UNIVERSIDAD DE MURCIA

ESCUELA INTERNACIONAL DE DOCTORADO

TESIS DOCTORAL

Implication of the NLRP3, NLRC4 and Pyrin inflammasomes in inflammatory diseases and sepsis

Implicación de los inflamasomas NLRP3, NLRC4 y Pirina en enfermedades inflamatorias y sepsis

Dña. Laura Hurtado Navarro

2023

UNIVERSIDAD DE MURCIA

ESCUELA INTERNACIONAL DE DOCTORADO

TESIS DOCTORAL

Implication of the NLRP3, NLRC4 and Pyrin inflammasomes in inflammatory diseases and sepsis

Implicación de los inflamasomas NLRP3, NLRC4 y Pirina en enfermedades inflamatorias y sepsis

Autora: Dña. Laura Hurtado Navarro

Director: D. Pablo Pelegrín Vivancos

UNIVERSIDAD DE MURCIA

DECLARACIÓN DE AUTORÍA Y ORIGINALIDAD
DE LA TESIS PRESENTADA PARA OBTENER EL TÍTULO DE DOCTOR
Aprobado por la Comisión General de Doctorado el 19-10-2022

D./Dña. LAURA HURTADO NAVARRO

doctorando del Programa de Doctorado en

INTEGRACIÓN Y MODULACIÓN DE SEÑALES EN BIOMEDICINA

de la Escuela Internacional de Doctorado de la Universidad Murcia, como autor/a de la tesis presentada para la obtención del título de Doctor y titulada:

Implication of the NLRP3, NLRC4 and Pyrin inflammasomes in inflammatory diseases and sepsis / Implicación de los inflamasomas NLRP3, NLRC4 y Pirina en enfermedades inflamatorias y sepsis

y dirigida por,

D./Dña. PABLO PELEGRÍN VIVANCOS

D./Dña.

D./Dña.

DECLARO QUE:

La tesis es una obra original que no infringe los derechos de propiedad intelectual ni los derechos de propiedad industrial u otros, de acuerdo con el ordenamiento jurídico vigente, en particular, la Ley de Propiedad Intelectual (R.D. legislativo 1/1996, de 12 de abril, por el que se aprueba el texto refundido de la Ley de Propiedad Intelectual, modificado por la Ley 2/2019, de 1 de marzo, regularizando, aclarando y armonizando las disposiciones legales vigentes sobre la materia), en particular, las disposiciones referidas al derecho de cita, cuando se han utilizado sus resultados o publicaciones.

Si la tesis hubiera sido autorizada como tesis por compendio de publicaciones o incluyese 1 o 2 publicaciones (como prevé el artículo 29.8 del reglamento), declarar que cuenta con:

- *La aceptación por escrito de los coautores de las publicaciones de que el doctorando las presente como parte de la tesis.*
- *En su caso, la renuncia por escrito de los coautores no doctores de dichos trabajos a presentarlos como parte de otras tesis doctorales en la Universidad de Murcia o en cualquier otra universidad.*

Del mismo modo, asumo ante la Universidad cualquier responsabilidad que pudiera derivarse de la autoría o falta de originalidad del contenido de la tesis presentada, en caso de plagio, de conformidad con el ordenamiento jurídico vigente.

En Murcia, a 1 de diciembre de 2023

Firmado por HURTADO NAVARRO LAURA - ***4539** el día 01/12/2023 con un certificado emitido por AC FNMT Usuarios

Fdo.: LAURA HURTADO NAVARRO

Esta DECLARACIÓN DE AUTORÍA Y ORIGINALIDAD debe ser insertada en la primera página de la tesis presentada para la obtención del título de Doctor.

Información básica sobre protección de sus datos personales aportados	
Responsable:	Universidad de Murcia. Avenida teniente Flomesta, 5. Edificio de la Convalecencia. 30003; Murcia. Delegado de Protección de Datos: dpd@um.es
Legitimación:	La Universidad de Murcia se encuentra legitimada para el tratamiento de sus datos por ser necesario para el cumplimiento de una obligación legal aplicable al responsable del tratamiento. art. 6.1.c) del Reglamento General de Protección de Datos
Finalidad:	Gestionar su declaración de autoría y originalidad
Destinatarios:	No se prevén comunicaciones de datos
Derechos:	Los interesados pueden ejercer sus derechos de acceso, rectificación, cancelación, oposición, limitación del tratamiento, olvido y portabilidad a través del procedimiento establecido a tal efecto en el Registro Electrónico o mediante la presentación de la correspondiente solicitud en las Oficinas de Asistencia en Materia de Registro de la Universidad de Murcia

The author of this thesis memory has jointed of PhD student fellowship "*Ayudas para la F.P.I. en Universidades y Organismos Públicos de Investigación de la R. de Murcia en los ámbitos académico y de interés para la industria*" (21214/FPI/19) from the Fundación Séneca, Región de Murcia (Spain). During the development of the Thesis, the author of the thesis also received a complementary mobility fellowship "*Ayudas para la realización de estancias externas destinadas a los Investigadores Predoctorales contratados con cargo al Subprograma Regional de Contratos de Formación de Personal Investigador"* with reference 21714/EFPI/22 to spend a short stay at the Radboud University Medical Center (Nijmegen, The Netherlands), whose research supervisor at host institution was Mihai G. Netea.

The research described in this thesis was financially supported by the projects:

1. Función del Inflamasoma en sepsis: un nuevo marcador temprano para predecir mortalidad (20859/PI/18), PI: Pablo Pelegrín, 2019-2022. Fundación Séneca (Spain).
2. Viabilidad de un test pronóstico para pacientes críticos con sepsis (Earlytest) (21081/PDC/19, IP: Pablo Pelegrín, 2020-2021. Fundación Séneca (Spain).
3. Pyroptotic cell death in the crossroad of the transition from health to disease (PID2020-116709RB-I00), PI: Pablo Pelegrín, 2021-2024. Ministry of Science, Innovation and Universities (Spain).
4. Desarrollo técnico de un equipo para determinar en el punto de atención la inmunosupresión de pacientes críticos con sepsis basado en la actividad del inflamasoma NLRP3 (DTS21/00080), PI: Pablo Pelegrín, 2022-2023. Institute of Health Carlos III (Spain).
5. Proof of concept of prognostic test for critical Septic Patients based in Early Detection of NLRP3 Inflammasome impairment activation (SPEDI-TEST), PI: Pablo Pelegrín, 2020-2021. European Research Council - Proof of Concept grant.

According to the declaration of interest, the author of this Thesis is co-founder of Viva In Vitro Diagnostics SL but declare that the research of the Thesis was conducted in the absence of any commercial or financial relationships that could be construed as a potential conflict of interest.

Tras cuatro años, la entrega de esta Tesis Doctoral supone para mí dejar por escrito el esfuerzo y dedicación que conlleva el culmen de la formación académica, alcanzar el título de Doctora. A lo largo de esta aventura me han acompañado innumerables personas a las que quiero dar las gracias.

Me gustaría comenzar agradeciendo a todos aquellos pacientes y a sus familiares, que con completa solidaridad acceden, en momentos tan delicados de la salud de un ser querido, que el personal médico, de enfermería… y, en mi caso, de investigación, podamos realizar nuestro trabajo. Es esta forma desinteresada y amable la que nos permite alcanzar nuevos hitos y descubrimientos científicos y, *por ende,* avances en la sociedad en la que vivimos. Tras una pandemia, ha quedado patente que todas y cada una de nosotras debemos remar en una misma y única dirección. Sin la aportación de cada uno de ellos esta Tesis no podría haberse llevado a cabo, de ahí mi especial gratitud.

De igual forma, mi más sincero agradecimiento a mi director y guía en esta Tesis, el Dr. Pablo Pelegrín. Gracias Pablo, por brindarme la oportunidad de acercarme a la investigación con las prácticas de la carrera y el TFG y por volver a confiar en mí durante cuatro años más. Tu supervisión, ayuda, tiempo y pasión por la ciencia han supuesto para mí un crecimiento personal y laboral del que estoy tremendamente orgullosa. Siempre te estaré agradecida.

Asimismo, me gustaría agradecer a todos los equipos clínicos y grupos de investigación con los que ha sido un placer colaborar. Al Dr. Carlos García Palenciano, por la obtención de muestras de pacientes sépticos desde la Unidad de Reanimación del Hospital Clínico Universitario Virgen de la Arrixaca. Gracias también a la Dra. Graciela Valero desde el Servicio de Cirugía General del Hospital Morales Meseguer, por facilitarnos la serie de pacientes control que, habiendo sufrido una cirugía abdominal, no desarrollaron sepsis. Al Dr. Juan Ignacio Arostegui, al Dr. José Hernández Rodríguez y a la Dra. Carmen Vargas, desde los Servicios de Enfermedades Autoinflamatorias y Reumatología del Hospital Clinic de Barcelona y del Hospital Virgen de la Macarena, por proporcionarnos las muestras de pacientes con enfermedades autoinflamatorias. Gracias al Dr. Manuel Comabella y al Dr. Sunny Malhotra, desde el Centro de Esclerosis Múltiple de Cataluña, por permitirnos estudiar pacientes con esclerosis múltiple. Gracias a la Dra. Francisca Ferrer y a Ernesto José Cuenca del Departamento de Hematología y Oncología Clínica del Hospital Morales Meseguer, por poder acercar la investigación a la clínica y ayudar en el entendimiento y la terapia de pacientes con leucemias monocíticas crónicas. Gracias a todos y a todas por haber confiado en mi trabajo.

Gracias a mis tutores académicos, Pedro Aparicio y Gonzalo Rubio, por su ayuda y consejo durante el desarrollo de esta Tesis Doctoral.

Gracias a Mihai G. Netea, por darme la oportunidad de formar parte de su equipo durante mi estancia en Países Bajos, destacando a Jorge Domínguez y Athanasios Ziogas, por su recibimiento, hospitalidad, ayuda y cariño.

A mis compañeros y compañeras de aventura: Cristina, Julio, Sandra, Adrián y Adriana. No he podido tener mejor apoyo que el vuestro. Sois, sin duda, el mejor descubrimiento de estos años.

Gracias a Diego y Alberto, por responder mis millones de preguntas siempre con cariño y paciencia. Gracias a Mª Carmen porque ese “pescozón”, cuando aún no sabía nada de ciencia, ha traído muchas cosas buenas detrás.

A Laura Martínez, gracias por ser mis manos, mis pies y mi voz con cada paciente. Descubrir, gracias a ti, el papel tan importante que tenéis las enfermeras y los enfermeros en la salud y en la vida de las personas hospitalizadas ha sido realmente un honor.

Al resto del equipo: Alejandro, Juan José, Santiago, Ana Isabel, Fernando, Cristina Alarcón, Curro, Carlos, Malvina, gracias por todo, no me he podido rodear de mejores personas.

Gracias a mis amigas, a mi núcleo fuerte, por haberme acompañado durante estos años de esfuerzo y sacrificio. Cris y Noe, gracias por estar siempre, aunque nos separen miles de kilómetros. Carmen, compartir contigo cada paso que doy es de las mejores cosas que tengo, gracias.

A María, gracias por ser Hogar y Suerte. Este éxito es mío, pero ha sido increíblemente bonito conseguirlo contigo a mi lado. Y, ‘que nada nos pare’.

Gracias a toda mi familia, por hacerme sentir siempre lo orgullosos y orgullosas que estáis de mí, me llena el alma teneros conmigo.

Papá, gracias por decirme cada mañana, durante cuatro años, que me coma el Mundo, que yo puedo con todo. Mamá, gracias por ser mi abrazo eterno, mis mimos constantes. Sois el ejemplo de superación, de lucha, y de amor más bonito que existe. María, gracias por ser siempre mi apoyo incondicional, mi media mitad, no he podido tener mejor hermana. Abuela, eres y siempre serás la mujer de mi vida, gracias por enseñármelo todo.

La ciencia es la expresión creativa de la razón y la libertad es la condición fundamental para que haya verdadera ciencia.

INDEX

INDEX

INDEX OF FIGURES

INDEX OF TABLES

ABBREVIATIONS

ABBREVIATIONS

AAD	Acidic activation domain
ACMG	American College of Medical Genetics and Genomics
ADCC	Antibody-dependent cellular cytotoxicity
AID	Autoinflammatory disease
AIM	Absence in melanoma
ALR	AIM-like receptor
APACHE	Acute physiology and chronic health evaluation
APC	Allophycocyanin
APP	Acute-phase protein
ARDS	Acute respiratory distress syndrome
ASC	Apoptosis-associated speck-like protein containing a caspase-recruitment domain
ATP	Adenosine-5'-triphosphate
BIR	Baculovirus inhibitor repeat
BMDM	Bone marrow-derived macrophages culture
BRET	Bioluminescent resistance energy transfer
CAPS	Cryopyrin-associated periodic syndromes
CARD	Caspase activation and recruitment domain
CCR	Cysteine-cysteine chemokine receptor
CD	Cluster of differentiation
CHS	Central helical scaffold
CIITA	MHC-class II transactivador complex
CINCA	Chronic infantile neurologic, cutaneous and articular syndrome
CLR	C-type lectin receptor
CMML	Chronic myelomonocytic leukemia
CNS	Central nervous systems
CO_2	Carbon dioxide
COVID-19	Coronavirus disease 2019

CRP	C-reactive protein
CXCR	Cysteine-X-cysteine chemokine receptor
DAMPs	Danger-associated molecular patterns
DMSO	Dimethilsulphoxide
DNA	Deoxyribonucleic acid
EDSS	Expanded disability status scale
EDTA	Ethylenediaminetetraacetic acid
ELISA	Enzyme-linked immunosorbent assay
FCAS	Familial cold autoinflammatory syndrome
FCS	Foetal calf serum
FiO_2	Fraction of inspired oxygen
FISNA	Fish-specific NACHT-associated domain
FITC	Fluorescein isothiocyanate
FMF	Familial Mediterranean fever
GBP	Guanylate-binding proteins
GM-CSF	Granulocyte-macrophage colony stimulating-factor
GoF	Gain-of-function
GSDMD	Gasdermin D
HD	Helical domain
HIF	Hypoxia inducible factor
HLA-DR	Human leukocyte antigen–DR isotype
HMGB1	High-mobility group box 1 protein
HRP	Horseradish peroxidase
HSC70	Heat shock cognate protein 70
HSCT	Hematopoietic stem cell transplantation
ICU	Intensive care unit
IFN	Interferon
IL	Interleukin

IL-1Ra	IL-1 receptor antagonist
IL-18BP	IL-18 binding protein
ILC	Innate lymphoid cell
INFI	INF-inducible protein
IRF	Interferon response factor
KRAS	*Kirsten* RAS
LDA	Linear discriminant analysis
LDH	Lactate dehydrogenase
LGP2	Laboratory of genetics and physiology 2 protein
LPS	Lipopolysaccharide
LRR	Leucine-rich repeat
Luc	Luciferase
MAP	Mean arterial pressure
MAPK	Mitogen activated protein kinases
MAS	Macrophage activation syndrome
MAVS	Mitofusin 2 and mitochondrial antiviral signalling
M-CSF	Macrophage colony-stimulating factor
MDA5	Melanoma differentiation-associated gene 5
MDS	Myelodysplastic syndromes
MHC	Major histocompatibility complex
MINCLE	Macrophage-inducible C-type lectin
mmHg	Millimetres of mercury
MNDA	Myeloid cell nuclear differentiation antigen
MPN	Myeloproliferative neoplasms
MRI	Magnetic resonance imaging
MS	Multiple sclerosis
mtDNA	Mitochondrial DNA
MTOC	Microtubule organizing centre

MWS	Muckle-Wells syndrome
MyD88	Myeloid differentiation primary response 88
NACHT	NAIP, CIITA, HET-E, and TP-1
NAIP	Neuronal apoptosis inhibitory protein
NBD	Nucleotide binding domain
NEK7	NIMA-related kinase 7
NF-kB	Nuclear factor kappa B
Nig	Nigericin
NINJ	Ninjurin
NK	Natural killer cell
NKT	Natural killer T cell
NLR	NOD-like receptor
NLR	Neutrophils-lymphocytes ratio
NOD	Nucleotide oligomerization binding domain
NOMID	Neonatal-onset multisystem inflammatory disease
NRAS	Neuroblastoma RAS
Nrf2	Nuclear factor erythroid 2-related factor
NT-proBNP	N-terminal brain natriuretic propeptide
OMV	Outer membrane vesicle
PAAD	Pyrin-associated dominant disease
PAAND	Pyrin-associated autoinflammation with neutrophilic dermatosis
PAMPs	Pathogen-associated molecular patterns
PaO_2	Partial pressure of oxygen
PB	Permeabilization buffer
PBMCs	Peripheral blood mononuclear cells
PCR	Polymerase chain reaction
PCT	Procalcitonin
pDC	Plasmacytoid dendritic cell

PE	Phycoerythrin
PJVK	Pejvakin
PLD	Phosphorylated linker domain
POP	PYRIN domain-only protein
PPMS	Primary progressive MS
PRR	Pattern-recognition receptor
PtdIns4P	Phosphatidylinositol 4-phosphate
PTM	Post-translational modification
PYD	Pyrin domain
qSOFA	Quick SOFA
RAGE	Receptor for advanced glycation end products
RAS	Rat sarcoma
REAu	Reanimation Unit
RLR	Retinoic acid-inducible gene (RIG)-I-like receptor
RNA	Ribonucleic acid
RNS	Reactive nitrogen species
ROC	Receiver operating characteristic analysis
ROS	Reactive oxygen species
RPM	Revolutions per minute
RRMS	Relapsing-remitting MS
RT	Room temperature
sAML	Secondary acute myeloid leukemia
SARS-CoV-2	Severe acute respiratory syndrome coronavirus 2
SB	Staining buffer
SDS	Sodium-docecyl-sulfate
SOFA	Sequential (Sepsis-related) Organ Failure Assessment
sPLS-DA	Latent structures-discriminant analysis
SPMS	Secondary progressive MS

T3SS	Type III secretion system
TACE	Matrix metalloproteinase TNF-α converting enzyme
TBS	Tris-buffered saline
Tcd	*Clostridium difficile* toxin
TCR	T cell receptor
TGF-β	Transforming growth factor β
TGN	*trans*-Golgi network
Th	Lymphocyte T helper
TIR	Toll/IL-1 receptor
TLR	Toll-like receptor
TNF	Tumor necrosis factor
TOFIE	Time-of-flight inflammasome evaluation
TRIF	TIR domain-containing adaptor inducing IFN-β
WBC	White blood cell
WHD	Winged helix domain
YFP	Yellow fluorescent protein

INTRODUCTION

1. Inflammation as a trigger of disease

Inflammation is an essential and evolutionarily conserved immune response of the organism, orchestrated by immune and non-immune cells, that protect the host of invading pathogens or endogenous signals, resulting in the elimination of the initial cause of injury and maintaining tissue homeostasis (Medzhitov, 2010; Netea et al., 2018).

Immunity and inflammation, as process that work together, have been studied since the dawn of medical practice in Ancient Egypt, in Classical Greece and in Ancient Rome (Cavaillon, 2018; Metwaly et al., 2021). Concretely, the roman doctor Cornelius Celsus (30 Before Christ to 38 Anno Domini) defines for the first time the *four-cardinal signs* (clinical symptoms) of inflammation as *rubor et tumor cum calore et dolore* (redness, swelling with warmth and pain). The *fifth cardinal sign* was added by Rudolf Virchow in 1858, *function laesa* or loss of function, which establish the cellular basis of the inflammatory response. In 1865, Max Schultze described different types of leucocytes in human blood, corresponding to those which are now known as monocytes, lymphocytes, neutrophilic and eosinophilic polymorphonuclear granulocytes and even documented the extracellular particles and the phagocytosis of these cells (Brewer, 1994; Medzhitov, 2010; Netea et al., 2018).

With the help of these investigations and all those that came in the following years, it is now established that a normal inflammatory response is a homeostatic mechanism that involve feed-forward (proinflammatory pathways) and feed-back (anti-inflammatory pathways) signals that lead to progressive attenuation of the acute inflammation response by the removal of the triggering stimulus, tissue regeneration and healing (Kotas & Medzhitov, 2015). However, the lack of removal of the triggering stimulus, which causes a persistent stimulation of the inflammatory cells, aggravated by certain factors (genetic, social, psychological and environmental), promote a state of low-grade, non-infective systemic chronic inflammation that at last causes collateral damage to tissues and organs over time (Furman et al., 2019; Straub & Schradin, 2016).

The Global Burden of Disease, a detailed scientific study made by the Institute for Health Metrics and Evaluation, measures the magnitude of diseases, injuries and risk factors to an individual's life across age groups, sexes, countries and time. According to the Global Burden Disease 2019, non-communicable diseases, including cardiovascular disorders, neoplasms, chronic respiratory diseases, kidney diseases and diabetes, account the half of overall global health loss (Abbafati et al., 2020). Decades ago, each non-communicable disease was considered as an independent condition, nevertheless, recent evidence suggests that there are a diverse group of chronic and highly disabling conditions that share

a state of low grade and sterile systemic chronic inflammation, called immune-mediated inflammatory diseases. Disorders belonging to this group are, among others, psoriasis, rheumatoid arthritis, spondylitis, inflammatory bowel disease, Chron's disease and ulcerative colitis. Their main commonalities in their pathogenesis are an imbalance in inflammatory cytokines and the influence of genetic predisposition (El-Gabalawy et al., 2010; Furman et al., 2019; Rahman et al., 2010).

The relationship between inflammation and diseases has encouraged researchers to further investigate the aetiology of these conditions, the mechanism that promote inflammation and cytokine dysregulation and, to develop mechanism-based treatment, such as novel biologic precise agents, that target the origin of inflammation improving quality of life and reducing the chances of people of suffer from immune-mediated inflammatory diseases (Baker & Isaacs, 2018; Kuek et al., 2007).

2. Immune system

All living beings, including plants and bacteria, are constantly threatened by the invasion of pathogens and have evolved several recognition mechanisms of immune defence to eliminate to vastly different groups of microorganisms. These recognition systems determine microbial location, viability, replication and pathogenicity (Iwasaki & Medzhitov, 2015).

Mammalian hosts provide a huge number of niches which can be colonized by microorganisms. Some of them, such as skin and colon, are colonized constitutively by an endogenous microbiota and other niches, as lower respiratory tract and the internal organs, are normally kept sterile. To get that, three anatomic and chemical barriers are present in mammals, (i) mechanical as body's epithelial surfaces, (ii) chemical and enzymatic systems like complement or lysozymes and (iii) microbiological barriers with the normal host-related microbiota. Commensal bacteria are critical for the breakdown of nutrients and for the development of an optimally functioning immune system, preventing colonization by potentially pathogenic bacteria. So that, the immune system is an interactive network of lymphoid organs, specific cells of innate and adaptative immune responses, humoral factors, cytokines and microbiota, which response to protect the organisms against infections and injuries (Kosiewicz et al., 2011; Medzhitov, 2007; Murphy & Weaver, 2017).

A pathogen that breaches the host's chemical and anatomic barriers will encounter with the cellular defences of innate immunity, which is an almost immediately immune response. It is orchestrated by the activation and functions of different sensor cells, as dendritic cells, granulocytes, natural killer cells (NKs), innate lymphoid cells (ILCs), monocytes

and macrophages, and blood proteins including the complement system, leukotrienes or prostaglandins among others (Eberl et al., 2015; Janeway & Medzhitov, 2002; Rapp et al., 2019). Innate immune cells recognize microorganisms and cellular damage through a limited number of germline-encoded pattern-recognition receptors (PRRs), which are activated via pathogen's products with immunostimulatory activity that share invariant structures such as lipopolysaccharide (LPS) in Gram-negative bacteria, double-stranded ribonucleic acid (RNA) in several groups of RNA viruses and mannans in yeast cell walls. Triggering these receptors, innate immune cells initiate an inflammatory response secreting proinflammatory cytokines and chemokines, which are responsible for the recruitment and activation of more immune cells at the site of infection or tissue injury, like neutrophils, that will amplify the response and initiate the adaptative immune response (Akira et al., 2006; Brubaker et al., 2015; Parkin & Cohen, 2001; Janeway & Medzhitov, 1997). It took almost a century, and it was not until the discovery of PRRs, to understand that innate immune system can provide protection against reinfection by building immunological memory in innate immune cells via epigenetic modifications in them, a process that ten years ago was called as trained immunity (Netea et al., 2011).

In parallel to innate immune activation or in the case that innate immunity was not able to eliminate the pathogens efficiently due to the high amount of virulence of invading microorganisms, adaptative immune mechanism are activated. It is mediated by different lymphocytes populations (principally T and B lymphocytes) that recognise specific portions of proteins or epitopes that are termed antigens. The downstream effects of lymphocyte activation through antigen-recognition are then extended by amplifying innate immune responses such as killing of pathogens, phagocytosis or providing signals to others immune cells. Upon a second encounter with the same pathogen, clonal expansion of lymphocytes induces a rapid and effective response (long-lasting immunity or immunological memory) (Farber et al., 2016; Parkin & Cohen, 2001; Netea et al., 2019). However, an incorrect adaptative immune response, such as production of antibodies against self-proteins, allows the development of autoimmune diseases, allergies and allograft rejection (Janeway & Medzhitov, 2002).

3. Cells of the immune system

Cells of the innate and adaptative immune system are generally originated in the bone marrow, where the majority of them maturate. Then, they are present as circulating cells in the blood and in the lymph, disseminated in tissues or as extravascular cells in

lymphoid organs. Myeloid cells include monocytes, macrophages, dendritic cells and granulocytes, among others, and their major roles are defence mechanisms by phagocytosis, production of cytokines, lipid mediators and antigen presentation. Lymphoid cells, for its part, include lymphocytes (B and T cells), NK cells and ILCs (Murphy & Weaver, 2017). Considering the importance of peripheral blood mononuclear cells (PBMCs) for this Thesis, they will be described in the following sections.

3.1 Lymphocytes

With exception of ILCs, which are important regulators of innate immunity through their rapid production of effector cytokines in response to tissue-derived signals, lymphocytes are the main cells of adaptative immunity. They are the only cells in the organism able to individually recognize and respond to each antigenic epitope. The most abundant subset of lymphocytes in peripheral blood are T and B lymphocytes. Mature T or B cells that have never encountered an antigen are considered naïve cells. Whereas, in response to them, activated lymphocytes differentiate into effector (capable of eliminating foreign antigens, T-effector cells; antibody-secreting cells, B-effector cells) or memory cells (cells which amplify the immune response after a re-infection) (Murphy & Weaver, 2017).

3.1.1 T lymphocytes

T cells coordinate multiple aspects of adaptative immunity including defence against extrinsic and intrinsic dangers (pathogens, allergens and malignant cells). They derive from precursors in the bone marrow and maturate in the thymus. The differentiation of T cell results in distinct subpopulations where the most important are T cytotoxic cells and T helper (Th) cells.

Cytotoxic T cells are effector cells which express differentially the cluster of differentiation (CD)-8 and are able to attack and kill cells that are malignant or infected with virus by exocytosis of cytolytic granules (e.g., granzyme B) or by Fas ligand-induce apoptosis cell death. On the other hand, T helper cells express CD4 and are in charge of the production of cytokines which stimulate B cells to generate antibodies. Th cells includes different subsets of cells which are distinguish based on their extracellular markers, their intracellular transcription profiles and their cytokine secretion profiles, highlighting Th1 and Th2 cells. Th1 cells are involved in cellular immunity against intracellular pathogens and in the development of autoimmune diseases, by producing inflammatory cytokines such as interleukin (IL)-2 and interferon (INF)-γ. Th2 cells are involved in the humoral immunity response

against allergens and extracellular pathogens in which Th2 cells initiate the secretion of cytokines like IL-4, IL-5, IL-10 and IL-13 (Kumar et al., 2019; Levy et al., 2000; Mousset et al., 2019; Saito et al., 2010).

3.1.2 B lymphocytes

B lymphocytes play a crucial role in humoral immunity responses against pathogens and tumours, promoting T cell response and production of specific antibodies. They are also implicated in the control and development of autoimmunity disorders, which are directly related to the production of auto-antibodies. The major part of B cells emerges from the bone marrow and are guided to the spleen, a secondary lymphoid organ, to continue their differentiation and maturation. Mature B cells can be subdivided into different subsets depending on their location, antigen specificity and cell surface phenotype. Between these population of cells, the more important are: plasma cells (antibody-secretory differentiated B-cell), memory B cells or regulatory B cells (functional subset of B cell which secrete IL-10 to suppress the excessive inflammatory response during unsolved infections or in autoimmune disorders) (Akkaya et al., 2020; Anaya et al., 2006; Rosser & Mauri, 2015).

3.2 Natural killer cells

Natural killer cells belong to a specific group of innate immune lymphocytes called ILCs and can be divided into two distinct subsets based on surface expression of CD56 and CD16. Their ability of cellular cytotoxicity allows them to induce a rapid and non-specific innate immune response against cells infected with intracellular viruses or pathogen and cancer cells. In order to distinguish between infected, damaged or malignant cells and host healthy cells, NK activation is governed by a balance between activating and inhibitory receptors (such as major histocompatibility complex (MHC)-1). Moreover, NK cells can also be directly activated by stimulation of cytokines such as IL-18, IL-2, IL-12 or IL-33, among others (Artis & Spits, 2015; Freud et al., 2014; Moritz Rapp, 2019). In addition to their cytotoxic functions, NK cells can secrete proinflammatory cytokines, such as INF-γ and tumor necrosis factor (TNF)-α, which amplify the inflammatory response during infections (Guo et al., 2017).

3.3 Dendritic cells

Dendritic cells are a heterogeneous sentinel myeloid group of innate immune cells. The main dendritic cells subsets include conventional dendritic cells, a specialized antigen-processing and presenting cells equipped with phagocytic activity, and plasmacytoid dendritic cells, specialized to respond to viral infection with a massive production of type I IFN (Cabeza-Cabrerizo et al., 2021; Morante-Palacios et al., 2021; Murphy & Weaver, 2017). Moreover, dendritic cells ingest large amounts of extracellular fluid and particles (clearance function) by a process known as micropinocytosis, in order to present antigens to the adaptative immune T lymphocytes by cell-cell interactions (Kratky et al., 2011; Swanson et al., 1995).

3.4 Granulocytes

Granulocytes are a subset of short-live polymorphonuclear leucocytes of myeloid origin which have densely staining granules containing a variety of toxic proteins and enzymes in their cytoplasm. Between this group of cells, basophils, eosinophils and neutrophils are found (Farahi et al., 2012; Geering et al., 2013; Pillay et al., 2010; Simon, 2009).

Eosinophils and basophils are important chiefly in defence against parasites, like helminths, and in allergic inflammatory responses contributing to the Th2 immune response through enhancing IL-4 (basophils) and IL-33 (eosinophils) production (Murphy & Weaver, 2017; Nadif et al., 2013; Rosenberg et al., 2013).

Neutrophils, for their part, are typically the first leucocytes to be recruited to areas of invasion by extracellular pathogens. They can contribute in the clearance of pathogens by three killing mechanisms: phagocytosis (engulfing of bacteria), degranulation (secretion of cytoplasmatic granules either into phagosomes or into the extracellular milieu) and releasing neutrophil extracellular traps. Neutrophil extracellular traps are structures composed by decondensed deoxyribonucleic acid (DNA), histones, proteins (e.g., lactoferrin) and enzymes (e.g., myeloperoxidase and elastase) that are released from neutrophils to attach and immobilize pathogens, facilizing their subsequent phagocytosis. Several studies indicate that a dysregulation on neutrophils activation and cell death and excessive neutrophil extracellular formation induce inflammation and organ injury in disorders like rheumatoid arthritis, systemic lupus erythematosus and sepsis (Alsabani et al., 2022; Chapman et al., 2019; Sun et al., 2021).

3.5 Monocytes and macrophages

Monocytes and macrophages are important phagocytic cells, being key during inflammatory responses and their resolution (innate and adaptative immune responses), pathogen clearance, tissue remodelling and repair, as well as in maintaining tissue homeostasis (Geissmann et al., 2010; Ginhoux & Jung, 2014; Hettinger et al., 2013).

Monocytes are known to be originated in the bone marrow from a common myeloid progenitor, shared with other leucocytes as neutrophils. Following tissue damage in response to infections, inflammation or neoplasia, monocytes are released into circulation and rapidly emigrate into tissues where they phagocytose infected or damaged cells and act as antigen-presenting cells to lymphocytes (Jakubzick et al., 2017). They constitute around the 10% of peripheral-blood leucocytes in humans, being the main phagocytic cell within the blood circulation, although they are also present in the bone marrow and spleen. Monocytes are heterogenous and can be divided into three subpopulations depending on the differential expression of surface markers and chemokine's profile. Classical monocytes are characterized for expressing high levels of CD14 and no expression of CD16 ($CD14^{++}CD16^{-}$) and high level of the cysteine-cysteine chemokine receptor (CCR)-2. When recruited to injured or infected sites, they act as the precursor of peripheral phagocytic cells and secrete proinflammatory cytokines. Intermediate monocytes express both CD14 and CD16 ($CD14^{++}CD16^{+}$) and non-classical monocytes express high level of CX3C motif chemokine receptor-1 (CX3CR1) and CD16 ($CD14^{+}CD16^{++}$). Intermediate and non-classical monocytes are implicated in vascular regeneration and homeostasis (Guilliams et al., 2018; Ziegler-Heitbrock & Hofer, 2013).

Monocytes differentiate into tissue-resident macrophages during inflammatory conditions. As monocytes, macrophages constitute a heterogenous phagocytic cell type whose functions, phenotypes and names depend on their resident tissue localisation (such as osteoclasts in bone or Kupffer cells in liver). Despite macrophages' heterogeneity, in the last decade it has been revealed that most tissue-resident macrophages (with the exception of the yolk-sac-derived macrophages) are developed during embryogenesis and maintain their population by tissue resident stem cells self-renewal. However, monocytes migrating to tissues could also transform into tissue resident macrophages (Guilliams et al., 2018; Schulz et al., 2012; Yona et al., 2014).

Macrophage activation and polarization occurs into two distinct varieties which differ in term of effector function, cytokine production, receptor expression and chemokine profile.

Classically activated or M1 macrophages are induced in presence of LPS, INF-γ or granulocyte-macrophage colony stimulating-factor (GM-CSF). Their principal functions are initiate the inflammatory response against microorganism and tumours, present antigen via MHC class II, recruit granulocytes to the infection site and polarize T cells to Th1. As explained above, Th1 cells and NK cells release INF-γ which amplify M1 polarization. Once M1 macrophages are active, they have a proinflammatory phenotype releasing, among others, IL-12, IL-23, IL-1β, TNF-α and reactive oxygen/nitrogen intermediates. On the other hand, alternative activated or M2 macrophages are polarized in presence of IL-4, IL-10, IL-13, glucocorticoids and M-CSF. M2-activated macrophages promote inflammation resolution and adaptative immune response, tissue healing and repair, angiogenesis and participate during allergy responses and helminth infections. Alternative macrophages are characterized for secreting high concentration of IL-10 and IL-1 receptor antagonist (IL1-Ra), both with anti-inflammatory properties, promoting a Th2 response (Chiu & Bharat, 2016; Mantovani et al., 2004; Martínez et al., 2009; Martínez & Gordon, 2014).

Several research have shown that M1 and M2 polarized macrophages are extremes of a continuum of functional states which depends on the microenvironment's signals. This plasticity allows M1 and M2 macrophages to be re-polarized by a secondary stimulus, e.g., reducing dampening inflammation via M1 to M2 re-polarization (López-Castejón et al., 2011; Pelegrín & Surprenant, 2009). Some studies indicate that M2 macrophages present more plasticity than M1 macrophages and rapidly change to an inflammatory M1 state (Biswas & Mantovani, 2010; Van den Bossche et al., 2016).

4. Exogenous and endogenous origin-inducers of the inflammatory response

As previously described, the role of the inflammatory response is to combat pathogens' infections and tissue damage. To achieve this, innate immune cells sense the presence of microorganisms and endogenous molecules released from damaged cells through their intracellular or surface-expressed PRRs. This initial recognition is mediated by innate immune cells, such as macrophages and neutrophils, and is a key step for phagocyting and killing pathogens and leading to the production of a wide variety of cytokines and chemokines. As well, PRRs signalling allows the activation of dendritic cells and the induction of the adaptative immune response by antigen presentation.

Exogenous inducers of the inflammatory response involve pathogen-associated molecular patterns (PAMPs) and virulence factors. Non-microbial inducers of inflammation are allergens, irritants, toxic compounds and foreign bodies. PAMPs are defined as a set of structurally diverse and molecularly conserved patterns present on microorganisms, that

are often essential for the life-cycle of the pathogen survival. The best-known examples of PAMPs include LPS from Gram-negative bacteria, lipoteichoic acid from Gram-positive bacteria, the bacterial protein flagellin or the fungal β-glucan, among others (Kumar et al., 2011; Medzhitov, 2008).

Danger- or damage-associated molecular patterns (DAMPs) are endogenous inducers of inflammation released during cellular stress, tissue damage (acting as alarmins) and death cells. DAMPs play an important role in regulating innate and adaptative immunity, as their signalling imply the sensing and repair of a damage cell or tissue and are capable of activate myeloid cells. Certain cellular constituents that are released when plasma membrane is disrupted during cell death, such as adenosine-5'-triphosphate (ATP), potassium ions, uric acid, several members of S100 calcium-binding protein family (S100A8, S100A9) and high-mobility group box 1 protein (HMGB1), are all endogenous signals triggering inflammation. Breakdown products from the extracellular matrix, such as hyaluronan, heat shock proteins and oxidized lipoproteins are also DAMPs (Newton & Dixit, 2012; Patel, 2018; Pelegrín, 2011).

5. Sensors of the inflammatory response: pattern recognition receptors

PRRs are germline-encoded sensors expressed in the majority of immune cells, like dendritic cells, macrophages, neutrophils and lymphocytes. Several non-immune cells also express PRRs, like epithelial cells. PRRs sense DAMPs and PAMPs, which induce their oligomerization and assemble into macromolecular complexes that initiate transcriptional pathways which lead to the release of immune mediators, such as proinflammatory cytokines, chemokines, type I IFN and antimicrobial proteins. PRRs activation also initiates non-transcriptional responses such as phagocytosis of infected or damaged cells, cytokine processing, cell death and induction of co-stimulatory molecules on antigen-presenting cells.

Most PRRs can be classified into five families depending on their protein domain homology. Toll-like receptors (TLRs) and C-type lectin receptors (CLRs) are membrane-bound receptors (plasma membrane or endocytic compartments) which sense pathogens' ligands within endosomes and the extracellular space. On the other hand, Nucleotide-binding domain, leucine-rich repeat (LRR)-containing (or NOD-like) receptors (NLRs), Retinoic acid-inducible gene (RIG)-I-like receptors (RLRs), and the Absence in melanoma (AIM)2-like receptors (ALRs) are intracellular receptors in charge of sensing cytosolic dangers. PRRs also differ in their expression patterns, in their recognition specificity (different PRRs react with specific PAMPs or DAMPs) and in the downstream signalling pathways they activate (Akira et al., 2006; Brubaker et al., 2015).

5.1 C-type lectin receptors

CLRs constitute a heterogeneous superfamily of receptors expressed mainly in myeloid cells and are characterized by sharing at least one carbohydrate recognition domain. On the basis of their structure, CLRs exist both as transmembrane and soluble proteins and are implicated in numerous physiological functions such as antigen-presentation for promoting T cells responses and induction of the inflammatory immune responses and the recognition of mannose, fucose and carbohydrate structures on microorganisms like bacteria, fungi and viruses (e.g., *Streptococcus pneumoniae, Candida albicans* and severe acute respiratory syndrome (SARS) coronavirus. The most studied CLRs are Dectin-1 (binds to fungal β-1,3-glucans), Dectin-2 (binds to α-mannans of fungal cell walls) and MINCLE (Macrophage-inducible C-type lectin; binds to glycolipids of pathogens and ligands released by dead cells) (Drouin et al., 2020; Fischer et al., 2022; Geijtenbeek & Gringhuis, 2009).

5.2 RIG-I-like receptors

RLRs are RNA sensors localized in the cytosol seinsing viral entry and replication. This family of proteins is composed of the melanoma differentiation-associated gene 5 (MDA5), RIG-I and laboratory of genetics and physiology 2 (LGP2) proteins. All RLRs are characterized for having a C-terminal regulatory domain, an intermediate DExD/H-box RNA helicase domain and, in the case of RIG-I and MDA5, they additionally have two N-terminal caspase activation and recruitment (CARD) domains. RIG-I and MDA5 are involve in antiviral defence (e.g., Influenza virus or Hepatitis C virus and encephalomyocarditis virus, respectively) and are potent inductors of type I IFN in virus infections, whereas, LGP2 regulates negatively RIG-I and MDA5 (Koyama et al., 2008; Rehwinkel & Gack, 2020; Wu & Chen, 2014).

5.3 AIM2-like receptors

ALRs are a novel family of PRRs, only described in mammals, involved in the detection of nuclear and cytosolic DNA of stressed or infected cells and the regulation and repair of chromatin structure. In human, the family is composed by four members: Absent in melanoma (AIM)2, INF-γ inducible protein 16 (IFI16), myeloid cell nuclear differentiation antigen (MNDA) and INF-inducible protein X (IFIX). Structurally, they are characterized for having a N-terminal pyrin domain (PYD) and a C-terminal HIN200 domain. The most studied ALR is AIM2, which activates in response to pathogens, such as *Streptococcus pneumoniae* and *Mycobacterium tuberculosis,* promote inflammasome formation and secretion of IL-1β

and IL-18 through pyroptosis cell death (Brubaker et al., 2015; Gray et al., 2016; Jiang et al., 2021).

5.4 Toll-like receptors

Toll-like receptors is one of the best-studied family of PRRs which recognize pathogen-derived components. They are widely distributed in all innate and adaptative immune cells, and also in non-immune cells like epithelial cells. TLR are transmembrane proteins which structurally contains LRRs for PAMPs recognition, a single central transmembrane domain and a cytosolic Toll/IL-1 receptor (TIR) domain in charge of transducing signals to downstream adaptors (Akira et al., 2006; Fitzgerald & Kagan, 2020).

TLRs are synthesized in the endoplasmic reticulum (ER) and then are transported to their ultimate locations in the cell. Human TLR1, TLR2, TLR5, TLR6 and TLR10 are located on the cell surface, whereas TLR3, TLR7, TLR8, TLR9 and TLR11, are exclusively expressed on intracellular vesicles (e.g., endosomes, phagosomes, lysosomes, endo-lysosomes). TLR4, for its part, can be expressed on the plasma membrane and also intracellularly (Newton & Dixit, 2012; O'Neill et al., 2013).

Their extensive distribution along the cell provides a comprehensive immune defence recognizing intracellular PAMPs and DAMPs and sensing extracellular microbial-derived compounds. In particular, TLR2 can sense (alone or heterodimerizing with TLR1 and TLR6) lipopeptides, teichoic acids, peptidoglycans and glycans from bacteria, fungi, yeast and viruses. TLR5 binds to flagellin and human TLR10 ligand remains undefined. On the other hand, TLRs found in endosomes are involved in nucleic acid sensing: TLR3 recognises double-stranded RNA during RNA virus replication in infected cells, TLR7 and TLR8 sense single-stranded RNA from virus and TLR9 is involved in the recognition of bacterial and viral unmethylated CpG motifs containing single-stranded DNA. TLR4 can detect a large repertoire of PAMPs and DAMPs as LPS from Gram-negative bacteria, heat shock proteins, HMGB1, S100 family proteins or the spike protein of SARS-CoV-2 virus among others (Akira et al., 2006; Fitzgerald & Kagan, 2020; Kumar et al., 2011; Liu et al., 2022; Newton & Dixit, 2012; O'Neill et al., 2013).

Once the endosomal or cytosolic TLR is activated, via PAMPs and DAMPs binding to their LRR domain, a signalling transduction pathway is promoted. There have been described two main adaptor pathways in TLRs signalling, called Myeloid differentiation primary response 88 (MyD88) and TIR domain-containing adaptor inducing IFN-β (TRIF) pathways. MyD88 is an adaptor protein which lead to the induction of gene expression through the

transcription factors nuclear factor kappa-light-chain enhancer of activated B cells (NF-κB) or interferon response factor (IRF), among others. In the case of the adaptor TRIF, it transmits the signal downstream through the IRF-3 and NF-κB together. Both signalling cascades culminate in the production of type I IFNs and the proinflammatory cytokines IL-1β and TNF-α. Interestingly, all TLRs with exception of TLR3, are able to induce MyD88 pathway. Remarkably, TLR4 is able to activate both pathways, initially leads to activation of the MyD88 pathway at the plasma membrane and then activates the TRIF pathway at the endosomes (Chen et al., 2016; Joosten et al., 2016; Wu & Chen, 2014).

5.5 NOD-like receptors

NOD-like receptors are cytosolic PRRs known for survey the cytoplasm homeostasis and the presence of PAMPs, and DAMPs playing an important role in innate immunity. In terms of structure, members of this family share a similar pattern of domain architecture which consist on: a N-terminal effector region such as CARD domain, CARD-like domain, Pyrin (PYD) or baculovirus inhibitor repeat (BIR), responsible for protein-protein interactions with adaptor molecules and required for signal transduction; a centrally located nucleotide-binding and oligomerization domain (NBD), also referred as NACHT (neuronal apoptosis inhibitor protein (NAIP), MHC-class II transactivador complex (CIITA), HET-E and TP-1), required for mediating self-oligomerization and activation of NLRs; and a C-terminal LRR domain involved in sensing microbial patterns and other ligands. NATCH domain includes a NDB domain with Walker A and B motigs, a helical domain (HD) 1, a winged helix domain (WHD) and a HD2 (**Figure 1**) (Bertin & DiStefano, 2000; Inohara et al., 2005; Newton & Dixit, 2012; Tschopp et al., 2003).

Depending on the nature of their N-terminal domain, the NLRs have been divided into subfamilies. When a CARD domain is present, the family is termed NLRC and it is composed by five members (NOD1, NOD2, NLRC-3/5). On the contrary, if the effector domain consists on a PYD domain, the family is called NLRP and comprises 14 members (NLRP-1/14). Alternatively, in some NLRs, BIR domain is present in the N-terminal and they are called NLRB or NAIP. Other member of the NLR family is CIITA complex which is characterized for the presence of an acidic activation domain (AAD) between CARD-like and NDB domains. At last, there is a slightly separated subfamily of a mitochondrial NLR termed NLRX with unknown functions and which N-terminal domain has no homology to other NLR

subfamily members (Carneiro et al., 2008; Martinon et al., 2009; Pedra et al., 2009) (**Figure 1**).

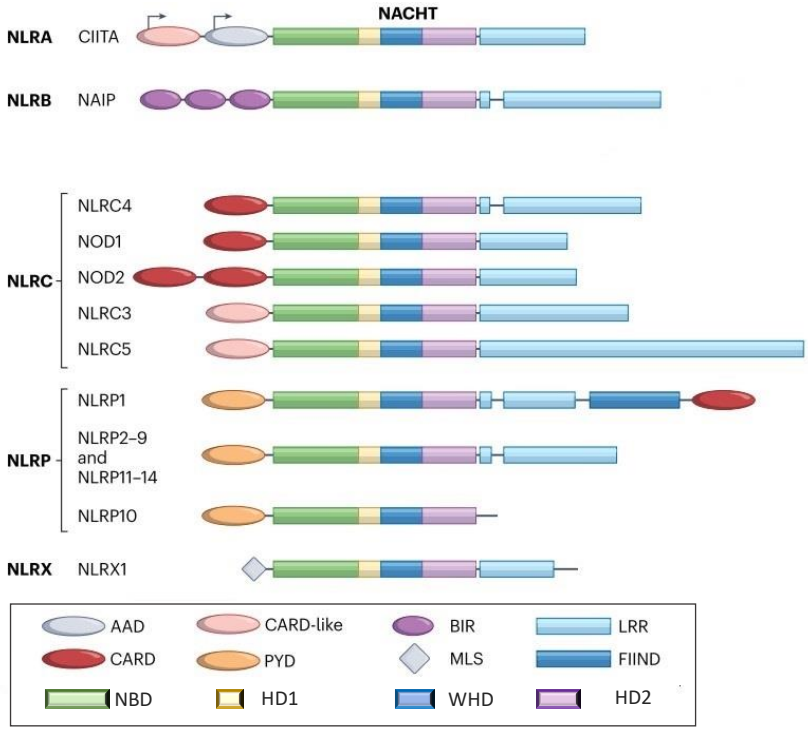

Figure 1. Structural organization of human NLRs according to subfamilies. AAD, acidic activation domain: BIR, baculovirus inhibitor of apoptosis repeat; CARD, caspase activation and recruitment domains; HD1/2, helical domain 1/2; WHD, Winged helix domain; FIIND, domain with function to find; MLS, mitochondrial localization signal; NOD, nucleotide-binding oligomerization domain; LRR, leucine-rich repeats; NATCH, NAIP, CIITA, HET-E and TP1 proteins; PYD, pyrin domain; CIITA, MHC-class II transactivador complex and NAIP, NLR family apoptosis inhibitory protein. Adapted from (Chou et al., 2023).

The different NLR members form molecular platforms that establish signalling complexes such as NOD signalosomes (NOD1 and NOD2) or inflammasomes (NLRC4 and NLRP1/2/3/6/10/12) (Martinon et al., 2009).

NOD1 and NOD2 are sensors of the breakdown products of bacterial cell wall molecules, as meso-diaminopimelic acid and muramyl dipeptide, respectively. Upon agonist sensing, both NLR recruit a serine/threonine kinase called RIP2, through CARD-CARD interactions, which initiate a proinflammatory response dependent on NF-κB and mitogen activated protein kinases (MAPK) pathways. The bifurcation in signalling involves differential PAMPs recognized and recruitment of adaptor proteins recruited to NOD signalosomes that signalise towards specific inflammatory responses (Saïd-Sadier & Ojcius, 2014; Yeretssian et al., 2011).

On the other hand, a number of NLR molecules have been shown to assemble a cytosolic high-molecular-weight multiprotein complexes called inflammasomes that, generally, mediate the activation of the inflammatory caspase-1 which initiates downstream responses including the release of IL-1β and IL-18 (Martinon et al., 2002). So that, inflammasomes have been recognized for their crucial role in host defence against pathogens and infections (Broz & Dixit, 2016; Lamkanfi & Dixit, 2014; Pedra et al., 2009). Although the major part of the NLRs act as pro-inflammatory molecules, it is important to stand out that there are some NLRs whose function is repressing the inflammatory response, such as NLRP10 (that acts as a suppressor of the cutaneous inflammatory response to *Leishmania major* infection), NLRP11 (that has a potential negative regulatory role in NF-κB and IFN pathways) and NLRP12 (that reduces NF-κB activation by TLR-signalling molecules after *Mycobacterium tuberculosis* infection (Clay et al., 2017; Ellwanger et al., 2018; Williams et al., 2005). In section 7 of this Thesis a detailed description of the different inflammasomes is present.

6. Inflammatory mediators: cytokines, alarmins and plasmatic factors

During an inflammatory process, epithelial cells, endothelial cells and immune cells trigger the production of numerous mediators including cytokines, chemokines, oxygen free radicals or plasmatic factors among others, which in turn amplify the immune response and alter the functionality of many organs and tissues. Though the majority of mediators have a proinflammatory role, others are implicated in repressing the immune response or maintaining tissue homeostasis (Medzhitov, 2008). In the following section, there will be explained the inflammatory mediators that have a major relevance in this Thesis.

6.1 The IL-1 family of cytokines

The interleukin-1 family comprises eleven cytokine members and ten receptors, with proinflammatory and anti-inflammatory properties, implicated in both the innate and the adaptative responses. The members of this family can be categorized into three subfamilies on the basis of the primary ligand binding receptor: IL-1α, IL-1β, IL-1 receptor antagonist (IL-1Ra) and IL-33 comprise the IL-1 subfamily and bind to the IL-1 receptor and the specific accessory protein IL-1R3 (also called IL-1RAcP); the IL-36 subfamily comprises IL-36α, IL-36β, IL-36γ, IL-36Ra and IL-38, which share the receptor IL-1R6; and IL-18 and IL-37 form the IL-18 subfamily that bind to the receptor IL-1R5. With the exception of IL-1Ra that presents a signal peptide and it is rapidly secreted upon expression, all IL-1 family members have to be cleaved to generate an optimal bioactive mature cytokine. To gain that, they

present a protease cleavage site normally located nine amino acids before a consensus sequence A-X-D, in which A may be any aliphatic amino acid followed by any amino acid (X) and then an aspartic acid (D) (Dinarello, 2009).

6.1.1 IL-1 subfamily

IL-1β is the most studied member of the IL-1 family and it is considered a central mediator of innate immunity and inflammation. It is primarily a product of myeloid cells although NK cells and B cells can also produce it. The conversion of the precursor pro-IL-1β into its mature and biologically active form represents an important step in its activation. Once the monocytes and macrophages are activated, pro-IL-1β is accumulated in the cytosol until being processed, which can be mediated by several mechanisms. That includes the activation of caspase-1 or other serine proteases (Dinarello, 2019; Netea et al., 2010). Mature IL-1β can then be released via exosomes, secretory lysosomes as a result of calcium influx or by the shedding of microvesicles from the plasma membrane. However, the main pathway inducing the release of IL-1β is caspase-1-dependent cell death (later explained in section 7.2). After IL-1β is released from the cell, its proinflammatory effects are exerted through binding to IL-1R1, inducing the MyD88 dependent pathway to activate NF-κB that ultimately lead to further production of proinflammatory cytokines. Based on data derived from patient cells, mice models and clinical trials the number and complexity of IL-1β-mediated autoinflammatory diseases (Broderick & Hoffman, 2022; Netea et al., 2015).

IL-1α is a constitutively expressed cytokine in many cells and is implicated in the first defence mechanisms of tissues with a barrier function. Its precursor (pro-IL-1α) and the cleavage form (obtained by the processing of membrane-associated calcium-dependent cysteine proteases like calpain II) are both biologically active and acts as IL-1R1 ligand. IL-1α is known to have a dual role since the pro-IL-1α have a nuclear localization signal. In the nucleus, it binds to the chromatin acting as a transcription factor regulating gene expression. In the cytoplasm, it binds to mitochondrial cardiolipin to regulate the activation and function of the NLRP3 inflammasome. Also, IL-1α acts as a soluble mediator (like IL-1β) in the extracellular space, binding to cell membrane IL-1RI and initiating signal transduction with the consequent activation of NF-κB and MAPK kinases pathways and stimulate the synthesis of inflammatory chemokines recruiting infiltrated neutrophils and monocytes to damaged or infected sites. During necrotic cell death, IL-1α is released to extracellular space where it, thus acting as an alarmin (Cavalli et al., 2021; Dagvadorj et al., 2021; Van de Veerdonk & Netea, 2013).

To prevent exacerbated activation and minimizing collateral damage of inflammation, the IL-1 family of cytokines is tightly controlled at different levels by antagonists, decoy receptors or scavengers, as some examples. Related to IL-1 subfamily, IL-1Ra and the decoy receptor IL-1R2, reduce both IL-1β and IL-1α signalling.

IL-1Ra was the first naturally cytokine described as a specific receptor antagonist (Arend, 1998). Specifically, IL-1Ra acts as a competitive inhibitor for the binding of IL-1β and IL-1α to their receptor IL-1R1 by preventing the recruitment of IL-1R3, which will impair intracellular signalling. IL-1 receptor antagonist is produced as four different isoforms, one is secreted (sIL-1Ra) while the others lack a signal peptide and remain intracellular (icIL-1Ra1, icIL-1Ra2 and icIL-1Ra3). Under certain circumstances, these intracellular isoforms can be released by dying cells or actively secreted by unconventional release pathways of proteins (Gabay et al., 2010; Garlanda et al., 2013). It should be highlighted that recombinant IL-1Ra, commercially named Anakinra, was approved in 2001 from the US Food and Drug Administration as a treatment for rheumatoid arthritis and Cryopyrin-associated periodic syndromes (CAPS) (Bedaiwi et al., 2021; Dinarello, 2018). Since then, Anakinra has been shown to be an efficacious therapeutic agent in a broad spectrum diseases as sepsis or Coronavirus disease 2019 (COVID-19) (Dinarello et al., 2012; Van De Veerdonk & Netea, 2020).

For its part, IL-1R2 is a dominant negative receptor that binds to IL-1β and IL-1α with high affinity without inducing intracellular signalling, therefore acting as a molecular trap. Concretely, IL-1R2 forms a complex with the protein IL-1R3, which is essential for IL-1 signal transduction. It also binds to IL-1Ra but with low affinity. Soluble and membrane bound IL-1R2 is found in healthy individuals' blood at high concentrations where it limits IL-1β mediated systemic inflammation. Intracellularly, in the cytosol, it interacts with pro-IL-1α protecting its cleavage and maturation and limiting IL-1α-depending inflammation during necrosis. Interestingly, during severe infections caspase-1 is able to cleavage IL-1R2, reverting the blockade made by this decoy receptor and restore the IL-1α activity (Garlanda et al., 2013; Smith et al., 2003; Zheng et al., 2013).

The fourth member of the IL-1 subfamily is IL-33. It is characterized for forming a heterotrimer with IL-1R4 receptor and the accessory protein IL-1R3. IL-33, as IL-1α and HMGB1, is normally found in the nucleus of the cells that expressed it constitutively or in an inducible manner, like epithelial, endothelial and hematopoietic cell types. Although the structure of IL-33 precursor contains a caspase-1 cleaving site, caspase-1 cleaving actually results in the inactivation of this cytokine (Cayrol & Girard, 2009). As other members of the

IL-1 family, the generation of a potent mature form is mediated by neutrophils serine proteases elastase and cathepsin G and, also, by mast cell proteases (Lefrançais et al., 2014). After processing and releasing, mature IL-33 acts as a proinflammatory alarmin. The principal biological activity of IL-33 is the promotion of Th2 responses, M2 macrophages polarization and type-2 immune responses driven by innate lymphoid cells, although under certain conditions it also promotes Th1 responses and INF-γ production (Kurowska-Stolarska et al., 2009; Schmitz et al., 2005; Smithgall et al., 2008). Interestingly, Bessa et al., showed that nuclear sequestration of IL-33 might protect from non-resolving and chronic inflammation that contribute to the pathogenesis of multiple condition such as sepsis (Bessa et al., 2014). Recent research also show that IL-33 plays a central role in all the pathogenesis of COVID-19, being considered as a biomarker of disease severity (Markovic et al., 2021; Zizzo & Cohen, 2020).

6.1.2 IL-18 subfamily

Interleukin-18 is a potent cytokine involved in host defence against infections regulating both innate and adaptative responses. Similar to IL-α and IL-33 and unlikely to IL-1β, many hematopoietic and non-hematopoietic cells constitutively express the IL-18 precursor, such as in Kupffer cells, circulating monocytes, resident macrophages, dendritic cells and keratinocytes, among others. Similarly to IL-1β, IL-18 is produced in the cytoplasm of the cells as an inactive cytokine (pro-IL-18) that required proteolytic processing to form a biologically active IL-18. The maturation of pro-IL-18 is via caspase-1/4/8 cleavage and its unconventional release mainly via pyroptotic cell death (Devant et al., 2023; Shi et al., 2023). Then, extracellular IL-18 form a signalling complex by binding to the receptor IL-1R5 (with low affinity) and the co-receptor IL-1R7 (with high affinity), inducing the MyD88-dependent pathway to activate NF-κB transcription factor. Functionally, IL-18 induces Th1 responses and INF-γ production in presence of IL-15 or IL-12, however if this synergism is absent, IL-18 entails an induction of Th2 responses. Also, IL-18 plays a major immunoregulatory role in NK cell responses and, in the adaptive immune system, IL-18 promotes activation and the differentiation of T cells (Dinarello et al., 2013; Novick et al., 2013; Teufel et al., 2022).

The interleukin-18 binding protein (IL-18BP) is a constitutive secreted protein that belongs to a separate family of proteins, which acts as an antagonist with an exceptionally high affinity for IL-18 in 1:1 ratio. In healthy individuals, circulating concentrations of IL-18BP are 10-20-fold molar excess over circulating IL-18. That implies that most circulating IL-18 is bound to IL-18BP and therefore is inactive. There are several immunologically mediated

diseases in which there is an imbalance of the IL-18:IL-18BP ratio, so that free IL-18 is elevated in the circulation, resulting in an exacerbated Th1 lymphocytes and macrophages activation (e.g., metabolic syndromes, psoriasis, inflammatory bowel disease, macrophage activation syndrome (MAS), sepsis and COVID-19 disease). The recombinant IL-18BP is being developed as therapeutical agent (Abbafati et al., 2020; Ihim et al., 2022; Lieben, 2018; Rodrigues et al., 2020).

IL-37 is a novel member of the IL-18 subfamily and is a broad suppressor of inflammation and adaptative immune responses. It has been reported that IL-37 promotes anti-inflammatory effects through IL-1R5, the same receptor that binds IL-18 cytokine but now using the co-receptor IL-1R8. However, IL-37 is not a classical receptor antagonist of IL-18. Following stimulation and similar to IL-33 and IL-1α, IL-37 can translocate to the nucleus after caspase-1 cleavage, where it acts as a transcriptional modulator inhibiting the production of inflammatory cytokines. Moreover, Li et al., showed that in addition to its nuclear function, IL-37 could act as an extracellular cytokine binding to IL-1R8 expressed in M1 macrophages and reduce IL-1β, IL-6 and TNF-α production. With respect to acquired immune responses, IL-37 is capable of tolerise DC cells or supress the expression of MHC class II. Due to the ability of IL-37 in blocking inflammatory processes, treatment of recombinant IL-37 is being studied as a possible novel therapeutic target in allergic diseases (Huang et al., 2019; Li et al., 2015; Nold et al., 2010).

6.1.3 IL-36 subfamily

IL-36 cytokines (IL-36α, IL-36β and IL-36γ) are agonists of the IL-1R6 and induce proinflammatory activation of NF-κB and MAPK kinases signalling cascades, while IL-36Ra specifically binds to that receptor preventing IL-36 cytokine-mediated signalling. Neither IL-36 nor IL-36Ra contain a caspase cleavage site, hence their N-terminal processing to produce active molecules require neutrophil's elastase and cathepsin G. IL-36 cytokines are mainly expressed in skin keratinocytes, brain tissue, bronchial epithelium, gut, monocytes and macrophages, where it plays an important role in first-line immune defence and tissue homeostasis. For example, IL36 cytokines are able to induce Th1 and Th17 responses with the consequent release of IL-2, IL-1β, IL-12 and IL-17 cytokines. A growing body of evidence associated IL-36 cytokines with inflammatory diseases, such as inflammatory bowel disease, rheumatoid arthritis, psoriatic arthritis and skin diseases where the most notable is psoriasis in which IL-36γ has been proposed as a biomarker (Buhl & Wenzel, 2019; Migliorini et al., 2020; Queen et al., 2019; Towne et al., 2011).

IL-38 cytokine is another member of the IL-36 subfamily. It is expressed in most tissues including spleen, thymus, skin and B cells. As IL-36 cytokines, IL-38 lacks a caspase-1 cleavage site and binds to IL-1R6 receptor. However, contrary to IL-36, once activated it could be released from apoptotic cells resulting in the suppression of the inflammatory response. As an example, in LPS-stimulated PBMCs upon *Candida albicans* infection, IL-38 reduces the IL-36γ-induced T-cell cytokines (Mora et al., 2016; Van De Veerdonk et al., 2012).

6.2 Others pro-inflammatory cytokines: TNF-α, IL-6, IL-8 and IL-15

TNF-α is a strong proinflammatory cytokine which plays important roles in acute and systemic inflammatory responses, cell proliferation, differentiation and cell apoptosis, while promoting the production of others cytokines and chemokines. It belongs to a superfamily of cytokines known as the TNF superfamily, being the most studied member. TNF-α is produced in two forms, membrane-bound and soluble form after cleavage by matrix metalloproteinase TNF-α converting enzyme (TACE), and signals through two transmembrane receptors called TNFR1 and TNFR2. T cells and macrophages are the main producers of TNF-α, although there are other cells that can also synthetize this cytokine, e.g., neutrophils, NK cells, adipocytes and B cells. Besides LPS, which is considered to be the main trigger of TNF-α expression, pathogen's antigens, immune complexes and other cytokines, such as IL-1β, IFN-γ, GM-CSF and transforming growth factor β (TGF-β), also induce its synthesis (Kalliolias et al., 2016; Ordás et al., 2007; Zelová & Hošek, 2013). TNF-α inhibitors are crucial therapeutics to treat severe autoimmune diseases and chronic inflammatory syndromes, like rheumatoid arthritis, psoriasis, systemic juvenile idiopathic arthritis and COVID-19 (Fisher et al., 2022; Guo et al., 2022; Monaco et al., 2015) .

IL-6 is a pleiotropic proinflammatory cytokine expressed in a broad range of immune cells and non-immune cells (e.g., fibroblasts, keratinocytes, malignant cells) in response to a wide variety of stimuli, such as ultraviolet irradiation, microbial products and viruses. IL-6 is highly induced by IL-1β. IL-6 exerts its biological functions by binding to the IL-6 receptor (IL-6R), which exits as a transmembrane protein in leucocytes and hepatocytes or soluble (sIL-6R) in human serum. Once the complex is formatted, homodimerization with the glycoprotein-(gp)-130 is induced. This heterotrimeric complex then mediates IL-6-signalling pathways: MAPK kinases and JAK/STAT pathways. Regarding to IL-6 functions, this cytokine is a vital inducer of acute phase proteins like serum amyloid A or C-reactive protein (CRP). Also, it is known that in combination with TGF-β, IL-6 favours Th17 differentiation. Moreover, IL-6 is implicated in the differentiation of T cells into Th2 lymphocytes. Due to its

pleiotropic activity, dysregulated or excessive production of IL-6 leads to a worsening of several diseases, among rheumatoid arthritis, systemic lupus erythematosus, sepsis or COVID-19 (Galil et al., 2015; Jekarl et al., 2013; Rincon, 2012). The development of Tocilizumab, a humanized monoclonal antibody that blocks the interactions of IL-6 to both cell surface IL-6R and sIL-6R, improved exacerbated inflammation of these diseases constituting an efficacy therapy of inflammatory and autoimmune diseases (Emery et al., 2019; Salama et al., 2021; Tanaka et al., 2016).

IL-8 is a proinflammatory and chemoattractant cytokine which signals via binding to the G protein-coupled receptors cysteine-X-cysteine chemokine receptor (CXCR) 1 and CXCR2. In response to infection or tissue injury, macrophages, endothelial cells and epithelial cells produce IL-8. Once localized to the damaged site, IL-8 promotes the recruitment of neutrophils and the release of neutrophil extracellular traps and activate the angiogenesis. Hence, IL-8 also serves to both resolve the inflammatory response and promote healing. However, these two activities foster its stimulatory effect on tumour growth. Tumour cells express IL-8 in order to recruits neutrophils and M2 macrophages that modify the composition of the tumour microenvironment to an immunosuppressive milieu (Cao et al., 2016; Fousek et al., 2021).

Interleukin-15 is a proinflammatory cytokine which belongs to the four α-helix family of cytokines that also includes IL-2, IL-4, IL-7, IL-9 and IL-21. It is expressed in many hematopoietic and non-hematopoietic cells, although the patterns of mature protein and messenger RNA (mRNA) levels differs greatly, suggesting a tightly control of cytokine production. Its synthesis is induced by a variety of stimulus, INF-γ, LPS, ultraviolet irradiation, viruses including herpes simplex virus and fungal and bacterial agents, such as *Escherichia coli*, *Staphylococcus aureus* and *Candida albicans.* IL-15 is widely known as a master regulator of innate and adaptative responses. Between the activities of this pleiotropic cytokine are activation and expansion of NK cells, $CD8^+$ effector memory cells, NKT cells and T lymphocytes. Also, IL-15 inhibits apoptotic cell death in myeloid cells, such as neutrophils, and is critical for the functional maturation of both macrophages and DC cells. Due to that functionality, IL-15 has been used as an adjuvant of many vaccines against infectious diseases, like influenza virus, and as a therapeutic tool against tumours, being considered a key cytokine for immunotherapy (Croce et al., 2012; Fiore et al., 2020; Patidar et al., 2016; Perera et al., 2012)

6.3 High-mobility group protein box 1.

HMGB1 is a highly conserved non-histone nuclear protein virtually expressed in all cell and tissues that, similar to IL-1α, has a dual function. Intracellularly, HGMB1 binds to DNA chromatin acting as a transcriptional regulator. Extracellularly, HMGB1 is actively released by non-apoptotic dying cells induced by LPS or INF-γ, constituting an important DAMP during inflammatory processes, or passively secreted by severely stressed or necrotic cells. Once released into the extracellular space, HMGB1 mediates the recruitment and activation of innate immune effector cells, angiogenesis, endothelial cell activation, tissue repair or healing among others. HMGB1 binds to the receptor for advanced glycation end products (RAGE) and/or TLR2 and TLR4. As an alarmin, HMGB1 potentially plays an important role in a widespread diversity of immunologically-mediated conditions that range from sepsis to autoimmunity diseases (Bianchi et al., 2017; Pisetsky et al., 2008; Saïd-Sadier & Ojcius, 2014).

6.4 Acute phase proteins

As explained above, when there is an infection, injury or trauma, there is a rapidly inflammatory response in order to neutralize pathogens and minimize tissue damage. The variety of local and systemic reactions in the host are collectively known as the acute-phase response. This is characterized by fever and an increase of vascular permeability. Also, proinflammatory mediators, such as IL-1β, TNF-α and IL-6, enhance the production by the hepatocytes of plasmatic proteins called acute-phase proteins (APPs). The maximum concentration of APPs is typically reached within 24 hours after infection or injury, and generally decline once there is a recovery from infection and the initial stimulus disappeared. The importance of APPs consists in their capacity to modulate the immune response by activating the complement system. The most studied acute phase proteins are C-reactive protein, procalcitonin (PCT) and serum amyloid P. C-reactive protein binds to phosphorylcholine on microorganisms and enhances phagocytosis by macrophages, complement activation and pathogen's opsonization. Procalcitonin, for its part, is a prohormone of the peptide calcitonin which in basal conditions is produced by the thyroid gland; however, under systemic infections, the hepatocytes produced and secreted it. Several studies have shown that systemic levels of CRP and PCT are elevated in septic patients' serum, so that, both have been suggested as sepsis-related biomarkers for disease severity (Jain et al., 2011; Jekarl et al., 2013; Panico & Nylen, 2013; Pierrakos & Vincent, 2010). However, it is important to stand out that both acute phase proteins are released in an early onset of sepsis and most of the available literature refers to small cohorts of patients. In fact, systematic and meta-analysis

reviews showed controversial results of their ability to differentiate sepsis from other non-infectious causes of a systemic inflammatory response (Hassan et al., 2022; Tang et al., 2007).

7. The inflammasomes

As described above in section 5.5 of this Thesis, inflammasomes are multiprotein complexes whose oligomerization occurs in response of a variety of physiological and pathogenic stimulus (infections, ionic imbalance, and mitochondrial dysfunction), that control immune response and coordinate host defence against pathogens and tissue injury by the activation of inflammatory caspases (Martinon et al., 2002).

7.1 Inflammasome signal transduction: adaptor ASC

Canonical inflammasomes (like NLRP3 and AIM2) consist of a sensor protein (NLR, ALR or pyrin), an enzymatic component (caspase-1) and a common adaptor protein known as apoptosis-associated speck-like protein containing a CARD domain (ASC).

ASC is a cytosolic soluble protein that contains two death-fold domains, a PYD domain and a CARD domain. Recognition of specific stimuli (PAMPs or DAMPs) by the inflammasome sensor (NLR, ALR or pyrin) results in its activation. Upon activation, several molecules of the inflammasome sensors oligomerize and recruit ASC via electrostatic and hydrophobic PYD-PYD homotypic interactions. Then, ASC^{PYD} domain recruits and interacts with other ASC molecules polymerizing in a prion-like fashion to form α-helical filaments (Cai et al., 2014; Lu et al., 2014). In these filaments, the ASC^{CARD} domain is exposed to the external side, connecting with other ASC filaments and forming a clustered structure called ASC speck or pyroptosome. The CARD domains in the ASC speck facilitate the recruitment of pro-caspase-1 via CARD-CARD interaction, inducing its dimerization, autoproteolysis and activation (Ball et al., 2020; Boucher et al., 2018). Active caspase-1 is then able to process the proinflammatory cytokines (pro-IL-1β and pro-IL-18) and induces their release through gasdermin D plasma membrane pores and pyroptotic cell death (Broz et al., 2020).

On the contrary, CARD-containing inflammasome sensors (as NLRC4 and NLRP1) are able to signal without the initial recruitment of adaptor ASC, directly recruiting (via CARD-CARD interaction) and activating pro-caspase-1. However, these inflammasome sensors can also recruit ASC via CARD-CARD interactions and form ASC specks to amplify caspase-1 activation (Hoss et al., 2017; Sharma & Kanneganti, 2016).

NLRC4, Pyrin and NLRP3 inflammasomes are central for this Thesis, so they will be described in more detail in Sections 7.3, 7.4 and 7.5 of the Introduction, respectively.

7.2 Inflammasome effector mechanisms

Upon activation, caspase-1 drives at least two proinflammatory responses. First of all, this enzyme cleavage pro-IL-1β and pro-IL-18 proinflammatory cytokines to their mature bioactive forms, which orchestrate immune responses and moderate adaptative immunity. Secondly, caspase-1 activation yields a necrotic cell death called pyroptosis (Dinarello, 2018).

In 2015, Feng Shao and Vishva Dixit discovered that the protein gasdermin-D (GSDMD) was a substrate of inflammatory-activated caspases, necessary for pyroptosis (Ding et al., 2016; Kayagaki et al., 2015; Sborgi et al., 2016). Importantly, there are other caspases (caspase-4/5 in human and caspase-11 in mice) that sense LPS through guanylate-binding proteins (GBPs), and independently of inflammasome activation pathways also cleavage GSDMD. This is known as the non-canonical inflammasome pathway (Hagar et al., 2013; Kayagaki et al., 2013; Meunier et al., 2014).

Under homeostatic conditions, full-length gasdermin D consists of an N-terminal domain, the cytotoxic part of the protein, and a C-terminal domain which serves as an inhibitory domain that keeps $GSDMD^{NT}$ inactive, both connected with a linker. When caspases cleavage GSDMD within its central linker, the N-terminal domain binds to negatively charged lipids of the membranes (e.g., cardiolipin and phosphoinositides) integrate into the membrane and form oligomeric pores. GSDMD pores allow the release of molecules smaller than the inner diameter of the pore (around of 215 Å and 20 nm), such as IL-1β and IL-18 (Evavold et al., 2018; Xia et al., 2021). Calcium influx through GSDMD pores can activate the endosomal sorting complexes required for transport (ESCRT) machinery to initiate repair of the damaged membranes (Rühl et al., 2018). If that repair is not efficient, pyroptotic cell death continues. Until a few years ago, it was assumed that after plasma membrane pore formation, the plasma membrane rupture and cell lysis was a passive process caused by water influx through the pores, an increase in osmotic pressure and osmotic lysis. However, recently, Kayagaki et al., found that PMR is executed by ninjurin-1 (NINJ-1) protein. NINJ-1 is a 16-kDa plasma membrane protein that has two transmembrane regions with both termini exposed to the surface cell. During cell lysis, NINJ1 monomers oligomerize into amphipathic filaments that rupture the plasma membrane thereby releasing intracellular contents. In fact, inhibition of NINJ1 by anti-NINJ1 monoclonal antibody or using glycine blocks NINJ1 oligomerization, preventing plasma membrane rupture (Borges et al., 2022;

Kayagaki et al., 2021, 2023) (**Figure 2**). Pyroptosis release cytosolic contents as the alarmins HMGB1 and galectin-3, lactate dehydrogenase (LDH), oligomeric inflammasomes or mitochondrial DNA, which can all act as danger signals (Baroja-Mazo et al., 2014; De Torre-Minguela et al., 2016; Franklin et al., 2014).

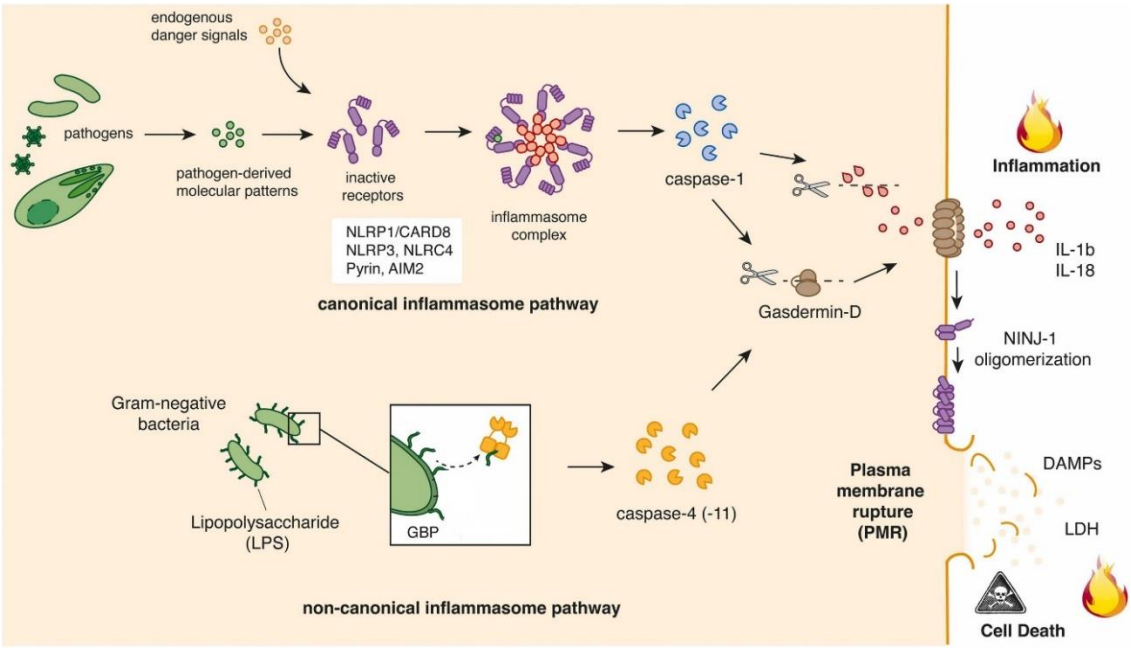

Figure 2. Role of GSDMD and NINJ1 in canonical and non-canonical inflammasome activation. In canonical inflammasome pathway, detection of pathogen-associated molecular patterns and endogenous danger signals initiates the assembly of inflammasome complexes which acts as an activation platform for caspase-1. Caspase-1 processes the pro-IL-1β and pro-IL-18 to their mature form. The non-canonical inflammasome pathway results in the activation of caspase-4 in human and caspase-11 in mice via guanylate-binding proteins (GBP) sensing of lipopolysaccharide (LPS) from Gram-negative bacteria. The activated caspases then cleave GSDMD, releasing its cytotoxic N-terminal domain which forms plasma membranes pores through which mature proinflammatory cytokines are released. GSDMD pore formation initiates the oligomerization of Ninjurin-1 into filaments which support plasma membrane rupture. Image adapted from (Broz, 2023).

Of note, GSDMD is not the only member of gasdermin family that can be processed by an inflammatory caspase. Gasdermin-D belongs to a highly conserved family composed by six members (GSDM-A/E) and Pejvakin (PJVK) (Angosto-Bazarra et al., 2022). With the exception of PJVK, gasdermin family members are cell death effectors defined by their N-terminal domain. GSDME can be cleavage and activated by caspase-3, causing pyroptosis or inducing secondary necrosis after apoptotic cell death (Rogers et al., 2017; Wang et al., 2017). It also has been suggested that caspase-8 can process GSDMD (Orning et al., 2018; Sarhan et al., 2018). Caspase-1 and granzyme A are in charge of GSDMB cleavage (Zhou et al., 2020), whereas GSDMA could be proteolyzed by the streptococcal pyrogenic exotoxin B (Deng et al., 2022). Therefore, it is now recognized that pyroptosis comprises a

repertoire of pathways that finalizes with cell lysis but, expands beyond GSDMD and the caspase family (Broz et al., 2020).

7.3 NLRC4 inflammasome

The NAIP family receptors, as explained in Introduction's section 5.5 of this Thesis, is a NLR family structurally characterized by containing at the N-terminal three BIR domains, a central NBD domain (composed by HD1, WDH and HD2 regions) and a LRR domain in the C-terminal. On the other hand, NLRC4 shares the domain organization of NAIPs but in the N-terminal it contains a CARD domain (**Figure 3A**). NAIP receptor family recognizes specific Gram-negative bacterial ligands. This ligand specificity depends on several largely α-helical domains associated with the NBD domain (Tenthorey et al., 2014). Concretely, mouse NAIP2 senses type III secretion system (T3SS) inner rod proteins, such as Prgj protein from *Salmonella*; mouse NAIP5 and NAIP6 recognize flagellin proteins of *Salmonella* and *Legionella* (Kofoed et al., 2012; Yue Zhao et al., 2011); and mouse NAIP1 senses needle proteins. In human, there is only one NAIP receptor which is able to respond to all three ligands (Yang et al., 2013). The pathogens deliver these virulence factors into the host cell cytoplasm upon infection.

Crystal structure of inactive monomeric NLRC4 showed that its LRR domain is curved, occluding the NBD domain and acting as an autoinhibitory domain (Hu et al., 2013). Recently, it has shown that ligand binding of NAIP5 with flagellin, induce a conformational change of WHD-HD2-LRR regions towards the active NAIP5 conformation (Paidimuddala et al., 2023). Once NAIPs are activated, they initiate an inflammatory response through the NAIP-NLRC4 inflammasome pathway. In deep, one ligand-bound NAIP uses it nucleating surface to interact with NLRC4. This interaction forces in NLRC4 a roughly 90 degrees rotation of the WDH-HD2-LRR domains, overcoming NLRC4 auto-inhibition. The activated NLRC4 recruits and activates nine new monomers (ten NLRC4 molecules in total) through its newly exposed nucleating surface, consequently forming twisted structures, wheel-like (Hu et al., 2015; Zhang et al., 2015) or spiral structures (Diebolder et al., 2015) (**Figure 3B**).

The oligomerization of NLRC4 enables the recruitment, via CARD-CARD interactions, of pro-caspase-1 molecules, triggering its dimerization, autoproteolysis and self-induced activation. The involvement of adaptor ASC in this inflammasome is unclear. Some studies revealed that in response to the intracellular pathogen *Salmonella typhimurium*, caspase-1 activation after NLRC4 oligomerization requires the ASC adaptor (Mariathasan et al., 2004); whereas others considered that ASC is dispensable for NLRC4-dependent caspase-1 activation (Case et al., 2009). Also, NLRC4 inflammasome is able to recruit and

activate caspase-8 in response to *Salmonella* infection independently on caspase-1 and GSDMD, thereby preventing pyroptosis and resulting in apoptotic cell death (Mascarenhas et al., 2017).

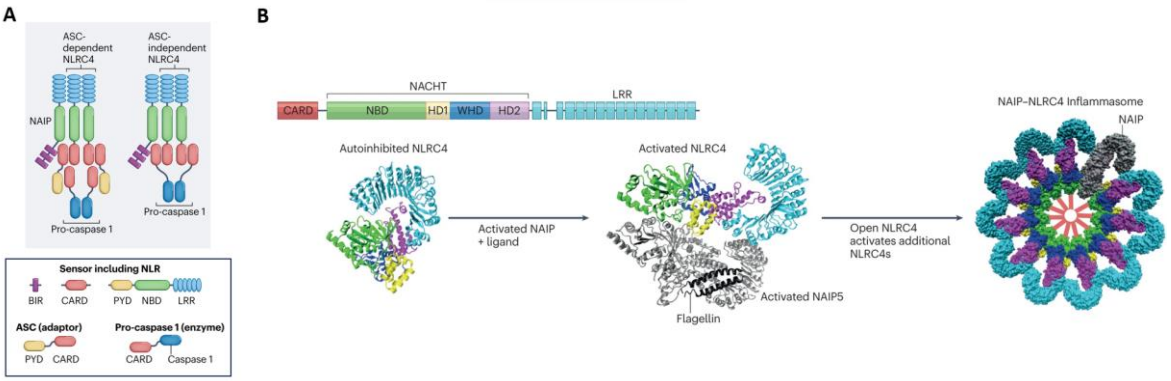

Figure 3. Schematic representation of NAIP/NLRC4 domain organization and activation. (**A**) NLRC4 inflammasome detects bacterial proteins via neuronal apoptosis inhibitory proteins (NAIPs) and can assemble an inflammasome in the presence or absence of ASC adaptor protein. (**B**) In left, crystal structure of autoinhibited NLRC4 (Protein Data Bank (PDB) 4KXF; adapted from (Hu et al., 2013)). In the middle, activated NAIP5 (in silver colour) with bound flagellin (in black colour) initiates a conformational change in NLRC4 (PDB 6b5b; adapted from (Tenthorey et al., 2014)). Finally, crystallographic structure of NAIP-NLRC4 inflammasome (PDB 3JBL; adapted from (Liman Zhang et al., 2015)). Colour coding for domains is replicated in the **A** and **B** structural depictions. Image adapted from (Chou et al., 2023).

7.4 Pyrin inflammasome

Human Pyrin protein, encoded by the *MEFV* gene, is an inflammasome composed by five main domains (from N-terminal to C-terminal): PYD domain, a phosphorylated linker domain (PLD) with connect PYD to B-box domain (which mediate protein-protein interactions), the central helical scaffold (CHS) or coiled-coiled domain (necessary for the dimerization of Pyrin), and the B30.2 domain (which functions are still enigmatic) (Mariathasan & Monack, 2007; Weinert et al., 2009). As most inflammasome sensors, Pyrin PYD interacts with the adaptor ASC to promote inflammasome activation. In fact, each PYD domain could recruit simultaneously up to three molecules of ASC PYDs (Vajjhala et al., 2014). At steady state, Pyrin inflammasome is in a autoinhibited stated due to intramolecular interactions between its PYD and B-box domains (Yu et al., 2007).

To be activated, Pyrin acts a sensor of the impairment of RhoA subfamily GTPases activity, implicated in actin cytoskeleton dynamics, that can results from either RhoA direct modifications, such as glycosylation or deamidation, or RhoA sequestration into cytosol (Xu et al., 2014). There have been described different RhoA inhibiting toxins that activated the pyrin inflammasome, including TcdA and TcdB from *Clostridium difficile*, VopS from *Vibrio*

parahaemolyticus, C3 from from *Clostridium botulinum*, YopE and YopT from *Yersinia species* and TecA from *Burkholderia cenocepacia* (extendedly reviewed in (Jamilloux et al., 2018).

Specifically, the kinases PKN-1/2, direct effectors of RhoA, phosphorylate Pyrin on two serine (S) residues (S208 and S242 in human). Consequently, phosphorylated Pyrin interacts with chaperone proteins from the 14-3-3 family that sequester it away from ASC. By different mechanisms, the virulence factors inhibit RhoA GTPases and decrease PKN-1/2 activity, leading to dephosphorylation of Pyrin and its release from 14-3-3 proteins (Masters et al., 2016; Park et al., 2016). However, Pyrin dephosphorylation is not sufficient to trigger the full inflammasome activation. The following recruitment and oligomerization of Pyrin and ASC it is mechanistically poorly understood. Some researchers suggest that microtubule-dependent mechanisms downstream of this dephosphorylation step are implicated at a late stage of inflammasome activation cascade. Indeed, colchicine, a drug that depolymerizes microtubules, blocks Pyrin activation by TcdB downstream of its dephosphorylation (Gorp et al., 2016). Furthermore, the histone deacetylase HDAC6 is a dynein adaptor indispensable for the microtubule transport and assembly of Pyrin (and NLRP3) inflammasomes at the microtubule organizing centre (MTOC). Chemical or genetic inhibition of *HDAC6* impairs Pyrin inflammasome activation, thereby suggesting that microtubule-mediated transport of Pyrin/ASC complex is necessary for the assemble of Pyrin inflammasome (**Figure 4**) (Magupalli et al., 2020).

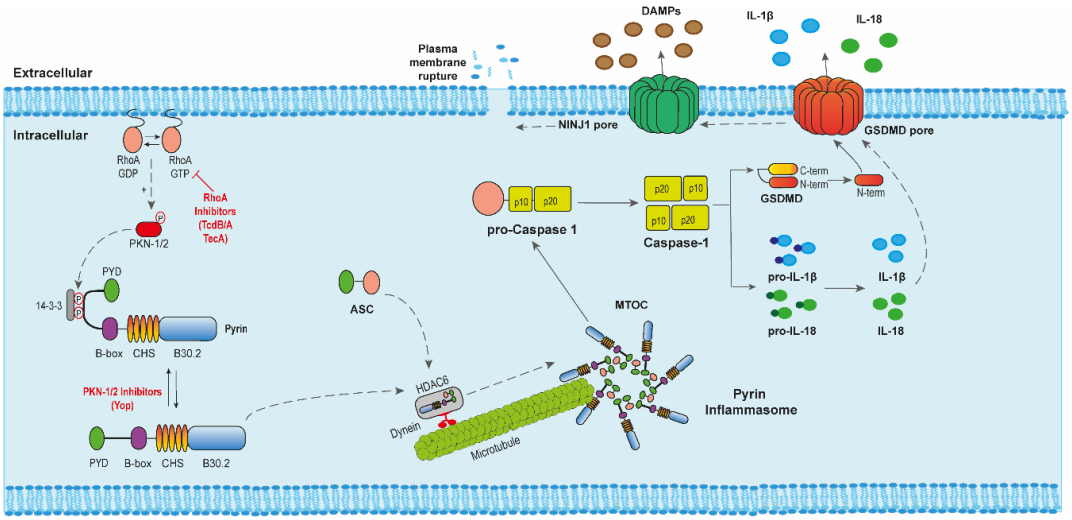

Figure 4. Pyrin inflammasome activation mechanism. Virulence bacterial factors (TcdB/A, Yop or TecA) by different mechanisms inhibit RhoA GTPases and PKN-1/2 kinases, leading to the dephosphorylation of Pyrin and its dissociation of 14-3-3 chaperones. The formation of an ASC speck in the Microtubule Organization Centre (MTOC) may require the transport of Pyrin/ASC complex through a polymerized microtubule by HDAC6 and dynein. Active inflammasome leads to caspase-1 dimerization and activation, cleavage of Gasdermin D (GSDMD) and proinflammatory cytokines, with the consequent gasdermin D pore formation, pyroptosis cell death, Ninjurin-1 (NINJ1) oligomerization and subsequent plasma membrane rupture.

7.5 NLRP3 inflammasome

The NLRP3 inflammasome is an immunological sensor that detect cellular stress, cell membrane damage and pathogen invasion. It is constitutively expressed in the majority of the innate immune cells, including cells of the myeloid lineage, but also in barriers cells and neurons. It is linked to many human diseases, counting inflammatory diseases, metabolic disorders, various cancers and disorders related to nervous system, e.g., as sepsis (Alarcón-Vila et al., 2020) or Alzheimer (Liu et al., 2020). Gain-of-function mutations in NLRP3 cause the dominantly inherited auto-inflammatory disease known as CAPS (Hoffman et al., 2001). NLRP3 is considered to form the most promiscuous nflammasome, as it can be activated by a large number of triggers. In the following sections of this Thesis, it will be explained in detail the NLRP3 canonical and non-canonical activation pathways, its structure and oligomerization process.

According to NLRP3 structure, it comprises a N-terminal PYD domain, a centrally located NBD-containing ATPase domain called NACHT (which includes FISNA (fish-specific NACHT-associated domain), HD1, WHD and HD2 domains) and a C-terminal LRR that consists of 12 repeats.

7.5.1 Canonical and non-canonical NLRP3 activation

The canonical NLRP3 inflammasome activation is a two-step process. The first signal, or priming, is typically provided by the recognition of IL-1β and TNF-α cytokines or PAMPs, which induce the expression of NLRP3 and pro-IL-1β (Bauernfeind et al., 2009; Franchi et al., 2009). Also, during the priming step, NLRP3 suffers different post-translational modifications (PTMs) in order to stabilize it in an inactive but signal-competent state. Multiple PTMs have been described for NLRP3, including ubiquitination, phosphorylation, and sumoylation (extendedly reviewed in (Gritsenko et al., 2020; McKee et al., 2021; Swanson et al., 2019).

The second signal, or activation, is provided by a versatile company of triggers (PAMPs, DAMPs and particulate matter) that include extracellular ATP, bacterial toxins such as nigericin, particulates like cholesterol crystals, amyloids, acid urid crystals, silica and some drugs such as imiquimod (Swanson et al., 2019). The chemical and structural diversity of NLRP3 triggers suggest that NLRP3 inflammasome sense a common cellular signalling instead of the direct binding of these stimuli to NLRP3. Multiple upstream processes are though to activate NLRP3, including an ion flux model, organelle dysfunction (lysosomal

damage, mitochondrial disruption and *trans*-Golgi disassembly) and metabolic changes (**Figure 5**).

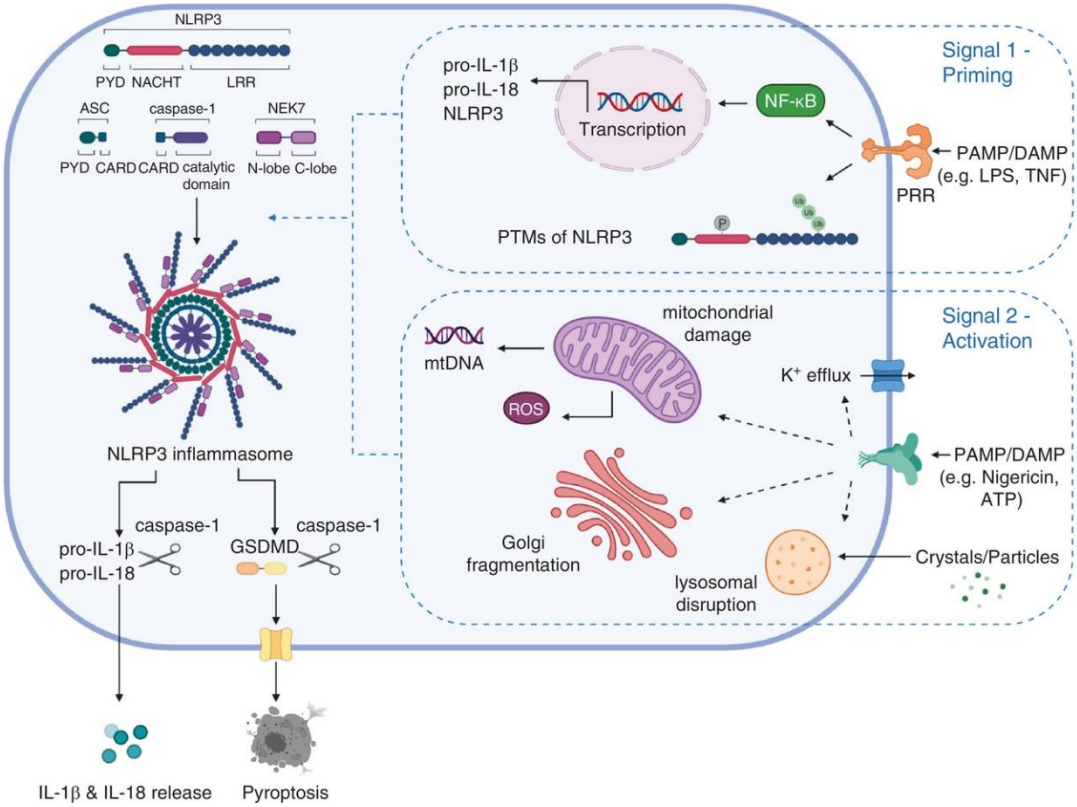

Figure 5. NLRP3 inflammasome priming and canonical activation. Priming stimuli (first signal) involves binding of PAMPs and DAMPs, such as LPS, IL-1β and TNF-α, to their pattern recognition receptors (PRRs), driving NF-κB-dependent expression of NLRP3, pro-IL-18 and pro-IL-1β. Also, priming implies post-translational modifications (PTMs) of NLRP3 to facilitate its further activation with the second signal. PAMPs and DAMPs, like nigericin and extracellular ATP respectively and crystal/particles activate NLRP3. Different types of NLRP3 stimuli trigger different intracellular events, including lysosomal disruption, mitochondrial damage (with the following release of reactive oxygen species (ROS) and mitochondrial DNA (mtDNA)), K^+ efflux and the dispersion of the *trans*-Golgi network. Following canonical priming and stimuli, activated NLRP3 form the inflammasome complex with ASC, pro-caspase-1 and NEK7. Caspase-1 is then activated, cleaving its effector substrates to their mature form, pro-IL-1β, pro-IL-18 and GSDMD. Mature cytokines are released from the cell through gasdermin D pores, which leads to pyroptosis cell death. Image obtained from (McKee & Coll, 2020).

The efflux of potassium (K^+) is a cellular event induced by almost all NLRP3-activating stimuli (Muñoz-Planillo et al., 2013). However, it may not be an absolute requirement as certain NLRP3 triggers, such as imiquimod, can activate NLRP3 inflammasome independently of K^+ efflux (Groß et al., 2016). Nigericin, a K^+ ionophore, and extracellular ATP mediated the activation of P2X purinoceptor 7 (P2X7R), which promote calcium and sodium influx and coordinate the K^+ efflux via the K^+ channel two-pore domain weak inwardly rectifying K+ channel 2 (TWIK2) (Di et al., 2018; Perregaux & Gabel, 1994). A recent study showed that low intracellular K^+ concentration induce a stable conformational change in the inactive NLRP3, promoting an open conformation, facilitated by NLRP3 FISNA domain and

flexible linker located between the PYD and FISNA domains (Tapia-Abellán et al., 2021). Also, decreased levels of cytosolic K^+ cause changes in the structure of the ASC speck that make ASC^{CARD} domains more accessible to enhance the recruitment of pro-caspase-1^{CARD} domain (Marín-Sánchez et al., 2023).

NLRP3 inflammasome is also activated by sensing organelle dysfunctions. Lysosomal damage and rupture, caused by phagocytosis of particulates such as silica, asbestos, uric acid or amyloid-β among others, induce NLRP3 inflammasome activation via K^+ efflux (Halle et al., 2008; Hornung et al., 2008). Also, the release of lysosomal cathepsin into the cytoplasm has been suggested to contribute to this ion efflux (Orlowski et al., 2015). In the same way, the mitochondrial dysfunction and the subsequent mitochondrial reactive oxygen species production and release have an emerging role in NLRP3 inflammasome activation (Dagvadorj et al., 2021; Holley & Schroder, 2020). In fact, ATP-induced mitochondrial damage leads to the release of oxidized mitochondrial DNA (mtDNA) that can promote NLRP3 activation (Shimada et al., 2012). The rapid response of NLRP3 to mitochondrial damage might in part be explained by the fact that, upon stimulation, NLRP3 change its localization, from cytoplasmatic or the endoplasmic reticulum to the mitochondria-associated endoplasmic reticulum membranes. This translocation appears to be mediated by the proteins cardiolipin, mitofusin 2 and mitochondrial antiviral signalling (MAVS) (Ichinohe et al., 2013; Iyer et al., 2013; Subramanian et al., 2013). In addition to mitochondria, Golgi apparatus provides a docking platform for NLRP3 inflammasome assemble. Recent studies showed that NLRP3 stimuli cause disassembly and dispersion of the *trans*-Golgi network (TGN) and that the recruitment of NLRP3 to the dispersed TGN is mediated by phosphatidylinositol 4-phosphate (PtdIns4P) vesicles (Chen & Chen, 2018). Furthermore, NLRP3-activating stimuli impaired retrograde vesicular trafficking of endosomes to the TGN, endosome recycling and endosome-to-lysosome trafficking, leading to the accumulation of PtdIns4P in endosomes (Lee et al., 2023; Zhang et al., 2023). These two recent studies suggested that NLRP3 can also sense endosomal dysfunction and that NLRP3 oligomerization and inflammasome formation could occur on endosomes.

At last, several studies suggest complex regulation of the NLRP3 inflammasome by intertwining metabolic pathways (glycolysis, tricarboxylic acid cycle and fatty acid metabolism) and metabolic reprogramming (extendedly reviewed in (Swanson et al., 2019; Xu & Núñez, 2023).

Once NLRP3 has sensed the second signal, NLRP3 was observed to be transported to microtubule organizing centre via microtubules where it can interact with a serine/threonine kinase contributing to mitosis, NIMA-related kinase 7 (NEK7), through multiple direct

binding where the LRR domain might be particularly important (Y. He et al., 2016; H. Shi et al., 2016). Cyro-electron microscopy of PYD-deleted-ADP-bound human NLRP3 in complex with a dimer of NEK7 showed that NEK-NLRP3 interactions forced NLRP3 into a semi-activated state but further rearrangement is needed for inflammasome activation (Sharif et al., 2019). Three recent publications revealing the human and mouse cyro-electron microscopy structure of full length inactive NLRP3 in the presence or absence of the NLRP3 inhibitor MCC950 showed that NLRP3 forms inactive oligomeric double-ringed cages trough LRR-LRR domain interactions. On the other hand, PYDs domains are shielded inside the cage, possibly preventing the NLRP3 activation (Andreeva et al., 2021; Hochheiser et al., 2022; Ohto et al., 2022). Xiao et al., reported the cyro-electron microscopy of active NLRP3, NEK7 and ASC, in which NEK7 binds to the LRR domain of NLRP3 disassembling the 'double ring' into a 'single ring' structure where NLRP3 exposed its PYDs. The NLRP3 PYD domains then form a PYD filament seed that recruits ASC PYDs to prompt downstream signalling (Xiao et al., 2023).

Upon activation, NLRP3 assembles and recruits the components to form the inflammasome complex, activating the inflammatory caspases which will process cytokines to form their mature forms and induce the pyroptotic cell death.

7.5.2 Non-canonical NLRP3 activation

On the other hand, the NLRP3 inflammasome can also be activated in a non-canonical pathway, in which mouse caspase-11 and its orthologous caspases-4/5 in human act as sensor of cytosolic LPS (Kayagaki et al., 2011; Shi et al., 2014) or certain endogenous oxidized phospholipids (Chu et al., 2018; Zanoni et al., 2016). In this pathway, extracellular LPS from Gram-negative bacteria activates TLR4 and induced type I interferon response that, together with the complement C3 axis, induces caspase-11 expression (Broz et al., 2012; Napier et al., 2016; Rathinam et al., 2012).

Moreover, pathogenic Gram-negative bacteria release outer membrane vesicles (OMVs), which present several surface antigens as LPS or lipoproteins. OMVs are internalized by macrophages and lysed by recruited guanylate-binding proteins and IRGB10, liberating LPS into the host cytosol (Man et al., 2016; Meunier et al., 2014; Santos et al., 2018). Direct recognition of LPS by caspase-11/4/5 triggers their oligomerization and activation by auto-proteolytic cleavage (Lee et al., 2018). Once activated, these inflammatory caspases cleavage GSDMD and induce pyroptosis cell death (Kayagaki et al., 2015; Shi et al., 2015). However, they cannot process pro-IL-1β. The potassium efflux caused by gasdermin D

pores, in turn, activate NLRP3-caspase-1 canonical inflammasome activation with the consequent maturation of IL-1β and IL-18 (Baker et al., 2015; Yang et al., 2015) (**Figure 6**).

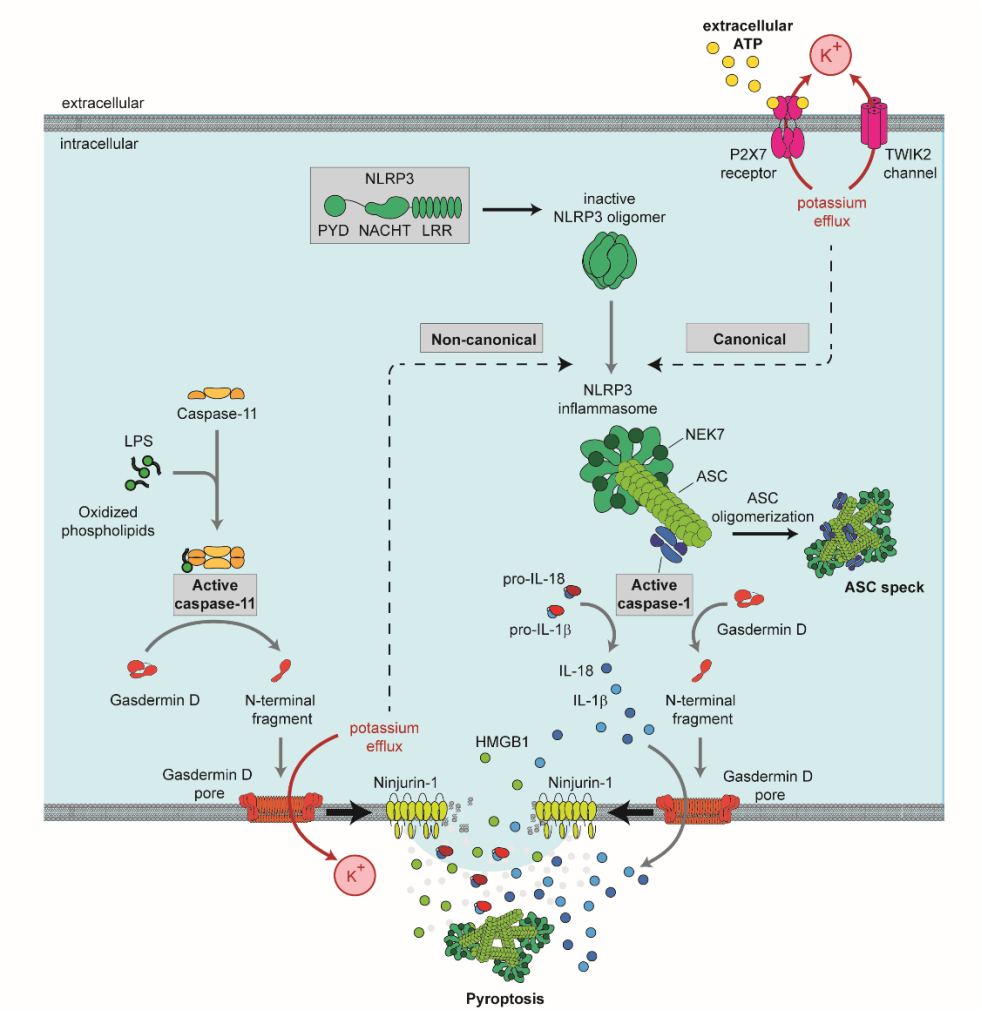

Figure 6. Schematic representation of canonical and non-canonical NLRP3 inflammasome pathways. In the canonical pathway, NLRP3 activation is mediated by K^+ efflux that can be induced by several PAMPs and DAMPs. An active inflammasome complex is then formed by activated NLRP3, ASC, pro-caspase-1 and NEK7. Active caspase-1 cleavages gasdermin D, pro-IL-1β and pro-IL-18, causing membrane pore formation and cytokine release. In the non-canonical pathway, bacterial lipopolysaccharides and host-derived oxidized phospholipids directly activate caspase-11, which cleavages gasdermin D and induce membrane pore formation. The consequent potassium influx activates the NLRP3 inflammasome. Both pathways culminate in Ninjurin-1-mediated lytic cell death via plasma membrane rupture. Image adapted from (Pizzuto et al., 2022).

7.5.3 Therapeutic opportunities targeting the inflammasome pathway

The NLRP3 inflammasome is an attractive drug target due to its implication in the development and pathogenesis of several human diseases. A number of small molecules have been described to target NLRP3 activation directly (extendedly reviewed in (Angosto-Bazarra et al., 2021; Coll et al., 2022). The most well-known inhibitor of NLRP3 is the sulfonylurea-containing compound MCC950 (also known as CRID3 and CP-456773) (Coll et

al., 2015). Concretely, MCC950 blocks NLRP3 ATPase activity and shifts NLRP3 from an active to an active conformation, preventing NLRP3 inflammasome assembly and activation (Coll et al., 2019; Tapia-Abellán et al., 2019). Another sulfonylurea is Glyburide, which blocks potassium transport across ATP-sensitive K^+ channels (Lamkanfi et al., 2009). Several covalent modifiers of the NLRP3 NATCH domain are also described, such as CY-09, that competes with ATP for binding to the Walker A site (Jiang et al., 2017) or Dapansutrile (also called OLT1177), which is a β-sulfonyl nitrile compound that not only reduces ATPase activity of NLRP3 but also, affects NLRP3 priming via affecting the NF-κB pathway (Marchetti et al., 2018). Moreover, others inhibitors like Oridonin or its metabolite derivate 4-octyl-itaconate (4-OI), attenuate NLRP3 interactions with NEK7, then affecting protein-protein interactions (He et al., 2018; Hooftman et al., 2020).

Similarly, small compounds have been developed to target downstream events of NLRP3 activation. Various caspase-1 inhibitors were described, including the peptidomimetic pro-drugs VX-740 and VX-765 (Boxer et al., 2010; Wannamaker et al., 2007). Both reversible inhibitors reached phase II clinical trials for the treatment of epilepsy and psoriasis respectively; however, they were discarded due to concerns around hepatotoxicity (Mangan et al., 2018).

Likewise, numerous efforts are being made to find more effective broader-spectrum therapeutics known as multi-inflammasome inhibitors. It mainly refers to strategies that inhibit the adaptor ASC, as it is a common element of many inflammasomes activation pathways. In 2021, Soriano-Teruel et al., described the first-in-class small molecule inhibitor of ASC, MM01, which disrupts ASC oligomerization and inhibit the downstream signalling (Soriano-Teruel et al., 2021). There are also endogenous inflammasome modulators, termed PYRIN domain-only protein (POPs), that compete with the ASC PYD domain preventing the assembly of ASC-containing inflammasomes and interfering with the ASC recruitment to activated PYR-NLRs (de Almeida et al., 2015; Dorfleutner et al., 2007). The high binding affinity and the ability to disrupt self-association of ASC have demonstrated that these natural modulators are potent suppressors of SARS-CoV-2-induced inflammasome activation (Ahn et al., 2023).

As well, gasdermin D has emerged as a target in the inflammasome pathway, as targeting GSDMD would block pyroptosis cell death and cytokine release. Punicalagin, the complex natural polyphenol, is a potent antioxidant that scavenge ROS preventing pore assembly of N-terminal GSDMD into the plasma membrane (de Torre-Minguela et al., 2021; Evavold et al., 2021; Martín-Sánchez et al., 2016). Additionally, pharmacological agents that directly bind or modify the amino acid cysteine 191 impair GSDMD pore formation, such as

disulfiram or dimethyl fumarate (Deng et al., 2020; Humphries et al., 2020). Importantly, given that these compounds act as covalent cysteine-modifiers, they react to several proteins, preventing off-target effects. Others attempts to limit excessive NLRP3-derived inflammation and cell death, results from anti-NINJ1 monoclonal antibody, blocking its oligomerization and preventing plasma membrane rupture (Kayagaki et al., 2023).

Finally, clinically approved strategies to prevent damaging inflammation from inflammasome activation has been focus on inhibiting IL-1 (Dinarello et al., 2012; 2019). Three different mechanisms of action of approved biologics have demonstrated efficacy in autoinflammatory diseases: IL-1 receptor antagonism (named Anakinra), IL-1 decoy receptors (called Rilonacept) and anti-IL-1 antibodies (termed Canakinumab). Anakinra treatment is based on the potential of IL-1Ra as anti-inflammatory (Arend et al., 1990; Granowitz et al., 1992), Rilonacept functions as a soluble recombinant receptor that binds to IL-1α and IL-1β preventing them from signalling (Economides et al., 2003) and, Canakinumab is a humanized antibody that binds to IL-1β with high affinity (Gram, 2020). Although Canakinumab is the most successful biological therapy to directly target and neutralize IL-1β, these three IL-1 blockers have been remarkably successful treatments for patients with several inflammatory conditions.

8. Autoinflammatory disorders: inflammasomopathies

Autoinflammatory diseases (AIDs) involve group of inflammatory autosomal dominant disorders characterized by fever, rash, joint pain, neutrophilia, an increase in inflammatory markers and absence of infection and neoplasia, as well as no evidence of autoantibody and autoantigen-specific T and B cells. The inflammasomopathies or inflammasomes-related AIDs are a category of monogenic AIDs which are a consequence of inappropriate activation of the inflammasome complex with the consequent exacerbated release of inflammatory cytokines, mainly IL-1β and IL-18 (Hoffman & Broderick, 2016; Nigrovic et al., 2020).

8.1 NLRP3 inflammasome-related diseases

Cryopyrin-associated periodic syndromes denotes the prototype of *NLRP3*-inflammasomopathies. Clinically, CAPS includes three different phenotypes with an increase in the severity: familial cold autoinflammatory syndrome (FCAS), the less severe of the spectrum, Muckle-Wells syndrome (MWS) as an intermediate phenotype, and the most severe

phenotype denoted the chronic infantile neurologic, cutaneous and articular (CINCA) syndrome, also known as NOMID (neonatal-onset multisystem inflammatory disease). Common clinical features include onset during childhood, recurrent fevers, arthralgias, conjunctivitis and urticaria-like skin rash, although other symptoms seem to be characteristic of a specific phenotype, such as AA-type amyloidosis in MWS, cold sensitivity in FCAS and central nervous system and bone disease in CINCA (Booshehri & Hoffman, 2019; de Torre-Minguela et al., 2017).

From a genetic point of view, CAPS are a consequence of germline or de novo heterozygous *gain-of-function* (GoF) variants in *NLRP3* gene. Most severe *NLRP3* pathogenic variants are single amino acids changes located in the NATCH domain (Nigrovic et al., 2020; Tartey & Kanneganti, 2020). To date, more than 150 variants of *NLRP3* gene have been included in Infevers database (de Menthière et al., 2003). Among then, the most frequent is R260W, which is associated to FCAS (Cuisset et al., 2011). Missense substitution T348M and D303N are the most common germline-inherit pathogenic variants and are associated to CINCA (Levy et al., 2015). On the other hand, there are *NLRP3* variants like V198M which has little significance and are considered low penetrance variants (Kuemmerle-Deschner et al., 2017).

CAPS patients have chronic, systemic and local inflammation due to a massive overproduction of IL-1β cytokine. Due to that, the gold-standard treatment used to treat the different phenotypes of CAPS syndromes is IL-1 blockage, with either IL-1β neutralizing drugs (e.g., Canakinumab) or with inhibitors of IL-1 receptor (e.g., Anakinra) (Broderick & Hoffman, 2022; Dinarello, 2019; Levy et al., 2015).

8.2 NLRC4 inflammasome-related diseases

Monoallelic GoF variants in the *NLRC4* gene are associated with a dominantly inherited autoinflammatory disease with a variable spectrum of phenotypes. The disease expressivity ranges from a milder phenotype similar to FCAS (Kitamura et al., 2014), known as FCAS type IV, to macrophage activation syndrome and severe life-threating enterocolitis (Canna, De Jesus, et al., 2014; Romberg et al., 2014). Also, erythematous nodules and cold-induced urticaria have been linked to variants in *NLRC4* (Volker-Touw et al., 2017). Generally, patients exhibit rash, fever, arthritis, hyperferritinemia, anemia and high levels of C-reactive protein (Romberg et al., 2017).

From a genetic point of view, similarly to CAPS, all pathogenic *NLRC4* variants have been identified in or near the central NATCH domain but, despite CAPS patients, the exacerbate activation of NLRC4 inflammasome provokes the persistence of high serum IL-18 levels instead of IL-1β. So that, patients with such alterations highly response and benefit from recombinant human IL-18 blocking therapy (Canna et al., 2017).

8.3 Genetic mosaicism: NLRP3 and NLRC4-somatic variants

The search for the genetic disease aetiology of patients with a classical presentation of NLRP3 and NLRC4 inflammasomopathies without detectable *NLRP3* and *NLRC4* variants by Sanger sequencing has resulted in the identification of patients with somatic mosaicism. This refers to genetic alterations that occurs postzygotic in cells (e.g., myeloid cells), leading to two genetically distinct population of cells within an individual and are not passed to progeny. In some cases, the variant allele fraction is less than 5% in peripheral blood, thus indicate that a small fraction of mutated cells were sufficient to cause systemic symptoms (Nakagawa et al., 2015; Tanaka et al., 2011).

Importantly, studies of variant allele fraction in blood samples of patients with late-onset but otherwise typical NLRP3 CAPS at the onset and approximately ten years ago, showed that the frequency of mutant allele can increase progressively over time, which implies a worsening of the clinical phenotype (Mensa-Vilaro et al., 2016; Rowczenio et al., 2017; Zhou et al., 2015).

Regarding to *NLRC4* genetic mosaicisms, only two children carrying post-zygotic *NLRC4* variants have been reported (Kawasaki et al., 2017; Liang et al., 2017) and two adults whose disease began during adulthood (Ionescu et al., 2022; Wang et al., 2022).

8.4 Pyrin inflammasome-related diseases

Different human inherited disorders have been associated to pathogenic variants in *MEFV* gene, which encoded the Pyrin inflammasome protein: Familial Mediterranean fever (FMF), Pyrin-associated autoinflammation with neutrophilic dermatosis (PAAND) and Pyrin-associated dominant disease (PAAD).

FMF is the most common inherited monogenic autoinflammatory disorder worldwide, highly prevalent in eastern Mediterranean region. FMF patients during childhood typically show self-limited acute febrile attacks (2-3 days long), fatigue, abdominal pain, occa-

sional episodes of erysipelas-like skin rash (every 3-4 weeks, arthritis, leucocytosis (neutrophilia and thrombocythemia) and marked increase of CRP in plasma. The most severe complication concerning FMF is the development of amyloidosis with increase in systemic amyloid A (Ben-Chetrit & Touitou, 2009; Marek-Yagel et al., 2009). The disease is therapeutically-controlled with the daily use of colchicine. From a genetic point of view, the majority of pathogenic mutations are located at the B30.2 domain of the pyrin protein. Interestingly, FMF was classically considered an autosomal recessive condition but, in the last two decades, different evidences of its mode of inheritance considered it as an autosomal-dominant disease (Marek-Yagel et al., 2009; Schnappauf et al., 2019).

PAAND is an inherited autosomal-dominant disorder characterized by childhood-onset, episodes of neutrophilic dermatosis, fever, arthralgia and cystic acne. The pathogenic *MEFV* variants causing PAAND are located in amino acid residues 242-244 and leads to a non-phosphorylated pyrin, thus losing its interaction with 14-3-3 proteins and thereby forming a constitute active inflammasome (Masters et al., 2016).

PAAD is an extremely rare and autosomal-dominant periodic inflammatory disease reported in different families. Affected individuals mainly presented long fever episodes, renal amyloidosis, and colchicine resistance. These phenotypes are caused by heterozygous variants in *MEFV* gene but, the exact pathophysiological mechanism of these variants are still unknown (Aldea et al., 2004; Schnappauf et al., 2019).

9. Sepsis

In 2016, the Third International Consensus for sepsis (Sepsis-3) defined sepsis as a life-threating organ dysfunction caused by a dysregulated host response to infection, being one of the most frequent causes of death in intensive care units (ICUs). About 15% of septic patients develop septic shock, which is now defined as a subset of sepsis in which cellular, circulatory and metabolic dysfunctions are associated with a higher risk of mortality (Rhodes et al., 2017; Singer et al., 2016).

In relation with its aetiology, sepsis can be caused by any infecting organisms (bacteria, fungi and viruses), although *Staphylococcus aureus* (Gram-positive) and *Pseudomonas* species and *Escherichia coli* (Gram-negative) are the most frequently identified organisms (Cecconi et al., 2018).

One of the most important aspects in the management of sepsis is its early recognition and diagnosis. Current guidelines recommend the use of clinical scales, such as SOFA score (Sequential (Sepsis-related) Organ Failure Assessment) or qSOFA (quick SOFA).

SOFA is a scoring system to codify the degree of organ dysfunction (**Table 1**), where score of 2 points or more is associated with a hospital mortality greater than 10%. For its part, qSOFA score system is a stratification tool used for the detection of patients at risk of sepsis likely to have poor outcomes. Patients are considered on a risk if the meet at least two of these criteria: altered level of consciousness (Glasglow Coma scale ≤ 13), systolic blood pressure ≤ 100 mmHg (millimetres of mercury) and respiratory rate ≥ 22 rpm (respirations per minute) (Cecconi et al., 2018; Rello et al., 2017). There are others severity scores, like APACHE II (Acute physiology and chronic health evaluation), which evaluate the risk of death at hospital discharge based on the data collection (physiologic measurements like health status, age or Glasgow Coma scale) during the first 24 hours in the ICU. However, it should be emphasized that others parameters, such as blood lactate concentration or HLA-DR (human leukocyte antigen–DR isotype) measurement, are now also considered to assessing and monitoring organ dysfunctions in critically ill septic patients (Moreno et al., 2023).

Table 1. Description of SOFA scoring system.

SOFA score	0	1	2	3	4
Respiratory system					
PaO_2/FiO_2 (mm Hg)	> 400	< 400	< 300	< 200	< 100
Coagulation					
Platelets ($\times 10^3/\mu L$)	> 150	< 150	< 100	< 50	< 20
Liver					
Bilirubin, mg/dL (µmol/L)	< 1.2 (< 20)	1.2–1.9 (20–32)	2.0–5.9 (33–101)	6.0–11.9 (102–204)	> 12 (204)
Cardiovascular system					
Hypotension	None	MAP < 70 mmHg	Dopamine <5 or dobutamine (any dose)	Dopamine > 5 or epinephrine ≤ 0.1 or norepinephrine	Dopamine > 15 or epinephrine > 0.1 or norepinephrine
Central nervous system					
Glasglow Coma scale	15	13–14	10–12	6–9	< 6
Renal system					
Creatinine, mg/dL (µmol/L)	< 1.2 (< 110)	1.2–1.9 (110–170)	2.0–3.4 (171–299)	3.5–4.9 (300–440)	> 5.0 (> 440)
OR urine output (mL/d)				< 500	< 200

MAP, mean arterial pressure; PaO_2, partial pressure of oxygen; FiO_2, fraction of inspired oxygen.

Regarding its clinical operationalization, sepsis involves cardiac dysfunction, hypotension and decreased effective circulating blood volume. So that, the main managements recommended to prevent organ dysfunctions are: early administration of broad-spectrum antibiotics (within 3 hours of recognizing sepsis and 1 hour if shock is present), oxygen and mechanical ventilation (as septic patients may develop respiratory dysfunction), source control (removal of infected tissue, device or drainage of an abscess) and, for patients with haemodynamic instability (defined by hypotension or elevated lactate concentration), it is

recommended rapid administration of crystalloid bolus, process that it is called hemodynamic resuscitation. If needed, other therapies (e.g., enteral nutrition, corticosteroids) are used (Cecconi et al., 2018; Dugar et al., 2020; Rello et al., 2017).

Despite the advances in medical care and the extensive research developed in the last decades, the incidence of sepsis and the number of sepsis-related deaths are rising (Martin et al., 2003). In search of new therapeutic approaches, several different animal models of sepsis, using high doses of endotoxins (like LPS) or bacteria, have been developed to mimic numerous clinical and laboratory features of human sepsis. In these studies, beneficial effects of inflammation response's blockade (e.g., IL-1β and TNF-α inhibition) were obtained. However, inadequate understanding of the pathophysiological mechanisms of sepsis led to the failure of numerous clinical trials in human. The fact that sepsis involves, not only an exacerbated inflammation but also an immunosuppressive state, make sepsis treatment a complex and multidisciplinary process (Buras et al., 2005; Fink, 2014; Rittirsch et al., 2007).

9.1 Physiopathology of sepsis

In sepsis disease it has been recognized two different responses, hyperinflammatory (proinflammatory) and immunosuppressive (anti-inflammatory), that occur rapidly and concomitantly. The fact that the anti-inflammatory response occurs simultaneously with a persistent exacerbated inflammation implies that the majority of elderly patients with comorbidities fail in the initial sepsis resolution which increase the risk of suffering secondary nosocomial infections, hence increasing long-term mortality (**Figure 7**) (Delano & Ward, 2016; Van Der Poll et al., 2017).

The early dominant hyperinflammatory phase is clinically characterized by shock and fever. On the onset of sepsis, the innate immune is strongly activated by PAMPs and DAMPs which, as explained previously, induce the transcription of proinflammatory genes, activate inflammatory signalling pathways and promote the oligomerization and activation of inflammasomes like NLRP3. These results in a persistent and severe inflammatory response characterized by an exacerbated systemic release of cytokines such as IL-1β, TNF-α, IL-6, INF-γ and IL-17, collectively known as "cytokine storm". This cytokine release, together with other chemokines and factors like HMGB1, PCT or CRP, induce the activation of the complement system, the coagulation system and the vascular endothelium, thus inducing tissue damage and organ dysfunction (Guo et al., 2017; Ljungström et al., 2017; Rittirsch et al., 2008; Schulte et al., 2013). Moreover, during the inflammatory response of sepsis, macrophages and neutrophils secrete large amounts of ROS and reactive nitrogen

species (RNS) resulting in an overwhelming oxidative stress. Both impair the activity of the nuclear factor erythroid 2-related factor (Nrf2), whose inhibition promotes an overaction of NLRP3 and AIM2 inflammasomes which further amplifies the inflammatory response (Bosmann & Ward, 2013; Hennig et al., 2018; Hurtado-Navarro, Angosto-Bazarra, et al., 2022) and, directly damage the respiratory chain of the mitochondria (Brealey et al., 2002). Also, exacerbated neutrophil extracellular traps formation via neutrophils activation have been shown to facilitate prothrombotic events, contributing to collateral tissue damage (Li et al., 2010).

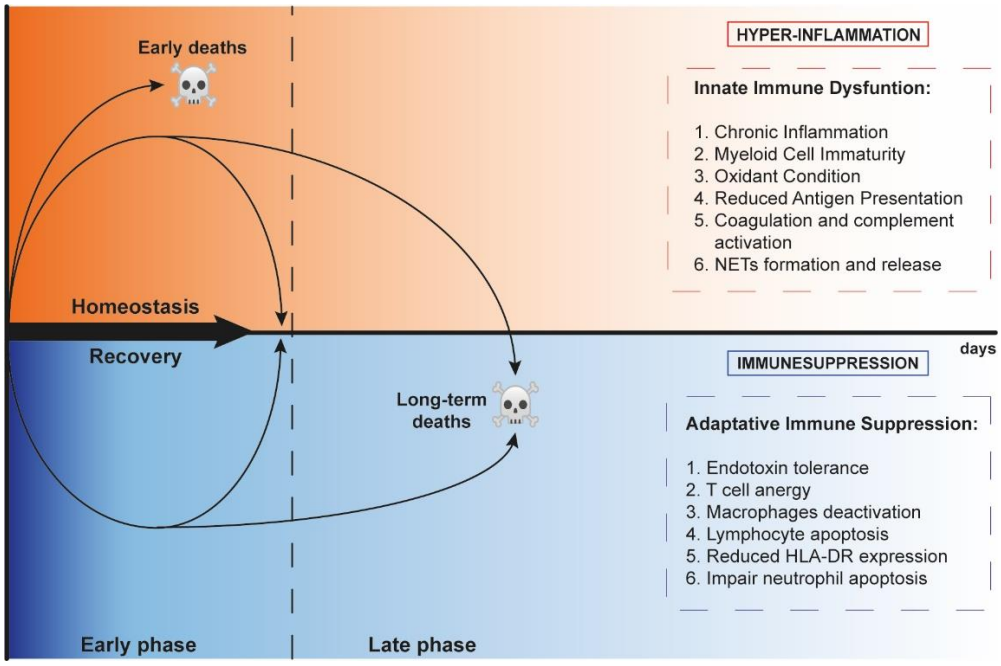

Figure 7. The host immune response during sepsis. At early state of sepsis, inflammatory and anti-inflammatory responses can occur simultaneously, giving to an hyperinflammatory response characterized by a “cytokine storm” and the development of multiple-organ dysfunction and early death. The anti-inflammatory response is prolonged at late state of sepsis, causing an immunosuppressive state that is associated with nosocomial and/or reactivation of latent viral infections and ultimately patient death. Adapted from (Hurtado-Navarro et al., 2023).

To compensate this imbalance response, sepsis involves an immune paralysis state at a later phase. This sepsis-induced immunosuppression involves both innate and adaptative immunity and is characterized by T-cell anergy, lymphocyte exhaustion and apoptosis (above all DCs, NK cell and B/T lymphocytes), diminished cytotoxicity, T cell-Th2 polarization, reduced expression of activating cell surface molecules like HLA-DR in macrophages and monocytes, enhanced expression of negative regulators of TLR signalling, increased secretion of anti-inflammatory cytokines (IL-10, IL-4, TGF-β and IL-1Ra) and epigenetics reprogramming of APCs (Bhan et al., 2016; Cavaillon & Adib-Conquy, 2006; Hotchkiss, 2013; Van Der Poll et al., 2017).

Additionally, leucocytes from patients with severe sepsis also displayed severe defects in their cellular energy metabolism. During the hyperinflammatory phase, leukocytes shift from oxidative phosphorylation to aerobic glycolysis (the Warburg effect), whereas it is reduced in the immunosuppressive phase ("immune-metabolic paralysis"). This effect could activate the NLRP3 inflammasome (Arts et al., 2017; Bar-Or et al., 2018; Cheng et al., 2016)

Neutrophils, for their part, showed a delayed apoptosis which impaired its bacterial clearance capacity and ROS release, a decrease in their chemotactic activity and an impaired kinase activity (Alves-Filho et al., 2010; Hoogendijk et al., 2019).

Monocytes from septic patients not only release proinflammatory cytokines during the "cytokine storm", but also, adopt an immunosuppressive phenotype during immunosuppression (Shalova et al., 2015). Several studies have shown that monocytes and macrophages exhibit a transient state in which they are unable to respond to endotoxin challenges (e.g., LPS), a phenomenon called endotoxic tolerance (Biswas & López-Collazo, 2009; López-Collazo & del Fresno, 2013). This reprogramming is mechanistically mediated by a pathway dependent of hypoxia inducible factor (HIF)-1α (Cubillos-Zapata et al., 2014; Shalova et al., 2015). For instance, septic monocytes present a down-regulation of TLR4, showing a reduced production of IL-1α, IL-1β, TNF-α and IL-6 after an *ex vivo* challenge with LPS (Cavaillon & Adib-Conquy, 2006; Munoz et al., 1991; Santos et al., 2016). Moreover, it has been reported that inflammasomes' components present changes in their gene expression in septic monocytes (Esquerdo et al., 2017). In deed, septic patients' monocytes with an impaired NLRP3 activation, via P2X7 receptor, are associated with a high rate of mortality (Martínez-García et al., 2019).

Overall, these immune alterations are very heterogeneous and results in a chronic state of immune paralysis, multiple-organ dysfunctions and often results in hospital readmission and long-term deaths. So that, it becomes necessary to find novel biomarkers and specific treatments for sepsis that improve this systemic condition.

10. Other inflammatory diseases of interest in this Thesis

10.1 COVID-19

COVID-19 is a viral disease develops after the infection with SARS-CoV-2, an enveloped RNA beta coronavirus, that according to the Johns Hopkins University COVID-19 dashboard, as of 10 March 2023 there have been over 675 million infections and 6.9 million deaths worldwide (coronavirus.jhu.edu/map.html). The diversification of SARS-CoV-2 into

variants with different transmissibility, severity and immune evasion mechanisms, has facilitated its spread globally (Carabelli et al., 2023; Markov et al., 2023).

SARS-CoV-2 principally infects cells predominantly in the respiratory tract causing a complex profile with many plethoric clinical symptoms, including in the severe cases pneumonia with hypoxia, acute respiratory distress syndrome (ARDS), lymphopenia and multisystemic dysfunctions (Vora et al., 2021). Patients with severe COVID-19 was shown to have an impaired activation of monocytes, macrophages and neutrophils (Courjon et al., 2021; Gibellini et al., 2020; Junqueira et al., 2022; Sefik et al., 2022; Veras et al., 2020) which entails abnormal blood levels of several proinflammatory cytokines and chemokines (including ferritin, C-reactive protein, D-dimers, IL-6, IL-15 and TNF-α, etc) (Abers et al., 2021; Del Valle et al., 2020).

This pathogenicity of the disease is associated with NLRP3 inflammasome activation. Several studies have demonstrated that SARS-CoV-2 proteins Orf3a, Orf8 and envelope protein (E) function as conductive transmembrane proteins (also called *viroporins* channels), which induced potassium and calcium influx that finally activate NLRP3 inflammasome (Bertoni et al., 2022; Nieto-Torres et al., 2015; Xu et al., 2022). Also, the nucleocapsid protein (N) could directly interact with NLRP3 to promote its assembly and activation (Pan et al., 2021). However, there are also negative regulatory mechanisms that limit inflammasome activation, for example the E protein or the non-structural proteins 1 and 13 block NLRP3 priming and the N protein inhibits pyroptosis by blocking GSDMD cleavage (Kim et al., 2021; Ma et al., 2021; Yalcinkaya et al., 2021). Therefore, there is a balance between these two signalling systems (positive and negative, hyperinflammatory and immunosuppressive) during NLRP3 inflammasome activation in cases of SARS-CoV-2 infection.

10.2 Multiple sclerosis

Multiple sclerosis is a chronic autoimmune, neurodegenerative and inflammatory disease of the central nervous systems (CNS) characterized by the infiltration into the CNS of autoreactive $CD4^+$ T cells, B cells and macrophages which results in axonal damage, demyelination, neuroinflammation and neurodegeneration. The phenotypical manifestations of the disease are diverse and includes ataxia, cognitive dysfunction, loss of coordination and blindness. The most common clinical form of MS is relapsing-remitting MS (RRMS), characterized by periods of symptoms followed by periods of recovery. RRMS often transitions into secondary progressive MS (SPMS), which is identified by a progres-

sive and irreversible accumulation of neurologic disability. Also, a smaller group of MS patients display a continuous deterioration of neurological functions from the onset of the disease, that it is called primary progressive MS (PPMS) (Charabati et al., 2023; Kuhlmann et al., 2023; Travers & Tsang, 2022).

Although there are no therapies that reverse or prevent completely the development of the MS, many disease-modifying therapies have been approved for MS treatment such as monoclonal antibodies (e.g., natalizumab which prevents immune cell infiltration into CNS or rituximab which selectively depletes B cells), injectable INF-β (that reduces proinflammatory cytokine levels and enhances Th2 cytokine production) and immunomodulatory oral agents (e.g., terifluromide, an inhibitor of the proliferation of activated B and T cells; dimethylfumarate, which shifts the cytokine profile of Th1 to an anti-inflammatory profile; and fingolimod (also known as FTY20), a sphingosine 1-phosphate modulator that inhibit lymphocytes cell migration within lymph nodes to the CNS) (Brinkmann, 2009; Callegari et al., 2021; Mehling et al., 2008; Murúa et al., 2021; Río et al., 2009).

Recent studies showed that the NLRP3 inflammasome plays an important role in the progression of MS by promoting the infiltration of autoreactive cells to the CNS and favouring the differentiation of $CD4^+$ T cells into the proinflammatory Th1 and Th17 subsets (Cui et al., 2022; Shao et al., 2021). Also, some NLRP3 variants, like Q703K, are associated with the disease severity (Soares et al., 2019). Moreover, MS therapies, as INF-β and fingolimod, have shown to block the NLRP3 assembly by down-regulating NLRP3, ASC and caspase-1, promoting and M2 response and reducing the levels of the proinflammatory TNF-α, IL-6 and IL-1β, hence alleviating the neuroinflammation (Guo et al., 2020; Malhotra et al., 2015, 2020; Yao et al., 2019).

10.3 Chronic myelomonocytic leukemia (CMML)

The 5th edition of the World Health Organization Classification of Haematolymphoid Tumours described CMML as a rare, age-related bone marrow derived myeloid malignancy with co-occurrence of pathological and clinical features of both myelodysplastic syndromes (MDS) and myeloproliferative neoplasms (MPN), with a white blood cell (WBC) count < or ≥ $13x10^9$/L, respectively (Arber et al., 2022; Khoury et al., 2022). CMML is characterized by sustained clonal monocytosis, morphologic dysplasia, cytopenia and an increased risk of transformation to a secondary acute myeloid leukemia (sAML). Moreover, acquired abnormal cytogenetics and presence of, at least, one myeloid associated mutation are also part of the diagnostic criteria for CMML (Arber et al., 2022; Itzykson et al., 2018; Lasho & Patnaik, 2021).

Retrospective studies showed that CMML-MP subtype confers an adverse prognosis in comparation to CMML-MD subtype (Patnaik & Lasho, 2020; Such et al., 2013). In fact, CMML-MP is frequently associated with mutations affecting rat sarcoma (RAS) pathway (implicated in cell growth and differentiation) which includes the oncogenes *KRAS* (Kirsten RAS) and *NRAS* (neuroblastoma RAS) (Itzykson et al., 2013; McCubrey et al., 2007). Recently, it was shown that *KRAS* mutations enhances the malignancy of CMML through activation of NLRP3 inflammasome via ROS production, suggesting a novel therapeutic approach to RAS-mutant myeloid malignancies based on NLRP3/IL-1β axis blockade (Hamarsheh et al., 2020).

The importance of the relationship between NLRP3 inflammasome and CMML pathogenesis results in the fact that, actually, the allogeneic hematopoietic stem cell transplantation (allo-HSCT) remains the only treatment recognized as curative for patients with CMML. So that, novel NLRP3 and/or IL-1β inhibitors offers new therapeutical promises in the treatment of myeloid malignancies (Patnaik & Tefferi, 2018; Robin et al., 2022; Sallman & List, 2019).

OBJECTIVES

The following specific aims were formulated for the present Thesis:

1. To characterize the inflammatory markers and the function of the NLRP3 and the Pyrin inflammasomes in septic patients.

2. To compare inflammatory markers between septic and COVID-19 patients.

3. To determine the function of *NLRP3*, *NLRC4* and *MEFV* with pathogenic variants on inflammasome activation.

4. To analyse the activation of the NLRP3 and Pyrin inflammasomes in CMML and MS patients before and after therapeutical treatments.

MATERIAL AND METHODS

1. Buffers and cell culture media

The essential buffers used in this Thesis were phosphate-buffered saline 1x (PBS, from Sigma-Aldrich) and Dulbecco's phosphate-buffered saline (Gibco).

Physiological buffer E-total (Et) was used to stimulate the cells. The composition of Et buffer was composed by: 13 mM D-glucose, 10 mM HEPES, 147 mM NaCl, 1 mM $MgCl_2$, 2 mM $CaCl_2$ and 2 mM KCl. The pH was adjusted to 7.4 at room temperature (RT).

Lysis buffer used to protein extraction was composed by 0.15M NaCl, 2% Triton X-100, 10% of 20mM Tris-NaOH (pH = 8) and 10% of a broad-spectrum cocktail for protease inhibitors (in order to inhibit serine, cysteine, acid proteases and aminopeptidase, from Sigma-Aldrich).

Tris-glycine buffer with or without Sodium-docecyl-sulfate (SDS) used in Western Blot assay were from Bio-Rad and Laemmli buffer 2x (Sigma-Aldrich) was composed by 4% SDS, 20% glycerol, 10% 2-mercaptoethanol, 0.004% bromphenol blue and 0.125 M Tris HCl, pH adjusted to 6.8.

Staining buffer composition (SB) used in flow cytometry samples preparation was PBS 1x, 1% foetal calf serum (FCS, from Cytiva) and 0.1% sodium azide (Sigma-Aldrich). Cell permeabilization buffer (PB), which permeate the membrane allowing the intracellular staining of proteins with antibodies to enter the cell effectively, was composed by PBS 1x, 1% FCS, 0.1% sodium azide and 0.1% saponin (Sigma-Aldrich). In the detection of intracellular ASC-speck formation in whole blood samples, BD FACS lysing/fixation solution was used in order to lyse erythrocytes under gentle hypotonic conditions while preserving and fixing the leucocytes, due to the fluorochrome-labelled antibodies bind specifically to leucocyte surface antigens.

With regards to the cell culture media, human peripheral blood mononuclear cells were cultured in Opti-MEM reduced serum media (Gibco). Whole peripheral blood samples were cultured with complete RPMI 1640 medium (Lonza) containing 10% FCS and 2 mM GlutaMax (Thermo Fisher Scientific). Dulbecco's Modified Eagle Medium:Nutrient Mixture F12 (DMEM:F12 (1:1), from Lonza) supplemented with 10% FCS, 2 mM GlutaMax (Cytiva) and 1% L-glutamine (Cytiva) was used to culture HEK293T cell line.

Cell freezing buffer to maintain viable cells in liquid nitrogen was composed by FCS and 10% dimethilsulphoxide (DMSO, from Sigma-Aldrich).

Macrophage differentiation medium was composed by high glucose DMEM (Biowest), 15% of FCS, 25% L929-cell culture supernatants as source of macrophage colony-stimulating factor (M-CSF), 1% of penicillin and streptomycin (Lonza), and 1% of L-glutamine (Lonza). Macrophage synchronization medium was composed by DMEM medium (Biowest) with 20% of FCS and 1% of penicillin and streptomycin.

2. HEK293T cell culture and transfection

HEK293T cell line (CRL-11268; American Type Culture Collection) was maintained in DMEM:F12 complete medium, as explained above. To seed HEK293T cells, cell culture media was removed using a vacuum pump and then cells were washed with PBS 1x. After washing, 1 ml of trypsin with 0.25% of ethylenediaminetetraacetic acid (EDTA, from Sigma-Aldrich) was added into the centre of the flask and after 3 min of incubation at 37 ºC temperature, 4 ml of fresh DMEM:F12 complete medium was added to inactivate trypsin. Then, the cell suspension was removed from the flask to a conical tube and centrifuged at 433 xg during 5 min; afterwards supernatant was discarded and new medium was added. Cells were counted using an automated cell counter (Countess II FL, from Life Technologies) and cultured on a well-plate and concentration specific for each experimental assay.

Cells were incubated at least 16 hours in a humidified incubator (Fisher Scientific) at 37 ºC with 5% of carbon dioxide (CO_2) to allow for adhesion to the plate before cationic lipid-based transiently transfection using Lipofectamine 2000 (Invitrogen) according the manufacturer's instruction. Briefly, two solutions of 50 µl of Opti-MEM containing a mix of 1 µg of total plasmid DNA (tube A) and 3 µl of Lipofectamine 2000 (tube B) were prepared and incubated 5 min at RT. After this period of time, the volume of DNA tube (A) was added into Lipofectamine 2000 tube (B), mixed gently and incubated 20 min at RT to allow lipid/DNA complexes formation and then added drop by drop to the cells. The plate was swirled gently and incubated at 37 ºC. Typically, fluorescent microscopy, Bioluminiscent Resistance Energy Transfer and flow cytometry assays were done 24 hours after transfection.

3. Human blood samples

All human samples and data from humans included in this Thesis were collected after written informed consent in accordance with the WMA Declaration of Helsinki. Human blood samples were collected and processed following standard operating procedures with appropriate approval of the Research Ethics Committees of the Clinical University Hospital *Virgen de la Arrixaca* (Murcia, Spain), the Clinical University Hospital *Morales Meseguer*

(Murcia, Spain) and the Clinical University Hospital *Vall d'Hebron* (Barcelona, Spain). The samples were stored in the *Biobanco en Red de la Región de Murcia*, BIOBANC-MUR and registered on the National Registry of Biobanks with registration number B.0000859. Whole blood samples were collected in EDTA anticoagulated tubes.

3.1 Patients enrolled in this Thesis

3.1.1 Sepsis

All septic patients enrolled in this Thesis met the definition for sepsis or septic shock that was established at the Sepsis-3 Consensus (Singer et al., 2016). The inclusion criteria for septic patients were (i) patients undergoing an elective primary colorectal surgery where they were diagnosed with intra-abdominal origin sepsis confirmed by exploratory laparotomy (presence of purulent, fecaloid or biliary material discovery in the abdominal cavity, acute cholecystic or peritonitis), (ii) with at least two diagnostic criteria for sepsis (fever or hypothermia; tachycardia; tachypnea, leukocytosis, or leukopenia) and (iii) multiple-organ dysfunction. We excluded patients who (i) were pregnant or (ii) at a paediatrics age (< 12 years old), (iii) were immunocompromised or present immunodeficiencies (including antineoplastic treatments during the month previous to the septic episode), (iv) were terminal oncologic and (v) hematologic neoplastic patients. Also, (vi) patients that had a delay of more than 24 hours from intra-abdominal sepsis diagnosis to surgery, (vii) patients who spent less than 24 hours in the Reanimation Unit and (viii) patients whose infection focus was not clearly specific from abdominal focus, were also excluded. Taking these criteria into account, septic patients' whole blood samples were collected at days 1, 3 and 5 after sepsis onset and development (n = 34). Blood from (n = 15) septic patients were also extracted as hospital discharge, after sepsis recovery.

Surgery controls (n = *36*), were patients undergoing an elective primary colorectal surgery without developing any symptoms of sepsis or septic shock (previously described).

Control donors (n = 34), were considered patients who were disease-free, such as neoplasms, at the time of blood collection. Previous diseases, as well as comorbidities, of these patients were taken into account during the study. Age and gender were statistically analysed in septic patients in comparison with healthy and surgery controls.

3.1.1.1 Clinical determinations

Within the first 24 h of sepsis-onset and hospital admission, several clinical, cellular and biochemical markers of sepsis were determined. PCR, CRP and lactate were detected as molecular markers of acute phase of sepsis. In blood samples, the number of circulating monocytes, lymphocytes, platelets, neutrophils and total leucocytes were analysed. As well as, the concentration of bilirubin, creatinine, urea, haemoglobin, fibrinogen and NT-proBNP (N-terminal brain natriuretic propeptide) were also determined. Clinical scores of severities we calculated as SOFA (three days tracing) and APACHE II (first 24 hours of hospital admission).

3.1.2 COVID-19 disease

Plasma samples of *n* = 208 recovered individuals diagnosticated of SARS-CoV-2 infection (positive reverse transcription polymerase chain reaction (RT-PCR) test, positive serology and/or positive rapid antigen test) were collected in the first days after diagnosis and hospital admission.

Patients were classified into their clinical spectrum of infection in three categories of disease severity (mild, moderate and severe), as described in the National Institutes of Health COVID-19 treatment guidelines at the time of sample and data collection (https://www.covid19treatmentguidelines.nih.gov/). Briefly, mild illness patients were those who (i) have at least one symptom associated with COVID-19 (such as fever, cough, loss of taste and smell, nausea, headache, etc.), (ii) have no shortness of breath, dyspnoea or (iii) oxygen supplementation and (iv) have no abnormal chest imaging. Moderate illness patients were patients satisfying (i) evidence of lower respiratory disease, (ii) an oxygen saturation (SpO_2) ≥ 94% on room air at sea level requiring and, in some cases, (iii) oxygen therapy. Severe illness is attributed to patients who were (i) hospitalized in the Critical Care Unit, (ii) with a respiratory rate of > 24 breaths per minute, (iii) a SpO_2 < 94% on room at sea level, (iv) have a highest level of oxygen therapy required, (v) have bilateral infiltrates of infection, (vi) and who die from respiratory failure caused by COVID-19 disease, septic shock or multiple-organ dysfunction.

Plasma from non-COVID-19 blood donors (*n* = 69) obtained before COVID-19 pandemic were also included in the study as the negative or healthy control group.

3.1.3 Autoinflammatory syndromes

Samples from autoinflammatory syndromes were collected from Hospital Clinic and Vall d'Hebron (Barcelona) and Hospital Virgen Macarena (Sevilla), in case of CAPS patients, and Hospital Virgen de la Arrixaca (Murcia) for FMF diagnosed individuals.

In particular, individuals with CAPS syndrome carrying the NLRP3 R260W variant (*n* = 1), V198M variant (*n* = 6), R488K variant (*n* = 3) and Q703K variant (*n* = 3) were included in this study. Moreover, individuals with the *MEFV* M694I variant in homozygosity (*n* = *4*) were also analysed. CAPS patients were asymptomatic and under therapy by the time blood was extracted and FMF patients were with inactive disease under colchicine or anakinra therapy by the time blood was extracted. Whole blood samples from healthy donors (*n* = *4*) were used as control group.

3.1.4 Multiple sclerosis

Patients with relapsing-remitting multiple sclerosis treated with fingolimod, from the Centre d'Esclerosi Multiple de Catalunya (Cemcat, Barcelona) were included in this Thesis.

Classification of patients into responders and non-responders was performed after one year treatment, following criteria described in (Río et al., 2009). Briefly, responders were patients (i) having no relapses, (ii) no progression on neurologic disability and (iii) no radiologic activity on the 12-month brain MRI (magnetic resonance imaging). Non-responders were patients satisfying at least one of the next criteria: (i) presence of one or more relapses, (ii) presence of ≥ 3 lesions on brain MRI and (iii) increase of 1 or more points in the Expanded Disability Status Scale (EDSS) score over the follow-up period.

Seven responders and five non-responders to fingolimod, either at baseline or after six months of treatment were studied. PBMCs from six donors without MS were also included in the study for comparison purposes.

3.1.5 Chronic myelomonocytic leukemia

This study started with an index patient diagnosed of a high-risk CMML myeloproliferative variant with a *KRAS*^{G12D} mutation from Hospital General Universitario Morales-Meseguer (Murcia). Clinical disease monitoring was done from him diagnosis until his clinical stabilization before and after anakinra treatment, up to HSCT of a haploidentical sibling. During this period of time (July 2020 – August 2021), blood samples were analysed at six time points, before and after anakinra treatment, were performed.

In order to analyse if other patients diagnosed of CMML would have similar biological characteristics in comparison with the index patient, whole blood samples of treatment-free patients with/without mutation in *KRAS*, CMML *KRAS*^{mut} (n = 5) and CMML *KRAS*^{WT} (n = 4), were included in this study.

CMML diagnosticated patients' samples were collected from: Clinical University Hospital *Morales-Meseguer* (Murcia, Spain), *La Fe* University and Polytechnic Hospital (Valencia, Spain); Clinical University Hospital *Valencia* (Valencia, Spain), University Hospital of *Salamanca* (Salamanca, Spain), University Hospital October 12 (Madrid, Spain), Hospital *del Mar*, and University Hospital of *Germans Trias i Pujol* (both located in Barcelona, Spain).

Moreover, samples from controls individuals without CMML (*n* = 9) matched in age and sex with the CMML *KRAS*^{mut} patients were used as controls.

3.2 PBMCs isolation

Peripheral blood mononuclear cells were isolated from whole blood samples using a Ficoll-based gradient separation method (Histopaque-1077, Sigma-Aldrich). Depending on the quantity of whole blood samples (3 to 5 ml or 10 ml), 5 ml or 15 ml of Ficoll with 1,077 g/ml density were added in the bottom of special Falcon tubes SepMate-15 or SepMate-50 respectively, until filling the chamber. These special tubes present two differential chambers connected to each other, preventing the layers from mixing and allowing a higher deceleration during centrifugation process and optimizing the PBMC isolation protocol. Then, whole blood was diluted in 1:1 proportion with warm PBS 1x and carefully was added on the top chamber. Once added, tubes were centrifugated at 1,200 xg during 10 minutes with the brake off and at RT. When centrifugation is performed, four phases are obtained according to their density (**Figure 8**):

- Plasma phase (the top phase).
- The PBMCs and platelets phase, forming a white ring. This was the layer used for the experiment of this Thesis.
- The Ficoll phase, which it is mostly acellular.
- Erythrocytes and polymorphonuclear cells phase, which are in the bottom due to they are in the highest density layer.

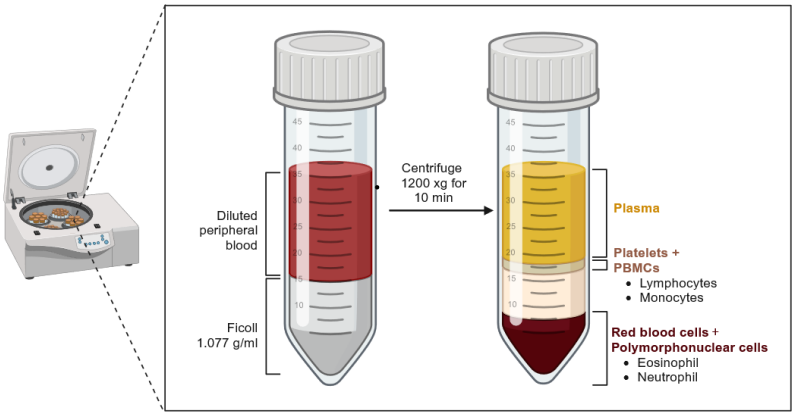

Figure 8. Schematic representation of the different phases of a Ficoll separation system based on density gradients. Four phases based on their density were obtained, from the less dense (plasma) to the densest (PMNs and erythrocytes). Between plasma and Ficoll phase, there are the PBMC cells ring, the layer of interest. Image created with Biorender.com.

After centrifugation, PBMCs and plasma were carefully and individually collected using a sterile Pasteur pipette (Deltalab) and deposited into differential Falcon tubes. Plasma was frozen and stored in the *Biobanco en Red de la Región de Murcia*. Instead, PBMCs were washed with 30 ml of warm sterile PBS 1x and centrifuged at 300 xg during 8 min at RT. Then, supernatant was discarded and PBMCs were suspended on 1 ml of Opti-MEM and were counted in a Bürker counting chamber (Marienfeld) diluting the cells 1:10 in tryplan blue (Sigma-Aldrich) to exclude permeable non-viable cells (death cells are stained). Bürker chamber contains nine quadrants of 1 mm^2 each making a big square. Each large square is subdivided by double lines into sixteen group squares. Three quadrants were counted diagonally in the chamber and the total counted cells were divided into three and multiplied by the chamber dimensions and the trypan blue dilution used, resulting in the number of cells in 1 ml of sample volume. Cells were counted using an inverted phase contrast AE200 microscope (Motic). Isolated and counted PBMCs were seeded on 24-well plates at a density of $5x10^5$ cells in 500 µl of Opti-MEM and the remaining cells were subsequently frozen at – 80ºC (explained in detail in next section).

3.3 PBMCs freezing and thawing

Remaining PBMCs were washed once with PBS 1x and harvested in foetal bovine serum (FBS, from Cytiva) with 10% DMSO at a concentration of 8-10 $x10^6$ cells/ml in a 2 ml cryotube. To achieve slow cooling rates of the cell solution (-1 ºC/minute), the optimal rate for cell preservation, cells were frozen down at -80 ºC in a Mr. Frosty freezing container (Sigma-Aldrich) provided with isopropanol (ITV Reagents, PanReac AppliChem). 24 hours after freezing, cells vials were transferred to -195.8 ºC liquid nitrogen for long-term storage.

In order to defrost the PBMC cells vials, cells were quickly thawed by immersion of the cryotube in a 37 ºC water bath and subsequently, cell culture media was added. Once added, tubes were centrifugated at 300 xg during 5 minutes at RT. Viable cells were enriched by a negative magnetic selection process using the OctoMACS MS separation columns and the dead cell removal kit (both from Miltenyi Biotec) according to manufacturer's recommendations. This procedure recognizes phosphatidylserine, that is translocated from the cytoplasmic face of the plasma membrane to the cell surface during cell death. Briefly, defrosted PBMCs were resuspended in 10 ml warm RPMI with 10% foetal bovine serum and were pelleted by centrifugation at 300 xg for 10 minutes. Up to 10^7 cells were resuspended in 100 µl of dead cell removal microbeads and incubated 15 min at RT. Next, the cells were added to calibrated columns (columns were calibrated with 500 µl of 1x binding buffer) and were washed three times with 500 µl of 1x binding buffer. The final volume of collected unlabelled live-cells (fluorescently propidium iodide negative stained population) was about 2 ml. Cells were then counted using a Bürker counting chamber were suspended and seeded in the specific densities needed by each experimental assay.

3.4 Cell stimulation

Whole peripheral blood and human PBMCs (cell density of 10^6 cells/ml), which were previous isolated using Ficoll, were cultured in RPMI complete media and Opti-MEM reduced serum media respectively at 37 ºC and 5% CO_2. Samples were stimulated with LPS (1.6 µg/ml) for 3 hours in the absence or presence of ATP (3 mM, added in the last 30 minutes of incubation, from Sigma-Aldrich), nigericin (10 µM, added in the last 30 minutes of incubation, from Sigma-Aldrich), TcdB (1 µg/ml, added in the last 1 hour of incubation, from Enzo Life Sciences) and with 4 µg of protective antigen (PA) and 2 µg of flagellin A lethal factor (LFn-FlaA) (here called FlaTox, kindly obtained from Prof. V. Mulero, University of Murcia) during 5 h. In some cases, 10 µM MCC950 (Sigma-Aldrich) was added 15 min before ATP, nigericin or TcdB and maintained during stimulation. In case of PBMCs isolated from auto-inflammatory patients, cells were primed as described previously but, cell cultures were maintained at 37 ºC or at 32 ºC during 3 hours in in a humidified 5% CO_2 incubator. Stimulations were done in 500 µl of final volume for 24-wells plates.

In flow cytometry experiments, ATP and TcdB stimulation's time were reduced to 15 or 30 minutes, respectively, in order to preserve cell viability.

In all experiments, cell supernatants were collected and centrifuged at 12856 xg during 30 seconds and the pellet were discarded. Supernatant was frozen at –80ºC or directly used for ELISA. Cells were lysed with 30 µl of cold lysis-buffer during 30 min at 4ºC

and centrifuged during 10 min at 12856 xg. Supernatant from lysed cells were collected and stored together clarified cell-free supernatants at -80ºC.

4. Bone marrow-derived macrophages (BMDMs)

C57BL/6 background mice with an age between 6 and 12 weeks were maintained under specific pathogen free in ventilated racks, with a constant temperature of 25 ºC, a light-dark cycle of 12 h and free access to sterile food and water.

Mice were euthanized with CO_2 inhalation and the long bones tibia and femur from the two hind paws were dissected. Bone marrow extraction was flushed from the medullar cavity by the irrigation of 20 ml (2.5 ml per bone) of differentiation medium (explained in Material and Methods' section 1) in sterile conditions. The bone marrow suspension was seeded into two p150 Petri dishes (CellStar) and plates were then incubated at 37 ºC with 5% of CO_2.

After two days of bone marrow culture, 20 ml of differentiation medium was added per Petri dish and cells where again incubated at 37 ºC and 5% of CO_2. After six days of bone marrow culture, macrophages were differentiated. Then, supernatant was discarded carefully and cells were washed with PBS sterile solution at 4 ºC during 5 min. In order to let detachment of the cells, BMDMs cells were manually scrapped and cells suspension was centrifuged at 400xg for 5 min. Supernatants were discarded and cells were cultured in 10 ml of synchronization medium. At last, BMDMs were counted and seeded into 12-well plates at a confluence of 10^6 cells per ml and used the following day for experiments.

5. Fluorescence microscopy

Fluorescence microscopy was used for experiment to visualize and analyse the NLRP3 inflammasome puncta formation. Cells were seeded at $3.5x10^5$ cells/ml in a 12-wells plate with 1 ml of completed DMEM:F12 medium and transiently transfected. 24 hours after transfection, cells were washed with PBS 1x and suspended in 1 ml of E-t buffer. Quantification of inflammasome spontaneous puncta distribution was done in 5 fields of view per condition/plasmid transfection and at least from n = 3 independent experiment.

Images were acquired with a Nikon Eclipse Ti microscope equipped with a 20× S Plan Fluor objective (numerical aperture, 0.45), and a digital Sight DS-QiMc camera (Nikon) and 472 nm/520 nm filter set (Semrock), and the NIS-Elements AR software (Nikon). Im-

ages were processed using the imaging processing software ImageJ and the image processing package Fiji (US National Institutes of Health). Contrast and brightness of the images were adjusted to improved data visualization when necessary.

6. Molecular biology: plasmid construction

Different mutations of human NLRP3 were generated by overlapping PCR to introduce a point mutation. As well, all the plasmids generated for being used in this Thesis were double tagged in the amino (N)-terminus with the yellow fluorescent protein (YFP) and in the carboxi (C)-terminus with *Renilla* Luciferase (Luc) using overlapping PCR. All plasmids generated for this work have been deposited in the plasmid repository of the Pelegrín's laboratory.

Site directed mutagenesis by overlap extension was achieved after consecutive PCR reactions run using the following protocol: 98ºC – 30 s, (98ºC – 10 s, 57ºC – 30 s, 72ºC – 2 min) x 15 cycles, 72ºC – 2 min, 4ºC - ∞. In all cases, the Platinum SuperFi high fidelity polymerase (Thermo Fisher Scientific) was used and a couple of specific primers designed (**Table 2**). After these two independent PCR reactions, two PCR amplicons were obtained and their DNA was purified using electrophoresis from a 0.5% agarose gel using the DNeasy gel purification kit (Qiagen) according to the manufacturer's instructions.

The reactions from both PCR were then combined by an overlapping PCR using the same PCR protocol than explained before and the specific combination of primers (**Table 2**) and the the Platinum SuperFi high fidelity polymerase. Then, final PCR fragment was purified using electrophoresis from a 0.5% agarose gel using the DNeasy gel purification kit according to the manufacturer's instructions. After obtaining the complete fragment including the desired NLRP3 mutation, the Taq-polymerase was used to add overhanging adenines at each end in order to facilitate its insertion into the pcDNA3.1/V5-His TOPO vector (Life Technologies). NLRP3 constructs were transformed into chemically competent TOP10 *E. coli* strain (Thermo Fisher Scientific) by heat-shock incubating the samples at 42 ºC during 30 s and subsequently for 2 min on ice. 250 µl of SOC medium were added to the mix and the bacteria were cultured for 1 h at 37 ºC and 500 revolutions per minute (rpm), that allow its exponential growth and recovery from the heat-shock. The culture was then streaked onto 5 ml of Luria-Bertani agar (LB, from Acros Organics) with 100 µg/ml of ampicillin (Sigma-Aldrich) Petri dishes and incubated at 37 ºC overnight to allow growth of single colonies.

Table 2. List of primers used during this Thesis.

Use		Sequence (5' to 3')	Length in nucleotides	GC content (%)
Introduction of NLRP3 V198M mutation	F	GTGAGAGCCCCATGAGTCCCATT	23	56.5
	R	AATGGGACTCATGGGGCTCTCAC		
Introduction of NLRP3 D303A mutation	F	GGACGGCTTCGCTGAGCTGCAAG	23	65.2
	R	CTTGCAGCTCAGCGAAGCCGTCC		
Introduction of NLRP3 D303G mutation	F	GGACGGCTTCGGTGAGCTGCAAG	23	65.2
	R	CTTGCAGCTCACCGAAGCCGTCC		
Introduction of NLRP3 D303H mutation	F	GGACGGCTTCCATGAGCTGCAAG	23	60.9
	R	CTTGCAGCTCATGGAAGCCGTCC		
Introduction of NLRP3 L305P mutation	F	CTTCGATGAGCCGCAAGGTGCCT	23	60.9
	R	AGGCACCTTGCGGCTCATCGAAG		
Introduction of NLRP3 Q306H mutation	F	TCGATGAGCTGCATGGTGCCTTTG	24	54.2
	R	CAAAGGCACCATGCAGCTCATCGA		
Introduction of NLRP3 F309S mutation	F	GAGCTGCAAGGTGCCAGTGACGAGCA	26	61.5
	R	TGCTCGTCACTGGCACCTTGCAGCTC		
Introduction of NLRP3 G326E mutation	F	GGCCGAGCGGGAAGACATTCTCCTG	25	64
	R	CAGGAGAATGTCTTCCCGCTCGGCC		
Introduction of NLRP3 L353P mutation	F	GACCTGTGGCCCCGGAGAAACTG	23	65.2
	R	CAGTTTCTCCGGGGCCACAGGTC		
Introduction of NLRP3 K355N mutation	F	CTGTGGCCCTGGAGAATCTGCAGCAC	26	61.5
	R	GTGCTGCAGATTCTCCAGGGCCACAG		
Introduction of NLRP3 M406V mutation	F	GTCCTCTTCACCGTGTGCTTCATCCC	26	57.7
	R	GGGATGAAGCACACGGTGAAGAGGAC		
Introduction of NLRP3 L411F mutation	F	GCTTCATCCCCTTCGTCTGCTGGA	24	58.3
	R	TCCAGCAGACGAAGGGGATGAAGC		
Introduction of NLRP3 T433I mutation	F	GAGCCTTGCCCAGATTTCTAAGACCACC	28	53.6
	R	GGTGGTCTTAGAAATCTGGGCAAGGCTC		
Introduction of NLRP3 R488K mutation	F	GAGTCCGACCTCAAGAATCATGG	23	52.2
	R	CCATGATTCTTGAGGTCGGACTC		
Introduction of NLRP3 Q703K mutation	F	GATATGGTGAAGTGTGTCCTCCC	23	52.2
	R	GGGAGGACACACTTCACCATATC		
Amplying initial part of the insert	F	AACATGGATTACAAAGACGATG	22	36.4
Amplying final part of the insert	R	TTCTTACTGCTCGTTCTTCAGCAC	24	45.8
Correct aligment of the plasmid in the vector	F	TAATACGACTCACTATAGGG	20	40
Correct aligment of the plasmid in the vector	R	GATCAGCGGGTTTAAACTC	19	47.4

The specific nucleotide(s) changed to performed mutation are represented in red. GC, guanine (G) and Cytosine (C); F, forward and R, reverse.

After incubation, 8-10 single colonies were picked from LB plate and the following PCR protocol 94ºC – 10 min, 94ºC – 3 min, (98ºC – 10 s, 57ºC – 30 s, 72ºC – 2 min) x 30 cycles, 4ºC - ∞, were performed to check if the desired construct was inside the vector and in the correct orientation using specific primers (**Table 2**). Positive bacteria colonies were then grown overnight in 5 ml of LB with 100 µg/ml of ampicillin at 37 ºC and gently agitation. After that, DNA plasmids were purified using the the QIAprep spin miniprep kit (Qiagen)

according to manufacturer's recommendations and the amount of DNA obtained was measured in a NanoDrop 2000/2000c spectrophotometer (Thermo Fisher Scientific). 500 µl of *E. coli* transformed bacteria with the plasmid of interest were conserved in glycerol stocks mixed with 500 µl 50% glycerol in water (volume/volume) and frozen at – 80 ºC.

Newly created plasmids were digested with 10 Units/µl of *NotI* and *BamHI* (both from Thermo Fisher Scientific) to confirm correct size between tags and the NLRP3 sequence. Finally, constructs were sequenced using Sanger sequencing and obtained sequences were pairwise aligned to the *in silico* engineered plasmid sequence to confirm the correct modification and the absence of unwanted mutations. Alignments were done using the Clustal Omega program of EMBL-EBI website.

7. Bioluminescent resonance energy transfer (BRET) assay

Bioluminescent resonance energy transfer is a natural phenomenon resulting in the transfer of non-radiative energy between a luminescence donor (*Renilla* luciferase) and a fluorescence acceptor (YFP). Energy transfer occurs when the distance and orientation between the donor and the acceptor is less than 100 Å and requires an overlapping among the emission and absorption spectrums of the donor and acceptor, respectively. In this Thesis, BRET assay was used to monitor conformational changes produced by the different NLRP3 plasmid constructs in HEK293T living cells before and during NLRP3 inflammasome activation.

Briefly, the following day of transient transfection, 1% of poly-L-lysine solution (Sigma-Aldrich) 1:100 in PBS 1x was prepared to added 100 µl of mix to each well in a coat 96-well white plate (Greiner Bio-One). Then, the plate was incubated 20 min at 37 ºC humidified incubator. In the meantime, transfected HEK293T cells were detached in 1 ml of DMEM:F12 complete medium by gently pipetting up to down. After poly-L-lysine incubation time, wells were washed twice with PBS 1x and 100 µl of cell suspension (approximately 100.000 cells/µl) were added to each well. For some experiments, 50 µl of the specific NLRP3 inhibitors MCC950 10µM and CY-09 10µM (or 50 µl of complete medium in controls wells) was added. Plates were incubated at 37ºC and 5% of CO_2 atmosphere during 24 hours. Then, cell culture media was removed using a vacuum pump and then cells were washed twice with warm PBS 1x.

In double-NLRP3 inhibitors experiments, 2 hours post-transfection, MCC950 10µM or CY-09 10µM was added to cell culture (24 h of first inhibitor; e.g, MCC950). The following day of transient transfection, once poly-L-lysine solution and washing step have been done,

100 µl of cell suspension containing the specific NLRP3 inhibitor (48 h of first inhibitor; e.g, MCC950) was added. 8 hours after, 50 µl of the other NLRP3 inhibitor was added to each well over-night (24 h of second inhibitor; e.g., CY-09).

To record BRET signal, 40 µl of Et-buffer with different treatments depending on the experimental assay was added to each well and BRET readings were performed 5 min after the automatic injection of 30 µM coelenterazine-H (Invitrogen) luciferase's substrate, in order to allow luciferase signal to stabilize. Final concentration of coelenterazine-h was 5 µM. In some experiments, cells were seeded with 40 µl of Et-buffer with 10 µM of nigericin and incubated during 30 min at 37ºC and 5% of CO_2 atmosphere, and then coelenterazine-H was added.

After incubation, luminescence was immediately read in a Synergy neo2 multi-mode plate reader (BioTek) at 480 and 530 nm every 150 s for 30 min with a gain of 110 units, and miliBRET units (mBU) were determined with the following equation:

$$\mathrm{BRET\ (mBU)} = \left(\left(\frac{\mathrm{Lum\ (535\ nm)}}{\mathrm{Lum\ (480\ nm)}} \right)^{\mathrm{donor+acceptor}} - \left(\frac{\mathrm{Lum\ (535\ nm)}}{\mathrm{Lum\ (480\ nm)}} \right)^{\mathrm{rLuc\ only}} \right) \times 1000$$

After BRET measurement, the expression of the NLRP3 BRET sensors in the different transfection and independent experiments were monitored by reading YFP fluorescence, which was measured by exciting at 480 nm and reading emission at 530 nm in the same wells. A NLRP3 construct without YFP, but with Luciferase was used as negative control (rLuc only) in all experimental assays.

8. Biochemical assays

8.1 Cytokine detection by enzyme-linked immunosorbent assay

The Enzyme-linked immunosorbent assay (ELISA) is a biochemical technique for detecting and quantifying specific proteins, antibodies, antigens and glycoproteins in biological samples such as plasma, serum or cell supernatant samples based on the antigen-antibody recognition (**Figure 9**).

In this Thesis, a quantitative sandwich ELISA system was used (**Figure 9**) to detect different cytokines: human IL-1β (Invitrogen), human TNF-α (R&D Systems), human IL-18 (MBL), human IL-6 (R&D Systems), human IL-18BP (Invitrogen), human HMGB1 (Arigo) and human Galectin-3 (Invitrogen) in PBMCs supernatants and complete whole blood; ELISA for mouse IL-1β (Invitrogen) and mouse TNF-α (Invitrogen); ELISAS for human ASC

(Cusabio), human TREM-1 (R&D Systems), human SIGLEC5 (Sigma-Aldrich) and human P2X7 receptor (Cusabio) in plasma.

ELISAs were done in 96-wells plate (Corning Costar). In brief, 100 µl of capture antibody diluted in coating buffer provided with the kit (dilution specific from each kit) per well was done overnight at 4 ºC or plates were previously pre-coated by the manufacturer. After coating, plates were washed three times with washing buffer (provided with the kit). Then, a standard with different dilutions of recombinant cytokine and samples were added according to manufacturer's recommendations. (Point 1 in **Figure 9**) and incubated to allow high specific binding between primary antibody and the antigen (Points 2 and 3 in **Figure 9**). Sample dilutions were done with the corresponding diluent buffer provided in the kit. After samples incubation and washing to eliminate avoid and excess of unspecific binding, the secondary antibody or detection antibody was added. In all ELISAs kit used, the secondary antibody was conjugated with horseradish peroxidase (HRP)-avidin or HRP-streptavidin (Point 4 in **Figure 9**). After secondary antibody incubation, samples were washed and 3,3',5,5'-tetramethybenzidine (provided with the kit) as substrate reagent was added in all assays and incubated protected from light. During this time, the enzyme reaction yields a blue product proportional to the amount of analyte presence in the sample that turned yellow when the provided stop solution was added (Point 5 in **Figure 9**). Absorbance at 450 nm was measured in a Synergy Mx plate reader (BioTek), using 570 or 620 nm wavelengths as reference. In all cases, manufacturers' protocols were followed.

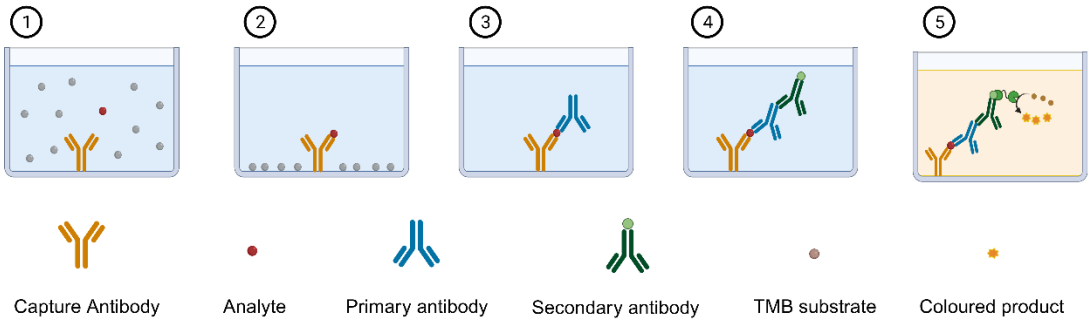

Figure 9. Schematic representation of sandwich ELISA protocol. Image created with Biorender.com.

8.2 Cytokine detection by Luminex

Plasma and cell-free supernatants from septic patients and controls group (abdominal surgery patients and healthy individuals), and plasma from patients with COVID-

19 (mild, moderate and severe), were used to measure the concentration of several cytokines, chemokines and plasmatic factors using different Luminex color-coded antibody-immobilized beads from Merck Millipore following the manufacturer's indications.

Specifically, multiplexing in human plasma for IL-15, IL-18, MCP-1, IL-2, IL-6 and IL-1Ra (HCYTA-60K) was performed in case of COVID-19 patients. On the same way, multiplexing in human plasma for IL-1α, IL-1Ra, IL-1β, IL-6, IL-8, IL-15, IL-18, GM-CSF, M-CSF, TNF-α (HCYTA-60K), IL-18BP (HFIB1-100K), HMGB1, IL-36β, IL-37, IL-38 (HCYP4MAG-64K) IL-33 (HCYP2MAG-62K), sIL-1RI and sIL-1RII (HSCRMAG-23K) was measured in septic patients and controls group. In case of cell-free supernatants from septic patients and controls groups, IL-18, TNF-α and IL-6 (HCYTA-60K) were quantified.

In brief, 25 µl of plasma samples was mixed with the appropriate antibody-immobilized beads (provided with the kit) and incubated with agitation on a plate shaker overnight at 4 ºC. After that, plate was washed twice and 25 µl of specific detection antibodies were added into each well and incubated with agitation on a plate shaker for 1 hour at RT. 25 µl of Streptavidin-Phycoerythrin is then added to each well and incubated for 30 minutes at RT. Finally, well contents were washed twice and 150 µl of drive fluid (provided with the kit) were added to all wells. The results were analysed in a Luminex MAGPIX instrument (Luminex Corporation).

8.3 Lactate dehydrogenase release

Extracellular LDH measurement was used to determine cell pyroptosis. In deep, LDH is a stable and soluble cytoplasmic glycolytic enzyme present in in most eukaryotic cells that leaks from cell upon plasma membrane damage. During pyroptosis, LDH leaks from the cell after NINJ1 plasma membrane rupture, but cannot permeate GSDMD pores. The LDH Cytotoxicity assay kit (Roche) was used following the manufacturer's indications (**Figure 10**).

In brief, 25 µl of cell-free culture supernatant sample was diluted 1:4 with Opti-MEM in 96-wells plate and 25 µl of cell-extracts were diluted 1:20 with Opti-MEM and then diluted again 1:4 in 96-wells plate to obtain the total cellular LDH content. 100 µl of freshly prepared LDH detection reagent mix was added to each sample well and absorbance was immediately read at 492 nm every 30 s during 10 min in a Sinergy MX plate reader (BioTek), using 620 nm wavelength as reference. The slope of the curve plotting absorbance *versus* time was calculated in order to obtain each sample's percentage of LDH leakage, calculated with the obtained LDH values from LPS treated cells that were lysed (100 % of LDH release).

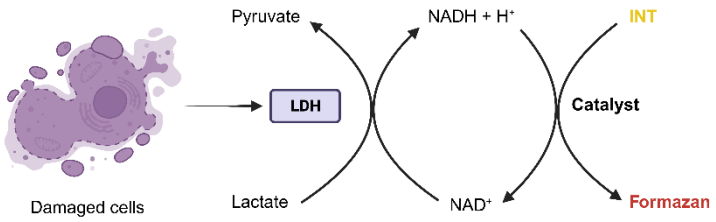

Figure 10. Schematic representation of LDH extracellular release assay principle. Extracellular LDH in the media could be quantified by a coupled enzymatic reaction. In the first step, LDH catalyses the conversion of lactate to pyruvate via NAD^+ reduction to $NADH+H^+$. Secondly, oxidation of $NADH+H^+$ by the catalyst diaphorase leads to the reduction of a yellow tetrazolium salt (INT) to a red formazam product which can be measured. Image created with Biorender.com.

9. Western-blot determination

In this Thesis, Western blot technique (**Figure 11**) has been used to confirm the correct expression of all NLRP3 wild-type and mutant constructs after transient transfection in HEK293T cells and to verify a similar expression between the NLRP3 mutant constructs and NLRP3 tagged with Flag vector in the flow cytometry heterozygous experimental assays.

Cell extracts obtained for $3.5x10^6$ HEK293T cells transient transfected with the different NLRP3 plasmid constructions were mixed with Laemmli buffer 1x (Bio-Rad) at 1:1 proportion in order to disrupt proteins' disulphide bonds and to avoid protein aggregation, as Laemmli buffer contains 2-mercaptoethanol. After that, samples were boiled at 95 ºC for 5 min to further denature protein structures, briefly spun down and loaded on the wells of an acrylamide gel. A single-phase 12% acrylamide gel was used to determine NLRP3 tagged with *Renilla* Luciferase (expression between NLRP3 mutants constructs) and a single-phase 10% acrylamide gel was used to determine NLRP3 in case of co-transfection of the NLRP3 mutants constructs with NLRP3 tagged with Flag vector. Samples were loaded into different gel wells together with a pre-stained protein standard (Life Technologies) and protein electrophoresis was performed at constant 200V for 50 min using a power supply from Bio-Rad (Point 1 in **Figure 11**). Then, immunoblotting was performed onto a 0.45 µM nitrocellulose membrane (Bio-Rad), Whatman® filter papers and casted into gel holders' cassettes (Bio-Rad) according to standard procedures (Point 2 in **Figure 11**). Protein transference was performed at constant 350 mA for 1 hour. Next, membranes were blocked to avoid unspecific antibody binding with skim milk (BD Biosciences) diluted at 5% in TBS Tris-buffered saline (TBS)-T (50 mM Tris, 150 mM NaCl, 0.05% Tween) for 1 hour at RT. After

that, primary antibody (**Table 3**) was added in TBS-T with 5% of milk and incubated overnight at 4 ºC (Point 3 in **Figure 11**). After overnight incubation, membranes were washed three times for 10 minutes with TBS-T to eliminate primary antibody that had not been bound and the secondary antibody conjugated with HRP (GE Healthcare) was added and incubated at 1:5000 dilution in TBS-T with 5% of milk for 1 hour with shaking at RT (Point 3 in **Figure 11**). At last, membranes were washed again before bioluminescent detection and were incubated for 5 min in dark with 1 ml of of enhanced chemiluminescence plus (Amhershan Biosciences) and light signal was detected using a ChemiDoc HDR (Bio-Rad) (Point 4 in **Figure 11**).

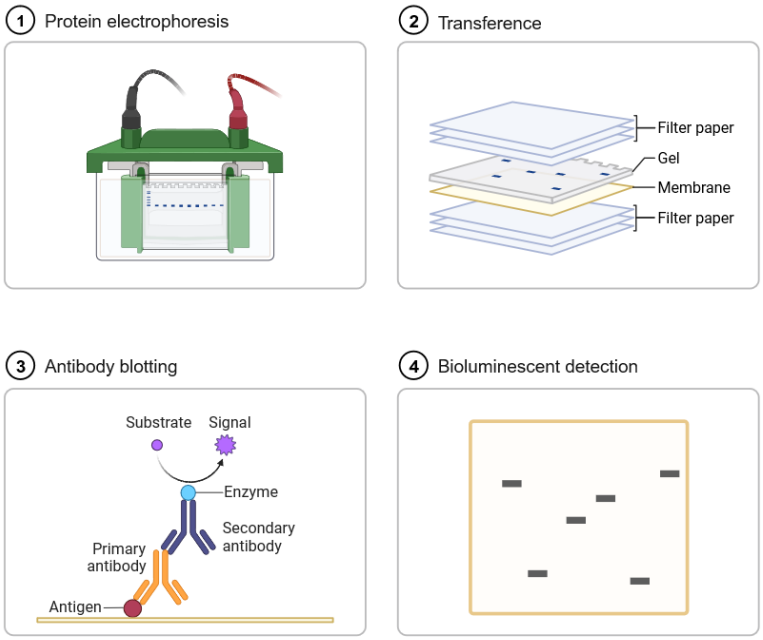

Figure 11. Graphic representation of Western Blot determination. Image created with Biorender.com.

Table 3. Antibodies used in Western Blot analysis.

Antibody	Host specie	Clonal expansion	Dilution	Company
Anti-*Renilla* Luciferase	Rabbit	Polyclonal	1:1000	MBL
Anti-NLRP3	Mouse	Monoclonal	1:1000	Adipogen
Anti-β-Actin	Mouse	Monoclonal	1:10000	Santa Cruz
Anti-rabbit IgG HRP Linked F(ab')2	Goat	Polyclonal	1:5000	Sigma-Aldrich
Anti-mouse IgG HRP Linked F(ab')2	Goat	Polyclonal	1:5000	Sigma-Aldrich

10.Flow cytometry

10.1 Determination of ASC oligomerization in whole blood

Intracellular ASC-speck formation in monocytes was detected following the protocol already published (Hurtado-Navarro et al., 2022). Briefly, ASC oligomerization in human monocytes was evaluated mixing 50 µl of individuals' whole blood samples in polystyrene flow cytometry tubes (Falcon) with 450 µl of complete RPMI 1640 medium.

Following stimulation, tubes were centrifuged 600 xg for 5 min to pellet floating cells and carefully remove supernatants. Then, resuspend the cells in 100 µl of SB containing mouse monoclonal PE-Cy7-conjugated anti-CD16 (1:10, clone 3G8, 557744, BD Biosciences), mouse monoclonal fluorescein isothiocyanate (FITC)-conjugated anti-CD14 (1:10, clone M5E2, 557153, BD Biosciences) and mouse monoclonal Allophycocyanin (APC)-conjugated anti-CD15 (1:40, clone HI98, 551376, BD Biosciences) for 30 min at RT in dark in order to stain the surface of monocytes ($CD14^+CD16^-$/$CD16^+CD15^-$). After incubation, 1 ml of SB was added and samples were centrifuged for 5 min at 600 xg, supernatants were then discarded. Cell pellets were resuspended in 1 ml of cell fixation/lysis buffer and incubated for 10 min on ice at dark, after which another wash was done.

After that, cells were stained for the detection of ASC specks by Time-of-Flight Inflammasome Evaluation (TOFIE) (Sester et al., 2015). For that, 250 µl of PB were added to each tube and also, 250 µl of a 1:100 dilution in SB of Phycoerythrin (PE)-conjugated mouse monoclonal anti-ASC antibody (653903, Biolegend) were added to achieve a final dilution of 1:200 in the desired tubes. Tubes were incubated 45 min in the dark at RT and after that, cell were washed again. Finally, cells were resuspended in 500 µl of SB and acquired analysing the staining of ASC in monocytes as well as the distribution of ASC-PE width *versus* ASC-PE area in $CD14^+CD16^+CD15^-$ monocytes to determine the quantify the percentage of ASC specking monocytes (**Figure 12**).

All samples were analysed by flow cytometry during 3 min at medium acquisition velocity using FACS Canto (BD Biosciences) and analysed using FCS express software (De Novo Software).

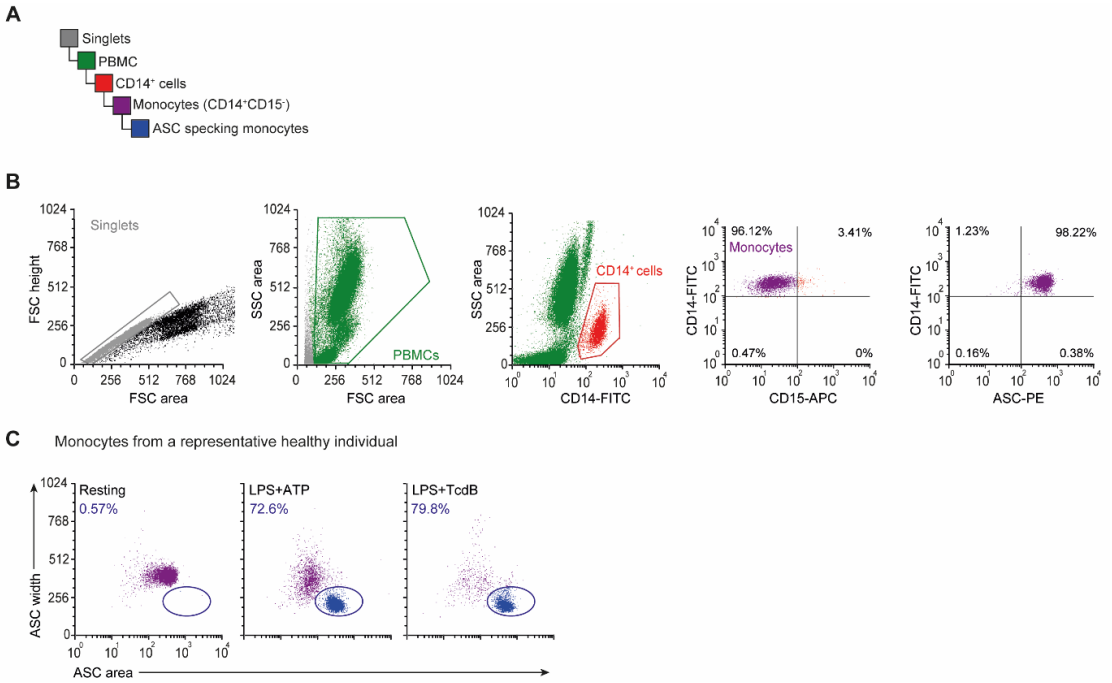

Figure 12. Gating strategy to identify monocytes with ASC specks. (**A**) Populations hierarchy analysed in flow cytometry experiments to determine ASC specking monocytes. (**B**) Peripheral blood mononuclear cells (PBMCs) were gated from total cells obtained after Ficoll-isolation selecting singlet cells in a forward scatter (FSC) height vs area dot plot and then excluding cell debris in a FSC vs side scatter (SSC) dot plot. Monocytes were gated from PBMCs by the positive staining with an anti-CD14 FITC monoclonal antibody in a SSC vs CD14 FITC dot plot and by the negative staining with an anti-CD15 APC monoclonal antibody in a CD14 FITC vs CD15 APC dot plot. ASC positive monocytes (>95%) were gated by the positive staining with an anti-CD14 FITC and anti-ASC PE monoclonal antibodies in a CD14 FITC vs ASC PE dot plot. (**C**) Time-of-flight inflammasome evaluation showing the quantification of ASC specking monocytes obtained from a representative healthy control. ASC specking monocytes were gated based in an ASC PE-width vs ASC PE-area dot plots after priming or not of the cells with LPS (1.6 µg/ml) during 2 h and then stimulated with ATP (3 mM) for 30 min or with TcdB (1 µg/ml) for 1 h.

10.2 Determination of intracellular ASC-speck formation in HEK293T cells

Intracellular ASC-speck formation was evaluated seeding $7x10^5$ HEK293T cells which were transfected with 0.1 µg of ASC-RFP plasmid and 0.1 µg of NLRP3 and NLRC4 plasmids (wild-type and mutants). Once plasmids are expressed (24 h post-transfection), the detection of ASC specks by TOFIE technic were analysed by flow cytometry using LSR-Fortessa (BD Biosciences) and the FCS express software (De Novo Software) (**Figure 13**).

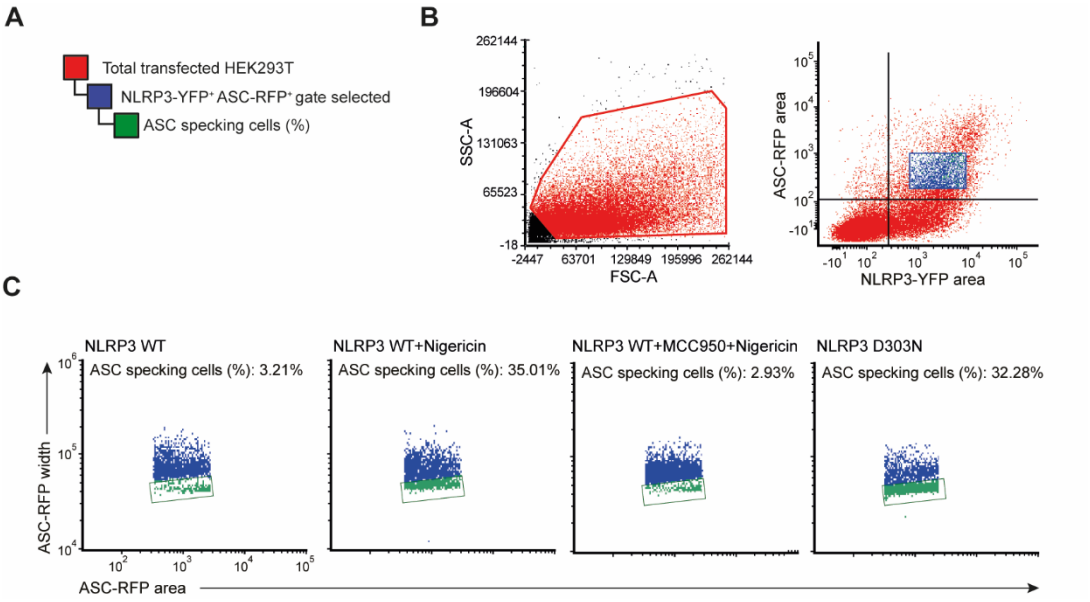

Figure 13. Gating strategy to identify the percentage of HEK293T cells with ASC oligomers. (**A**) Populations hierarchy analysed in flow cytometry experiments to determine ASC specking cells. (**B**) HEK293T transfected cells were gated from total cells using side scatter (SSC) area vs forward scatter (FSC) area dot plot. Co-transfected cells were gated by the positive expression of NLRP3-YFP (area) and ASC-RFP (width) dot plot. (**C**) Four different gates with increased expression of NLRP3-YFP wild type (WT) or D303N calculated as mean fluorescence intensity (MFI). NLRP3 WT was untreated or activated for 30 min with nigericin (10 μM). MCC950 (10 μM) was added to HEK293T transfected cells after 3 h post-transfection and maintained 24 hours in cell culture.

In some experiments, intracellular ASC-speck formation was studied in different gates with increasing mean fluorescence intensity for NLRP3-YFP (**Figure 14**). Likewise, in other set of experiments, transfected HEK293T cells were incubated for 3 hours at 37 ºC or 32º C and were untreated or activated for 30 min with nigericin (10 μM).

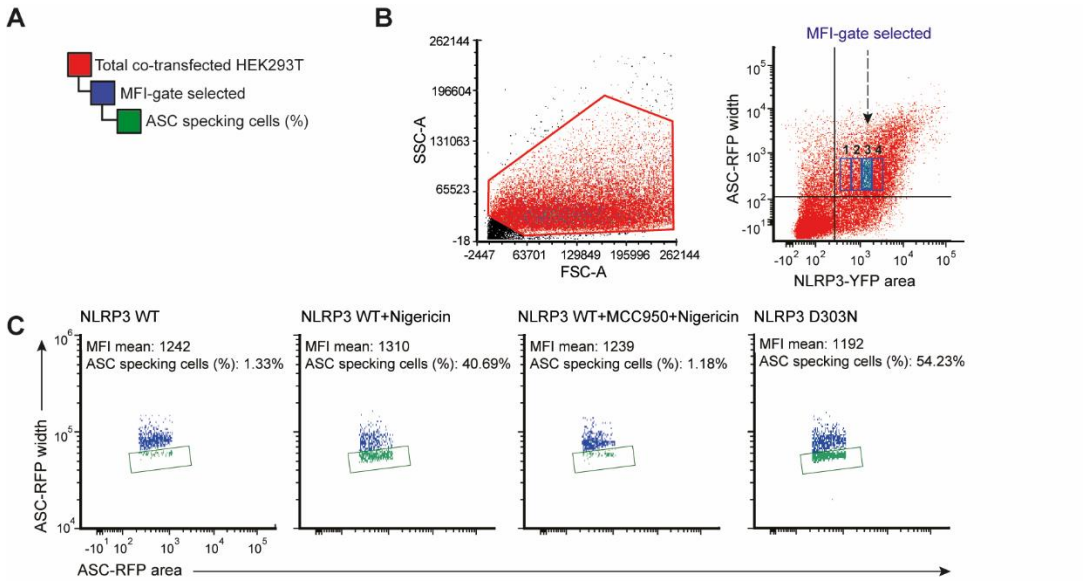

Figure 14. Gating strategy to analyse the percentage of ASC specking cells in different gates with increased expression of NLPR3. (**A**) Populations hierarchy analysed in flow cytometry experiments to determine ASC specking cells. (**B**) HEK293T transfected cells were gated from total cells

using side scatter (SSC) area vs forward scatter (FSC) area dot plot. Co-transfected cells were gated by the positive expression of NLRP3-YFP (area) and ASC-RFP (width) dot plot. As example, the percentage of ASC specking HEK293T cells is shown in the gate number three for NLRP3 expression. (**C**) Four different gates with increased expression of NLRP3-YFP wild type (WT) or D303N calculated as mean fluorescence intensity (MFI). NLRP3 WT was untreated or activated for 30 min with nigericin (10 μM). MCC950 (10 μM) was added to HEK293T transfected cells after 3 h post-transfection and maintained 24 hours in cell culture.

11. Bioinformatics data analysis

In order to analyse all variables associated to septic patients (clinical, demographic, biochemical, cellular and functional), bioinformatics data analysis was performed through the Biomedical Bioinformatics Platform of the Biomedical Research Institute of Murcia (IMIB-Pascual Parrilla).

To generate the chord plot or chord diagram, all patients' variables were correlated with each other. Using the correlation coefficient (R^2 value) of those correlations with a significant *p* value, a new data table was generated and imported into the 'Circlize' R package (Gu et al., 2014; R Core Team, 2014).

On the other hand, to reduce the dimensionality of the database, those variables and individuals with more than 20% missing data were eliminated. With the remaining data and using the 'Mice' R package with the 'Random Forests' method, the rest of the missing data were imputed (this process is defined as a method to give value to an item that previously was missing) (van Buuren & Groothuis-Oudshoorn, 2011). After this, the data were normalized using the 'preProcess' function of the 'Caret' R package (Kuhn, 2008). Different bioinformatics analyses were then carried out from the normalized data.

Firstly, two classical statistical machine-learning methods were used. Specifically, the linear discriminant analysis (LDA) function of the 'MASS' R package and the sPLS-DA (latent structures-discriminant analysis) function of the 'mixOmics' R package (Rohart et al., 2017; Venables & Ripley, 2002). Both algorithms allow to visualize a large set of data in a two-dimensional space. To do this, they identify and classify the variables by their similarity, minimizes the distance among samples belonging to the same class and increases the distance among samples belonging to different classes (in our case, classifying patients as 'healthy controls or surgery controls' *versus* 'septic patients').

Secondly, we wanted to create a predictive algorithm to classify individuals based on the values of the set of variables studied. To do this, individuals were classified into 'septic patients' and 'controls' ('healthy' and 'surgery' controls in the same category). Next, a multivariable logistic regression was applied ('nnet' R package) and those variables that

best classified patients between 'septic' and 'controls' were selected ('stepAIC' function from the 'MASS R' package and the 'backward and forward' method) (Venables & & Ripley, 2002). Once these variables were obtained (plasma concentration of: sSIGLEC5, sTREM-1, IL-1β, IL-1RA, IL-18BP, sIL-1RII and creatinine, with IL-1β release in whole blood stimulated with LPS+TcdB), 80% of the data was separated to train the algorithm and the remaining 20% to test it. In this way, we can predict which class an individual with certain characteristics (variables) should belong to, obtaining the probability of belonging to each of the classes. This process has been carried out with the 'createDataPartition' function of the 'Caret' R package (Kuhn, 2008). Finally, to generate a ROC curve with the results, the probabilities obtained in the previous step have been used together with the real data of membership of each individual to the specific class. This process has been repeated 50 times (that is, 80-20% of the data have been randomly separated, generating a predictive model and testing the generated algorithm), obtaining average values of Accuracy, Sensibility, Specificity and AUC. This process has been carried out with the 'ROC' function of the 'pROC' R package (Robin et al., 2011).

12. Statistical analysis

Statistics were calculated using GraphPad Prism 9 software (Graph-Pad Software, Inc.) or R-Studio (Posit, PBC). Normality of the samples was determined with D'Agostino and Pearson omnibus K2 normality test to observe if samples follow or not a Gaussian distribution. For two-groups comparation, parametric *t*-test for normal distributed data and Mann-Whitney U test for non-parametric data were used to determine the statistical significance. For multigroup comparison, one-way analysis of variance (ANOVA) test for normal distributed data and Kruskal-Wallis test for non-parametric data were used to determine the statistical significance. Data are shown as mean values and error bars represent standard error from the number of independent assays indicated in the figure legend. *p*-value is indicated as *p < 0.05; **p < 0.01; ***p < 0.001; ****p < 0.0001; > 0.05 not significant (*ns*).

Moreover, Chi-square (χ^2) test was used to determine differences between clinical variables among septic patients and control groups. Pearson correlation for normal distributed data and Spearman correlation for non-parametric data were used to measure linear correlations between two variables. Kaplan-Meier was used to compare the survival rate of NLRP3 immunocompromised and non-immunocompromised septic patients. ROC analysis was used for sensitivity and specific assessment of clinical, biochemical and experimental variables among septic patients and control groups and inside septic patients to differentiate

non immunocompromised *versus* immunocompromised individuals. Chord diagram analysis was performed to show in colour significant correlations between clinical, biochemical and experimental variables between septic patients and controls groups, as well as NLRP3 immunocompromised and non-immunocompromised septic patients. Coloured links represents correlation with a significant *p* value ($p > 0.05$) and width of the links correspond to the squared correlation (R^2).

RESULTS

Chapter 1:
The inflammatory response in infection

1. 1. Role of NLRP3 and Pyrin inflammasomes in sepsis

1.1.1 Inflammasome markers in sepsis

To achieve some understanding on how the inflammatory response occurs during infection, we analysed a cohort of intra-abdominal origin septic patients (*n* = 34), a control group of abdominal surgery patients that did not develop sepsis (*n* = 36) and a healthy control group (*n* = 35, **Table 4**).

Table 4. Demographics and clinical characteristics of enrolled patients with intra-abdominal sepsis and control groups.

	Healthy controls	Abdominal surgery controls	Intra-abdominal origin septic patients
N	35	36	34
Age, mean (range) ± SD	48.18 (26-63) ± 8.56	67.94 (32-85) ± 12.50	67.18 (40-89) ± 14.14
p value against septic group	*p*< 0.0001****	*p*> 0.05^{ns}	
Gender, N (%)			
Male	8 (22.86)	21 (58.33)	18 (55.88)
Female	27 (77.14)	15 (41.66)	15 (44.12)
p value against septic group	*p* = 0.007**	*p*> 0.05^{ns}	
Comorbilities			
Diabetes Mellitus II, N (%)	2 (5.71)	10 (27.77)	8 (23.53)
p value against septic group	*p* = 0.021*	*p*> 0.05^{ns}	
High Blood Pressure, N (%)	5 (14.28)	21 (58.33)	19 (55.88)
p value against septic group	*p* = 0.0001***	*p*> 0.05^{ns}	
Oncologic patients, N (%)	1 (2.86)	25 (69.44)	16 (47.06)
p value against septic group	*p* <0.001 ****	*p* = 0.047 *	
Clinical data (only for septic patients)			
Anatomical location of the initial focus, N (%)			
Stomach			4 (11.77)
Duodenum			3 (8.82)
Gallbladder			4 (11.77)
Liver			1 (2.94)
Small intestine			4 (11.77)
Large intestine			1 (2.94)
Colon			6 (17.65)
Appendix			4 (11.77)
Ilion			2 (5.88)
Rectum			1 (2.94)
Sigmoid colon			4 (11.77)
APACHEII score at admission			
mean (range) ± SD			17.21 (10-32) ± 6.441
SOFA score at admission			
mean (range) ± SD			5.412 (0-13) ± 3.619
Days in Surgical Critical Unit			
mean (range) ± SD			11.47 (1-72) ± 15.29
Days Hospitalized			
mean (range) ± SD			28.29 (3-249) ± 42.71
Days of mechanical ventilation			
mean (range) ± SD			3.606 (0-28) ± 6.991
Septic Shock, N (%)			15 (44.12)
Mortality, N (%)			9 (24.47)

SD, standard deviation; ns, not significant difference (p >0.05); Chi-square (χ^2) test was used except for the age that ANOVA test was used.

As an indication that our cohort of septic patients presented elevated systemic inflammation, we found high levels of PCT and CRP in the plasma 24 hours after sepsis initiation in comparation with the surgery control group (**Figure 15A**). Septic patients presented an averaged SOFA score of 5.412 ± 3.619 (range 0 to 13, average ± standard error) and APACHE II score 11.47 ± 15.29 (range 1 to 72), with dysfunction of one or more vital organ, together with an increase in the blood leucocytes, neutrophils, urea and creatinine (**Figure 15B, C** and **Table 5**). On the contrary, the number of lymphocytes and hemoglobin in blood was reduced when compared to the standard threshold of healthy individuals (**Figure 15B, C**). Platelets and bilirubin only presented a significant increase with respect to surgery controls, whereas monocytes and lactate did not (**Figure 15B, C**). Moreover, the neutrophils to lymphocytes ratio (NLR), an emerging marker of inflammatory status, was highly elevated in septic patients compared to healthy and surgery individuals (**Figure 15D**), supporting the inflammatory state of septic patients at sepsis onset.

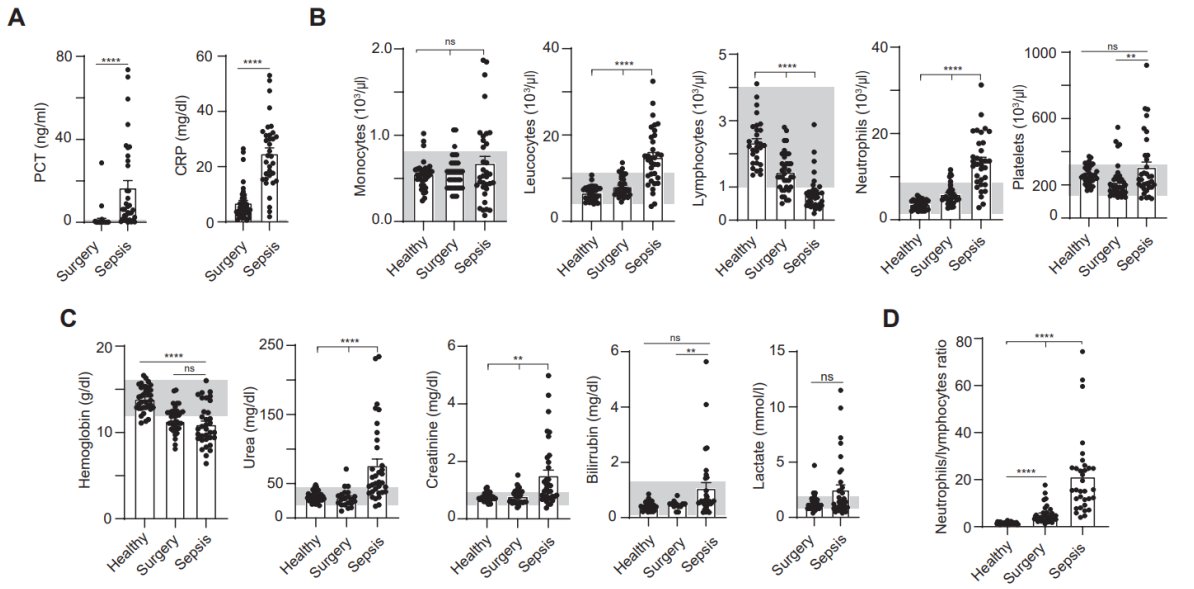

Figure 15. Acute phase proteins in plasma and clinical parameters of septic patients within the first 24 hours of admission at the Reanimation Unit. (**A**) Plasma concentration of PCT and CRP, (**B**) number of monocytes, leucocytes, lymphocytes, neutrophils and platelets, (**C**) concentration of hemoglobin, urea, creatinine, bilirubin and lactate, and (**D**) neutrophils-lymphocytes ratio from patients enrolled in this study (healthy controls, abdominal surgery patients and intra-abdominal origin septic patients). Each dot corresponds to an induvial patient; data is represented as mean ± SEM; grey shadow on graphs indicates the normal range in healthy population for each parameters analysed; *t*-test in (**A**) and Kruskal-Wallis test or ANOVA test in (**B-D**); ****p < 0.0001, **p<0.005, and ns, no significant difference (p>0.05).

Table 5. Clinical and demographic data of septic patients.

	Total septic patients
N	34
Age	
Mean (range) ± SD	67.18 (40-89) ± 14.14
Gender, N (%)	
Male	18 (55.88)
Female	15 (44.12)
Clinical data	
Diabetes Mellitus II, N (%)	8 (23.53)
High Blood Pressure, N (%)	19 (55.88)
Oncologic, N (%)	16 (47.06)
Infection acquired, N (%)	
Nosocomial	18 (52.94)
Community	16 (47.06)
Organ dysfuntion, N (%)	
Renal	18 (52.94)
Respiratory	11 (32.35)
Cardiovascular	8 (23.53)
Hepatic	4 (11.76)
Hematological	15 (40.12)
Mortality	
N (%)	9 (24.47)
Initial multi-organic failure*	6 (66.67)
Secondary complications**	1 (11.11)
Other pathologies	2 (22.22)

*Mortality due to the initial organ dysfunction without clear recuperation after initial admission. **Recuperation of initial organ dysfunction after admission, mortality due to acquisition of new infectious processes that could result in another multiple organ dysfunction. SD, standard deviation.

As the IL-1 cytokine family exert pleiotropic effects on intercellular signalling leading to anti- or pro- inflammatory responses, we aimed to study the plasma presence of IL-1 members in sepsis. We found a significant increase of IL-1β, IL-1α, IL-18, sIL-1RI, sIL-1RII, IL-1RA and IL-18BP in the plasma of septic patients when compared to surgery and healthy controls, indicating a dual inflammatory response during sepsis (**Figure 16**). IL-33, IL-36β, IL-37 and IL-38 were similar among all group of individuals studied (**Figure 16**).

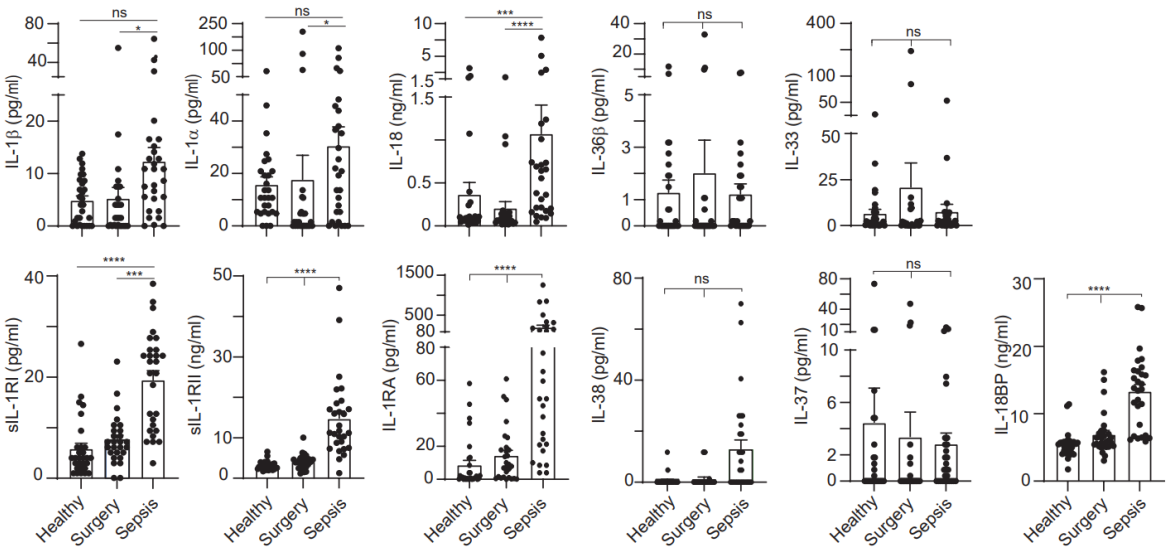

Figure 16. IL-1 cytokines released on septic patients' plasma within the first 24 hours of admission at the Reanimation Unit. Concentration of IL-1β, IL-1α, IL-18, IL-36β, IL-33, sIL-1RI, sIL1-RII, IL-1RA, IL-37, IL-38 and IL-18BP in the plasma of healthy controls, abdominal surgery patients and intra-abdominal origin septic patients enrolled in this study. Each dot corresponds to an induvial patient; data is represented as mean ± SEM; ANOVA test; ****p<0.0001, ***p<0.0005, *p<0.05 and ns, no significant difference (p>0.05).

As expected, IL-6 and IL-8 cytokines were also elevated in the plasma of septic patients when compared to control surgery and healthy groups (**Figure 17A**), supporting the potential diagnostic use of these cytokines in patients with sepsis (Harbarth et al., 2001; Zeng et al., 2022). Likewise, TNF-α, M-CSF and IL-15 were elevated in the plasma of septic patients (**Figure 17A**). However, no significant differences were found when the concentration of the alarmin HMGB1 was evaluated between control and septic groups (**Figure 17A**).

We also explored the potential prognostic value on serum levels of ferritin, soluble SIGLEC5 (sSIGLEC5) and soluble TREM-1 (sTREM-1), as predictors of mortality in infections (He et al., 2023; Lozano-Rodríguez et al., 2023; Wright et al., 2020). All were found augmented in our cohort of septic patients compared to healthy and surgery groups, with the exception of ferritin that did not present significant differences with surgery individuals (**Figure 17B**). Neither the concentration in plasma of ferritin nor IL-18 or sSIGLEC5 in our septic cohort were associated with death, with a higher risk of suffering septic shock or with an increase in the Reanimation Unit stay (**Figure 18**). However, we were able to find correlations between sTREM-1, TNF-α, IL-6 and IL-8 concentration in the plasma and sepsis mortality, or PCT concentration in plasma with a higher risk of suffering septic shock, among others (**Figure 18** and **Tables 6-8**).

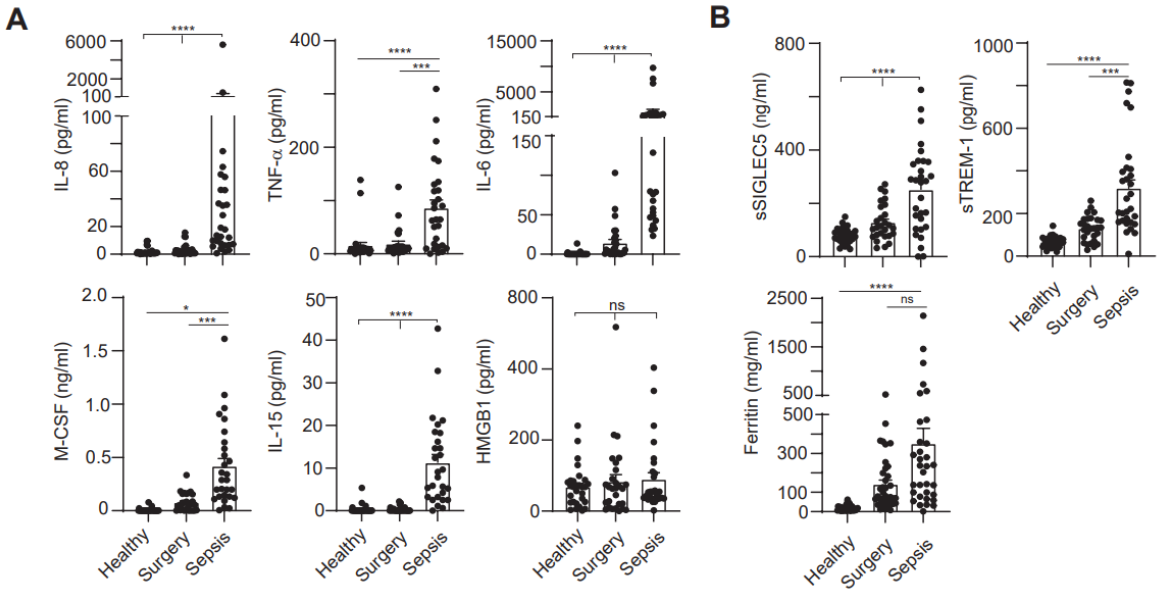

Figure 17. Pro-inflammatory cytokines and prognostic inflammatory markers in the plasma of septic patients. Concentration of IL-8, TNF-α, IL-6, M-CSF, IL-15 and HMGB1 (**A**), and levels of sSIGLEC5, sTREM-1 and ferritin (**B**) in the plasma of healthy controls, abdominal surgery patients and intra-abdominal origin septic patients enrolled in this study. Each dot corresponds to an induvial patient; data is represented as mean ± SEM; ANOVA test; ****p<0.0001, ***p<0.0005, *p<0.05 and ns, no significant difference (p>0.05).

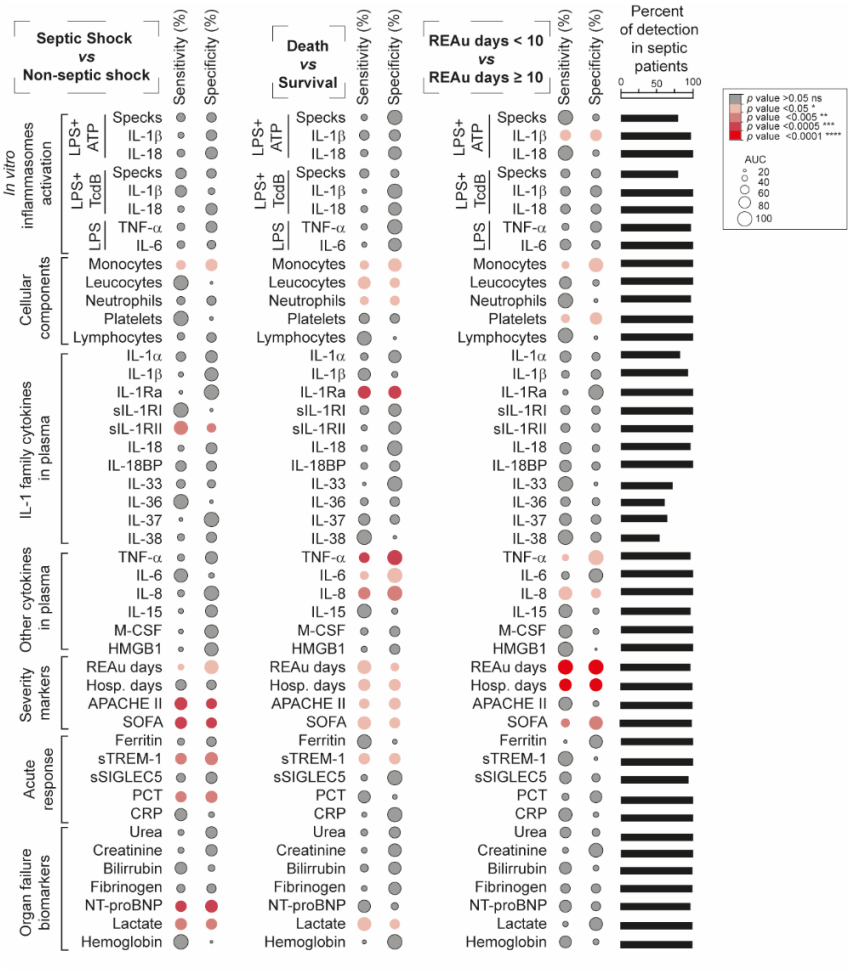

Figure 18. Schematic representation of receiver operating characteristic (ROC) analysis for functional, cellular, biochemical and severity parameters comparing control *vs* septic individuals. AUC, area under the curve; REAu, Reanimation Unit; IL, interleukin; CRP, C-reactive protein; PCT, procalcitonin. Control group included healthy donors and abdominal surgery controls (n = 72), and sepsis group included n = 34. Percentage of detection indicated indicates the percentage of septic individuals who presented measurable concentrations of each variable analysed. t-test; ****p<0.0001, ***p<0.0005, **p<005, *p<0.05 and ns, no significant difference (p>0.05).

Table 6. ROC analysis of total parameters analysed in this study for septic shock diagnosis comparing control *vs* septic individuals.

			Septic Shock	Non-septic shock	AUC±SE	*p* value	Cut-off	Sensitivity (%)	Specificity (%)
In vitro activation	LPS + ATP	Specks ASC	15.77	17.85 ns	0.54±0.115	0.7189	> 16.80	60	66.67
		IL-1β	477.3	510.1 ns	0.51±0.101	0.9454	> 1281	42.11	73.33
		IL-18	0.60	1.04 ns	0.68±0.098	0.0871	> 0.9688	54.55	83.33
	LPS + TcdB	Specks ASC	52.58	58.31 ns	0.66±0.111	0.1828	> 54.86	73.33	66.67
		IL-1β	1027	1270 ns	0.63±0.098	0.2149	> 629.1	78.95	46.67
		IL-18	5.37	7.83 ns	0.58±0.107	0.5146	> 8.852	45.83	80
	LPS	TNF-α	53.99	88.51 ns	0.66±0.098	0.179	> 81.34	54.17	77.78
		IL6	13.36	14.85 ns	0.54±0.108	0.7239	> 14.20	54.17	60
Cellular components		Monocytes	0.44	0.69 *	0.71±0.092	0.0387	> 0.5600	63.16	80
		Leucocytes	13.56	15.12 ns	0.54±0.106	0.9407	> 6.915	100	20
		Neutrophils	12.59	13.62 ns	0.52±0.109	0.8006	> 13.22	57.89	64.29
		Platelets	212	234 ns	060±0.100	0.319	> 136.0	100	26.67
		Lymphocytes	0.69	0.78 ns	0.55±0.101	0.6013	> 0.7750	52.63	66.67
IL-1 family cytokines in plasma		IL-1α	35.36	16.44 ns	0.64±0.124	0.2674	< 21.43	66.67	81.82
		IL-1β	11.86	8.216 ns	0.62±0.112	0.315	< 5.383	35.71	91.67
		IL1-RA	59.45	48.72 ns	0.60±0.109	0.3686	< 9.249	26.67	100
		sIL1RI	24.23	18.44 ns	0.66±0.104	0.122	< 31.30	100	23.0
		sIL1RII	17056	9637 **	0.82±0.081	0.0054	< 16700	93.33	61.54
		IL-18	642.6	345.7 ns	0.56±0.114	0.65	< 214.0	42.86	76.92
		IL-18BP	1568	1208 ns	0.58±0.119	0.967	< 1412	73.33	69.23
		IL-33	2.58	3.49 ns	0.52±0.145	0.923	> 3.035	61.54	57.14
		IL-36	106	1.49 ns	0.51±0.151	0.3188	< 5.247	100	25
		IL-37	2.80	2.30 ns	0.53±0.138	0.3089	> 9.572	27.27	100
		IL-38	18.87	22.47 ns	0.57±0.155	0.6723	> 24.26	50	71.43
Other cytokines in plasma		TNF-α	64.27	57.04 ns	0.62±0.111	0.209	< 39.48	50	84.62
		IL-6	210.3	79.53 ns	0.59±0.112	0.4397	< 738.3	93.33	38.46
		IL-8	13.63	17.91 ns	0.63±0.110	0.2539	< 7.013	46.67	100
		IL-15	9.66	8.46 ns	0.52±0.114	0.8673	> 17.20	35.71	84.62
		M-CSF	357.7	287.9 ns	0.61±0.108	0.3562	< 127.3	33.33	92.31
		HMGB1	46.7	53.15 ns	0.54±0.112	0.7079	< 34.72	33.33	92.31
Acute phase response		Ferritin	202.9	253.9 ns	0.53±0.103	0.8096	> 255.3	50	66.67
		sTREM-1	377.1	166.1 **	0.82±0.078	0.0015	< 205.7	76.47	86.67
		SIGLEC-5	295823	160112 ns	0.65±0.105	0.1548	< 200550	62.5	78.57
		PCT	29.6	4.4 **	0.77±0.091	0.008	< 6.240	73.68	80
		CRP	21.61	25.65 ns	0.55±0.104	0.7972	> 16.16	84.21	40
Organ failure biomarkers		Urea	51	52 ns	0.56±0.101	0.5776	< 43.50	42.11	80
		Creatinine	1.16	0.94 ns	0.59±0.100	0.3674	< 0.7850	42.11	80
		Bilirrubin	0.54	0.6 ns	0.69±0.096	0.1699	> 0.5350	82.35	46.67
		Fibrinogen	646	669 ns	0.58±0.103	0.393	> 660.0	57.89	64.29
		NT-proBNP	2705	763.5 ***	0.79±0.090	0.0076	< 1189	75	84.62
		Lactate	2.4	1 **	0.79±0.085	0.0033	< 1.450	78.95	73.33
		Hemoglobin	10.4	10.4 ns	0.52±0.101	0.6751	< 14.50	100	20
Severity markers		REAu days	8	4 *	0.71±0.088	0.0346	< 2.500	42.11	93.39
		Hospitalized days	25	13 ns	0.68±0.098	0.078	< 20.50	73.68	66.67
		APACHEII score	20.5	12.5 ***	0.85±0.066	0.0003	< 17.50	85	71.43
		SOFA score	7.5	3.5 ***	0.83±0.073	0.001	< 6.500	80	71.43

AUC, area under the curve; REAu, Reanimation Unit; IL, interleukin; CRP, C-reactive protein; PCT, procalcitonin. Control group included healthy donors and abdominal surgery controls (n = 72), and sepsis group included n = 34. The median and cut-off values are expressed in the same units as Figure 15-17. *t*-test; ****p< 0.0001, ***p<0.0005, **p<0.005, *p<0.05 and ns, no significant difference (p>0.05).

Table 7. ROC analysis of total parameters analysed in this study for mortality diagnosis comparing control *vs* septic individuals.

			Death	Survival	AUC±SE	*p* value	Cut-off	Sensitivity (%)	Specificity (%)
In *vitro* activation	LPS + ATP	Specks ASC	13.7	20.65 ns	0.72±0.099	0.0919	> 38.67	45	100
		IL-1β SC	220.8	668.2 ns	0.70±0.097	0.086	> 441.9	68	77.78
		IL-18	0.5227	0.9761 ns	0.69±0.097	0.1018	> 0.9688	52	88.89
	LPS + TcdB	Specks ASC	52.79	56.81 ns	0.54±0.135	0.9311	> 52.99	65	57.14
		IL-1β SC	796.3	1048 ns	0.60±0.104	0.4192	> 2694	32	100
		IL-18	5.27	7.861 ns	0.64±0.100	0.2308	> 8.852	48	88.89
	LPS	TNF-α	51.73	94.43 ns	0.72±0.091	0.0738	> 148.3	44	100
		IL6	13.08	14.96 ns	0.60±0.107	0.4192	> 27.48	36	88.89
Cellular components		Monocytes	0.4	0.6 *	0.74±0.110	0.0307	> 0.5400	60	88.89
		Leucocytes	8.8	15.17 *	0.8±0.091	0.0103	> 10.74	84	66.67
		Neutrophils	8.41	13.62 *	0.78±0.102	0.0218	> 9.990	80	75
		Platelets	203	250 ns	0.58±0.119	0.4652	> 206.0	72	66.67
		Lymphocytes	0.69	0.72 ns	0.57±0.115	0.5451	> 0.3700	96	22.22
IL-1 family cytokines in plasma		IL-1α	29.73	19.23 ns	0.65±0.122	0.2663	< 20.06	52.94	85.71
		IL-1β	12.84	8.65 ns	0.65±0.120	0.2437	< 15.88	85.71	42.86
		IL1-RA	502.7	37.84 ***	0.93±0.049	0.0002	< 133.0	85.71	85.71
		sIL1RI	25.4	18.44 ns	0.75±0.105	0.0534	< 21.91	61.9	85.71
		sIL1RII	11748	11251 ns	0.58±0.120	0.5329	< 10327	42.86	85.71
		IL-18	657.3	336.6 ns	0.65±0.105	0.2404	< 214.0	45	100
		IL-18BP	1380	1362 ns	0.51±0.126	0.9183	< 1274	47.62	71.43
		IL-33	3.94	3.49 ns	0.55±0.164	0.8035	< 1.890	25	100
		IL-36	1.49	1.06 ns	0.59±0.147	0.571	< 1.277	54.55	66.67
		IL-37	7.43	2.30 ns	0.68±0.142	0.3799	< 5.366	80	66.67
		IL-38	18.91	18.87 ns	0.51±0.201	0.978	< 66.28	100	25
Other cytokines in plasma		TNF-α	178.6	51.43 ***	0.90±0.062	0.0009	< 74.90	70	100
		IL-6	630.7	76.13 *	0.81±0.089	0.0143	< 79.18	57.14	100
		IL-8	46.56	9.987 **	0.89±0.062	0.0012	< 31.69	80.95	100
		IL-15	14.62	8.46 ns	0.63±0.144	0.0732	< 20.69	95	42.86
		M-CSF	199.4	342.9 ns	0.53±0.117	0.8438	> 315.4	52.38	71.43
		HMGB1	54.77	46.7 ns	0.54±0.120	0.7851	< 37.90	42.86	71.43
Acute phase response		Ferritin	240.5	218.7 ns	0.53±0.131	0.8337	< 660.4	95.83	33.33
		sTREM-1	401.7	201.1 *	0.77±0.099	0.0258	< 345.1	75	75
		SIGLEC-5	294673	229750 ns	0.61±0.099	0.6684	< 158917	45.45	100
		PCT	7.66	6.23 ns	0.52±0.119	0.8782	> 1.260	84	33.33
		CRP	18.52	28.07 ns	0.65±0.095	0.1565	> 31.32	36	100
Organ failure biomarkers		Urea	46	59 ns	0.54±0.109	0.7228	> 62.50	48	77.78
		Creatinine	1.19	0.96 ns	0.58±0.108	0.5198	< 0.7850	40	88.89
		Bilirrubin	0.6	0.55 ns	0.68±0.113	0.7253	< 0.5600	56	85.71
		Fibrinogen	618.5	666 ns	0.62±0.106	0.3789	> 741.5	40	87.50
		NT-proBNP	2417	1152 ns	0.64±0.124	0.2574	< 3446	85.71	50
		Lactate	4.3	1.2 *	0.74±0.116	0.0357	< 2.950	92	66.67
		Hemoglobin	11.5	10.4 ns	0.63±0.109	0.1864	< 9.150	28	100
Severity markers		REAu days	20	4 *	0.73±0.113	0.043	< 18.50	92	55.56
		Hospitalized days	34	13 *	0.76±0.104	0.0186	< 27.00	80	77.78
		APACHEII score	20	14 *	0.74±0.100	0.0335	< 16.50	68	77.78
		SOFA score	8	5 *	0.75±0.110	0.0244	< 7.500	88	66.67

AUC, area under the curve; REAu, Reanimation Unit; IL, interleukin; CRP, C-reactive protein; PCT, procalcitonin. Control group included healthy donors and abdominal surgery controls (n = 72), and sepsis group included n = 34. The median and cut-off values are expressed in the same units as Figure 15-17. *t*-test; ****p< 0.0001, ***p<0.0005, **p<0.005, *p<0.05 and ns, no significant difference (p>0.05).

Table 8. ROC analysis of total parameters analysed in this study for an increase in Reanimation Unit comparing control *vs* septic individuals.

			REAu Days <10	REAu Days ≥10	AUC±SE	*p* value	Cut-off	Sensitivity (%)	Specificity (%)
in vitro activation	LPS + ATP	Specks ASC	23.45	15.77 ns	0.59±0.109	0.4815	< 38.67	100	47.37
		IL-1β	1281	194.9 *	0.75±0.089	0.0213	< 363.5	72.73	77.27
		IL-18	1.08	0.76 ns	0.65±0.093	0.1567	< 1.401	100	45.45
	LPS + TcdB	Specks ASC	56.89	52.99 ns	0.55±0.117	0.9413	< 54.86	62.50	63.16
		IL-1β	1359	606.8 ns	0.69±0.100	0.0742	< 769.3	66.67	77.27
		IL-18	8272	5.32 ns	0.59±0.103	0.4230	< 5.572	66.67	68.18
	LPS	TNF-α	80.09	66.41 ns	0.60±0.103	0.3847	< 55.28	50	76.19
		IL6	17.95	5.99 ns	0.67±0.093	0.1096	< 14.85	75	59.09
Cellular components		Monocytes	0.64	0.39 *	0.75±0.087	0.0145	< 0.3500	50	95.45
		Leucocytes	14.92	13.90 ns	0.61±0.099	0.194	< 15.46	83.33	45.45
		Neutrophils	13.67	12.59 ns	0.62±0.099	0.2186	< 20.38	100	28.57
		Platelets	258	193.5 *	0.71±0.097	0.0485	< 202	58.33	81.82
		Lymphocytes	0.68	0.775 ns	0.54±0.101	0.7024	< 1.035	100	27.27
IL-1 family cytokines in plasma		IL-1α	36.01	20.88 ns	0.62±0.121	0.3598	< 32.54	77.78	57.14
		IL-1β	8.65	11.87 ns	0.58±0.116	0.5311	> 11.38	54.55	66.67
		IL1-RA	48.72	147 ns	0.65±0.121	0.1951	> 320	45.45	100
		sIL1RI	20.74	23.07 ns	0.54±0.111	0.7734	> 21.91	63.64	58.82
		sIL1RII	11189	13054 ns	0.59±0.117	0.5784	> 11500	63.64	58.82
		IL-18	310.6	649.9 ns	0.54±0.117	0.7486	> 336.6	80	52.94
		IL-18BP	1164	1443 ns	0.63±0.107	0.3830	> 1274	81.82	58.82
		IL-33	3.49	3.49 ns	0.51±0.133	0.9848	< 9.733	100	27.27
		IL-36	1.06	1.49 ns	0.54±0.146	0.8265	> 1.277	66.67	54.55
		IL-37	1.81	5.12 ns	0.66±0.148	0.3005	> 2.550	83.33	66.67
		IL-38	26.06	11.75 ns	0.81±0.113	0.1002	< 20.67	100	70
Other cytokines in plasma		TNF-α	63.31	118.9 *	0.72±0.106	0.0288	> 154.6	45.45	100
		IL-6	79.53	630.7 ns	0.68±0.119	0.1219	> 619.1	54.55	94.12
		IL-8	9.64	35.78 *	0.74±0.095	0.0326	> 12.43	90.91	64.71
		IL-15	9.45	9.08 ns	0.52±0.117	0.8652	< 15.41	90.91	43.75
		M-CSF	287.9	287.9 ns	0.55±0.110	0.6853	> 139.4	90.91	41.18
		HMGB1	49.92	54.77 ns	0.52±0.110	0.8856	> 29.20	100	16.67
Acute phase response		Ferritin	202.9	237.5 ns	0.55±0.109	0.6779	> 569.6	25	90.48
		sTREM-1	201.8	338 ns	0.56±0.103	0.5701	> 151.8	100	26.32
		SIGLEC-5	165704	299652 ns	0.65±0.1159	0.0980	> 200550	81.82	57.89
		PCT	6.96	3.6 ns	0.53±0.115	0.79	< 2.84	50	81.82
		CRP	25.65	19.99 ns	0.58±0.099	0.6965	< 31.32	92.31	38.10
Organ failure biomarkers		Urea	47	65.5 ns	0.64±0.103	0.2006	> 49	75	54.55
		Creatinine	1.01	0.98 ns	0.52±0.127	0.8941	< 0.69	41.67	95.45
		Bilirrubin	0.56	0.57 ns	0.60±0.106	0.1268	< 0.535	83.33	40
		Fibrinogen	695	600 ns	0.68±0.093	0.1162	< 653.0	69.23	65
		NT-proBNP	877	2604 ns	0.72±0.099	0.0531	> 1149	83.33	64.71
		Lactate	1.1	1.5 ns	0.60±0.109	0.3209	> 3.65	38.46	90.48
		Hemoglobin	10.8	9.9 ns	0.60±0.102	0.3278	< 11.7	83.33	40.91
Severity markers		REAu days	3	20.5 ****	1±0	<0.0001	> 9	100	100
		Hospitalized days	11	36.5 ****	0.89±0.059	<0.0001	> 24.5	83.33	86.36
		APACHEII score	15	17 ns	0.65±0.095	0.1583	> 12.50	91.67	40.91
		SOFA score	4.5	8 **	0.80±0.079	0.0017	> 7.5	58.33	90.91

AUC, area under the curve; REAu, Reanimation Unit; IL, interleukin; CRP, C-reactive protein; PCT, procalcitonin. Control group included healthy donors and abdominal surgery controls (n = 72), and sepsis group included n = 34. Evaluation of Reanimation Unit at day 10 was performed as it was the average of septic patients' stay in the hospital unit. The median and cut-off values are expressed in the same units as Figure 15-17. *t*-test; ****p< 0.0001, ***p<0.0005, **p<0.005, *p<0.05 and ns, no significant difference (p>0.05).

The percentage of monocytes with ASC speck formation in septic patients was reduced after the canonical activation of NLRP3 inflammasome with LPS and ATP, but not after the activation of the Pyrin inflammasome with LPS and TcdB, when compared to healthy and surgery control groups (**Figure 19A**). Despite the increase of IL-1β in plasma of septic patients, PBMCs from this cohort presented a decrease of IL-1β release upon NLRP3 inflammasome activation induced by LPS and ATP stimulation and upon Pyrin inflammasome activation induced by LPS and TcdB compared to surgery individuals, which corroborates previous studies (Giamarellos-bourboulis et al., 2011; Martínez-García et al., 2019) (**Figure 19B**). These defective inflammasomes activation was also found when IL-6 cytokine released was evaluated in septic patients, whereas did not occur in case of IL-18 and TNF-α released (**Figure 19C, D**).

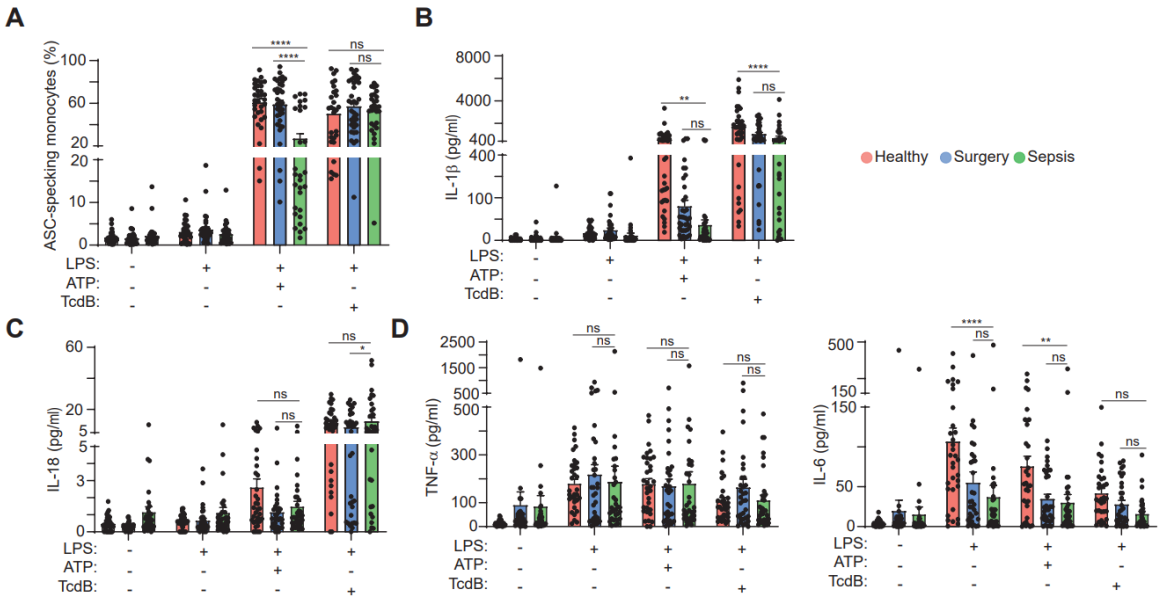

Figure 19. NLRP3 and Pyrin inflammasomes activation in sepsis. (**A-D**) Percentage of ASC-specking monocytes determined by time-of-flight assay (**A**) and ELISA for IL-1β in whole blood (**B**) and multiplexing for IL-18, TNF-α and IL-6 (**C-D**) supernatants from PBMCs isolated from septic patients within the first 24 hours of admission in the Reanimation Unit and control groups after NLRP3 inflammasome activation by LPS (1.6 µg/ml, 3 hours) and ATP (3 mM, 15 min in (**A**) or 30 min) and after Pyrin inflammasome activation by LPS (1.6 µg/ml, 3 hours) and TcdB (1 µg/ml, 30 min in (**A**) or 1 hour) treatments. Each dot corresponds to a different individual; data is represented as mean ± SEM; ANOVA test; ****p< 0.0001, **p<0.005, *p<0.05 and ns, no significant difference (p>0.05).

Also, the proportion of the different subsets of monocytes were evaluated. As expected, $CD14^{+}CD16^{++}$ inflammatory monocytes population increased after the priming with LPS (**Figure 20**). However, after NLRP3 and Pyrin inflammasome activation this population of monocytes decreased, being more remarkable in case of the canonical activation of the NLRP3 inflammasome (**Figure 20**).

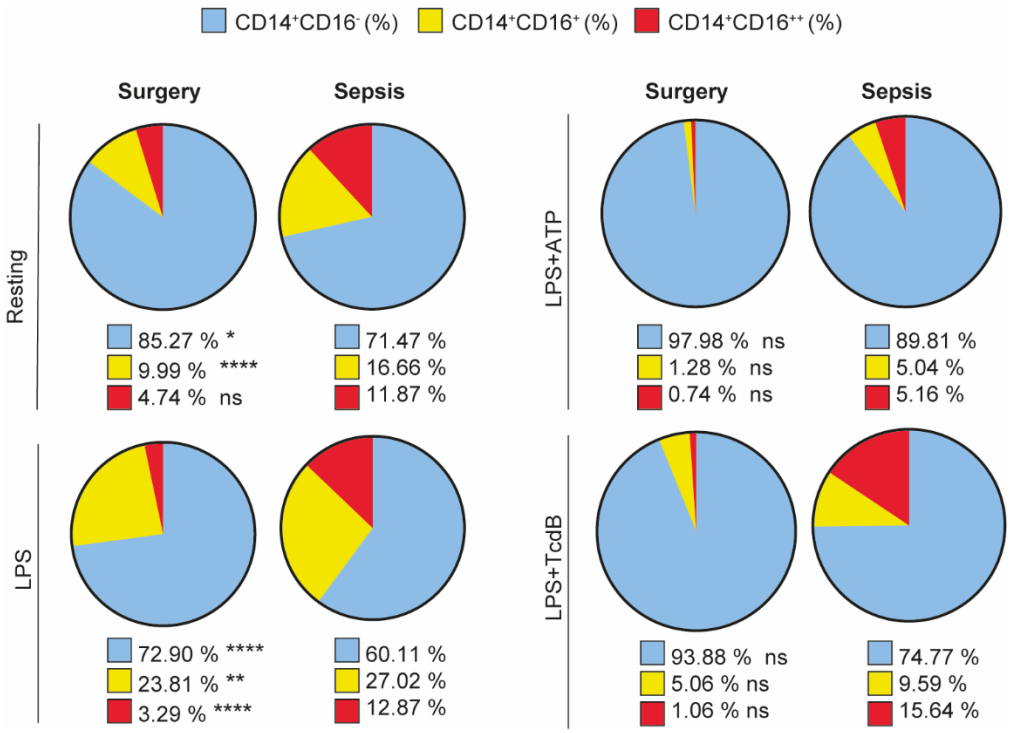

Figure 20. Percentage of monocytes phenotypes during sepsis. Sector graphs for the percentage of different monocytes populations from surgery controls or septic patients at day 1 after NLRP3 inflammasome activation by LPS (1.6 µg/ml, 3 hours) and ATP (3 mM, 15 min) and after Pyrin inflammasome activation by LPS (1.6 µg/ml, 3 hours) and TcdB (1 µg/ml, 30 min) treatments. ANOVA test; ****p< 0.0001, **p<0.005, *p<0.05 and ns, no significant difference (p>0.05).

In order to analyse the possible interactions between all the parameters studied in our septic cohort getting insight into a more globally inflammatory response during infection, we correlated all the variables studied in these patients. We found a positive association between the number of monocytes in blood with the percentage of ASC-specking monocytes after the canonical activation of NLRP3 inflammasome (LPS and ATP treatment) and with the IL-1β released after Pyrin inflammasome activation (LPS and TcdB treatment). In line with that, there was a positive correlation between the percentage of monocytes with ASC oligomers and the release of IL-1β, IL-18, TNF-α and IL-6 independently of which inflammasome was activated, thus indicating a positive feed-back between the pro-inflammatory response to infection (**Figure 21A**). Interestingly, we found an inverse association between the concentration of IL-1β in plasma, which was increased in septic patients when compared to healthy and surgery controls (**Figure 16**), with the *in vitro* activation of NLRP3 and Pyrin inflammasomes (**Figure 21B**). Also, others anti-inflammatory cytokines such as IL-37 and IL-38 correlated negatively with the percentage of ASC-specking monocytes after Pyrin and NLRP3 inflammasome activation, respectively (**Figure 21B**).

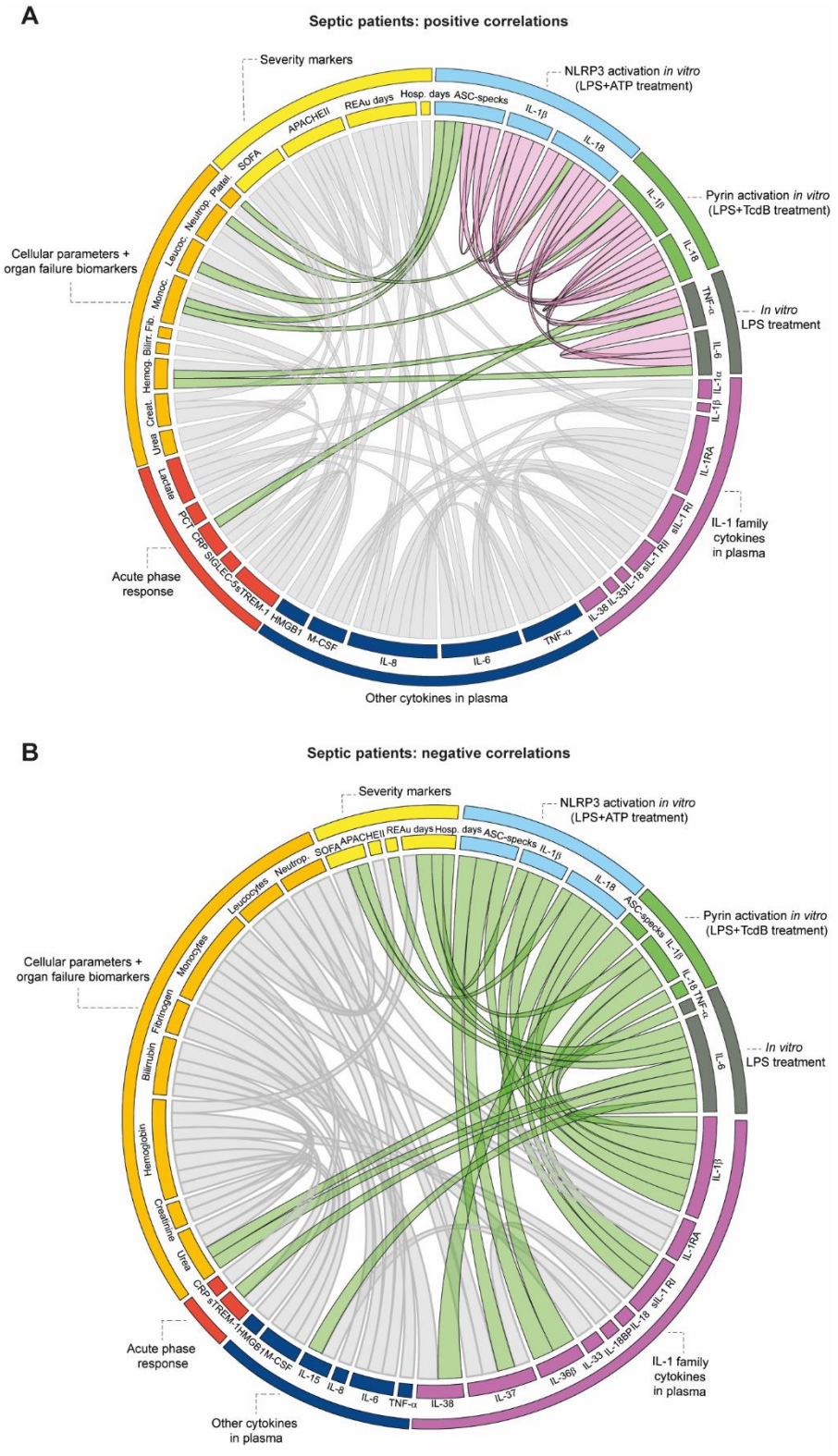

Figure 21. Sepsis biomarkers associations. (**A-B**) Chord diagrams of positive (**A**) and negative (**B**) associations between all the parameters studied in the intra-abdominal origin septic cohort. Only significant correlations (p value <0.05), calculated by Spearman and Pearson test, were evaluated. Width of the links correspond to the correlation coefficient. Some associations were underlined with colour patterns; purple lines indicate associations between *in vitro* assays and green lines between *in vitro* assays and the rest of parameters.

Taking into account all the previous results, we were able to verify that intra-abdominal origin septic patients on day 1 presented a different landscape than the control groups. This was confirmed by linear discriminant analysis clustering method (**Figure 22A**). Moreover, a multivariate logistic regression showed that the plasma concentration of sSIGLEC5, sTREM-1, IL-1β, IL-1RA, IL-18BP, sIL-1RII and creatinine, as well as the release ofd IL-1β in whole blood stimulated with LPS and TcdB identified septic patients among all the individuals studied with an area under the curve in the receiver operating characteristic (ROC) analysis of 0.925 (**Figure 22B**). In line, ROC analysis segregating septic patients from the control group identified several variables with high sensitivity and specificity (**Figure 22C** and **Table 9**).

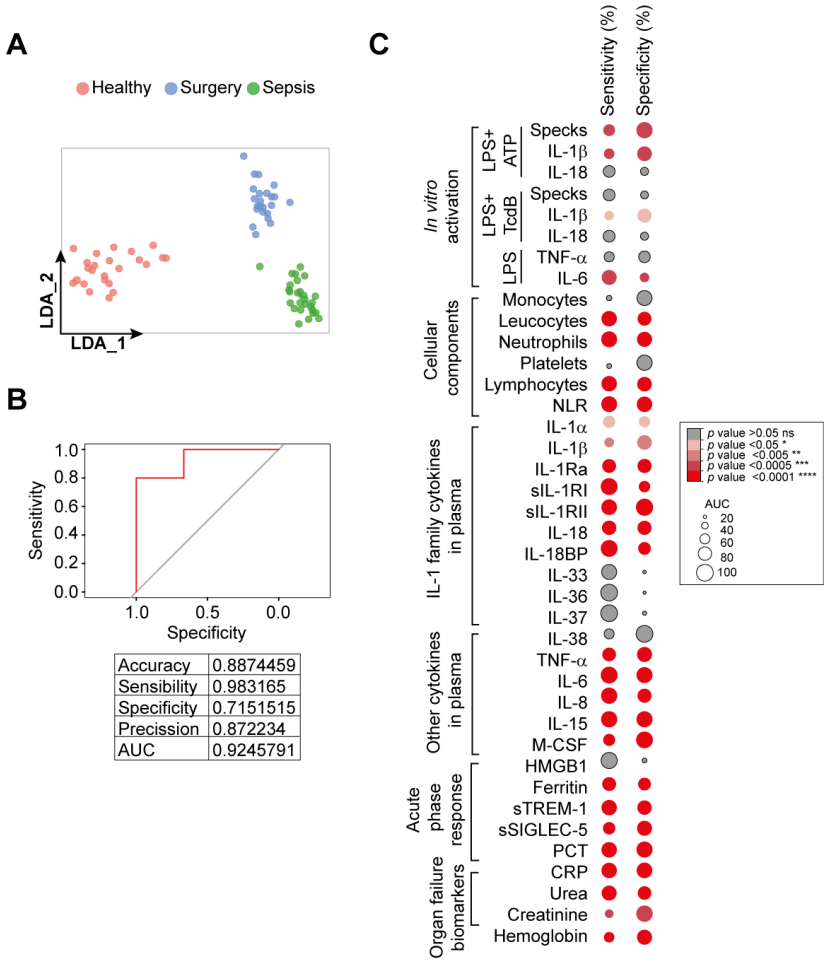

Accuracy	0.8874459
Sensibility	0.983165
Specificity	0.7151515
Precission	0.872234
AUC	0.9245791

Figure 22. Sepsis landscape at day 1 differs from healthy and surgery control groups. (**A**) Linear discriminant analysis (LDA) plot of clustering results of sepsis and control cohorts included in this study. (**B**) Screening accuracy and predictive power of the multivariate logistic regression predictive model generated from individuals included in this study. (**C**) Schematic representation of receiver operating characteristic (ROC) analysis for functional, cellular, biochemical and severity parameters comparing control *vs.* septic individuals. AUC, area under the curve; REAu, Reanimation Unit; IL, interleukin; CRP, C-reactive protein; PCT, procalcitonin; NLR, neutrophil-lymphocyte ratio. Control group included healthy donors and abdominal surgery controls (n = 72), and sepsis group included n = 34. Percentage of detection indicated indicates the percentage of septic individuals who presented measurable concentrations of each variable analysed. *t*-test; ****p<0.0001, ***p<0.0005, **p<005, *p<0.05 and ns, no significant difference (p>0.05).

Table 9. ROC analysis of total parameters analysed in this study comparing control *vs* septic individuals.

			Median control	Median sepsis	AUC±SE	*p* value	Cut-off	Sensitivity (%)	Specificity (%)
NFkB - NLRP3 - Pyrin *in vitro* activation	LPS + ATP	Specks ASC	61.59	16.57 ****	0.83±0.05	<0.0001	< 26.05	66.67	92.65
		IL-1β	1721	507.6 **	0.69±0.06	0.0019	< 513.1	58.82	84.29
		IL-18	1.134	0.8715 ns	0.57±0.6	0.2341	< 1.267	70.59	48.39
	LPS + TcdB	Specks ASC	54.11	56.72 ns	0.5±0.06	0.951	> 51.82	70.37	47.06
		IL-1β	1028	460.2 ***	0.71±0.06	0.0006	< 642.6	75.76	60.56
		IL-18	9.61	6.849 ns	0.52±0.07	0.7665	< 9.125	64.71	55.38
	LPS	TNF-α	151.8	78.82 ns	0.61±0.06	0.0788	< 98.11	60.61	69.70
		IL6	59.36	14.2 ***	0.72±0.05	0.0002	< 53.35	85.29	53.03
Cellular components		Monocytes	0.54	0.525 ns	0.51±0.07	0.8933	> 0.8300	32.35	89.55
		Leucocytes	7.085	14.45 ****	0.88±0.05	<0.0001	> 8.260	88.24	78.79
		Neutrophils	4.44	12.88 ****	0.93±0.03	<0.0001	> 6.450	90.91	85.94
		Platelets	223	233 ns	0.57±0.06	0.2324	> 347.0	29.41	91.3
		Lymphocytes	1.7	0.705 ****	0.88±0.04	<0.0001	< 1.190	88.24	83.08
		Neutrophil-lymphocyte ratio	2,199	15,65 ****	0.96±0.017	<0,0001	> 6.372	90.91	88.81
IL-1 family cytokines in plasma		IL-1α	10.74	25.39 *	0.67±0.07	0.0221	> 13.64	69.57	63.41
		IL-1β	5.225	10.87 **	0.70±0.07	0.0053	> 10.37	53.85	82.93
		IL1-RA	6.262	54.09 ****	0.87±0.04	<0.0001	> 20.31	78.57	80.39
		sIL1RI	5.065	21.91 ****	0.88±0.04	<0.0001	> 6.676	96.43	64.29
		sIL1RII	3345	11500 ****	0.95±0.04	<0.0001	> 6618	89.29	98.25
		IL-18	84.95	554.1 ****	0.83±0.05	<0.0001	> 159.8	81.48	80.36
		IL-18BP	552.7	1371 ****	0.91±0.03	<0.0001	> 614.7	96.43	71.93
		IL-33	2.578	3.492 ns	0.52±0.08	0.8128	> 1.431	90	20.73
		IL-36	1.92	1.49 ns	0.58±0.093	0.4069	< 8.740	100	19.05
		IL-37	3.81	2.55 ns	0.61±0.092	0.2654	< 17.23	100	25
		IL-38	11.75	18.87 ns	0.78±0.111	0.0978	> 15.31	60	100
Other cytokines in plasma		TNF-α	8.844	64.27 ****	0.83±0.05	<0.0001	> 15.07	77.78	85.71
		IL-6	0.41	49.95 ****	0.97±0.018	<0.0001	> 30.54	96.43	91.43
		IL-8	1.086	15.77 ****	0.92±0.03	<0.0001	> 2.902	92.86	80
		IL-15	0.9475	9.076 ****	0.93±0.04	<0.0001	> 2.340	92.59	91.67
		M-CSF	73.96	287.9 ****	0.83±0.058	<0.0001	> 191.3	67.86	96
		HMGB1	67.79	49.92 ns	0.52±0.07	0.7754	> 25.27	96.43	28.57
Acute phase response		Ferritin	38.5	234.5 ****	0.810±0.5	<0.0001	> 76.15	78.79	72.46
		sTREM-1	84.88	214.8 ****	0.90±0.04	<0.0001	> 149.7	87.5	82.14
		SIGLEC-5	87689	281125 ****	0.8±0.06	<0.0001	> 151841	70	85.45
		PCT	0.14	6.24 ****	0.93±0.03	<0.0001	> 0.7200	88.24	91.89
		CRP	4.4	23.82 ****	0.90±0.04	<0.0001	> 13.06	88.24	89.19
Organ failure biomarkers		Urea	28.5	51.5 ****	0.86±0.05	<0.0001	> 35.50	85.29	76.92
		Creatinine	0.73	1.005 ***	0.72±0.06	0.0003	> 1.135	47.06	94.03
		Hemoglobin	12.8	10.4 ****	0.74±0.06	<0.0001	< 10.95	58.82	85.51

AUC, area under the curve; REAu, Reanimation Unit; IL, interleukin; CRP, C-reactive protein; PCT, procalcitonin. Control group included healthy donors and abdominal surgery controls (*n* = 72), and sepsis group included *n* = 34. The median and cut-off values are expressed in the same units as Figure 15-17. *t*-test; ****p< 0.0001, ***p<0.0005, **p<0.005, *p<0.05 and ns, no significant difference (p>0.05).

1.1.2 Sepsis compromises NLRP3 inflammasome activation in patients with low survival

Despite the inflammatory response observed in the septic patients, we found that the majority of the septic patients analysed for the formation of ASC specks in monocytes (18 out of 27) after ATP stimulation presented very low percentage of ASC oligomers (from 3 to 24%) compared to the average from healthy and surgery control groups (60%) (**Figure 23A**). This allowed us to initially stratify septic patients into two groups, a group of patients with defective NLRP3 activation and another group with “normal” NLPR3 activation with no

significant differences when compared to control groups (**Figure 23B**). In both cases, septic patients presented a non-impaired activation of the Pyrin inflammasome (**Figure 23B**). We next found that this group of NLRP3-immunocompromised patients accumulated all of the deaths registered on the group of septic patients during their stay in Reanimation Unit, from day 1 to 89 (**Figure 23C** and **Table 10**). No deaths were registered on patients with normal activation of the NLRP3 inflammasome (**Figure 23C** and **Table 10**). Different clinical and biochemical parameters used to assess the severity of septic patients in the sepsis initiation were not able to accurately discriminate the group with profound NLRP3 immunosuppression, such as APACHE II score (**Figure 23D**), or PCT and CRP acute phase proteins (**Figure 23E**). Nevertheless, patients with severe NLRP3 suppression presented higher SOFA score, a longer stay at the Reanimation Unit and required more days of mechanic ventilation, but without statistical differences (**Figure 23D, F, G**). The evolution of clinical parameters, such as ΔSOFA, an accurate late-prognostic marker for sepsis-related deaths (Jones et al., 2009) calculated as the change in SOFA from day 1 to day 3, did not increase in these patients (**Figure 23H**).

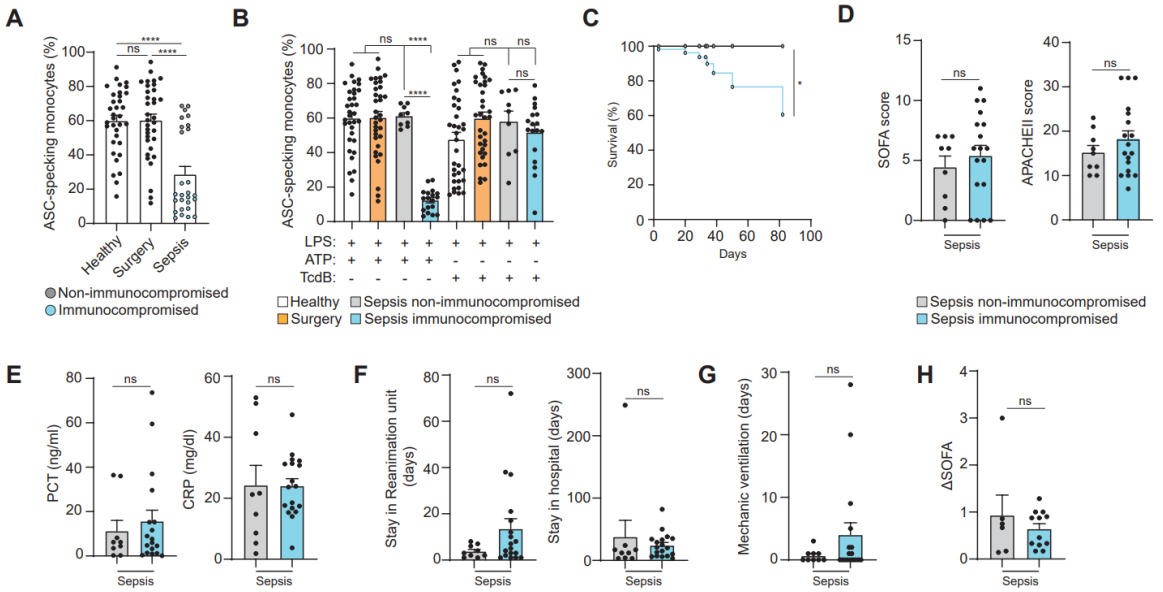

Figure 23. NLRP3 inflammasome activation is compromised in septic patients with high mortality. (**A**) Percentage of ASC-specking monocytes determined by time-of-flight assay in whole blood from septic patients within the first 24 h of admission at the Reanimation unit and control groups after NLRP3 inflammasome activation by LPS (1.6 μg/ml, 3 h) and ATP (3 mM, 15 min) treatment. There are two differently groups whose monocytes present normal ASC speck formation (grey dots) and other group with defective NLRP3 inflammasome activation (blue dots). (**B**) Percentage of ASC-specking monocytes from same samples as in (**A**) but where the septic patients were separated into two groups: non-immunocompromised (the grey dots in (**A**), represented by a grey bar) and immunocompromised (the blue dots in (**A**), represented by a blue bar). NLRP3 inflammasome was stimulated as in (**A**) and Pyrin inflammasome was activated by LPS (1.6 μg/ml, 3 h) and TcdB (1 μg/ml, 30 min) treatments. (**C**) Kaplan-Meier representation of non-immunocompromised (grey line) and immunocompromised (blue line) septic patients' survival. (**D-H**) SOFA and APACHEII scores (**D**), concentration of C-reactive protein (CRP) and procalcitonin (PCT) in plasma (**E**), days of stay on the

Reanimation unit and hospitalized (**F**), days of mechanical ventilation (**G**) and ΔSOFA calculated as the change in SOFA from day 1 to day 3 (**H**) in non-immunocompromised (grey bar) and immunocompromised (blue bar) septic patients at day 1. Each dot represents an individual patient; data is represented as mean ± SEM; Kruskal-Wallis test for (**A**); ANOVA test for (**B**); log-rank test for (**C**); and Mann-Whitney test for (**D-H**).

Table 10. Clinical and demographic data of septic patients with/without NLRP3 immunosuppression.

	NLRP3-IC septic patients	NLRP3-non-IC septic patients
N	18	9
Age		
Mean (range) ± SD	69.06 (42-89) ± 13.49	57.67 (40-72) ± 13.42
p value non-IC *vs* IC		$p > 0.05^{ns}$
Gender, N (%)		
Male	10 (55.55)	5 (55.55)
Female	8 (44.44)	4 (44.44)
p value non-IC *vs* IC		$p > 0.05^{ns}$
Clinical data		
Diabetes Mellitus II, N (%)	4 (22.22)	3 (33.33)
p value non-IC *vs* IC		$p > 0.05^{ns}$
High Blood Pressure, N (%)	11 (61.11)	3 (33.33)
p value non-IC *vs* IC		$p > 0.05^{ns}$
Oncologic, N (%)	7 (38.89)	4 (44.44)
p value non-IC *vs* IC		$p > 0.05^{ns}$
Infection acquired, N (%)		
Nosocomial	7 (38.89)	5 (55.55)
Community	11 (61.11)	4 (44.44)
p value non-IC *vs* IC		$p > 0.05^{ns}$
Organ dysfuntion, N (%)		
Renal	8 (44.44)	5 (55.55)
Respiratory	7 (38.89)	2 (22.22)
Cardiovascular	2 (11.11)	3 (33.33)
Hepatic	0	2 (22.22)
Hematological	7 (38.89)	3 (33.33)
p value non-IC *vs* IC		$p > 0.05^{ns}$
Mortality		
N (%)	6 (33.33)	0
Initial multi-organic failure*	4 (66.67)	
Secondary complications**	1 (16.66)	
Other pathologies	1 (16.66)	

*Mortality due to the initial organ dysfunction without clear recuperation after initial admission. **Recuperation of initial organ dysfunction after admission, mortality due to acquisition of new infectious processes that could result in another multiple organ dysfunction. IC, immunocompromised; SD, standard deviation; ns, not significant difference (p> 0.05) Chi-square (χ2) test.

Table 11. Peritoneal microbial isolation at sepsis onset in intra-abdominal origin septic patients.

	Total septic patients	NLRP3-IC septic patients	NLRP3-non-IC septic patients
N	34	18	9
Peritoneal isolation, N (%)			
Gram-negative bacteria			
Escherichia coli	21 (61.76)	12 (66.67)	7 (77.78)
Morganella morganii	3 (8.82)	3 (16.67)	0
Klebsiella sp.	8 (23.53)	2 (11.11)	2 (22.22)
Bacteroides sp.	6 (17.65)	5 (27.78)	1 (11.11)
Pseudomonas aeruginosa	5 (14.71)	3 (16.67)	1 (11.11)
Enterobacter sp.	3 (8.82)	2 (11.11)	1 (11.11)
Aeromonas sobria	1 (2.94)	0	1 (11.11)
Haemophilus parainfluenzae	1 (2.94)	1 (5.56)	0
Acinetobacter baumannii	1 (2.94)	0	1 (11.11)
Proteus sp.	3 (8.82)	1 (5.56)	1 (11.11)
Gram-positive bacteria			
Streptococcus sp.	6 (17.65)	5 (27.78)	1 (11.11)
Enterococcus sp.	6 (17.65)	3 (16.67)	2 (22.22)
Staphylococcus sp.	9 (26.47)	5 (27.78)	1 (11.11)
Fungi			
Candida sp.	9 (26.47)	4 (22.23)	3 (33.33)
Saccharomyces cerevisiae	1 (2.94)	1 (5.56)	0
Aspergillus sp.	1 (2.94)	0	0
Negative	3 (8.82)	0	1 (11.11)
p value against septic group		$p > 0.05^{ns}$	$p > 0.05^{ns}$
p value non-IC *vs* IC			$p > 0.05^{ns}$

NLRP3-IC, immunocompromised; ns, not significant difference (p >0.05) with Chi-square (χ^2) test.

Moreover, peritoneal microorganisms' isolation in this cohort of septic patients revealed that the majority of detected infections were polymicrobial developed by Gram negative bacteria (**Table 11**). In particular, *Escherichia coli* was present in more than 60% of patients, followed by *Klebsiella sp.* Between Gram positive isolated bacteria, *Staphylococcus sp.,* was the most frequently found (26.47%). In addition, *Enterococcus sp.* and *Streptococcus sp.* were identified in six septic patients. Furthermore, *Candida sp.* fungal isolation was also frequent (26.47%). In three septic patients the microbial isolation was negative, although exploratory laparoscopy showed clear signs and symptoms of intra-abdominal infections (**Table 11**). So that, infection type and specific organ dysfunction were also not able to differentiate septic patients, as well as differences in distribution of isolated bacteria (**Tables 5, 10 and 11**).

Furthermore, with the exception of the number of monocytes and neutrophils, which were found decreased in the NLRP3 immunocompromised septic patients, there were also no differences among cellular and biochemical parameters evaluated in both groups of septic patients (**Figure 24A, B, C**). IL-1β and IL-37 cytokines in plasma were the only cytokines associated with NLRP3- immunocompromised septic patients among all the IL-1 family members and related cytokines and plasmatic factors analysed (**Figure 24D, E, F**).

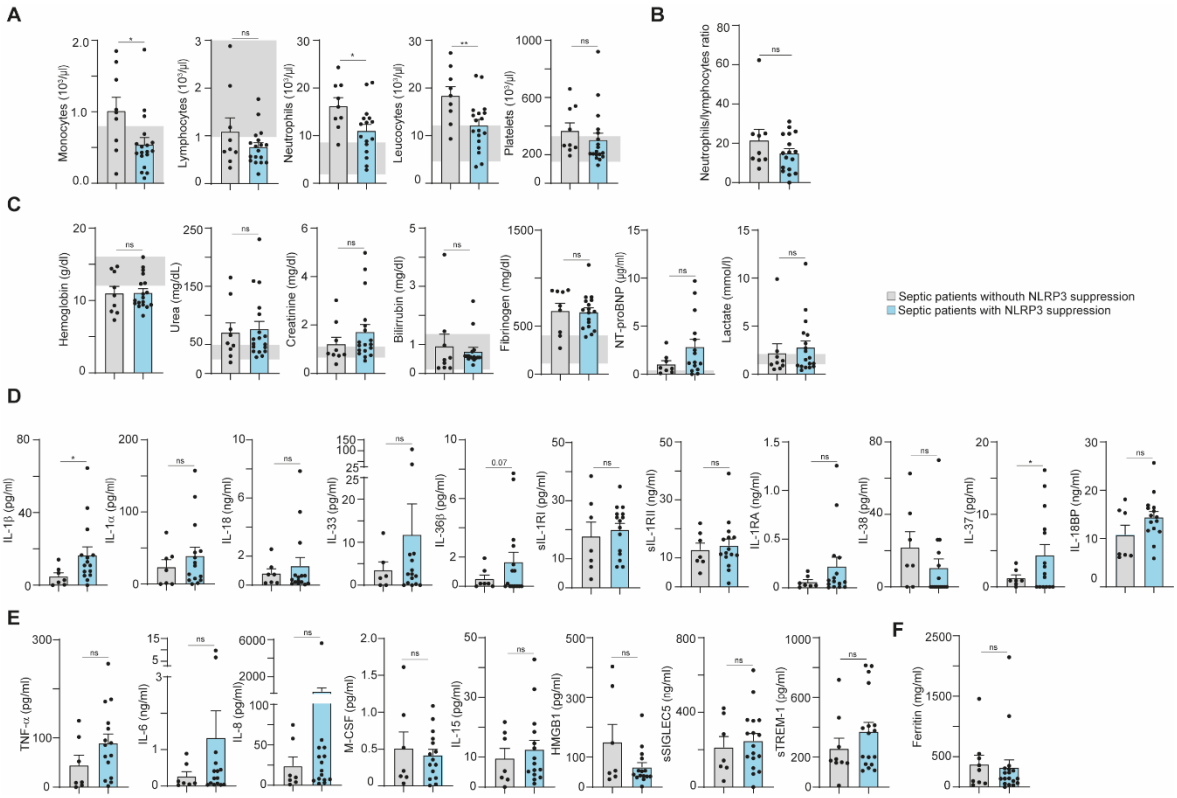

Figure 24. Inflammatory and biochemical determinations in septic patients. (**A**) Different cellular markers in the blood from septic patients at day 1. (**B**) Neutrophils-lymphocytes ratio. (**C-E**) Cellular components (**C**), IL-1 family members (**D**) and other cytokines and plasmatic factors related (**E**) in the plasma from septic patients at day 1. (**F**) Ferritin level in plasma. Blue represents septic patients with a profound deactivation of the NLRP3 inflammasome; grey shadow on graphs indicates the normal range in healthy population for each parameters analysed; each dot represents an individual patient; data is represented as mean ± SEM; *t*-test; **p<0.005, *p<0.05 and ns, no significant difference (p>0.05).

Patients with severe NLRP3 suppression also had defective production of IL-1β and IL-18 when compared to healthy controls and to NLRP3 non-immunocompromised septic patients after NLRP3 and Pyrin inflammasomes activation (**Figure 25A, B**). However, TNF-α and IL-6 did not identify the group with impaired NLRP3 inflammasome activation (**Figure 25C**).

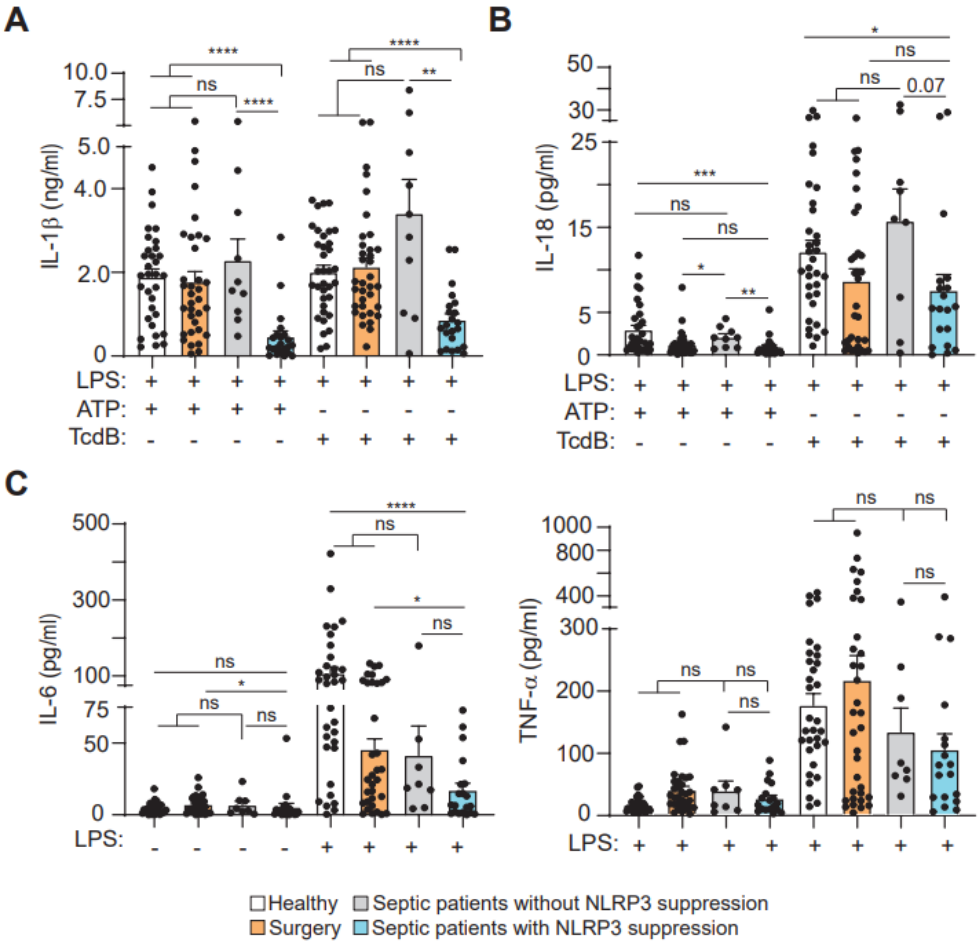

Figure 25. Proinflammatory cytokine released in NLRP3 immunocompromised septic patients. (**A-C**) ELISA for IL-1β in whole blood (**A**) and multiplexing for IL-18, TNF-α and IL-6 (**B, C**) supernatants from PBMCs isolated from septic patients within the first 24 hours of admission in the Reanimation Unit and control groups after NLRP3 inflammasome activation by LPS (1.6 µg/ml, 3 hours) and ATP (3 mM, 30 min) and after Pyrin inflammasome activation by LPS (1.6 µg/ml, 3 hours) and TcdB (1 µg/ml, 1 hour) treatments. Blue represents septic patients with a profound deactivation of the NLRP3 inflammasome; each dot corresponds to a different individual; data is represented as mean ± SEM; ANOVA test; ****p< 0.0001, ***p<0.0005, **p<0.005, *p<0.05 and ns, no significant difference (p>0.05).

In order to analyse the global inflammatory landscape in the group of septic patients with impaired NLRP3 inflammasome activation, an analysis of parameters' correlations was performed. Positive and negative associations between all the parameters analysed from both groups of septic patients were shown in **Figure 26.** Interestingly, the chord diagrams revealed visually that the inflammatory environment of both septic groups were different. In NLRP3 immunocompromised septic patients there was a positive correlation between the mortality predictors sTREM-1 and sSIGLEC5 with the severity scores APACHEII and SOFA. In line with that, the reduction in monocytes number presented in these patients correlated negatively with the last of these severity scores (**Figure 26A, B**), thus indicating a worst outcome for the patients that presented early impairment of NLRP3 activation.

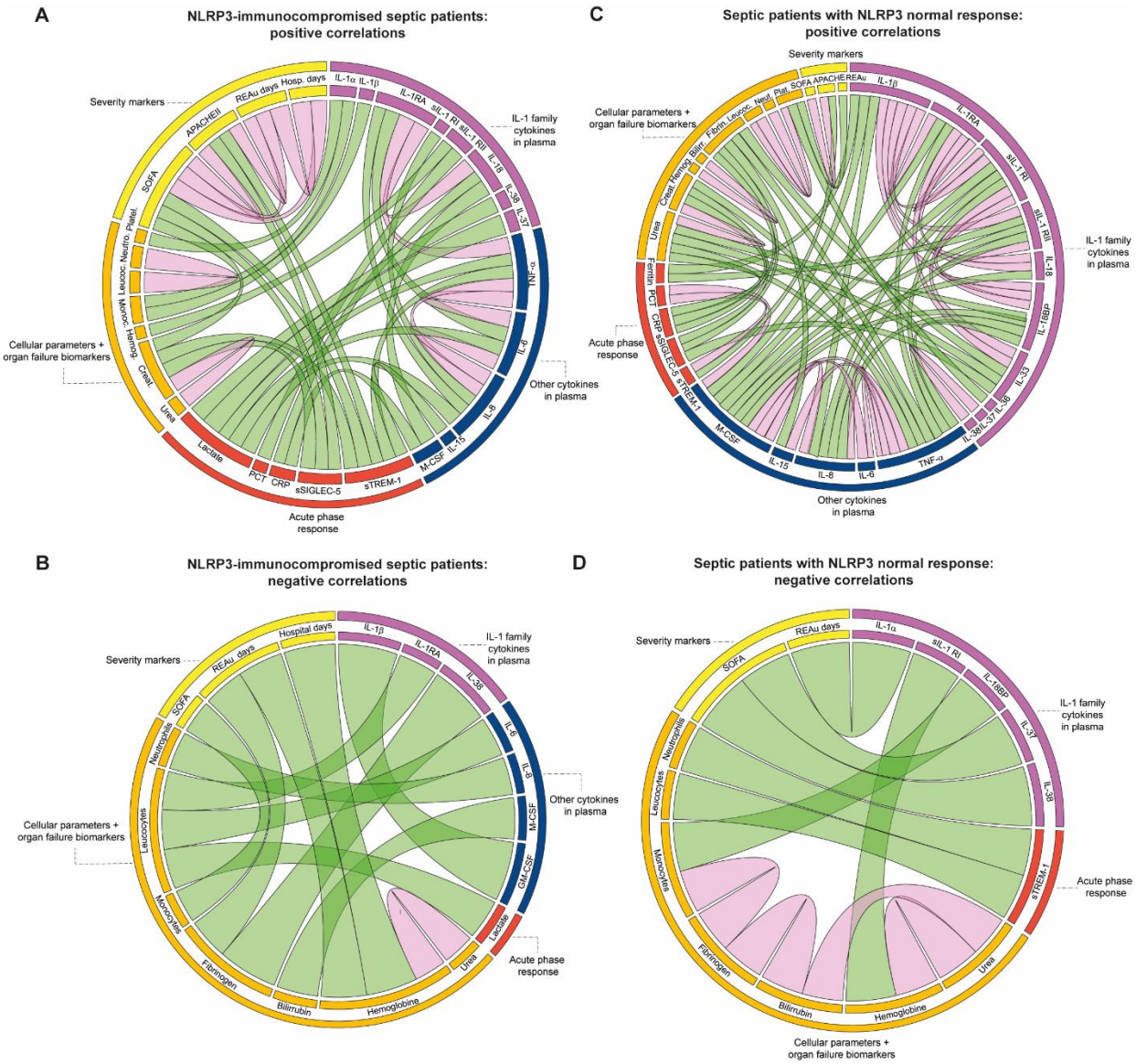

Figure 26. Septic patients with or without NLRP3 suppression's biomarkers associations. (**A-D**) Chord diagrams of positive (**A, C**) and negative (**B, D**) associations between all the parameters studied in the NLRP3 immunocompromised septic patients (**A-B**) and septic patients with normal NLRP3 activation (**C-D**). Only significant correlations (*p* value <0.05), calculated by Spearman and Pearson test, were evaluated. Width of the links correspond to the correlation coefficient. Purple lines indicate associations between the same parameters' category and green lines indicate associations among different categories.

This different landscape among septic individuals was confirmed by the latent structures-discriminant analysis (**Figure 27A**). In addition, ROC analysis segregating septic patients into these two groups showed that the release of IL-1β after NLRP3 and Pyrin inflammasomes activation identify the group with impaired NLRP3 inflammasome activation, with an area under the curve of 0.82-0.92 (**Figure 27B** and **Table 12**). Likewise, the concentration of IL-1β and IL-37 in plasma also differentiate the group of NLRP3 immunocompro-

mised patients inside the septic group, with an area under the curve of 0.8 and 0.9 respectively (**Figure 27B** and **Table 12**). Therefore, not only the group with impaired NLRP3 inflammasome activation present a worse prognosis but also, with the actual clinical scores and biomarkers currently employed in hospitals, the clinician cannot accurately predict septic patients presenting an immunosuppressive status with a high risk of death.

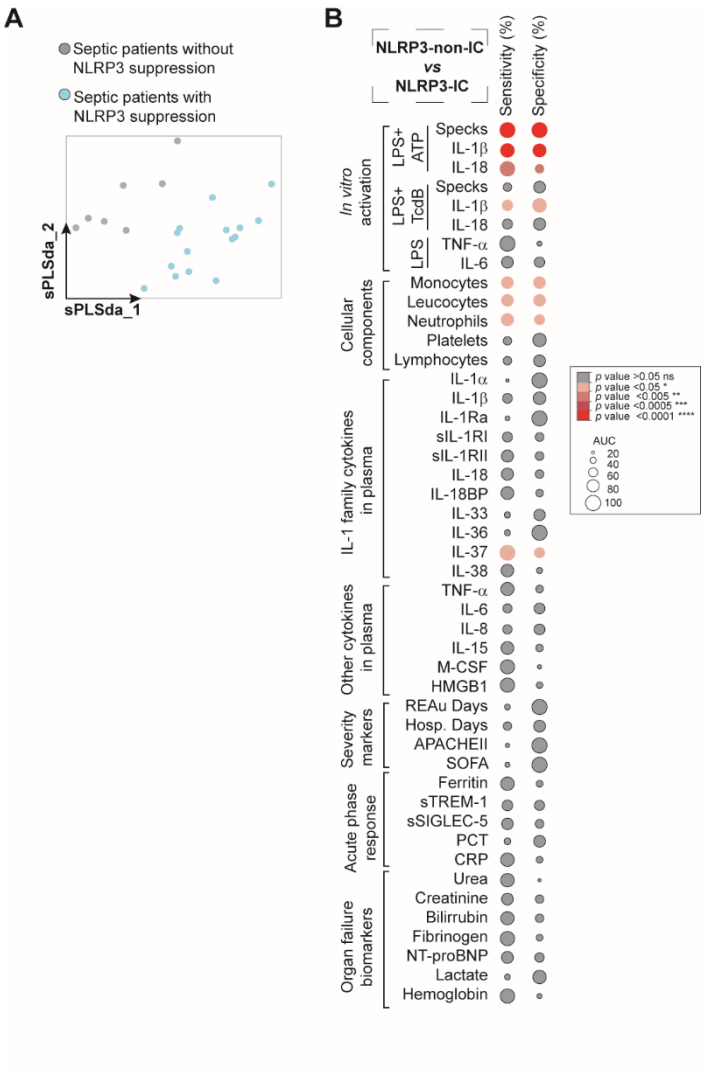

Figure 27. Inflammatory profile of NLRP3 immunocompromised landscape. (**A**) Latent structures-discriminant analysis (sPLS-da) plot of clustering results of impaired and non-impaired NLRP3 inflammasome activation. (**B**) Schematic representation of receiver operating characteristic (ROC) analysis for functional, cellular, biochemical and severity parameters comparing NLRP3 non-immunocompromised septic patients *vs.* NLRP3 immunocompromised septic patients. AUC, area under the curve; REAu, Reanimation Unit; IL, interleukin; CRP, C-reactive protein; PCT, procalcitonin; IC; immunocompromised. Non-immunocompromised included *n* = 9 individuals and NLRP3 immunocompromised septic patients included *n* = 18. Percentage of detection indicated indicates the percentage of septic individuals who presented measurable concentrations of each variable analysed. *t*-test; ****p< 0.0001, ***p<0.0005, **p<0.005, *p<0.05 and ns, no significant difference (p>0.05).

Table 12. ROC analysis of total parameters analysed in this study comparing NLRP3 non-immunocompromised *vs* immunocompromised septic patients.

			Median NLRP3-IC septic patients	Median NLRP3-non-IC septic patients	AUC±SE	*p* value	Cut-off	Sensitivity (%)	Specificity (%)
In vitro activation	LPS + ATP	Specks ASC	13.58	61.79 ****	1±0	<0,0001	> 38.67	100	100
		IL-1β	238	1666 ****	0.92±0.047	<0,0001	> 768.2	90	86.36
		IL-18	0.55	2.039 **	0.82±0.079	0.0051	> 0.6614	100	60
	LPS + TcdB	Specks ASC	54.86	63.9 ns	0.61±0.355	0.4441	> 63.02	55.56	77.78
		IL-1β	702	3115 **	0.82±0.098	0.003	> 2011	70	90.91
		IL-18	5.57	15.99 ns	0.68±0.115	0.1397	> 12.30	66.67	80
	LPS	TNF-α	71.65	82.59 ns	0.65±0.110	0.2317	> 28.39	100	33.33
		IL6	6.85	21.37 ns	0.71±0.104	0.0852	> 16.12	77.78	68.42
Cellular components		Monocytes	0.445	0.990 *	0.77±0.11	0.0268	< 0.5850	77.78	77.78
		Leucocytes	12.12	18.40 *	0.79±0.096	0.0146	< 14.96	77.78	77.78
		Neutrophils	11.10	16.03 *	0.75±0.103	0.0428	< 13.70	81.25	66.67
		Platelets	267.0	216.5 ns	0.67±0.107	0.1601	< 227.5	55.56	88.89
		Lymphocytes	0.72	0.565 ns	0.65±0.117	0.2261	< 0.6150	55.56	77.78
IL-1 family cytokines in plasma		IL-1α	27.56	35.36 ns	0.51±0.1489	0.9876	> 76.83	21.43	100
		IL-1β	11.85	4.759 *	0.80±0.107	0.0342	> 9.758	64.29	83.33
		IL1-RA	65.24	38.22 ns	0.60±0.114	0.2052	> 262.0	31.58	100
		sIL1RI	23.07	12.75 ns	0.56±0.154	0.6237	> 15.59	66.67	57.14
		sIL1RII	11748	10312 ns	0.58±0.139	0.5815	> 10327	80	57.14
		IL-18	380.9	735.4 ns	0.57±0.135	0.6298	< 712.9	80	57.14
		IL-18BP	1380	1103 ns	0.54±0.140	0.6489	> 757.6	84.21	50
		IL-33	3.035	3.177 ns	0.52±0.162	0.9291	> 5.541	41.67	75
		IL-36	1491	0.623 ns	0.70±0.135	0.2023	> 2.551	40	100
		IL-37	7434	0.864 *	0.90±0.083	0.0233	> 1.099	100	66.67
		IL-38	22.47	26.06 ns	0.57±0.183	0.7577	< 33.32	83.33	40
Other cytokines in plasma		TNF-α	85.54	31.25 ns	0.66±0.140	0.2648	> 11.47	86.68	51
		IL-6	218.6	79.53 ns	0.58±0.130	0.5815	> 169.4	60	71.43
		IL-8	17.91	9.642 ns	0.57±0.147	0.6298	> 12.44	61	71.44
		IL-15	9.66	4.28 ns	0.62±0.126	0.3329	> 3.213	84.21	50
		M-CSF	357.7 ns	204.5 ns	0.51±0.143	0.614	< 934.9	93.33	28.57
		HMGB1	47.52	54.77 ns	0.63±0.142	0.3477	< 141.9	93.75	42.86
Acute phase response		Ferritin	140.3	280.7 ns	0.59±0.126	0.4873	< 355.0	88.89	44.44
		sTREM-1	360.1	177.3 ns	0.61±0.117	0.3958	> 193.7	70.59	66.67
		SIGLEC-5	220432	142480 ns	0.56±0.139	0.6403	> 148500	76.47	57.14
		PCT	6.82	6.23 ns	0.56±0.118	0.6679	> 8.570	44.44	77.78
		CRP	23.82	21.22 ns	0.55±0.142	0.9618	> 15.05	88.90	44.45
Organ failure biomarkers		Urea	55	52 ns	0.51±0.124	0.9501	> 33.50	88.89	22.22
		Creatinine	1195	0.82 ns	0.65±0.117	0.2265	> 0.8800	77.78	55.56
		Bilirrubin	0.57	0.47 ns	0.65±0.141	0.6184	> 0.4850	87.5	55.56
		Fibrinogen	652	712 ns	0.57±0.138	0.8543	< 829.0	94.12	44.44
		NT-proBNP	1698	616.5 ns	0.71±0.1129	0.1266	> 763.5	78.57	62.5
		Lactate	2189	2.783 ns	0.59±0.116	0.4865	> 2.550	38.89	88.89
		Hemoglobin	10.2	10.7 ns	0.54±0.134	0.9260	> 8.800	94.44	33.33
Severity markers		REAu days	6	3 ns	0.66±0.104	0.1947	> 9	38.89	100
		Hospitalized days	20.5	12 ns	0.64±0.119	0.2466	> 18.50	55.56	77.78
		APACHEII score	16	15 ns	0.58±0.110	0.325	> 23.50	27.78	100
		SOFA score	6	6 ns	0.57±0.111	0.5065	> 7.500	33.33	100

AUC, area under the curve; REAu, Reanimation Unit; IL, interleukin; CRP, C-reactive protein; PCT, procalcitonin; IC, immunocompromised. Non-immunocompromised included *n* = 9 individuals and NLRP3 immunocompromised septic patients included *n* = 18. The median and cut-off values are expressed in the same units as Figure 15-17. *t*-test; ****p< 0.0001, **p<0.005, *p<0.05 and ns, no significant difference (p>0.05).

We have shown that acute phase proteins were increased during the first 24 hours after sepsis onset (**Figure 15A**). However, plasma concentration of CRP and PCT decreased after 3, 5 and 10 days of sepsis, reaching normal levels before hospital discharge (**Figure 28A**). Thus, denoting a gradual decrease of sepsis-related systemic inflammation. Moreover, we were able to obtain a blood sample from *n* = 8 NLRP3 immunocompromised patients that survived sepsis, once recovered at hospital discharge. Half of them were able to normally activate the NLRP3 inflammasome whereas the Pyrin inflammasome activation did not change (**Figure 28B**).

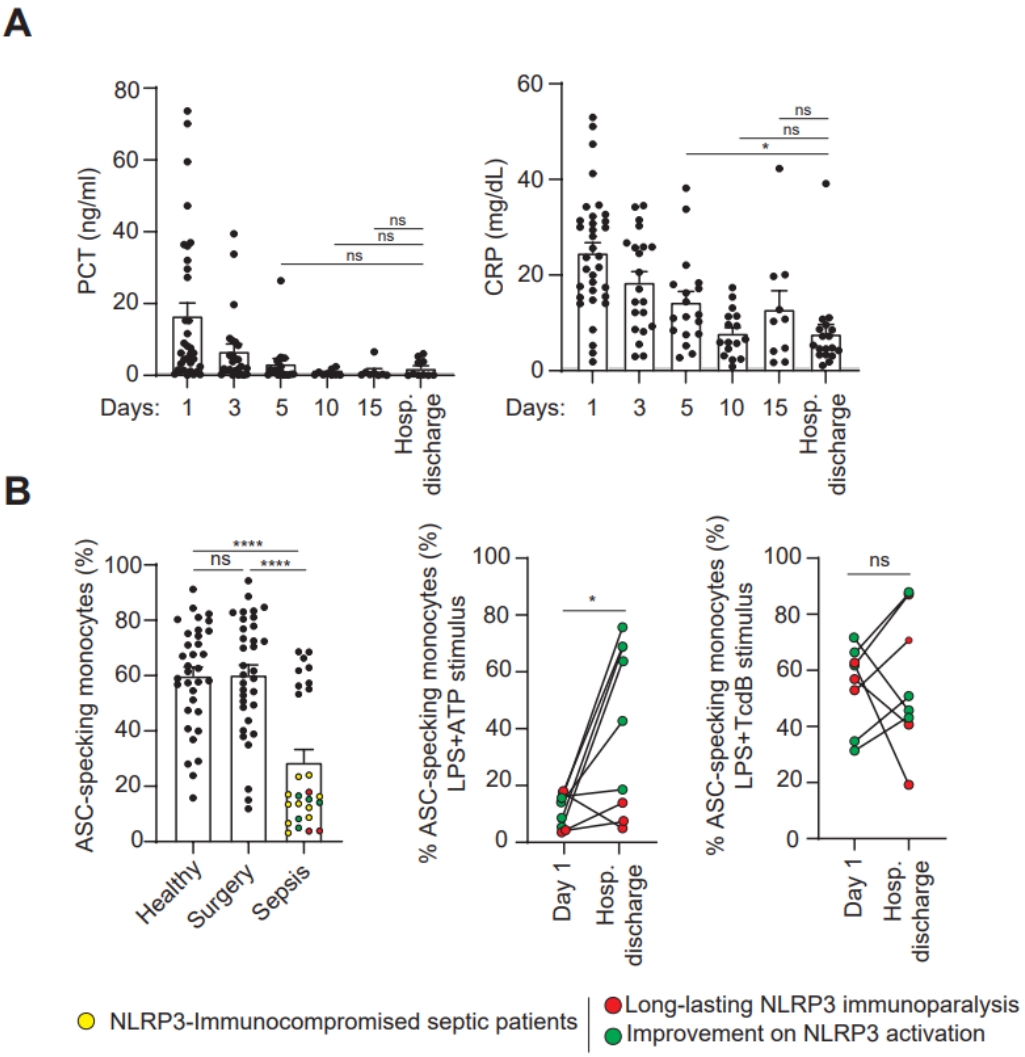

Figure 28. NLRP3 impairment during sepsis is transitory. (**A**) Concentration of procalcitonin (PCT) and C-reactive protein (CRP) in plasma of septic patients at day 1, 3, 5, 10, 15 and at hospital discharge. (**B**) Percentage of ASC-specking monocytes determined by time-of-flight assay in whole blood from septic patients at day 1 and at hospital discharge. NLRP3 inflammasome activation by LPS (1.6 µg/ml, 3 hours) and ATP (3 mM, 15 min) and after Pyrin inflammasome activation by LPS (1.6 µg/ml, 3 hours) and TcdB (1 µg/ml, 30 min) treatments. Each dot corresponds to a different individual; grey shadow on graphs indicates the normal range in healthy population for each parameters analysed; data is represented as mean ± SEM; ANOVA test in (**A**); *t*-test in (**B**); ****p< 0.0001, *p<0.05 and ns, no significant difference (p>0.05).

In *n* = 4 of these patients, NLRP3 activation continued impaired at hospital discharge. For one of these septic patients there is no clinical explanation, however we observed that another of these patients died a few days later from a severe deterioration caused by an unrelated disease. The two septic patients patients left were readmitted months later for a possible reinfection of the initial sepsis (**Figure 28B**). These results suggest that the NLRP3 inflammasome impairment during sepsis is a transitory state and could serve as a hospital discharge marker.

1. 2. Comparison of inflammatory markers between patients with COVID-19 and sepsis

Table 13. Demographic and clinical characteristics of the COVID-19 individuals included in this study.

	Healthy donors *n* = 69	Total COVID patients *n* = 208	Mild n= 41	Moderate *n = 128*	Severe *n = 39*
Age, mean (range) ± SD	48.26 (20-94) ± 18.44	64.31 (20-92) ± 15.56	72.86 (42-89) ± 14.16	61.20 (25-91) ± 14.16	71.49 (20-92) ± 17.07
p value		*p* <0.0001 *vs* Healthy donors			
Gender, N (%)					
Male	33 (47.8%)	88 (42.3%)	24 (58.5%)	71 (55.5%)	25 (64.1 %)
Female	36 (52.2%)	120 (57.7%)	17 (41.5%)	57 (44.5%)	14 (35.9 %)
p value		*p*>0.05 *vs* Healthy donors			
Patients with available clinical data (%)		89.9	80.5	92.9	89.7
Days of hospitalization, mean (range) ± SD		8.123 (1-133) ± 11.07	3.78 (1-13) ± 2.631	8.151 (1-34) ± 6.782	12.11 (1-133) ± 21.68
Supplemental O_2 (*n* (%))		157 (75.5%)	15 (36.5%)	105 (82.1%)	37 (94.8%)
Nasal glasses		98 (47.1%)	36.5%	59.3%	17.9%
Face mask ventilation		44 (21.2%)	-	21.1%	43.5%
Non-invasive Mechanical Ventilation / Intubation		15 (7.2%)	-	1.6%	33.3%
Critical Unit / ICU		39 (18.75%)	-	1.6%	94.8%
Lung disease due to COVID-19					
None		15 (7.2%)	21.9%	4.6%	-
Pneumonia		44 (21.2%)	31.7%	14.1%	33.3%
Bronchopneumonia		95 (45.7%)	29.2%	49.3%	51.2%
Bilateral Pneumonia		52 (25.0%)	14.6%	32.1%	12.8%
Death		29 (13.9%)	-	-	74.3%
Comorbidities (N (%))					
Hypertension		98 (47.1%)	41,4%	45,3%	58,9%
Dyslipidaemia		72 (34.6%)	24,3%	33,6%	48,7%
Diabetes		49 (23.6%)	9,7%	26,6%	28,2%
Hypothyroidism		43 (20.7%)	26,8%	6,2%	61,5%
Obesity		32 (15.4%)	12,2%	17,2%	12,8%
Heart disease		40 (19.2%)	26,8%	10,9%	38,4%

Bacterial sepsis and SARS-CoV-2 infection are life-threatening infectious diseases in which inflammatory markers can have prognostic value. Both pathologies are characterized by an exacerbated inflammatory response mediated in part by a cytokine storm. To gain insight into the inflammatory response during infection, we aimed to analyse a set of inflammatory cytokines and biomarkers in plasma between the group of patients with intra-abdominal sepsis (previously explained) and COVID-19 patients. As explained in Section 3.1.2 of this Thesis, plasma from a cohort of 208 individuals with COVID-19 disease were collected. Among these individuals, the largest group were those with mild symptoms (*n* = 128), followed by those with mild severity (*n* = 41) and those with severe symptomatology (*n* = 39) (**Table 13**).

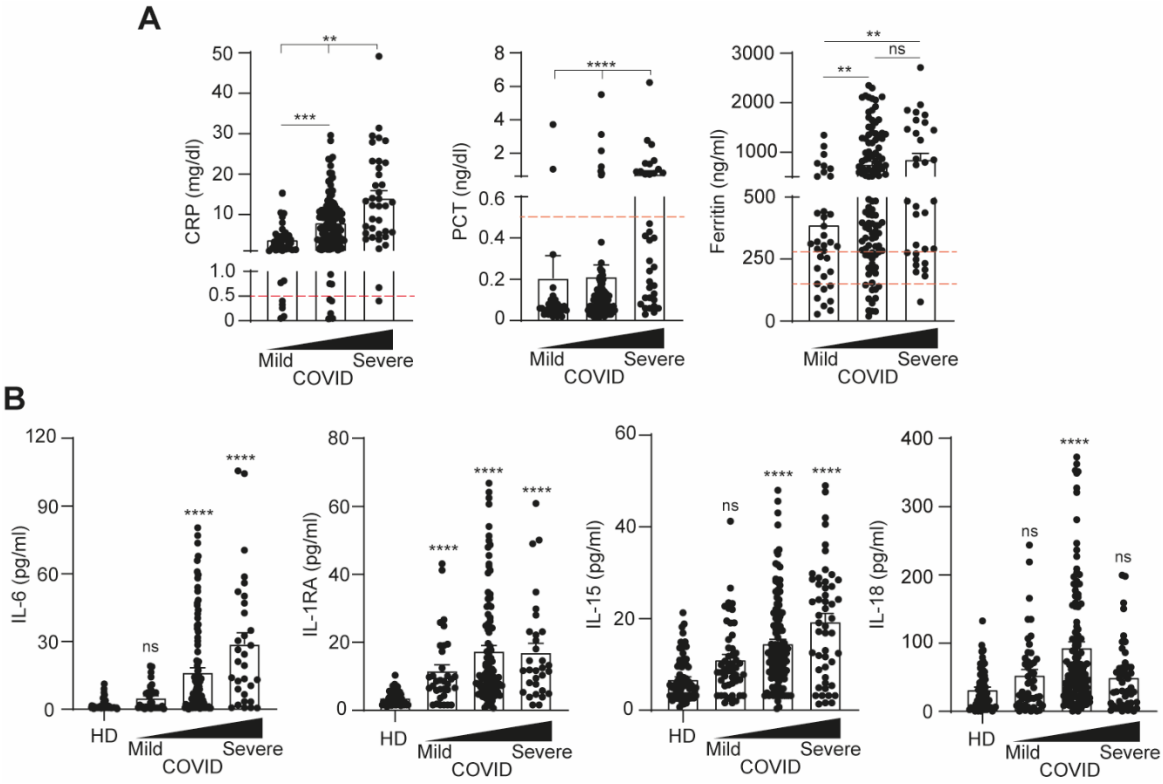

Figure 29. Biomarkers and inflammatory cytokines are markedly augmented in COVID-19 patients. (**A**) Concentration of C-reactive protein (CRP), procalcitonin (PCT) and Ferritin in plasma of COVID-19 patients. (**B**) IL-6, IL-1RA, IL-15 and IL-18 cytokines levels in plasma of healthy donors (HD) and COVID-19 patients in association with the clinical spectrum of SARS-CoV-2 infection (mild, moderate and severe). Each dot corresponds to an induvial patient; data is represented as mean ± SEM; dotted lines represent the normal range for each parameter analysed (the upper line in Ferritin's graph corresponds to the normal range for healthy men and bottom line for healthy women); Kruskal-Wallis test in (**A, B**); ****p < 0.0001, ***p<0.0005, **p<0.005, and ns, no significant difference (p>0.05).

COVID-19 patients presented elevated levels of CRP in the plasma following hospital admission, being the level of 90.9% of the patients above the standard threshold. As shown, the concentration of CRP significantly increased with the illness severity categories (**Figure 29A**). According to PCT levels, it was only significantly elevated in the severe

COVID-19 group, with only 10.6% of the COVID-19 above the standard of healthy threshold (**Figure 29A**). Whereas, ferritin, which was increased in the mild and severe groups, was above the standard healthy threshold in the 71.2% of the COVID-19 patients (taking into account male and female thresholds, **Figure 29A**). Moreover, the inflammatory cytokines IL-6 and IL-15 were significantly increased in the moderate and severe groups, but not in the mild group, when compared to healthy controls (**Figure 29B**). For their part, IL-1RA was elevated in the plasma of COVID-19 across all severity groups in comparation with healthy controls, while IL-18 plasma levels were increased only in moderate COVID-19 patients (**Figure 29B**).

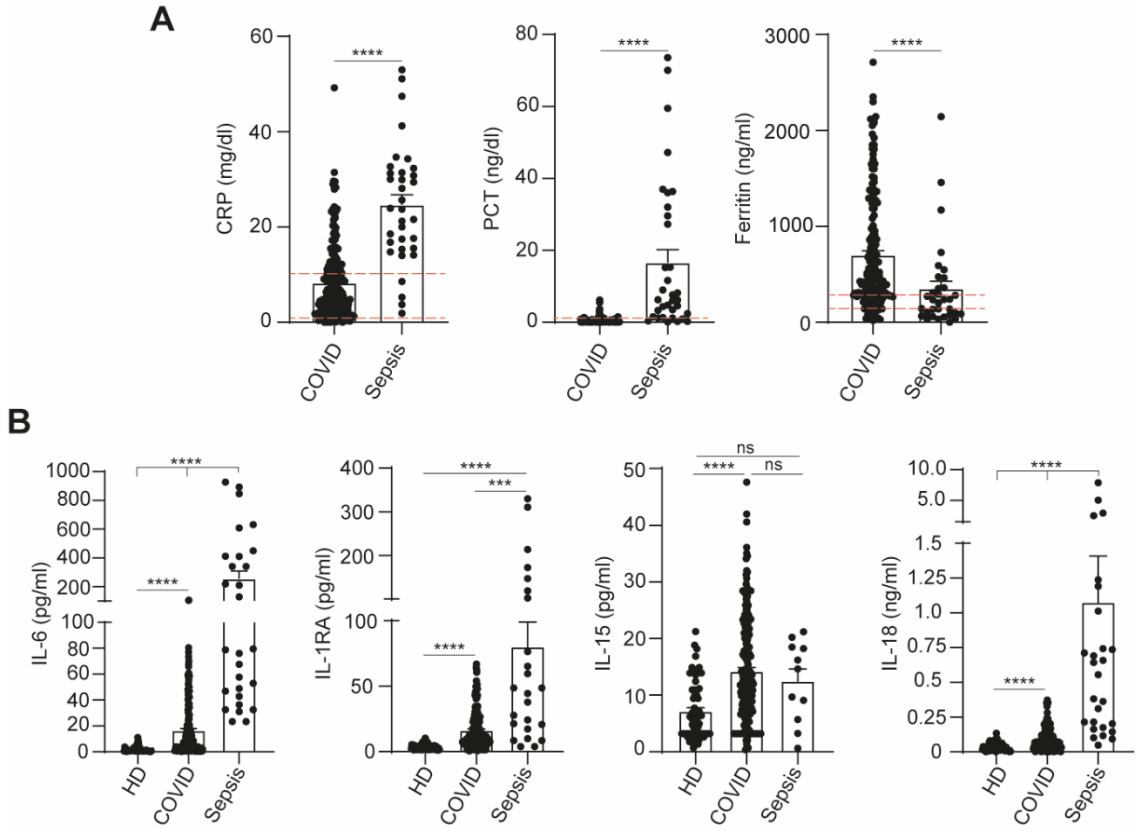

Figure 30. Inflammatory parameters at hospital admission in the plasma of patients with bacterial sepsis or COVID-19. (**A**) Concentration of C-reactive protein (CRP), procalcitonin (PCT) and Ferritin in plasma of sepsis and COVID-19 patients. (**B**) IL-6, IL-1RA, IL-15 and IL-18 cytokine levels in plasma of healthy donors (HD), intra-abdominal septic patients and COVID-19 patients. Each dot corresponds to an induvial patient; data is represented as mean ± SEM; dotted lines represent the normal range for each parameter analysed (the upper line in Ferritin's graph corresponds to the normal range for healthy men and bottom line for healthy women); *t*-test in (**A**) and Kruskal-Wallis test in (**B**); ****p < 0.0001, ***p<0.0005, and ns, no significant difference (p>0.05).

Differences on inflammatory markers were found between intra-abdominal septic patients and COVID-19 individuals. There was a higher level of CRP and PCT in patients with bacterial sepsis than in patients with COVID-19 (**Figure 30A**). On the contrary, a

marked decreased in Ferritin levels was found in the sepsis group compared to COVID-19 cohort (**Figure 30B**). These finding were in line with previous publications (Linarez-Ochoa et al., 2022; Perschinka et al., 2022). As expected, the IL-6 cytokine was elevated in both patients' cohort, being significantly augmented in septic patients (**Figure 30B**). The same results were obtained when the concentration of IL-1RA and IL-18 in plasma were evaluated between both groups of patients (**Figure 30B**). However, other cytokines like IL-15 presented no significant differences among bacterial sepsis and COVID-19 patients, neither sepsis patients compared to healthy donors' concentration (**Figure 30B**).

Chapter 2:

Inflammasome activation in autoinflammatory syndromes

2.1 Evaluation of NLRP3 and NLRC4 autoinflammatory-associated mutations in recombinant HEK293T cells

2.1.1 Expression of NLRP3 pathogenic mutations

We first generated 20 different mammalian vectors carrying different NLRP3 with autoinflammatory-associated mutations: V198M, R260W, D303A, D303G, D303H, D303N, E304K, L305P, Q306H, F309S, G326E, T348M, L353P and K355N (all found in the NBD of the NATCH domain); M406V, L411F and T433I (found in the HD1 of the NATCH domain), R488K (found in the WHD of the NATCH domain) and Q703K (found in the LRRs domain) (**Figure 31A**). It is important to stand out that mutations encounter within Walker B motif (residues between 295 to 304) affect an essential motif for NLRP3 activity because it is implicated in ATP-hydrolysis. Expression of all NLRP3 constructions after transient transfection in HEK293T cells were evaluated by immunoblot and fluorescence microscopy (**Figure 31B**). For all mutants, a punctua distribution for NLRP3 was found (**Figure 31C**).

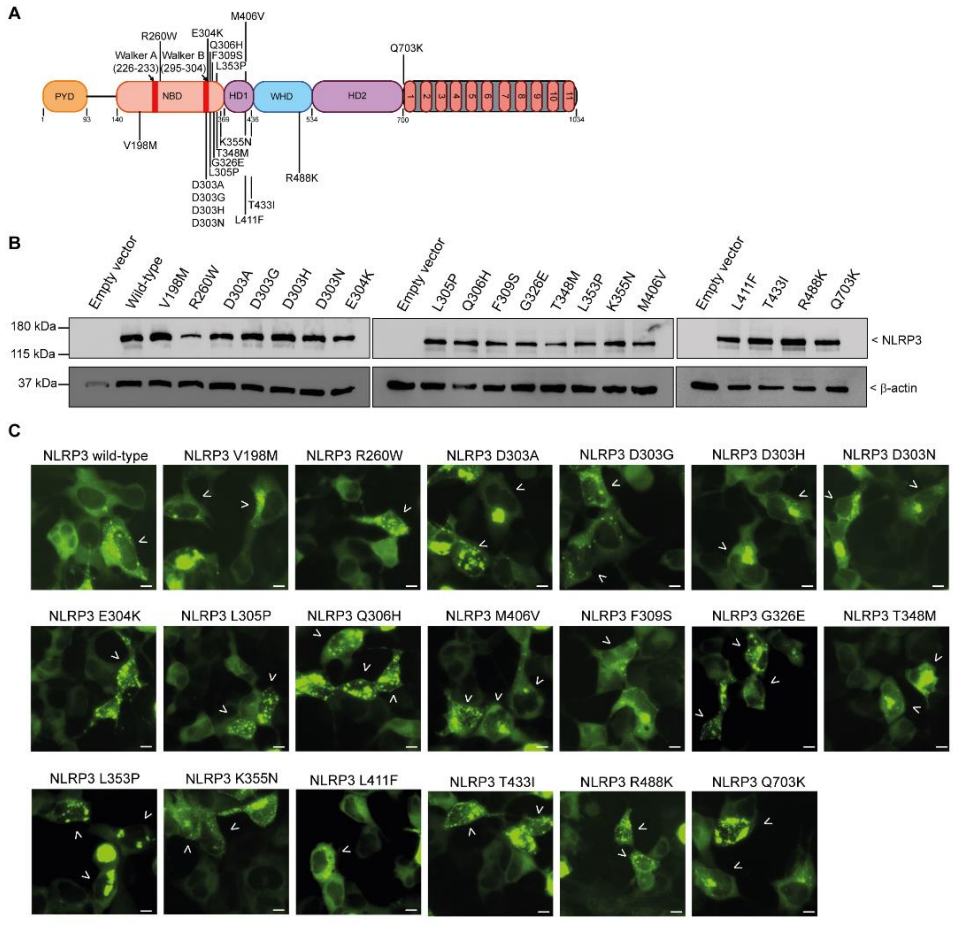

Figure 31. NLRP3 pathogenic mutants studied in this Thesis. (**A**) Schematic representation of amino acids changes and the position of the mutations along the NLRP3 inflammasome structure. (**B**) Immunoblot of lysates for the expression of empty-vector, NLRP3 wild-type or different NLRP3 mutants in transient transfected HEK293T cells. (**C**) Representative fluorescence microscopy images of HEK293T cells expressing NLRP3 wild-type or the different NLRP3 mutants tagged with YFP (green). Arrows indicate cells with NLRP3 puncta; scale bar 10 μm.

As indicated in **Table 14**, the different autoinflammatory-associated mutations of NLRP3 have been differentially identified in CAPS patients carrying mosaicism or germline diverse variant classification of the American College of Medical Genetics and Genomics, (variant of unknown significance (VUS), likely pathogenic, and pathogenic), different clinical CAPS phenotype and frequency in world-wide population. They also include a variety of changes in the polarity and charge of the amino acid changed. So that, this variability allows us to study a wide range of mutations associated with NLRP3 inflammasome.

Table 14. NLRP3 variants included in this Thesis.

Domain	Mutation	Mosaicism or Germline	ACMG Classification	Clinic	Polarity and charge changed by mutation: FROM	TO	Variant frequency/cases
	V198M	G	VUS	Uncertain	Non-polar	Non-polar	>200
	R260W	G	Pathogenic	FCAS/MWS	Basic (+)	Non-polar	>20
Walker B	D303A	M/G	Likely pathogenic	MWS	Acidic (-)	Non-polar	<5
	D303G	M/G	Pathogenic	NOMID	Acidic (-)	Non-polar	5 to 10
	D303H	M	Likely pathogenic	NOMID	Acidic (-)	Basic (+)	5 to 10
	D303N	M/G	Pathogenic	NOMID	Acidic (-)	Polar-Neutral	>20
	E304K	G	Pathogenic	NOMID	Acidic (-)	Basic (+)	<5
	L305P	G	Pathogenic	FCAS	Basic (+)	Non-polar	5 to 10
	Q306H	M	Likely pathogenic	Late-Onset MWS	Polar-Neutral	Basic (+)	<5
	F309S	G	Likely pathogenic	NOMID	Non-polar	Polar-Neutral	<5
	G326E	G	Likely pathogenic	NOMID	Non-polar	Acidic (-)	5 to 10
	T348M	M/G	Pathogenic	MWS	Polar-Neutral	Non-polar	>20
	L353P	G	Likely pathogenic	FCAS	Basic (+)	Non-polar	<5
HD1	K355N	M	Likely pathogenic	NOMID	Basic (+)	Polar-Neutral	<5
	M406V	M	Likely pathogenic	NOMID	Non-polar	Non-polar	<5
	L411F	M	Likely pathogenic	MWS	Basic (+)	Non-polar	<5
	T433I	M	Likely pathogenic	NOMID	Polar-Neutral	Non-polar	<5
	R488K	G	VUS	Uncertain	Basic (+)	Basic (+)	>100
	Q703K	G	VUS	Uncertain	Polar-Neutral	Basic (+)	>200

HD1, helical domain 1; VUS, variant of uncertain significance; FCAS, Familial cold autoinflammatory syndrome; MWS, Muckle-Wells syndrome; NOMID, Neonatal onset multisystem inflammatory disease; M, mosaicism; G, germline and ACMG, American college of medical genetics and genomics.

2.1.2 NLRP3 wild-type and uncertain significance NLRP3 variants have similar functionality

Low-penetrance NLRP3 variants have been identified at low frequencies in normal control populations and in some unaffected family members. However, there are individuals

in which have been associated to inflammatory symptoms, such as fever, cold-rash or headache, but symptoms occurred intermittently and their autoinflammatory phenotype is less pronounced in comparation with CAPS features (Aróstegui et al., 2004; Kuemmerle-Deschner et al., 2017). These characteristics make low-penetrance NLRP3 variants to be considered as variant of uncertain significance, as it is not clear if they could be pathogenic or not.

The recombinant function of NLRP3 with the V198M, R488K and Q703K variants have been analysed in this Thesis (**Table 14**). V198M and R488K have been associated with FCAS phenotype (Aróstegui et al., 2004), so that, we have tested the effect of the exposure of cells to different temperatures (37 ºC and 32 ºC) to assess if temperature has some effect on NLRP3 with VUS. Tapia-Abellán et al., demonstrated that HEK293T cells expressing NLRP3-associated variants result on a reduced BRET signal compared with wild-type receptor, suggesting an open conformation for active NLRP3 (Tapia-Abellán et al., 2019). In order to make a conformational BRET study of NLRP3 VUS variants, we aimed to express at the same level all mutant NLRP3 BRET sensors in transient transfected HEK293T cells and compare to wild-type NLRP3.

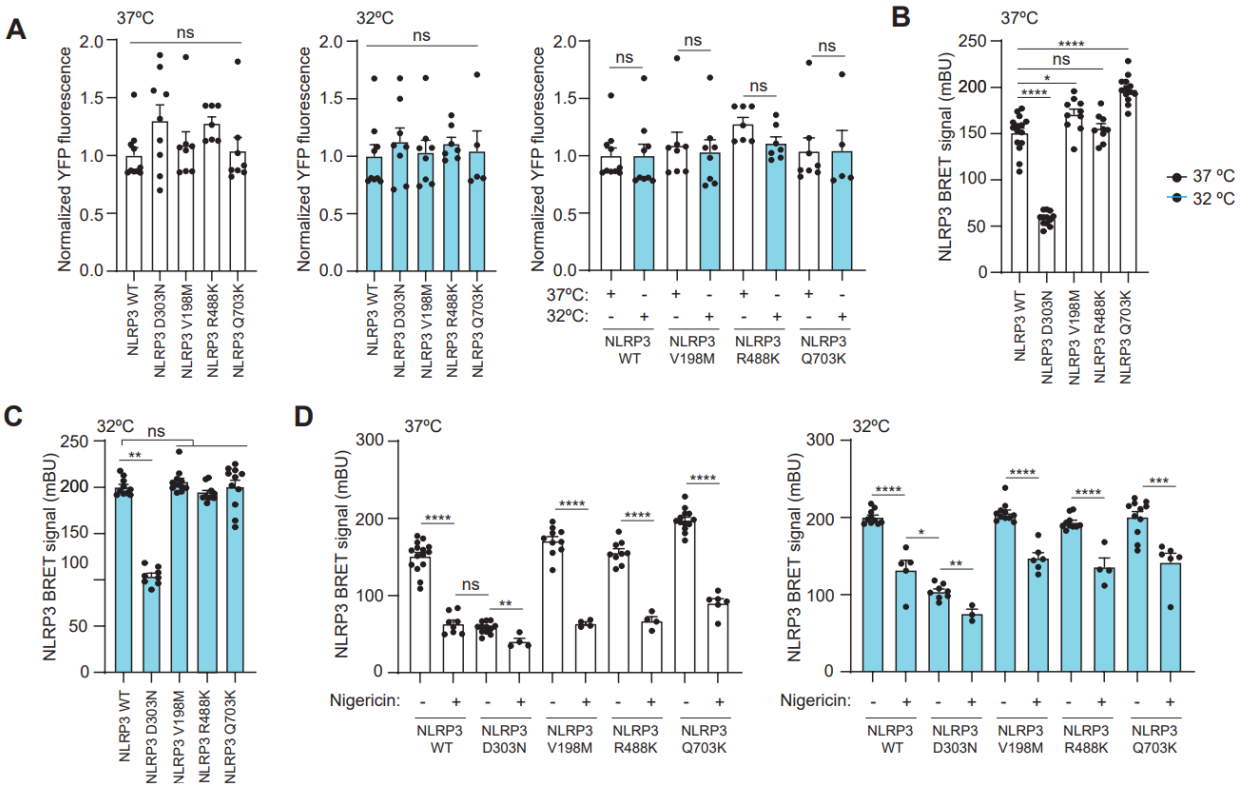

Figure 32. BRET signal of NLRP3 VUS variants. (**A**) Normalized YFP fluorescence and (**B, C, D**) BRET signal of HEK293T cells expressing wild-type and different YFP-NLRP3-Luc VUS variants. In (**D**), cells were activated or not for 30 min with nigericin (10 µM). Cells were incubated for 3 hours at 37 ºC (white columns) or 32º C (blue columns); data is represented as mean ± SEM; *n* = 3-15 independent experiments; ANOVA test in (**A**) and *t*-test; ****p<0.0001, ***p<0.0005, **p<0.005, *p<0.05 and ns, no significant difference (p>0.05).

First, we measured the YFP fluorescence by exciting it at 480 nm to assure equal expression and found that wild-type, D303N (used as a pathogenically mutant control) and NLRP3 VUS variants, presented a similar YFP signal and therefore similar expression independently of temperature (**Figure 32A**). BRET study shows that VUS variants have a significant higher BRET signal than D303N variant but similar than wild-type receptor (**Figure 32B**). Also, NLRP3 VUS were not affected when cells were incubated at 32 ºC (**Figure 32C**). Stimulated HEK293T cells expressing the wild-type BRET sensor with nigericin results in a decrease of BRET signal (Tapia-Abellán et al., 2019, 2021). We found that similarly to wild-type NLRP3 receptor, nigericin treatment induced a decrease of the BRET signal of NLRP3 carrying VUS variants (**Figure 32D**).

To assess the potential of NLRP3 VUS variants to induce ASC oligomerization, we co-expressed them with ASC and performed a Time-of-flight inflammasome evaluation by flow cytometry (Sester et al., 2016), as described in Material and Methods' section 10.2 of this Thesis. We gated cells with low expression of ASC and NLRP3, where we found an active NLRP3. As it shown in **Figure 33A**, the absence of the domains required for the oligomerization of NLRP3 and ASC, as well as, specific mutations affecting Walker B motif, impairs the formation of ASC oligomers. We found that neither V198M nor Q703K variants resulted in a basal increase of ASC positive cells and, similarly, wild-type NLRP3 was induced after nigericin treatment. However, R488K presented approximately 15-20% of cells with ASC oligomers at baseline, which were not increase after nigericin treatment (**Figure 33B**). This data suggests that, with exception for R488K, NLRP3 VUS variants present a similar structure and function than wild-type NLRP3.

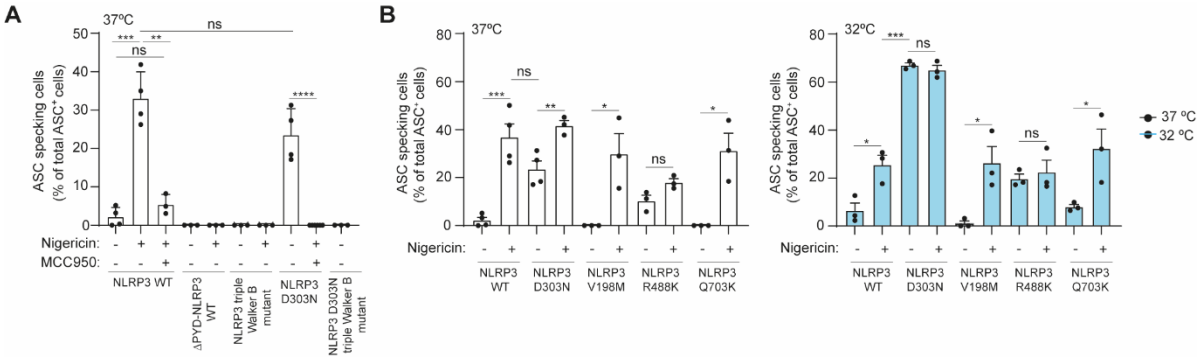

Figure 33. Percentage of ASC specking HEK293T cells expressing ASC-RFP and different BRET sensors of NLRP3 wild-type, D303N and VUS variants. (**A**) Percentage of ASC specking HEK293T cells expressing ASC-RFP and the BRET sensors of NLRP3 wild-type, ΔPYD-NLRP3 wild-type, NLRP3 wild-type triple mutated in Walker B motif, D303N and D303N triple mutated in Walker B motif. (**B**) Percentage of ASC specking HEK293T cells expressing ASC-RFP and the BRET sensors of NLRP3 wild-type, D303N and NLRP3 VUS variants. Cells were activated or not for 30 min with nigericin (10 µM) and incubated for 3 hours at 37 ºC (white columns) or 32º C (blue columns); cells were treated or not with MCC950 (10 µM) overnight; data is represented as mean ± SEM; *n* = 3-4 independent experiments; *t*-test; ****p<0.0001, ***p<0.0005, **p<0.005, *p<0.05 and ns, no significant difference (p>0.05).

We were able to obtain blood samples of individuals carrying the different NLRP3 VUS variants (**Table 15**). Then, we analysed the percentage of monocytes with ASC specks and, we found that there was a small trend to increase ASC specking monocytes at baseline when compared with monocytes from healthy donors (**Figure 34A**). This trend was also present when monocytes where primed with LPS but disappeared after the canonical activation of NLRP3 with ATP (**Figure 34A**). In fact, neither an asymptomatic individual nor a good-responder colchicine-treated patient carrying the V198M variant did not responded to ATP stimulation. When measuring IL-1β release from PBMCs, we observed a similar release to healthy donors when the cells were stimulated with LPS and LPS+ATP, except for a patient with the Q703K variant that presented a decrease in cytokine release (**Figure 34B**). Also, supporting our previous observation that R488K variant could favours inflammasome activation (**Figure 33**), one patient with the R488K variant presented elevated release of IL-1β in basal conditions and after priming with LPS (**Figure 34B**). According to the release of TNF-α and IL-6, patients carrying the NLRP3 VUS variants presented a decrease in cytokine release when the cells were treated with LPS (**Figure 34C, D**). However, in PBMCs from patients carrying the R488K variant there was a basal release of TNF-α and IL-6 (**Figure 34C, D**).

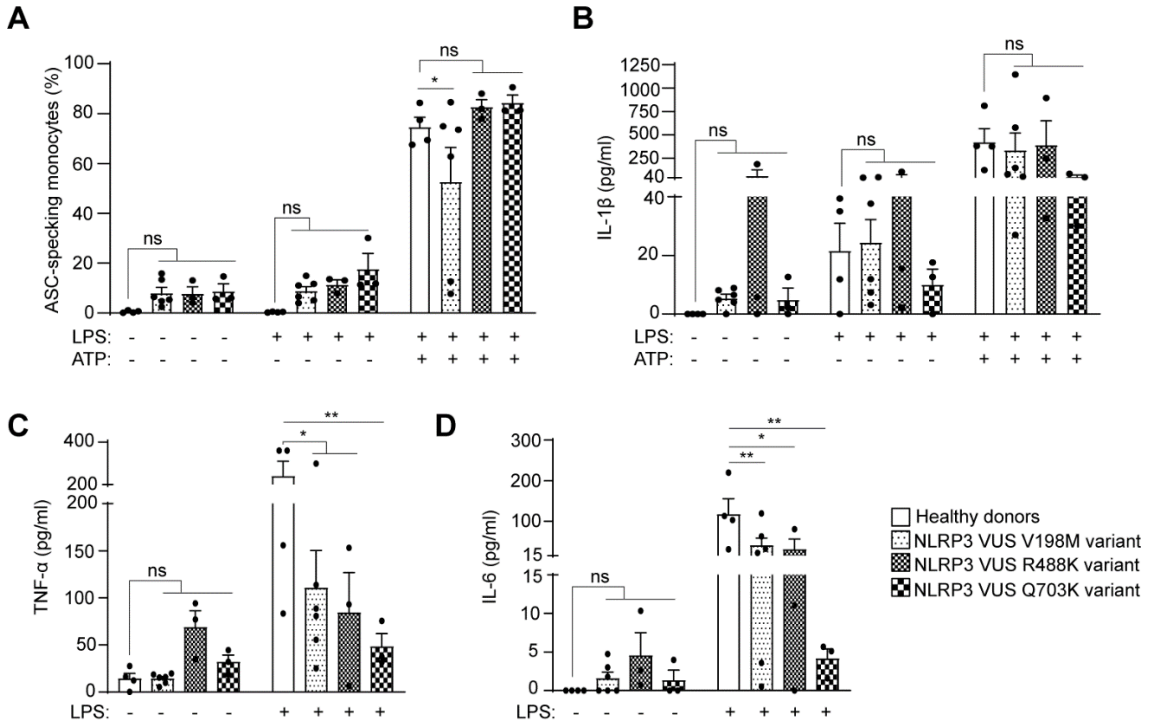

Figure 34. NLRP3 inflammasome activation in VUS variant patients. (**A**) Percentage of ASC-specking monocytes determined by time-of-flight assay in whole blood, (**B**) IL-1β, (**C**) TNF-α and (**D**) IL-6 in cell-free supernatants from PBMCs of healthy individuals and from patients with NLRP3 VUS variants primed with LPS (1.6 μg/ml for 3 hours) and stimulated with ATP (3 mM for 30 min) (**A, B**). Each dot represents an individual patient; data is represented as mean ± SEM; ANOVA test; **p<0.005, *p<0.05 and ns, no significant difference (p>0.05).

Table 15. Clinical and demographics characteristics of patients with NLRP3 VUS variants included in this Thesis.

Patient ID	Sex	Age	*NLRP3* Mutation	Phenotype	Age at disease onset	Age at diagnosis	Actual Treatment	Treatment started at diagnosis	Response to treatment
1	F	48	V198M	UAD	33	45	None	No	N/A
2	F	18	V198M	MWS	Birth	11	Steroids on flare, Antihistamines	Yes	Good
3	F	26	R488K	Not defined	27	27	Steroids, Azathioprine	Yes	Good
4	F	43	R488K	UAD	6	42	Colchicine, NSAID	Yes	Good
5	M	61	V198M	Not defined	40	40	None	No	N/A
6	M	25	V198M	FCAS/MWS	12	15	Colchicine, Steroids on flare	Yes	Good
7	F	22	V198M	Not defined	21	22	Hormone Therapy	No	N/A
8	F	31	V198M	UAD	18	28	Colchicine	Yes	Good
9	M	23	R488K	FCAS	15	19	NSAID	No	Good
10	M	39	Q703K	UAD	29	30	Anakinra	Yes	Good
11	M	35	Q703K	UAD	28	34	Colchicine	Yes	Good
12	M	59	Q703K	UAD	40	54	Steroids on flare	Yes	Good
13	M	73	R260W	MWS	Childhood	61	Canakinumab	Yes	Good

F, Female; M, male; NOMID, Neonatal, multisystemic, inflammatory disorder; MWS, Muckle-Wells Syndrome; FCAS, Familial Cold Autoinflammatory Syndrome; UAD, Undefined Autoinflammatory Disease; NSAID, Non-Steroidal Anti-Inflammatory Drugs and N/A, not applicable.

2.1.3 NLRP3 FCAS variants are activated by cold, while NLRP3 wild type is blocked

As described in **Table 15**, we analysed three FCAS variants (R260W, L305P, L353P), although R260W has been found in patients with FCAS and MWS phenotypes (Aganna et al., 2002; Hoffman et al., 2003). FCAS-associated NLRP3 mutants have been suggested to be active upon cold exposure, process mediated by the heat shock cognate protein 70 (HSC70) (Karasawa et al., 2022; Raghawan et al., 2023). To gain insights into the conformation of NLRP3 with FCAS-associated mutations, we next assessed NLRP3 BRET signal at 37 ºC and 32ºC. FCAS variants presented a similar expression level with independence of temperature, as assessed by YFP fluorescence (**Figure 35A**). The conformational studies by BRET revealed that the three variants presented a decrease in BRET signal in comparation with wild-type receptor (**Figure 35B**), being similar to the BRET signal of the D303N variant (MWS/CINCA) (**Figure 32B, C**) and wild-type NLRP3 receptor after nigericin treatment (**Figure 35C**). However, while wild-type NLRP3 showed a highly significant increase of the mutation associated to BRET signal upon cold temperature, FCAS-associated NLRP3 variants were not changing their BRET signal when exposed to 32 ºC (**Figure 35B**). That suggests that wild-type NLRP3 structure could be closed and inhibited at low temperatures, whereas FCAS-associated variants were insensible to cold exposure.

In fact, nigericin stimulation induced a higher decrease of the BRET signal in wild-type NLRP3 at 32ºC than FCAS-associated NLRP3 variants which did not change (**Figure 35C**).

Supporting these results, the analysis of ASC specking positive cells after co-expression of NLRP3 wild-type receptor with ASC showed that nigericin treatment induced less cells with ASC specks at 32ºC than at 37ºC in case of (**Figure 35D**). On the other hand, FCAS–associated NLRP3 variants presented an increase of basal ASC oligomers at 32ºC (**Figure 35D**). Moreover, macrophages expressing wild-type NLRP3 release less IL-1β with similar TNF-α release after the canonical activation of NLRP3 inflammasome at 32ºC (**Figure 35E**). Surprisingly, the NLRP3 L305P FCAS-associated variant presented a basal increase of ASC specking cells, not only at 32ºC, but also at 37ºC, probably because this pathogenic variant could be inducing spontaneous inflammasome activation.

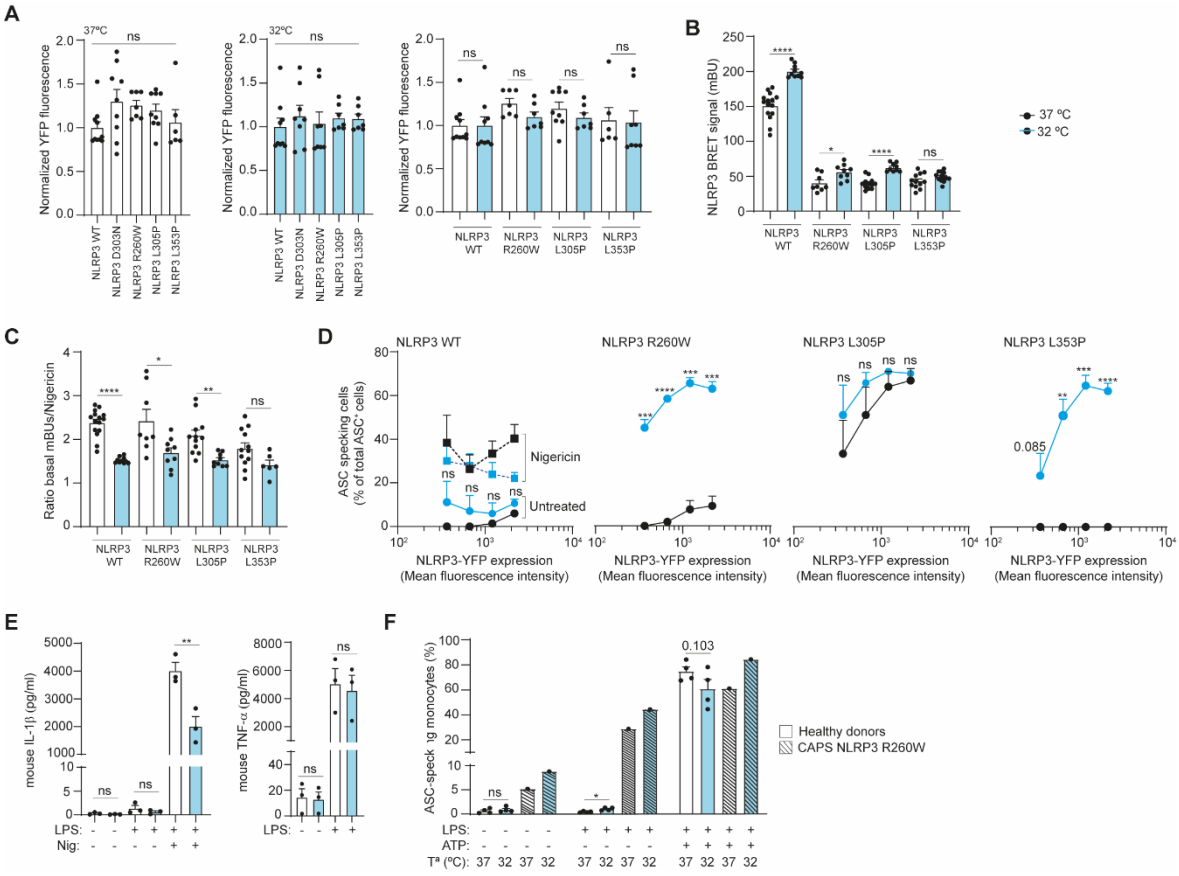

Figure 35. Conformational and functional study of NLRP3 FCAS-associated variants. (**A**) Normalized YFP fluorescence and (**B**) BRET signal of HEK293T cells expressing wild-type and different YFP-NLRP3-Luc FCAS variants. (**C**) Ratio obtained by comparing the BRET signal at baseline and after the activation for 30 min with nigericin (10 μM) of HEK293T cells expressing wild-type and different YFP-NLRP3-Luc FCAS variants. (**D**) Percentage of ASC specking HEK293T cells expressing ASC-RFP and the BRET sensors of NLRP3 wild-type and FCAS variants. (**E**) IL-1β (left) and TNF-α (right) release from mouse bone marrow derived macrophages (BMDMs) treated for 2 h with LPS (1 μg/ml) and for 30 min with nigericin (10 μM). (**F**) Percentage of ASC-specking monocytes determined by time-of-flight assay in whole blood from healthy individuals and from the patient with NLRP3 p.R260W variant primed with LPS (1.6 μg/ml, 3 hours) and stimulated with ATP (3 mM, 30

min). In (**A, B, C, D**), *n* = 4-15 independent experiments. Each dot represents an individual experiment or a different patient; cells were incubated for 3 hours at 37 ºC (white columns) or 32º C (blue columns); data is represented as mean ± SEM; ANOVA test in (**A**) and *t*-test; ****p<0.0001, **p<0.005, *p<0.05 and ns, no significant difference (p>0.05).

To confirm this hypothesis, we analysed a blood sample of a CAPS patient with the R260W variant. This individual presented clinical symptoms of MWS since childhood, although was diagnosed to MWS syndrome at 61 years old. Actually, he is under Canakinumab treatment with a good response. We found that monocytes from this CAPS patient had an increase of ASC specks at baseline and after incubation at 32ºC. However, healthy donors presented a slightly decrease of monocytes with ASC oligomers upon canonical NLRP3 inflammasome stimulation at 32ºC (**Figure 35F**).

2.1.4 Functional analysis of CAPS-associated NLRP3 mutations present in mosaicism and germline

We then studied different CAPS associated NLRP3 variants that have been associated with MWS and CINCA clinical phenotypes and are described either in germline and mosaicism (**Table 13**). The expression of all of them in HEK293T cells resulted in a similar expression as denoted by similar YFP fluorescence (**Figure 36A**). BRET analysis revealed that all NLRP3 variants tested presented a decrease in the BRET signal in comparation with the wild-type NLRP3 (**Figure 36B**). In fact, this decrease was similar to the BRET signal obtained in wild-type after nigericin treatment (**Figure 36B**). The NLRP3 variants D303G and E304K, both in the Walker B motif (**Table 14**), showed the highest reduction in BRET signal (**Figure 36B**). With the exception of D303A variant, all CAPS-associated NLRP3 mutants were able to induce basal ASC oligomerization (**Figure 36C**). Indeed, the variants Q306H, K355N, M406V and T433I presented the higher percentage of cells with ASC specks (approximately 70%). These four variants have been only described in mosaicism (Nakagawa et al., 2015; Tanaka et al., 2011). Therefore, suggesting that the strong activation of the inflammasome in these variants would not be compatible with viable development.

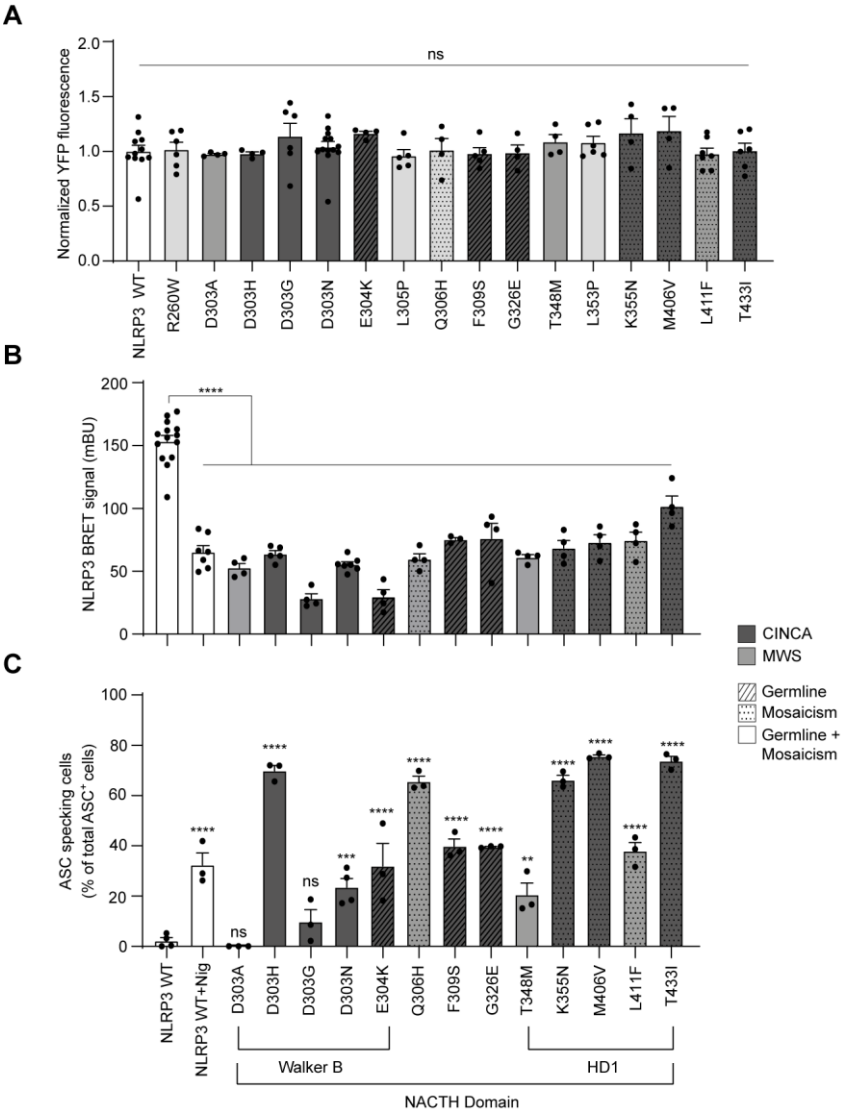

Figure 36. Conformational and functional study of CAPS-associated NLRP3 mutants. (**A**) Normalized YFP fluorescence, (**B**) BRET signal and (**C**) percentage of ASC specking HEK293T cells expressing the BRET sensors of NLRP3 wild-type and the different CAPS-associated NLRP3 variants**.** NLRP3 wild-type was activated or not for 30 min with nigericin (10 µM). Data is represented as mean ± SEM; *n* = 3-15 independent experiments; ANOVA test; ****p<0.0001, ***p<0.0005, **p<0.005 and ns, no significant difference (p>0.05).

2.1.5 Effect of the NLRP3 inhibitor MCC950 on CAPS-associated NLRP3 variants

The cyro-electron microscopy structure of NLRP3 bound to the inhibitor molecule MCC950 suggests that this molecule stabilize the closed cage structure of NLRP3, impairing its activation (Andreeva et al., 2021; Hochheiser et al., 2022; Ohto et al., 2022). In this line, Tapia-Abellán et al., demonstrated that MCC950 was able to increase the BRET signal of three different NLRP3 mutants (R260W, D303N and T348M), suggesting that MCC950 closes NLRP3 active conformation (Tapia-Abellán et al., 2019).

Here, we have studied the effect of MCC950 in the 17 CAPS–associated NLRP3 variants used in this Thesis. We found that MCC950 was able to increase the BRET signal in all the NLRP3 variants analyzed (**Figure 37A**). Also, we found that MCC950 was able to abolish the basal ASC oligomerization induced by all the NLRP3 mutants, except for the E304K variant (**Figure 37B**). That confirms the importance of this residue of the Walker B on MCC950 action, as was previously described (Tapia-Abellán et al., 2019). In addition, MCC950 was also able to increase BRET signal at 32ºC in FCAS-associated variants and reduce their basal ASC oligomerization (**Figure 37C, D**).

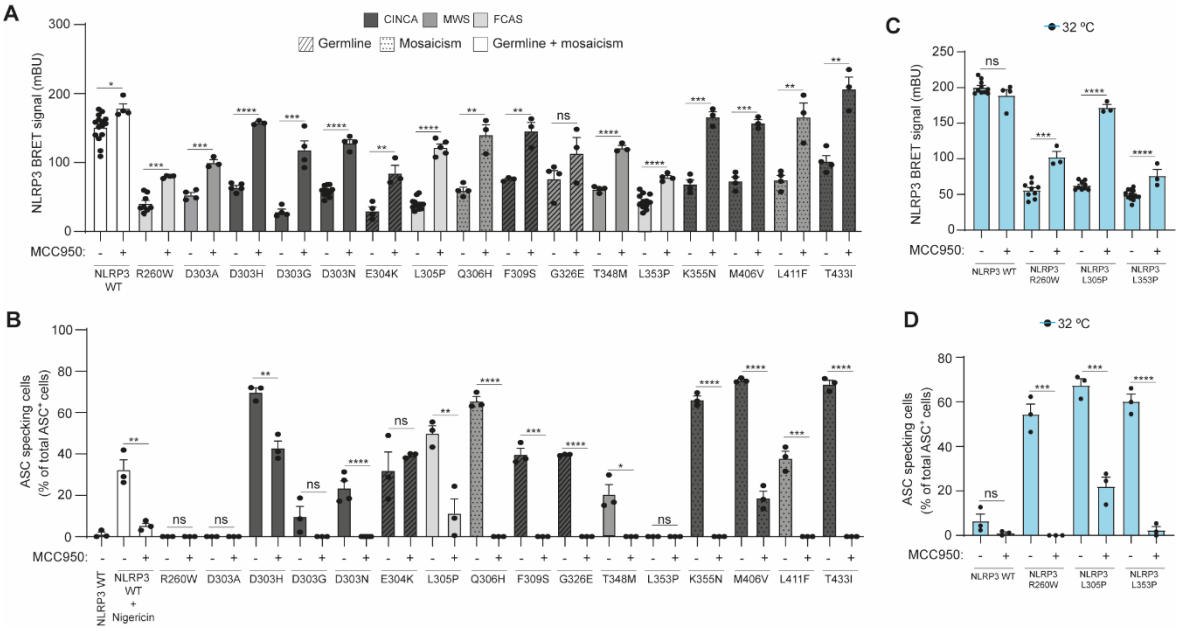

Figure 37. Conformational and functional study of CAPS-associated NLRP3 mutants treated with the MCC950 inhibitor. (**A**) BRET signal and (**B**) percentage of ASC specking HEK293T cells expressing the BRET sensors of NLRP3 wild-type and the different CAPS-associated NLRP3 variant. NLRP3 wild-type was activated or not for 30 min with nigericin (10 μM). Effect of MCC950 NLRP3 inhibitor on the BRET signal (**C**) and percentage of ASC-specking HEK293T cells (**D**) expressing wild-type and different NLRP3 FCAS variants incubated for 3 hours at 32º C (blue columns). In all cases, cells were treated or not with MCC950 (10 μM) overnight. Each dot represents an individual experiment; *n* = *3*-15 independent experiments; data is represented as mean ± SEM; *t*-test; ****p<0.0001, ***p<0.0005, **p<0.005, *p<0.05 and ns, no significant difference (p>0.05).

2.1.6 Effect of the NLRP3 inhibitor CY-09 on CAPS-associated NLRP3 variants

As explained in the section 7.5.3 of the Introduction of this Thesis, CY-09 is a covalent modifier of the NLRP3 inflammasome. Jiang and colleagues confirmed that CY-09 competes with ATP for binding to the Walker A motif of NLRP3, inhibiting its activation independently of the first signal (NLRP3 and pro-IL-1β expression) (Jiang et al., 2017).

Here, we have studied the effect of CY-09 in the 17 CAPS–associated NLRP3 variants used in this Thesis. Surprisingly, we found that, unlike MCC950, CY-09 inhibitor was able to significantly reduce the BRET signal in the wild-type NLRP3 receptor and D303N

variant (**Figure 38A**). Indeed, this reduction was similar to the decrease of the BRET signal produced by nigericin, which was no further able to reduce the BRET signal of NLRP3 carrying D303N variant when added at the same time with CY-09 (**Figure 38A**). Also, with the exception of the variants R260W, D303G, E304K, K355N, M406V and L411F, the CY-09 inhibitor was able to significantly decrease the BRET signal in the NLRP3 variants analyzed (**Figure 38B**).

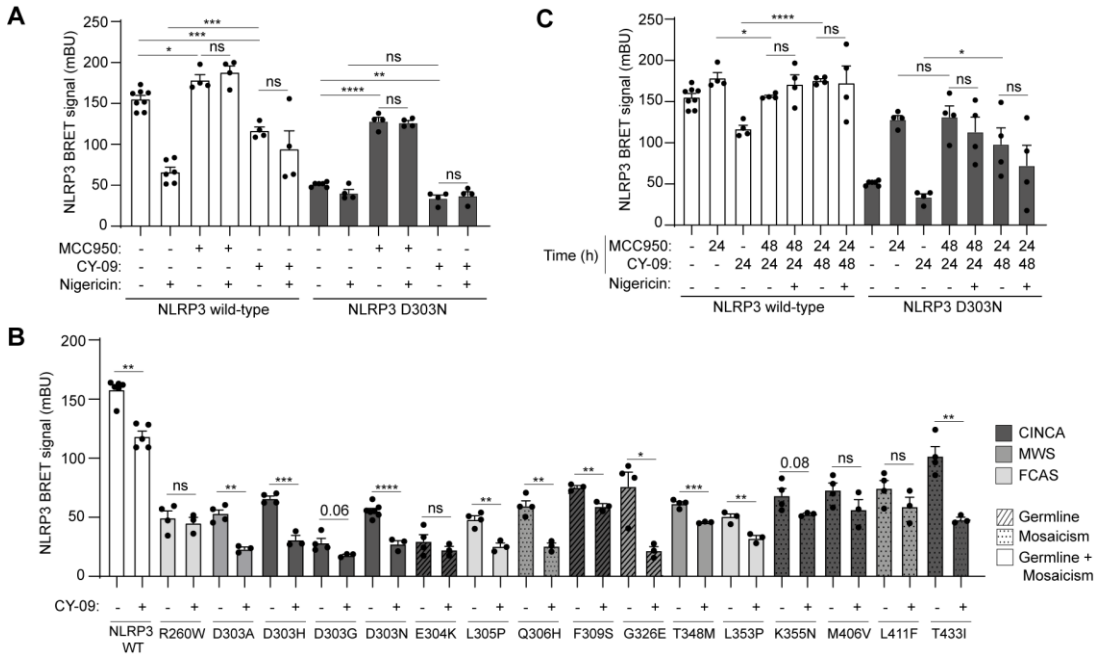

Figure 38. Conformational BRET study of CAPS-associated NLRP3 mutants treated with the NLRP3 inhibitors MCC950 and CY-09. (**A**) BRET signal of HEK293T cells expressing wild-type and NLRP3 D303N variant incubated or not with MCC950 (10 μM), CY-09 (10 μM) over-night and nigericin (10 μM) for 30 min. (**B**) Effect of CY-09 (10 μM over-night) in the BRET signal of HEK293T cells expressing wild-type and different CAPS-associated NLRP3 variants. (**C**) BRET signal of HEK293T cells expressing wild-type and NLRP3 D303N variant incubated or not with the NLRP3 inhibitors MCC950 (10 μM) and CY-09 (10 μM) during 24 hours or 48 hours and with nigericin (10 μM) for 30 min. Each dot represents an individual experiment; *n* = *3*-8 independent experiments; data is represented as mean ± SEM; *t*-test; ****p<0.0001, ***p<0.0005, **p<0.005, *p<0.05 and ns, no significant difference (p>0.05).

As MCC950 and CY-09 resulted in different BRET change, we next aimed to use subsequently both inhibitors. MCC950, independently of the presence of CY-09, was able to increase the BRET signal of NLRP3 wild-type and D303N variant (**Figure 38C**). On the contrary, if CY-09 was added as the second inhibitor, only in NLRP3 wild-type was shown a small reduction of the BRET signal produced by MCC950 (**Figure 38C**). In no case nigericin was able to reduce the BRET signal when both inhibitors were simultaneously blocking NLRP3 activation (**Figure 38C**). These results suggest that MCC950 and CY-09 do not bind at the same motif of NLRP3 inflammasome. Whereas MCC950 stabilizes the NACHT and LRR domains relative to each other facilitating the ‘closed’ conformation (both monomeric

and double-ring cage forms), CY-09 presumably stabilizes an 'open' inactive conformation of NLRP3.

2.1.7 Functional analysis of NLRC4 variants associated to autoinflammatory disease

Different NLRC4 variants have been associated to autoinflammatory diseases. We aimed to analyzed the functional consequences of these changes in NLRC4 and their ability to activate the inflammasome.

To do that, we used 12 different plasmids carrying NLRC4 with pathogenic mutations. Along NLRC4 structure, S171F and T177A are found in the NBD domain; T337N, T337S and V341A in the HD1 domain; H443P and S445P in the WHD domain; and G633dup, W655C, Q657L, C697S and D1009G in the LRR domain (**Figure 39A**). It is important to stand out that, here we described for first time that G633 duplication, C697S and D1009G variants in NLRC4 which are associated with autoinflammatory patients (**Table 16**).

When ASC oligomerization was studied in response to the expression of these variants, we found that S171F and T117A induce an increase of ASC-specking cells at baseline (**Figure 39B**). To a lesser extent, T337N, T337S, S445P and W655C NLRC4 variants presented a small, but significant increase, of basal ASC oligomers (**Figure 39B**). The rest of the variants were not able to induce ASC oligomers (**Figure 39B**). This result could be explained by the fact that NLRC4 activation and oligomerization do not strictly require ASC assembly to activate caspase-1, as their CARD domains could interact and enable the recruitment of pro-caspase-1 molecules (Saïd-Sadier & Ojcius, 2014).

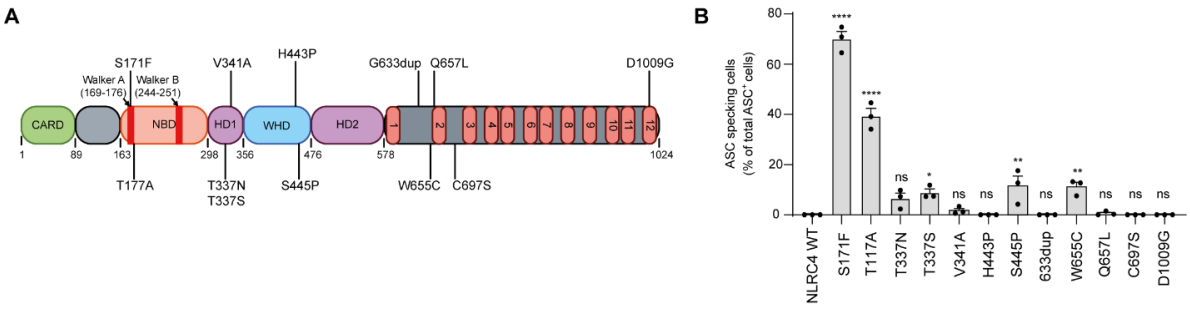

Figure 39. NLRC4 variants analysed in this Thesis. (**A**) Schematic representation of amino acids changes and the position of the mutations along the NLRC4 inflammasome structure. (**B**) Percentage of cells with ASC oligomers among HEK293T cells expressing wild-type or different NLRC4 variants. Significance is indicated above each column. Data is represented as mean ± SEM; *n*=3 independent experiments; ****p<0.0001, **p<0.005, *p<0.05 and ns p>0.05.

Table 16. NLRC4 variants included in this Thesis.

Domain	Mutation	Mosaicism or Germline	ACMG Classification	Clinic	Polarity and charge changed by mutation: FROM	TO	Variant frequency/cases
NBD	S171F	M	Likely pathogenic	NLRC4-AID	Polar-Neutral	Non-polar	<5
	T177A	M	Likely pathogenic	NOMID-like disease	Polar-Neutral	Non-polar	<5
HD1	T337N	G	Likely pathogenic	NLRC4-AIFEC	Polar-Neutral	Polar-Neutral	<5
	T337S	G	Likely pathogenic	NLRC4-Recurrent MAS	Polar-Neutral	Polar-Neutral	<5
	V341A	G	Likely pathogenic	NLRC4-AIFEC	Non-polar	Non-polar	10 to 20
WHD	H443P	G	Likely pathogenic	NLRC4-FCAS	Basic (+)	Non-polar	10 to 20
	S445P	G	Likely pathogenic	Erythematous skin nodules + FCAS	Polar-Neutral	Non-polar	<5
LRR	G633dup	G	Likely pathogenic/VUS	Not yet available	-	-	<5
	W655C	G	Likely pathogenic	NLRC4-Recurrent MAS	Non-polar	Non-polar	<5
	Q657L	G	Likely pathogenic	NLRC4-AIFEC	Polar-Neutral	Basic (+)	<5
	C697S	G	Likely pathogenic	Not yet available	Non-polar	Polar-Neutral	<5
	D1009G	G	Likely pathogenic	Not yet available	Acidic (-)	Non-polar	<5

HD1, helical domain 1; NBD, nucleotide-binding and oligomerization domain; WHD, winged helix domain; LRR, leucine-rich repeat; VUS, variant of uncertain significance; FCAS, Familial cold auto-inflammatory syndrome; NOMID, Neonatal onset multisystem inflammatory disease; MAS, macrophage activation syndrome; AID, autoinflammatory disease; AIFEC, autoinflammation with infantile enterocolitis; M, mosaicism and G, germline.

2.2 Evaluation of inflammasome activation in autoinflammatory syndromes

2.2.1 Monocytes from CAPS-associated NLRP3 variants, but not FMF patients, present a constitutive active inflammasome

Cryopyrin-Associated Periodic Syndromes and Familiar Mediterranean fever encompass two prototypical hereditary autoinflammatory diseases, characterized by recurrent episodes of fever, urticaria-like rash and joint inflammation, as a result of mutations in *MEFV* and *NLRP3* genes. Both autoinflammatory syndromes are different from a genetic point of view, CAPS-associated *NLRP3* variants are typically considered gain-of-function mutations and FMF-associated *MEFV* variants could be due to homozygous variants or gain-of-function mutations, resulting in both cases in an overactivation of NLRP3 and Pyrin inflammasomes, respectively. Due to that, CAPS and FMF patients are commonly treated with IL-1 blockers for a complete resolution of inflammatory flares.

During this Thesis, we collected whole blood samples from individuals with CAPS (MWS) carrying the NLRP3 R260W (*n* = 1), D303N (*n* = 1), T348M (*n* = 1) and A439T variants (*n* = 4) and from individuals with the *MEFV* M694I variant in homozygosity (*n* = *4*).

In all cases, patients were with inactive disease under colchicine or IL-1 blocking therapy by the time blood was extracted.

To determine whether these variants resulted in a constitutive activation of the inflammasome in monocytes, we analysed the formation of ASC oligomers in $CD14^+$ cells. We found that untreated monocytes from CAPS patients presented an increase in the percentage of ASC specks when compared with healthy individuals and FMF patients (**Figure 40A**). Stimulation with LPS led to an enhancement of the percentage of ASC-specking monocytes in CAPS patients, meanwhile this increase in the monocytes from FMF patients and healthy individuals were smaller (**Figure 40A**). In CAPS, this LPS-mediated increase was dependent on the time of stimulation (**Figure 40B**) and was reduced after MCC950 treatment (**Figure 40C**). These results suggest that circulating monocytes from CAPS patients, but not FMF patients, present a constitutively formation of ASC-dependent NLRP3 inflammasome that could be further induced by LPS stimulation.

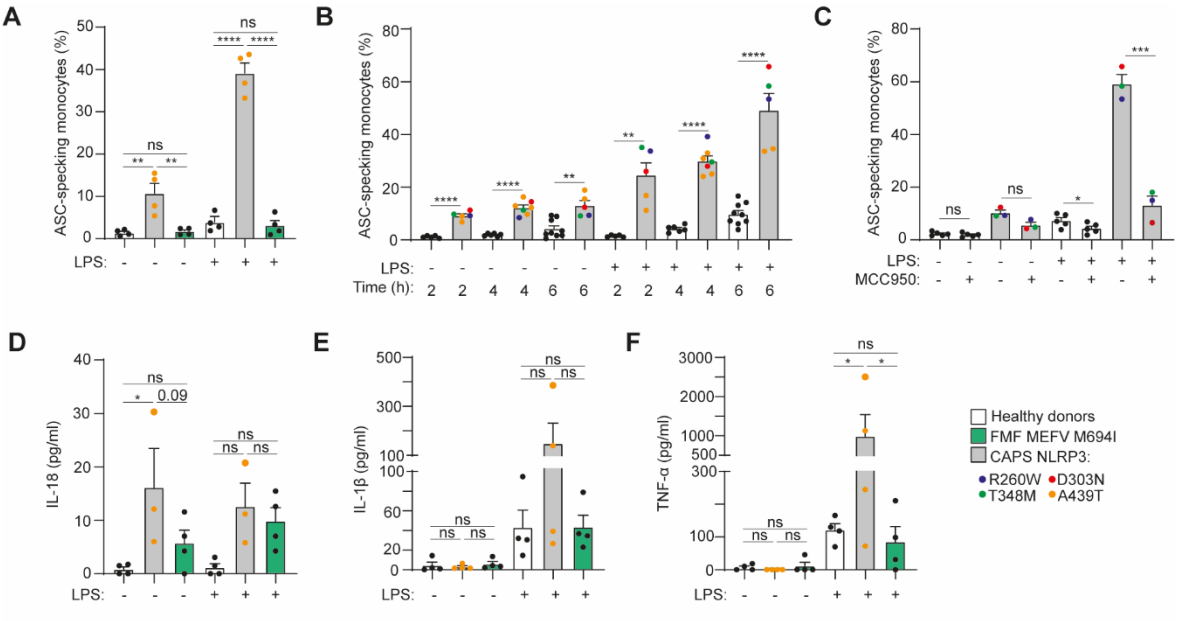

Figure 40. Monocytes from CAPS patients, but not from FMF individuals, present a constitutive inflammasome activation. (**A**) Percentage of ASC specking monocytes from healthy donors and CAPS patients (NLRP3 p.A439T) after whole blood treated or not for 3h with LPS (1.6 μg/ml). (**B**) Percentage of ASC specking monocytes from healthy donors and CAPS patients (NLRP3 p.R260W, p.D303N, p.T348M and p.A439T) after whole blood untreated/treated for different times with LPS (0.1 μg/ml). (**C**) Percentage of ASC specking monocytes from healthy donors and CAPS patients (NLRP3 p.R260W, p.D303N and p.T348M) after whole blood treated or not for 6 h with LPS (0.1 μg/ml), in the presence or absence of MCC950 (10 mM). (**D-F**) ELISA for IL-18 (**D**), IL-1β (**E**) and TNF-α (**F**) release from PBMCs treated as in panel A. Each dot corresponds to a different donor, and for CAPS each colour represents a different mutation (NLRP3 p.R260W, p.D303N and p.T348M, n = 1; p.A439T, n = 4); data is represented as mean ± SEM; t-test; ****p<0.0001, ***p<0.0005, **p<0.005, *p<0.05 and ns, no significant difference (p>0.05).

In line with that, although there was a slightly increase in the release of the cytokine IL-18 in untreated PBMCs from FMF patients, only in CAPS patients it was significant (**Figure 40D**). However, neither CAPS patients nor FMF individuals released IL-1β or TNF-α in unstimulated conditions (**Figure 40E, F**). LPS-treated PBMCs increased IL-1β, IL-18 and TNF-α release in CAPS and FMF patients (**Figure 40D-F**). These results suggest that CAPS NLRP3-inflammasome activation occurs in a constitutive manner, not present in FMF patients.

2.2.2 S171F *NLRC4* variant induces increased inflammasome activation

NLRC4-associated inflammatory disease is an inflammasomopathies that is a consequence of gain-of-function mutations in the *NLRC4* gene. Similarly to CAPS, both diseases debut onset during childhood and are characterized by fever, systemic inflammation and cutaneous lesions (Nigrovic et al., 2020; Romberg et al., 2014). Unlike *NLRP3*, in which there has been found both germline and post-zygotic variants as causes of disease, only children carrying post-zygotic *NLRC4* variants have been reported (Kawasaki et al., 2017; Liang et al., 2017).

During this Thesis, we were able to obtain whole blood samples of a 57-year-old woman with a late-onset autoinflammatory disease, suffering from systemic inflammation, recurrent episodes of fever and abdominal pain, which were partially controlled with interleukin-1 blockade. Genetic analysis revealed she carried the post-zygotic variant c.512C>T in the *NLRC4* gene, which lead to the S171F variant, that has already been classified as pathogenic (Volker-Touw et al., 2017).

We found that the proportion of monocytes with ASC oligomers was constitutively elevated in the patient with the S171F variant when compared to healthy controls (**Figure 41A**). LPS treatment increased the percentage of ASC-specking monocytes from the patient compared to healthy individuals but, these differences disappeared when the NLRP3 inflammasome was activated with LPS and ATP (**Figure 41A**). The patient's PBMCs released higher amount of IL-18 in all conditions studied when compared to healthy controls (**Figure 41B**), however they failed to release IL-1β even after the canonical activation of NLRP3 inflammasome (**Figure 41C**). This deficiency in IL-1β release and the basal level of monocytes with ASC oligomers were not dependent on an altered number of monocytes in the patient's sample (**Figure 41D**). Moreover, a similar release of LPS-induced TNF-α (**Figure 41E**, right) and IL-6 (**Figure 41E**, left) was seen in both healthy controls and the patient. That ruled out a potential defect on LPS priming. Finally, NLRC4 activation in the patient's

PBMCs with FlaTox resulted in an increase of the percentage of monocytes with ASC oligomers (**Figure 41F**), suggesting that mutant NLRC4 could be potentiated with specific NLRC4 stimuli.

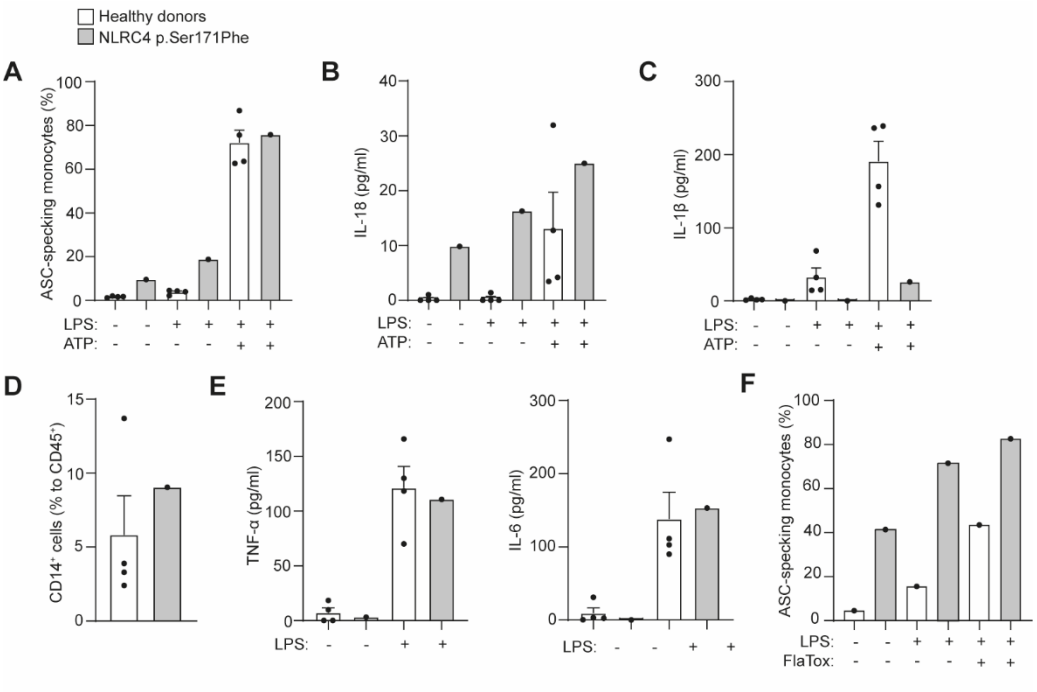

Figure 41. NLRC4 S171F variant induces increased inflammasome activation. (**A**) Percentage of ASC-specking monocytes identified by the time-of-flight assay, ELISA for IL-1β (**B**) and IL-18 (**C**) from healthy individuals (white bars) and from the patient with NLRC4 S171F variant untreated, primed with LPS alone or stimulated with LPS and ATP. (**D**) Percentage of $CD14^+$ monocytes (on total $CD45^+$ cells) in the PBMCs from the patient and from healthy controls. (**E**) ELISA for TNF-α (left) and IL-6 (right) release detected in cell-free supernatants of PBMCs untreated or primed with LPS from the patient and healthy controls. (**F**) Percentage of ASC-specking monocytes identified by the time-of-flight assay from healthy individuals (white bars) and from the patient with NLRC4 S171F variant untreated, primed with LPS alone or stimulated with LPS and FlaTox. In all experiments LPS was used at 1.6 μg/ml for 3 hours; ATP was used at 3 mM for 30 min and FlaTox was used at 2 μg during 5 hours. Each dot represents an independent individual; data is represented as mean ± SEM.

Chapter 3:

NLRP3 activity in monocytes of MS and CMML patients as a marker for treatment response

3.1 MS patient's refractory to fingolimod treatment present elevated NLRP3 inflammasome activation

Fingolimod is a sphingosine analogue approved for the treatment of multiple sclerosis, as it has a significant neuroprotective role in central nervous system. In the recent years, increasing evidence has related the oral therapy fingolimod to the inhibition of NLRP3 inflammasome activation (Guo et al., 2020; Yao et al., 2019). Because of that, the aim of this part of the Thesis was to determine whether the NLRP3 inflammasome activation was affected during the therapeutic treatment with fingolimod in patients with relapsing-remitting MS.

To do that, patients with RRMM treated with oral fingolimod (n = 12) were evaluated before and after six months of treatment. During this period of time, clinicians in charge of these patients classified them into responders and non-responders according the treatment response criteria. As a redout for inflammasome activation, the percentage of monocytes with ASC oligomers were measured. We found that, there was no differences in the formation of ASC-specking monocytes under unstimulated conditions between responders and non-responders either at baseline or after six months of treatment (**Figure 42A**). Stimulation with LPS alone was associated with a slightly increase of ASC oligomers in comparation with untreated monocytes in MS patients and healthy individuals (**Figure 42A**). Canonical activation of NLRP3 inflammasome with LPS and ATP stimulus, resulted in an increase in the percentage of ASC specks from responders and non-responders. However, this percentage was significantly lower in non-responders compared with responders and healthy individuals (**Figure 42A**). Surprisingly, after six months of fingolimod treatment, the response was opposite between responders and non-responders. The ASC oligomers formation after LPS and ATP treatment was increased in non-responders and inhibited in responders (**Figure 42A**). To assess if these changes were due to possible differences among monocytes subsets, the percentage of classical ($CD14^{+}CD16^{-}$), intermediate ($CD14^{+}CD16^{+}$) and non-classical monocytes ($CD14^{+}CD16^{++}$) was investigated. As shown in **Figure 42B**, no significant differences were observed in fingolimod RRMS treatment patients either before or after six months treatment.

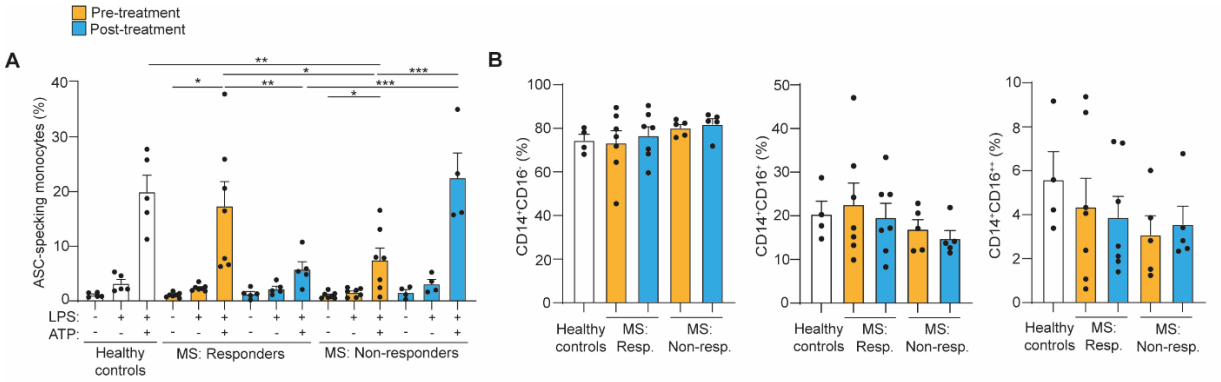

Figure 42. ASC oligomers formation in responders and non-responders to fingolimod MS patients. (**A**) Percentage of monocytes with ASC oligomers determined by time-of-flight inflammasome evaluation and (**B**) percentage of classical ($CD14^+CD16^-$), intermediate ($CD14^+CD16^+$), and non-classical ($CD14^+CD16^{++}$) monocytes in healthy controls (*n* = 5, white bars) and in responders (*n* = 7) and non-responders (*n* = 5) to fingolimod at baseline (pre-treatment, orange bars) and after 6 months of treatment (post-treatment, blue bars). Whole blood samples were untreated, primed with LPS (1.6 µg/ml, 3 hours) and, in some cases, stimulated with ATP (3 mM, 15 min). Each dot corresponds to a different donor and patients; data is represented as mean ± SEM; ANOVA test in (**A**) and *t*-test in (**B**); ***p<0.0005, **p<0.005, *p<0.05 and ns p>0.05.

We next aimed to analysed the release of the pro-inflammatory cytokines IL-1β and IL-18. IL-1β and IL-18 concentration were similar between responders and non-responders at baseline and after six months of fingolimod treatment and, also, with respect to healthy individuals (**Figure 43A, B**). Supporting the fact that non-responders had an increase in the ASC-specking monocytes after six months treatment, IL-18 release were significantly increased in PBMCs from non-responders in that time-point after LPS and ATP stimulation (**Figure 43B**). Also, a similar release of TNF-α and IL-6 was shown at baseline and after treatment in responders and non-responders. However, although LPS-induced a significant increase in TNF-α and IL-6 release in responders after treatment, in non-responders the levels of TNF-α and IL-6 were higher under unstimulated conditions, therefore LPS failed to promote a similar cytokine increase in these patients (**Figure 43C**). Moreover, we asked if this increase in NLRP3 inflammasome activation in oral fingolimod non-responders was associated with higher pyroptosis in this group of patients. For that, we evaluated the release of extracellular galectin-3, an alarmin secreted after pyroptosis cell death, and found that galectin-3 was significantly higher in LPS and ATP stimulated PBMCs from non-responders in comparation to responders after fingolimod treatment (**Figure 43D**).

Taking all these data into account, we suggest that fingolimod treatment results in an increase NLRP3 inflammasome activation and pyroptosis, which could aggravate disease symptoms in these patients.

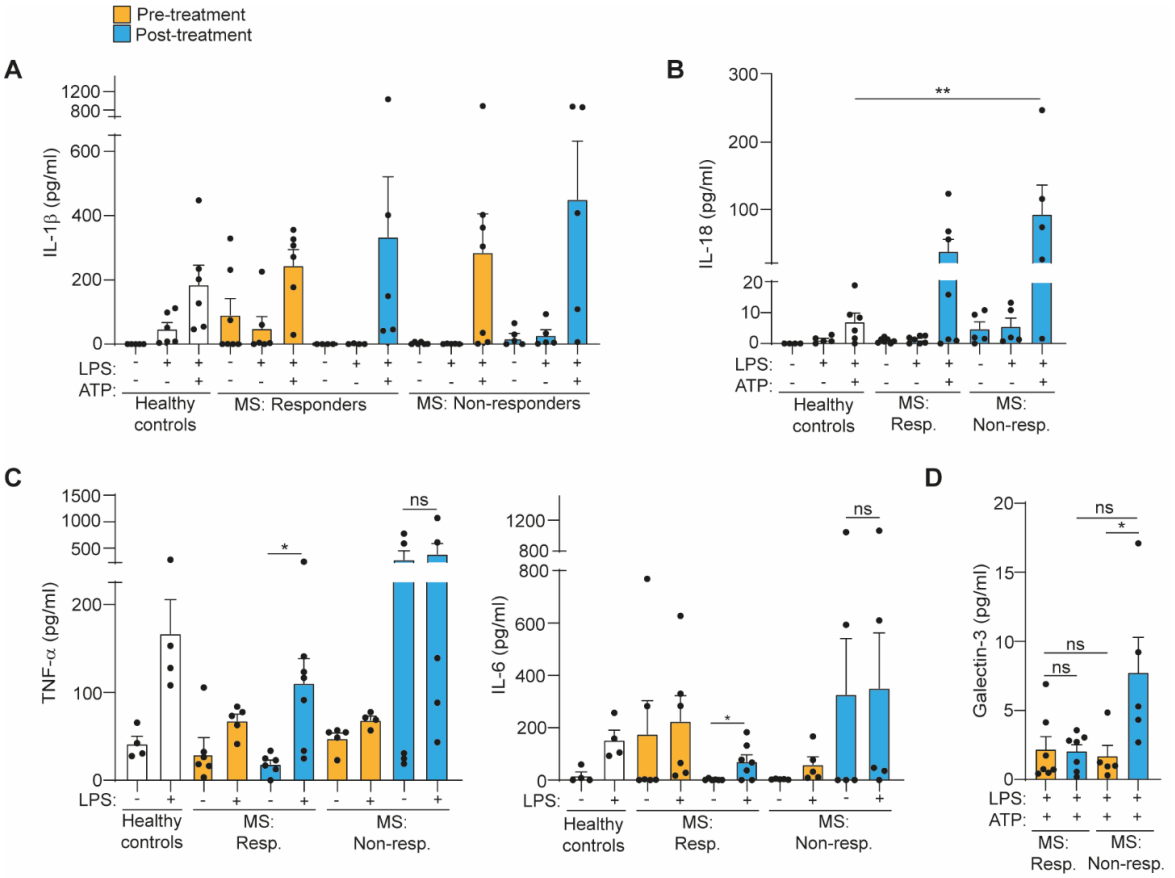

Figure 43. **NLRP3-related release of proinflammatory cytokines in responders and non-responders at baseline and after fingolimod treatment.** (**A-C**) ELISA for IL-1β (**A**), IL-18 (**B**), TNF-α (left) and IL-6 (right) (**C**) release in cell-free supernatants from PBMCs untreated, primed with LPS (1.6 μg/ml, 3 hours) and, in some cases, stimulated with ATP (3 mM, 30 min) in healthy controls (*n* = 4-6, white bars) and in responders (*n* = 7) and non-responders (*n* = 5) to fingolimod at baseline (pre-treatment, orange bars) and after 6 months of treatment (post-treatment, blue bars). (**D**) ELISA for galectin-3 release in cell-free supernatants from PBMCs primed with LPS (1.6 μg/ml, 3 hours) and stimulated with ATP (3 mM, 30 min) in responders (*n* = 7) and non-responders (*n* = 5) to fingolimod at baseline (pre-treatment, orange bars) and after 6 months of treatment (post-treatment, blue bars). Each dot corresponds to a different donor and patients; data is represented as mean ± SEM; *t*-test; **p<0.005, *p<0.05 and ns, no significant difference (p>0.05).

3.2 NLRP3 inflammasome and NLRP3-related cytokine signature in CMML patients with *KRAS* mutation

In order to study the mechanisms underlying the NLRP3/IL-1β axis disruption and *RAS* mutations in patients with CMML, we started studying an index patient with c.35G>A, G12D variant in the *KRAS* gene (allelic burden of 48.9%). He was clinically diagnosed of a high-risk CMML myeloproliferative variant at the age of 54 years (July 2020). Since that date until October 2020, the patient was treated with low-dose of corticosteroids and colchicine. However, colchicine treatment was discontinued because of digestive intolerance. In the following two months, the patient suffered various episodes of autoinflammation. We

found that the IL-1β release from PBMCs of the patient was elevated in comparation with healthy controls (**Figure 44**).

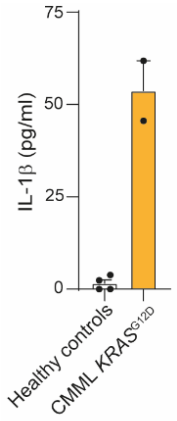

Figure 44. Level of IL-1β of CMML *KRAS*^{G12D} patient. ELISA for IL-1β release in cell-free supernatants from PBMCs untreated in healthy controls (n = 4, each dot represents an independent donors) and in the index patient (each dot represents a technical replicate). Data is represented as mean ± SEM.

Since PBMCs from the index patient released high levels of IL-1β (**Figure 44**), we wanted to know if this release was dependent on NLRP3 inflammasome activation. We found that, in contrast to healthy controls, in PBMCs from the index patient no increase of IL-1β release was observed after the canonical activation of NLRP3 with LPS and ATP compared to LPS alone, but it was observed upon activation of the Pyrin inflammasome with LPS and TcdB (**Figure 45A**). Also, the treatment of PBMCs with MCC950 inhibitor decreased the IL-1β release in all conditions, with except to under the stimulation of the Pyrin inflammasome (**Figure 45A**).

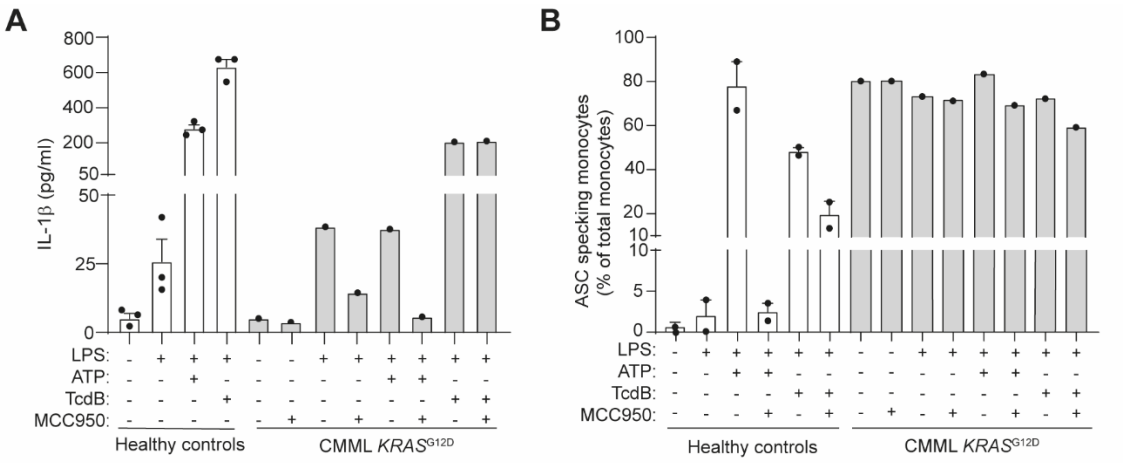

Figure 45. Constitutive basal activation in CMML *KRAS*^{G12D} patient. ELISA for IL-1β release (**A**) and percentage of ASC-specking monocytes (**B**) in the index patient (grey bars) and healthy controls (white bars), at baseline or after the stimulation of NLRP3 (LPS and ATP) and Pyrin (LPS and TcdB) inflammasomes. In all experiments, LPS was used at 1.6 µg/ml for 3 hours; ATP was used at 3 mM for 30 min in (**A**) or 15 min in (**B**), TcdB was used at 1 µg/ml for 1 hour in (**A**) or 30 min in (**B**) and MCC950 was added 15 minutes before second stimuli at 10 mM and maintained during stimulation. Each dot corresponds to a different individual; data is represented as mean ± SEM.

Next, we analysed the formation of ASC oligomers in monocytes as a readout of active inflammasome formation by flow cytometry. Unexpectedly, around 80% of monocytes from the index patient presented ASC specks at baseline, and the stimulation of the NLRP3

or Pyrin inflammasomes was not able to further induce any changes (**Figure 45B**). The NLRP3 inflammasome specific blocker, MCC950, was not able to reduce the percentage of ASC-specking monocytes in the index patient (**Figure 45B**). On the contrary, ASC oligomerization only occurred after NLRP3 and Pyrin inflammasomes activation in healthy controls, as expected (**Figure 45B**). These data suggest a maximal constitutive activation of NLRP3 inflammasome, as the ASC oligomerization is a final and irreversible step of inflammasome activation, which could also explain the small release of IL-1β after NLRP3 and Pyrin inflammasomes activation.

Five months after his diagnosis, coinciding with the second wave of COVID-19 and the impossibility of performing an allogeneic hematopoietic stem cell transplantation, anakinra was chosen as a treatment. The index patient presented then a good clinical response (weight gain, monocyte count stabilization and no treatment toxicity). However, four months later, he presented new episodes of autoinflammation, bilateral pneumonitis, severe heart failure and a life-threatening situation. As antibiotic treatment was needed, anakinra was discontinued and restarted three weeks after discontinuation. During to this period of time, four time-points were experimentally examined. As it is shown in **Figure 46A,** after the first administration of anakinra, while the patient was clinically stable, the percentage of basal ASC-specking monocytes decreased and remained low. Likewise, the discontinuation of anakinra and the new episodes of autoinflammation coincided with an increase in the percentage of ASC oligomers, which decreased again after the reintroduction of anakinra treatment (**Figure 46A**). Furthermore, while the percentage of monocytes with ASC specks remained stable around 60% during anakinra treatment, this therapy also favored a reduction of ASC-specking monocytes after the canonical activation of NLRP3 inflammasome with LPS and ATP stimulus (**Figure 46B**). In line with that, during anakinra treatment, *ex vivo* PBMCs primed with LPS or stimulated with LPS and ATP did not induce IL-1β (**Figure 46C**) and IL-18 (**Figure 46D**) release, but they were provoked when Pyrin inflammasome was activated with LPS and TcdB (**Figure 46C, D**). Similarly, during such treatment, PBMCs from index patient presented a slightly increase in TNF-α and IL-6 levels after LPS stimuli when compared with untreated conditions (**Figure 46E**), but this increase was less than the observed in healthy controls' PBMCs (**Figure 46E**). Altogether, these results suggest that anakinra treatment impaired NLRP3, but not Pyrin inflammasome, basal activation.

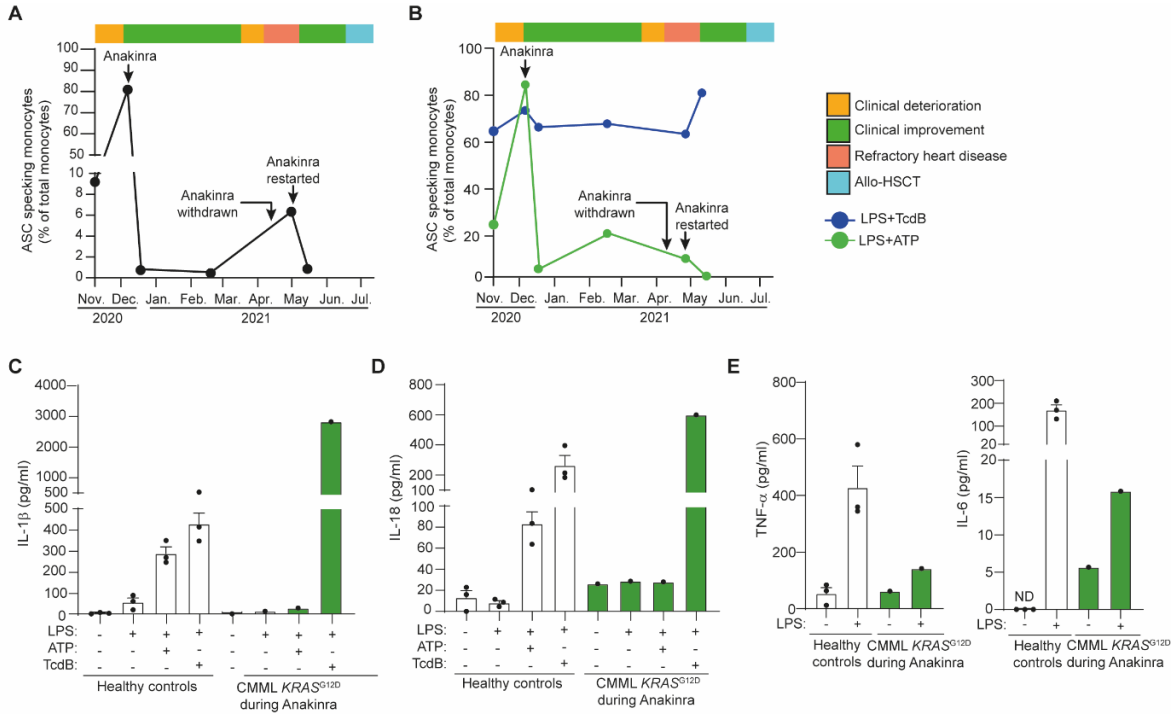

Figure 46. Anakinra treatment reduces NLRP3 inflammasome activation. (**A-B**) Percentage of monocytes with ASC oligomers from the index patient over the time point studied before, during and after anakinra treatment at baseline (**A**), and after NLRP3 inflammasome activation with LPS and ATP (green line) or Pyrin inflammasome activation with LPS and TcdB (blue line). (**C-E**) ELISA for IL-1β (**C**), IL-18 (**D**), TNF-α (left, **E**) and IL-6 (right, **E**) release in cell-free supernatants from PBMCs untreated or stimulated with LPS and ATP (NLRP3 inflammasome) or LPS and TcdB (Pyrin inflammasome) in healthy controls (white bars) and the index patient (green bars) during anakinra treatment. In all experiments, LPS was used at 1.6 µg/ml for 3 hours; ATP was used at 3 mM for 30 min in (**A**, **B**) and 30 min in (**C-E**), TcdB was used at 1 µg/ml for 30 min in (**A**, **B**) and 1 hour in (**C-E**). Each dot corresponds to a different donor and patients; data is represented as mean ± SEM.

As the activation of the NLRP3 inflammasome and caspase-1 can led to the release of oligomeric ASC particles (Baroja-Mazo et al., 2014), we next measure the ASC specks in the patient's plasma. We found that the concentration of ASC in plasma decreased after anakinra treatment and clinical improvement of the index patient and increase after anakinra withdrawn, overlapping with the clinical deterioration of the patient (**Figure 47**). That correlates with the profile of the percentage of monocytes with basal intracellular ASC speck (**Figure 46A**), suggesting that during periods of high ASC-specking monocytes, pyroptosis could be occurring *in vivo* in the patient and releasing ASC.

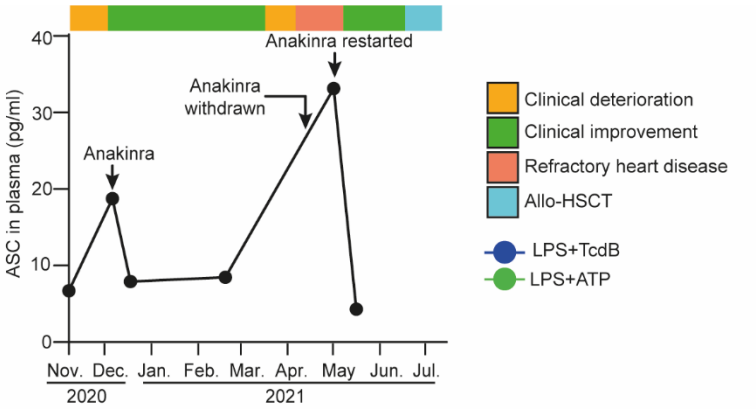

Figure 47. Anakinra treatment reduces levels of ASC oligomers in plasma. Plasma levels of ASC oligomers in the index patient along the time points studied before, during and after anakinra treatment., LPS was used at 1.6 µg/ml for 3 hours, ATP was used at 3 mM for 15 min and TcdB was used at 1 µg/ml for 30 min.

Taking into account the findings obtained in the index patient, we asked whether other patients with CMML or MDS/MPN and mutation in *KRAS* would have similar characteristics. To achieve that, and thanks to the collaboration of the Spanish Group of Molecular Biology and Hematology, we retrospectively identified 19 patients with similar clinical-biological characteristics of which we were able to collect and analyse fresh whole blood samples of five patients in the CMML *KRAS*^{mut} cohort and from four CMML *KRAS*^{WT} cohort. Equally to the index patient, all CMML *KRAS*^{mut} individuals had a significantly increase percentage of monocytes with ASC oligomers under untreated conditions and LPS stimulation when compared to either healthy controls or CMML *KRAS*^{WT} patients (**Figure 48A**). Moreover, only the stimulation of the Pyrin inflammasome with LPS and TcdB, but not the canonical activation of NLRP3 inflammasome with LPS and ATP, was able to increase the basal high percentage of ASC-specking monocytes. That suggest that the are some monocytes in which Pyrin, but not NLRP3, could be further activated (**Figure 48A**). As expected, in healthy controls and CMML *KRAS*^{WT} patients, the ASC oligomerization occurred only after the activation of NLRP3 and Pyrin inflammasomes with LPS and ATP or LPS and TcdB, respectively (**Figure 48A**). The IL-1β release after LPS and LPS and ATP stimulus in CMML *KRAS*^{mut} patients were reduced by the specific NLRP3 inhibitor, MCC950 (**Figure 48B**). According to its specificity, MCC950 was not able to reduce either the IL-1β or the ASC specks after activation of the Pyrin inflammasome with LPS and TcdB (**Figure 48B, C**). Whereas, the percentage of ASC-specking monocytes were slightly decreased by MCC950, being statistically significant when the NLRP3 inflammasome was activated (**Figure 48C**), according to recent studies showing that MCC950 is effective over the inactive NLRP3 structure and maybe is not able to disturb the irreversible NLRP3-ASC oligomer already formed (Hochheiser et al., 2022).

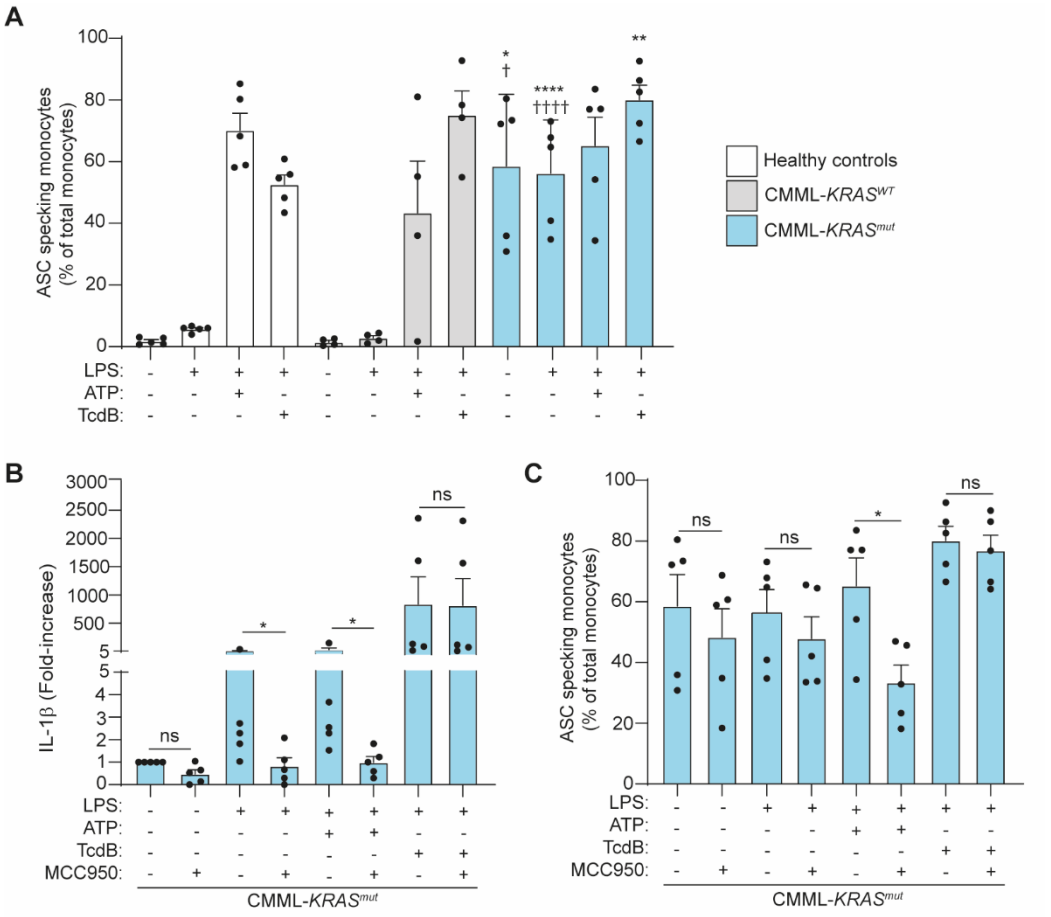

Figure 48. CMML *KRAS*^{mut} patients present a constitutive inflammasome activation. (**A**) Percentage of monocytes with ASC oligomers in healthy controls (white bars), CMML *KRAS*^{WT} patients (grey bars) and CMML *KRAS*^{mut} patients (blue bars) at baseline or treated with LPS and ATP (for NLRP3 inflammasome activation) and with LPS and TcdB (for Pyrin inflammasome activation). ELISA for IL-1β release (**B**) and percentage of ASC-specking monocytes (**C**) in CMML *KRAS*^{mut} patients at baseline or after the stimulation of NLRP3 (LPS and ATP) and Pyrin (LPS and TcdB) inflammasomes, in the presence/absence of MCC950. Fold-increase in (**B**) was calculated to untreated conditions. In all experiments, LPS was used at 1.6 µg/ml for 3 hours; ATP was used at 3 mM for 15 min in (**A, C**) and 30 min in (**B**), TcdB was used at 1 µg/ml for 30 min in (**A, C**) and 1 hour in (**B**) and MCC950 was added 15 minutes before second stimuli at 10 mM and maintained during stimulation. Each dot corresponds to a different individual; data is represented as mean ± SEM; ANOVA test was used in (**A**) (* compares CMML *KRAS*^{mut} vs healthy controls; † compares CMML *KRAS*^{mut} vs. CMML *KRAS*^{WT}) and *t*-test was used in (**B, C**); * or † p<0.05; **p<0.01; ***p<0.001; **** or †††† p<0.0001, ns, no significant difference (p>0.05).

CMML is characterized by sustained clonal monocytosis, so that we found an increase in the percentage of circulating monocytes in our cohort of CMML patients (*KRAS* wild-type and mutated) when compared to healthy controls (**Figure 49A**). This result correlates with the fact that there is a defective apoptosis of monocytes in these patients (Geissler et al., 2016; Sevin et al., 2021). In fact, analysis of the GEO dataset GSE135902 (Franzini et al., 2019) shows that in CMML patients with mutation in *RAS* gene there were less expression of *GSDMD*, in spite of the elevation of *NLRP3* and *IL1B* gene expression (**Figure 49B**). Furthermore, extracellular LDH levels normalized to the percentage of monocytes did

not increase in untreated PBMCs from CMML *KRAS*^{mut} patients (**Figure 49C**). This suggest that despite the basal activation of NLRP3 inflammasome in these patients, their monocytes could have an impaired pyroptosis cell death. This could be due to a hyperactive state of the monocytes in which activation of the inflammasome would produce a IL-1β release from living cells (Evavold et al., 2018; Lieberman et al., 2019; Zanoni et al., 2016). Also, in CMML *KRAS*^{mut} patients' plasma there was an increase in HMGB1 and P2X7 receptor (**Figure 49D**), suggesting that cell death was occurring in these individuals.

Taking all these data into account, we suggest that CMML patients with mutation in *KRAS* are associated with a basal overactivation of NLRP3 inflammasome, which blocking by the recombinant IL-1R antagonist resulted in a clinical improvement.

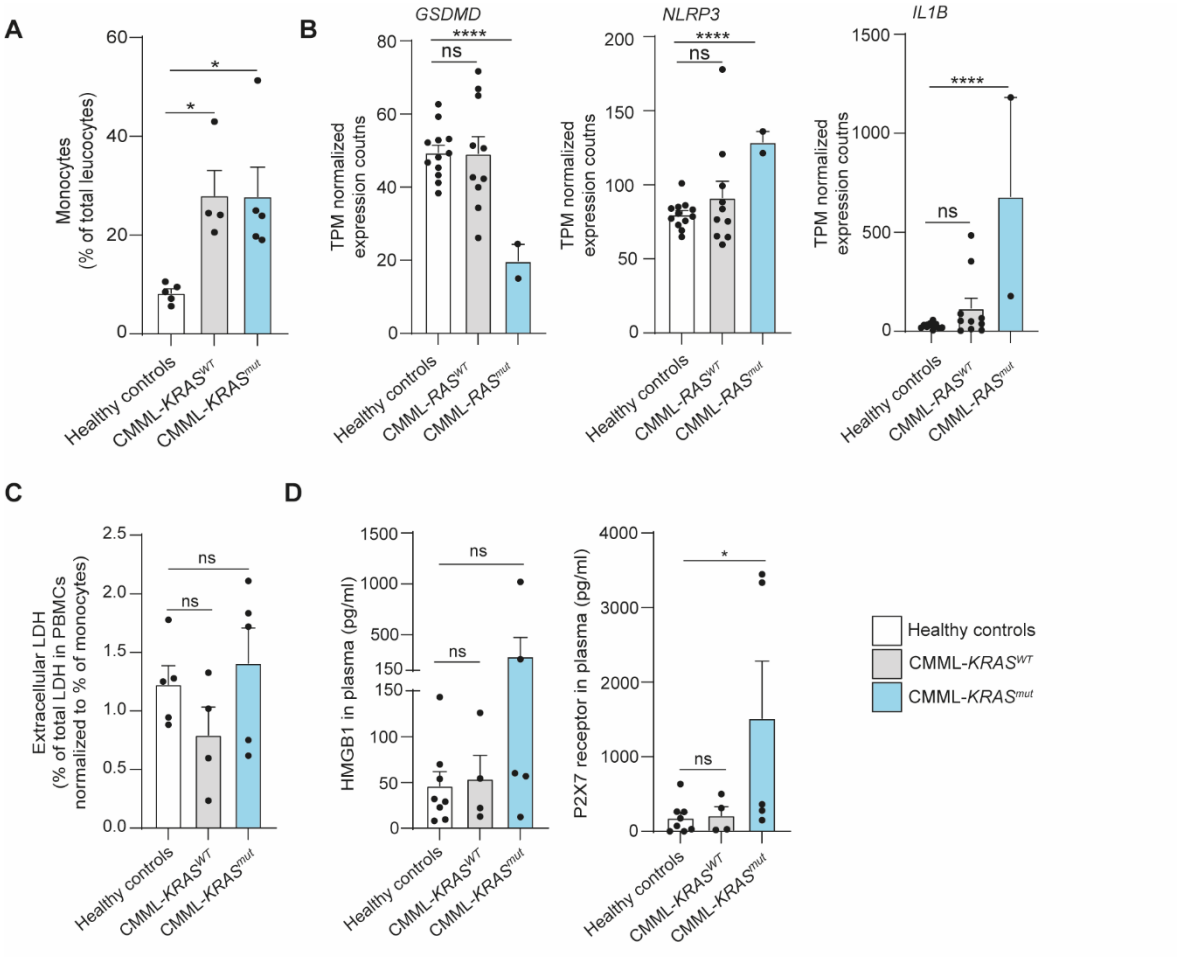

Figure 49. Percentage of monocytes, omnibus data gene expression and cell death. (**A**) Percentage of monocytes from the total leucocytes from healthy controls (white bars), CMML *KRAS*^{WT} patients (grey bars) and CMML *KRAS*^{mut} patients (blue bars). (**B**) *GSDMD, NLRP3* and *IL1B* mRNA expression in whole blood cells of healthy controls and CMML patients with *RAS*^{WT} and *RAS*^{mut} (using dataset GSE135902). (**C**) Percentage of extracellular LDH normalized to the percentage of monocytes from untreated PBMCs from healthy controls, CMML *KRAS*^{WT} patients and CMML *KRAS*^{mut} patients. (**D**) ELISA for HMGB1 (left) and P2X7 receptor (right) in plasma from healthy controls, CMML *KRAS*^{WT} patients and CMML *KRAS*^{mut} patients. Each dot corresponds to a different individual; data is represented as mean ± SEM; ANOVA test; ****p<0.0001, *p<0.05 and ns, no significant difference (p>0.05).

DISCUSSION

1. NLRP3, but not Pyrin inflammasome, is impaired in septic patients

Despite the extensive research, the clinical studies and the development of standardized protocols for critical care, sepsis remains one of the leading causes of death in critical patients. Sepsis initially exhibits a systemic inflammatory response to infection driven by an exacerbated production of proinflammatory cytokines, followed by a late immunosuppressive phase (Hotchkiss & Karl, 2003).

Our study demonstrates that at day one, intra-abdominal origin septic patients present a systemic acute inflammatory response, characterized by high concentration in plasma of acute phase proteins and organ failure markers, and with alterations of cellular counts, similarly to previous results obtained by our group and other studies with septic patients (He et al., 2023; Lozano-Rodríguez et al., 2023; Martínez-García et al., 2019).

To our knowledge, this is the first study determining the complete IL-1 family of cytokines in septic patients. The proinflammatory cytokine IL-18 and the anti-inflammatory proteins IL-18BP, IL-1RA, sIL-1RI and sIL-1RII were markedly higher in sepsis when compared to controls. Moreover, cytokines such as IL-6, IL-8, TNF-α, M-CSF and IL-15 were also elevated in septic patients at the illness onset. These results were in agreement with previous studies that found increased in sepsis, both proinflammatory and anti-inflammatory proteins (Bozza et al., 2007; Harbarth et al., 2001; Zeng et al., 2022), supporting the idea that in critically ill patients both inflammatory responses could coexist at the same time (Xiao et al., 2011). Interestingly, in our study the circulating IL-18 failed to correlate with mortality as previously demonstrated (Eidt et al., 2016), however, the predictors of poor outcome IL-6, IL-8, IL-1RA and TNF-α were strongly associated with death (Bozza et al., 2007; Chaudhry et al., 2013). In addition, in the last few years, ferritin, sTREM-1 and, recently, sSIGLEC5 have been proposed as markers of immune dysregulation due to infection (He et al., 2023; Lozano-Rodríguez et al., 2023; Wright et al., 2020), and although an increase of all of them were found in our septic cohort, only sTREM-1 predict septic shock and mortality. These differences could be due to the fact that our study focus in a well-defined population of intra-abdominal origin septic patients while in other studies there are different ranges of aetiologies on the septic patients enrolled.

As previously described (Martínez-García et al., 2019), our study also supports that during the initial inflammatory response of sepsis, there is a subgroup of patients who present an early impairment on the activation of the NLRP3 inflammasome, evidenced by the dysfunctional ability to form ASC oligomers after *ex vivo* stimulation of monocytes with LPS and ATP. This subgroup account higher mortality and higher state of severity. On the con-

trary, all septic patients presented a non-impaired priming and activation of the Pyrin inflammasome after LPS and TcdB treatment when analyse the percentage of ASC-specking monocytes. Importantly, individual and not averaged data allowed us to discriminate the group of NLRP3 immunocompromised septic patients at day one. Indeed, the group of patients with a NLRP3 inflammasome immunoparalysis was not identified with the different clinical scores to assess sepsis severity at early phase, the leucocytes counts or the biochemical parameters analysed. Also, these patients presented an impaired production of other cytokines when their PBMCs were cultured and stimulated *ex vivo*, suggesting a general suppression of the innate immunity. This distinction among septic patients was detected previously by the reduced expression of HLA-DR in monocytes (Döcke et al., 1997), confirming the role of blood monocytes in the development of an immunosuppressive long-term state in sepsis (Albertsmeier et al., 2017; Biswas & López-Collazo, 2009), in our study the reduction in ASC-specking monocytes correlates with the decrease in monocyte number.

The immunosuppression of the NLRP3 inflammasome found at day one was reversed upon patient recovery, indicating that the impairment in NLRP3 inflammasome activation was transitory. Whereas, the Pyrin inflammasome response was similar in septic patients during sepsis onset and at hospital discharge, suggesting that Pyrin inflammasome presents different regulation mechanisms during sepsis.

When the inflammatory landscape of septic patients with or without impairment of the NLRP3 inflammasome was compared, we found that the plasma concentration of IL-1β and IL-37 were able to define these septic patients with high mortality. IL-37 appears to downregulates the production of the LPS-induced proinflammatory cytokines, including IL-1β, IL-18 and IL-6 in human blood monocytes. In mice model of sepsis, IL-37 enhances the suppressive activity of T cells protecting animals from endotoxemia and mortality (Li et al., 2015; Nold et al., 2010). IL-1β is widely known for being a robust proinflammatory cytokine and recombinant human IL-1RA, anakinra, has been shown to be a safe and effective treatment in patients with bacterial sepsis (Fisher et al., 1994). Therefore, our results may us to hypothesize that both cytokines might be favouring the dysregulation of innate and adaptative responses that occurs in the immunocompromised septic patients, as these cytokines could be produced *in vivo* by NLRP3 inflammasome activation.

In definitive, our study differentiates from previous work that failed to identify predictive clinical markers and blood-cytokines associated to severity and deaths in septic patients (Fahy et al., 2008). We confirm previous results in a new cohort of patients which NLRP3 inflammasome is compromised in septic patients with high mortality (Martínez-García et al.,

2019). Moreover, the restauration of NLRP3 inflammasome activation in monocytes of septic patients who present an early impairment of the NLRP3 inflammasome could be an indicator of immune recovery. So that, this Thesis advances towards a personalized biomarker that could stratify septic patients with worse prognosis, being that an important advance for the diagnostic and therapeutical election in sepsis.

2. Differences in inflammatory cytokines between bacterial sepsis and COVID-19 disease

COVID-19, as sepsis, causes significant infection-related morbidity and mortality. In both infectious diseases, advanced aged and comorbidities can increase the risk of suffering a severe pathology and a poor clinical outcome. Similarly to sepsis, COVID-19 patients show high levels of circulating inflammatory cytokines which are associated with an unfavourable progression of the disease (López-Collazo et al., 2020; Zafer et al., 2021). According to data, the cytokine storm and the inflammatory burst present in severe cases, result in respiratory failure, the onset of sepsis and ultimately death (Guan et al., 2020; Zhou et al., 2020).

In this Thesis we compared the concentration in plasma cytokines between COVID-19 patients and intra-abdominal origin sepsis patients, additionally to other factors associated with severity such as procalcitonin, C-reactive protein and ferritin.

We found that the concentration of CRP and PCT in the plasma of COVID-19 patients significantly increased in line with the categories of illness severity, accordingly to different studies (Tan et al., 2020; Yang et al., 2020). Serum ferritin, a prognostic marker of immune dysregulation and a risk factor for disease severity (Henry et al., 2020; Vargas & Rojo, 2020), was also increased in the mild and severe group of COVID-19 patients. We also found that the concentration of four cytokines associated with the cytokine storm (IL-6, IL-1RA, IL-15 and IL-18) are consistent with previous reports demonstrating higher levels of inflammatory cytokines among COVID-19 patients with more severe disease (Zhao et al., 2020; Zhou et al., 2020). Moreover, in our COVID-19 cohort, IL-6 is one of the key cytokines that is correlated with disease severity, supporting the fact that various clinical trials have included IL-6 inhibitors to prevent COVID-19 disease progression (Atal & Fatima, 2020; Buonaguro et al., 2020; Liu et al., 2020).

When comparing COVID-19 to bacterial sepsis we showed that PCT and CRP levels were dramatically higher in bacterial sepsis compared to severe COVID-19, while ferritin displayed the opposite behaviour, similarly to other studies (Linarez-Ochoa et al., 2022; Perschinka et al., 2022; Wilson et al., 2020). Although ferritin is elevated in both sepsis and

COVID-19, the hyperferritinemia may influence the severity of COVID-19, as this is considered a marker of uncontrolled inflammation.

In addition, the proinflammatory cytokines IL-6 and IL-18 are markedly elevated in sepsis when compared with COVID-19 patients. IL-18, similar to IL-1β, is a potent proinflammatory cytokine involved in host defence against infections, and IL-6 is a cytokine produced downstream from IL-1β. Therefore, our results suggest a stronger production of these inflammatory cytokines in response to bacterial sepsis than COVID-19 patients.

3. Functional analysis of NLRP3 variants associated to autoinflammatory disease

NLRP3-associated autoinflammatory diseases encompasses a diverse of clinical manifestations in which only the 30% of pathogenic mutations have been associated with clinical phenotypes and have been confirmed through *in vitro* assays (Infevers database: https://infevers.umai-montpellier.fr/web/search.php). In this Thesis we functionally characterized 20 NLRP3 variants *in vitro* and for four of them, results were confirmed on monocytes from 13 patients. Noteworthy, expression of all the NLRP3 variants studies in transient transfections was similar, excluding any technical artifact caused by overexpression of a particular mutants.

In patients with variant of uncertain significance, the symptomatology of the AIDs varies widely and the genotype-phenotype correlation is generally difficult to assess. Moreover, the activation of the NLRP3 inflammasome in response to triggers in the absence of priming has not been considered for low-penetrance NLRP3 variants (Rieber et al., 2015). Our results showed that VUS variants V198M and Q703K did not result in a constitutively active NLRP3 inflammasome, suggesting that these mutations are functionally similar to wild-type. However, in the presence of the activation signal nigericin, and without LPS priming, they were able to induce ASC oligomers. On the contrary, R488K low-penetrance variant could favours inflammasome activation at baseline. Importantly, the exacerbated inflammatory phenotype of CAPS patients was not observed when testing PBMCs from patients with the low-penetrance NLRP3 variants. These results suggest that NLRP3 VUS variants present an inactive structure, similar to NLRP3 wild-type, in which the activation signal, at least, is involved in destabilizing the inactive form of the inflammasome. This is in line with previous studies in which low-penetrance NLRP3 variants displayed an intermediate biological phenotype compared to wild-type and pathogenic NLRP3 variants (Cosson et al., 2023; Kuemmerle-Deschner et al., 2017).

In this Thesis we also studied the functionally of NLRP3 with FCAS-variants. Although FCAS disorder is characterized by cold-induce hyperinflammation and fever, the molecular mechanisms by which cold exposure regulates the NLRP3 inflammasome activity in FCAS remain unclear (Brydges et al., 2013; Rosengren et al., 2007). In the recent years, it has been proposed that cold-triggered inflammasome activation is controlled by the chaperone HSC70. Concretely, at physiological temperature, HSC70 interacts and supresses the activity of NLRP3, being this suppression enhanced in NLRP3 mutants when compared to wild-type. However, upon cold exposure, HSC70 undergoes conformational changes with the consequent loss of interaction between HSC70 and the NLRP3 variants, favouring the formation of active NLRP3 inflammasomes (Karasawa et al., 2022; Raghawan et al., 2019, 2023). Our results have provided evidence that NLRP3 FCAS variants present an 'open' structure in comparation with wild-type, similarly than other NLRP3 CAPS–associated variants (Tapia-Abellán et al., 2019), which may facilitate their interaction with HSC70. Upon cold-exposure to 32ºC, FCAS–associated NLRP3 variants presented an increase ASC oligomer, suggesting that for these variants the activation of the NLRP3 inflammasome is induced by cold.

We also analysed different NLRP3 variants that have been described in mosaicism or germline. The low allele frequency of somatic NLRP3 mutations (under 15% of total cases) could be because they are highly detrimental and incompatible with embryonic development and with life (Lasigliè et al., 2017; Solís-Moruno et al., 2021). In fact, the detection of NLRP3 somatic mosaicism in CAPS has been directly associated with the severe clinical phenotype NOMID (Tanaka et al., 2011). Our results support that when NLRP3 variants affect to key amino acids required for Walker B ATPase function (residues from 295 to 304 in human NLRP3), autoinflammatory-related NLRP3 mutants present an active 'open' conformation with a high ASC oligomerization, similarly as previously described for variants E304K and D303N (Brinkschulte et al., 2022; Tapia-Abellán et al., 2019). Moreover, and in accordance with the recent studies resolving the cyro-electron microscopy structure of the NLRP3 inflammasome (Hochheiser et al., 2022; Xiao et al., 2023), the different NLRP3 variants found in mosaicism, which have a high percentage of cells with ASC oligomers (K355N, M406V and T433I), are located near the nucleotide-binding site in the NBD and next to the beginning of the WHD. This position is near the pivot point necessary for the conformational change leading to activation and thus causing an exacerbated auto-activation of the NLRP3 inflammasome. This could be either by destabilizing the inactive conformation or stabilizing the active conformation of NLRP3.

In this Thesis, we also performed a comparison of the sensitivity of the different NLRP3 mutants to two inhibitors, MCC950 and CY-09. We found that MCC950 was able to

significantly increase the BRET signal and abolish ASC oligomerization in the majority of NLRP3 variants studied, except for the E304K mutant, confirming that this residue is critical for ATP hydrolysis in NLRP3 as was previously described (Brinkschulte et al., 2022; Tapia-Abellán et al., 2019). Interestingly, the NLRP3 variants found in mosaicism, D303H and M406V, presented a partial sensitivity to MCC950 suggesting that higher dose will be needed to block the active conformation of these mutants. On the other hand, CY-09 was proposed to abrogate the NLRP3 inflammasome formation by direct interaction with the ATP-binding motif of Walker A/B sites (Jiang et al., 2017). However, a recent study reported that CY-09, like MCC950, do not impair NLRP3 ATP hydrolysis activity (Brinkschulte et al., 2022). Our experimental observations showed that CY-09 diminished BRET signal in most of the NLRP3 variants. This effect was the opposite than MCC950. Furthermore, when CY-09 is added after MCC950, it was not able to decrease the BRET signal, and therefore not able to alter the 'closed' conformation favoured by MCC950. We can propose that, while MCC950 stabilizes the NACHT and LRR domains, CY-09 induces to an 'open' inactive conformation of NLRP3 inflammasome.

Although our results are not identical in all the mutations studied, it is important to keep in mind the variability between the domains in which they are found, the polarity and charge of the mutated amino acids and the clinical phenotype to which they are associated. This highlight that NLRP3 blockers will not work with the same potency in all CAPS patients and personalized dose will be required. Altogether, our study constitutes a comprehensive analysis of NLRP3-associated autoinflammatory disease mutants, revealing the functional diversity of gain-of-function variants that could be take in consideration for diagnosis and treatment of autoinflammatory disorders.

4. Functional analysis of NLRC4 variants associated to autoinflammatory disease

NLRC4 is a cytosolic NLR that is activated by several bacterial proteins, like flagellin, which are first sensed by receptors of the NAIP family. Activated NAIP binds NLRC4, inducing a conformational change on it, which further allows the recruitment of inactive NLRC4 molecules in a prion-like polymerization event. NLRC4 activation induces caspase-1 activation and promotes the secretion of inflammatory cytokines of the IL-1 family. Pathogenic gain-of-function NLRC4 mutations are believed to cause dominantly inherit autoinflammatory diseases with variable clinical presentations, which include enterocolitis, recurrent episodes of MAS, a familial form of cold-induced autoinflammatory syndrome and painful subcutaneous nodules. Increasing evidence suggest that IL-18, instead of IL-1β, has an important role in the progression of NLRC4-inflammasomopathies, making its blockade a successful experimental therapy (Canna et al., 2017; Hafner-Bratkovič, 2017).

In this Thesis, we evaluated an adult patient carrying the postzygotic NLRC4 S171F variant present in mosaicism, suffering from systemic inflammation and recurrent fever. This variant was previously reported in a 28-week preterm infant with clinical features of MAS who died at 2 months of age without any functional research performed, which would likely be informative in the differential diagnosis and therapy strategies (Liang et al., 2017). To address the functional consequences of this variant, *in vitro* and *ex vivo* analysis was performed. *In vitro* assays revealed an increase in the ASC speck formation when mutant NLRC4 was expressed together with ASC molecule in HEK293T cells, compared with cells expressing wild-type NLRC4. Similarly, the proportion of ASC-specking monocytes in a single sample from the patient was constitutively increase when compared to healthy controls, thus indicating the expected behaviour of a gain-of-function variant. In line with previous studies on NLRC4-associated MAS, the patient's PBMCs showed enhanced secretion of IL-18 (Canna et al., 2014). However, patient's PBMCs failed to release high amount of IL-1β, in contrast to previous data (Canna et al., 2014). The deficiency in IL-1β could not be attributed to a defect in LPS priming and impaired NF-κB activation, as LPS-induced TNF-α and IL-6 released in a similar manner between the patient and healthy controls, or due to a decrease in the number of the monocytes in the patient's PBMCs sample. The differences found among this patient and others reported in the bibliography (Canna et al., 2014) in which a higher release of IL-1β and IL-6 was found after LPS priming could be due to the stimulation protocol (6h of LPS treatment against 3 hours in our study) or the differences in the degree of mosaicism (2-4% in the patient described herein versus 25% mutant allele fraction in the described fatal case). Overall, the evidence obtained in this Thesis supports a GoF behaviour of the S171F NLRC4 variant, being the patient described previously, the first case reported of a late-onset NLRC4-associated autoinflammatory disease caused by somatic NLRC4 mosaicism.

Additionally, to the S171F NLRC4 variant, we also studied in this Thesis other NLRC4 autoinflammatory-associated mutations using a recombinant HEK293T system. In the mutation T177A, similarly to S171F, the percentage of HEK293T cells with ASC oligomers was highly augmented when the variant was expressed with ASC. A three-dimensional model structure of this variant was performed by Kawasaki et al., and showed that the residue threonine 177 of human NLRC4 directly faces the ADP in the binding pocket, which seem important for NLRC4 auto-inhibition. So that, substitution of this amino acid could induce auto-activation of the NLRC4 inflammasome (Kawasaki et al., 2017). Likewise, the mutation S445P presented a pronounced increase in the ASC-speck formation, which could be related with the severe symptomatology presented in patients carrying this mutation

(Volker-Touw et al., 2017). Indeed, functional studies indicated that the S445P NLRC4 variant is able to recruit ASC and assemble a constitutively active oligomeric inflammasome (Gil-Lianes et al., 2023).

The mutations T337N and T337S increase the number of cells with ASC oligomers, being statistically significant only in the last variant, in accordance with previous results showing that substitution of threonine 337 could destabilize the WHD and NDB interactions, essential to maintain NLCR4 in an inactive state (Canna et al., 2014).

In the case of the mutation W655C, a slightly increase in the formation of ASC oligomers was observed when compared to NLRC4 wild-type. Moghaddas *et al.* showed that tryptophan 655 substitution with cysteine facilitates the engagement of two neighbouring NLRC4 monomers during NLRC4 oligomerization, stabilizing the final NLRC4 complex (Moghaddas et al., 2018). This result could be in consonance with the fact that, in comparation with others NLRC4 variants like T177A or S171F, W655C mutation did no induce a high number of cells with ASC oligomers. The same behaviour has been described for the mutation Q657L, also in agreement with our flow cytometry results detecting ASC oligomers (Chear et al., 2020).

Regarding the NLRC4 variants G633dup, C697S and D10009G, all of them are novel mutations that have not yet been described. Although the clinical features and the genetics analysis of the individuals carrying these mutations are ongoing, they correlate with a NLRC4-autoinflammatory disease. None of them resulted in an increase of the ASC speck formation when mutants NLRC4 were expressed together with ASC in HEK293T cells. The same result was obtained for the mutations H443P and V341A, both of which have been widely described as pathogenic NLRC4 variants that cause severe phenotypes of autoinflammation (Barsalou et al., 2018; Kitamura et al., 2014; Raghawan et al., 2019; Romberg et al., 2014). A possible explanation could be that NLRC4 exists in an autoinhibited monomeric conformation in which the C-terminal LRR domain occludes the central NBD, which is necessary for the NLRC4 oligomerization. The inactive state of NLRC4 depends on an auto-inhibitory mechanisms that require the interaction between its NBD and WHD domains, mediated by ADP binding and the stabilization of the HD1 domain. Activating mutations that affect amino acids contained in the LRR domain (such as D10009G) or that destabilize the NBD–WHD interaction (like V341A), could lead a conformational change exposing the NBD motif, similar than what is produced after NLRC4 activation, which appears to be sufficient to assembly fully functional NLRC4 inflammasomes in an ASC-independent manner (Duncan & Canna, 2018). Moreover, the H443P mutation appears to consistently manifest as FCAS, being induced by exposure to cold temperature (Kitamura et

al., 2014; Raghawan et al., 2019), hence our *in vitro* experiments could not mimic the physiological conditions that autoactivate this NLRC4 variant.

It is important to stand out that the system in which the NLRC4 oligomerization was analysed in Thesis is based on overexpression of proteins in HEK293T cells, which is a limitation of this work as these conditions could not entirely reproduce what occurs in human cells that normally are in heterozygosis. Despite our recombinant system only expressed mutant NLRC4, its expression was controlled to low expressing cells by flow cytometry MFI gating. Thus, future experiments should be focus on the study of more physiological systems and primary human samples, where display functional studies to confirm the gain-of-function behaviour of NLRC4 variants.

5. Inflammasome activation in monocytes from CAPS and FMF patients

Cryopyrin-Associated Periodic Syndrome and Familiar Mediterranean fever are two autoinflammatory conditions resulting from monoallelic variants in the *NLRP3* and the *MEFV* genes, respectively. The aberrant activation of the NLRP3 and the Pyrin inflammasomes in the patients, mediated by gain-of-function variants, cause inflammatory flares characterized by a dysregulated production of proinflammatory cytokines (Booshehri & Hoffman, 2019; de Torre-Minguela et al., 2017). In this Thesis, we aimed to study the activation of the NLRP3 and the Pyrin inflammasomes in monocytes from CAPS and FMF patients which were with inactive disease under colchicine and IL-1 blocking therapy.

Our study reveals that gain-of-function NLRP3 variants associated with CAPS, but not mutations affecting Pyrin inflammasome in FMF patients, lead to the formation of a constitutively active NLRP3 inflammasome even in the absence of triggers or priming signals. Indeed, triggers activating NF-κB signalling pathway, like LPS, enhance ASC oligomerization in monocytes of CAPS-associated NLRP3 variants, which seem to be NLRP3-dependent as the specific NLRP3 inhibitor MCC950 could reduce the percentage of ASC-specking monocytes in these patients.

According to the release of IL-1β and IL-18 cytokines in blood cells from CAPS and FMF patients, there are discrepancies in the bibliography. Some studies showed that PBMCs or monocytes from patients do not release constitutively the proinflammatory cytokines when maintained in culture untreated or primed with LPS (Magnotti et al., 2019; Moghaddas et al., 2017; Repa et al., 2015). However, other studies that reported cultures of blood cells from patients with Familiar Mediterranean fever had a constitutive increased IL-1β release (Ibrahim et al., 2014; Omenetti et al., 2014). The findings from our study confirm that neither CAPS patients nor FMF patients release detectable IL-1β or TNF-α in basal

unprimed cells. On the contrary, CAPS patients showed a constitutive release of the cytokine IL-18. The differences among studies could be due to various aspects: (i) the culture period of the unprimed cells in the studies which results in different activation of the NLRP3 inflammasome, (ii) the absence or presence of inflammatory flares at the time of blood collection and analysis, and (iii) the fact that different gain-of-function variants may lead to the constitutive formation of active inflammasomes but its downstream signalling could be differentially regulated.

Consequently, measurement of IL-1β release in FMF- and CAPS-related cells should not be considered as the sole marker of inflammasome activation. In conclusion, CAPS-associated NLRP3 variants can form constitutively active inflammasomes.

6. NLRP3 inflammasome activation in MS patient's refractory to treatment with fingolimod

Fingolimod (also known as FTY720) is the first-class modulator with highly effectivity approved for the therapy of RRMS. Functionally, it antagonizes the sphingosine 1-phosphate receptor (S1P) on T cells, causing its internalization and degradation, thus preventing the S1P-dependent lymphocyte egress from secondary lymphoid organs. Consequently, it reduces the number of autoreactive cells that recirculate through blood and lymph to the central nervous system, leading to a reduction of 60 to 80% in blood absolute lymphocyte counts (Brinkmann, 2009; Callegari et al., 2021; Mehling et al., 2008). Several studies have proposed different biomarkers to fingolimod response, like the levels of cerebrospinal mitochondrial or the monocyte-derived microvesicles (Leurs et al., 2018; Quirant-Sánchez et al., 2018). However, none of these could be used routinely by clinicians.

Recent studies in animal models of depression and Parkinson disease (Guo et al., 2020; Yao et al., 2019) showed that fingolimod, not only alleviated the neuronal damage and oxidative stress, but also inhibited the NLRP3 inflammasome assembly. Due to that, we aimed to study the potential role of NLRP3 inflammasome in the therapeutic response to fingolimod.

To do that, we analysed a cohort of patient with RRMS treated with fingolimod (n = 12), which were classified into responders and non-responders after 12 months of treatment according to the radiologic and clinical parameters. In line with previous findings in animal models, we found that fingolimod reduces the percentage of monocytes with ASC oligomers in responders patients after 6 months of treatment when the canonical activation of NLRP3 inflammasome with LPS and ATP was used. On the contrary, fingolimod failed to inhibit

NLRP3 inflammasome activation in non-responders, as the number of cells with ASC oligomers and the pyroptosis, measured by the extracellular concentration of galectin-3, were enhanced in this group of patients after 6 months of treatment in comparation with the pre-treatment levels. Neither of these results could be attributed to a difference in the proportion of the different monocyte phenotypes, as the percentage of classical, intermediate and non-classical monocytes were similar in fingolimod responders and non-responders either before or during treatment.

The fact that fingolimod has been shown to downregulate the NF-κB signalling pathway (Shi et al., 2021; Ling Zhang et al., 2022) may provide an explication of these differences among RRMS patients, as a lack of inhibition of NF-κB would result in a higher NLRP3 inflammasome activation in non-responders. Indeed, the PBMCs from these patients release higher levels of IL-6 and TNF-α release in the absence of LPS stimulation after fingolimod treatment. Whereas, the release of these NF-κB-dependent cytokines were significantly lower in fingolimod responders.

Taking together, our study suggests that fingolimod treatment may exert part of its beneficial effects by inhibiting the NLRP3 inflammasome activation. Moreover, the lack of inhibition of NLRP3 inflammasome activation in patients with RRMS treated with fingolimod, could emerge as a biomarker of non-responders to treatment, who may benefit of other MS therapies.

7. NLRP3 inflammasome activation in CMML patients with *KRAS* mutation is reverted by IL-1R-antagonist treatment

RAS mutations are considered adverse prognostic factors of unfavourable survival and are found in approximately 30% of all human malignancies. In particular, in chronic myelomonocytic leukemia are reported between 7% to 22% of the diagnosticated individuals (Patnaik & Lasho, 2020). The RAS proteins, KRAS and NRAS, are GTPases involved in several cellular signalling pathways, such as, in the regulation of cell proliferation and in apoptosis. Mutations affecting the GTP-binding site led to a continued activation of their downstream mechanisms, favouring cell survival (Johnson et al., 2017; Pantsar, 2020).

In the last few years, numerous studies have attempted to investigated whether myeloid clonal proliferation may be mediated by a combination of an inflammatory environment and oncogenic stimulus. Since that, models of NLRP3-deficient mice and animals treated with experimental NLRP3 blockers have implicated the NLRP3 inflammasome in diseases

like myelodysplastic syndromes (Coll et al., 2022; Mangan et al., 2018). However, few studies address the relationship between NLRP3 and malignant disorders in the context of human disease.

In this Thesis, we have analysed blood samples of a cohort of CMML patients with and without mutations in *KRAS*. We found that *KRAS*-mut CMML presented an increased percentage of circulating monocytes with ASC oligomers under basal conditions. This high percentage has not even described and is far above for the obtained from CAPS patients, who present gain-of-function mutations in NLRP3. Moreover, no increase of IL-1β release was achieved after the canonical activation of NLRP3 inflammasome with LPS and ATP. When the blood was cultured with the specific NLRP3 inhibitor MCC950, the release of IL-1β was significantly reduced while the percentage of ASC-specking monocytes slightly decreased. These results are in line with the fact that the NLRP3 inflammasome activation is a cellular irreversible mechanism once ASC oligomerize and supports the idea that mutations in the oncogene *KRAS* may be inducing the NLRP3 inflammasome activation, similarly to the results obtained in a mouse model and human leukemia cells with a *KRAS* mutation in the residue G12 (Hamarsheh et al., 2020).

Importantly, Basiorka *et al*. found that mutations in other myeloid genes can also induce the activation of the NLRP3 inflammasome (Basiorka et al., 2016). In our cohort of CMML patients, 4 of the 5 *KRAS*-mut patients studied had only mutations in that gene, whereas each of the 4 *KRAS*-WT patients carried a different mutational profile. Although we cannot conclude that other myeloid mutations may also influence inflammasome activation, due to the small size of our cohort, the main difference between the two cohorts of CMML patients is the presence of the mutation in *KRAS*, thus the high basal percentage of monocytes with ASC oligomers can only be explained by aberrant RAS signalling.

Moreover, we studied the extracellular LDH levels in unstimulated cultured PBMCs. We found that the basal activation of the NLRP3 inflammasome in *KRAS*-mut CMML patients was not associated with an increase of the pyroptosis of the monocytes. That suggests that the IL-1β release could result from living hyperactive monocytes with defective pyroptosis, representing this another mechanism of cell survival together with the impaired apoptosis found in CMML monocytes (Evavold et al., 2018; Lieberman et al., 2019; Sevin et al., 2021; Zanoni et al., 2016). On the contrary, in the CMML patient's plasma we found an increase in HMGB1, P2X7 receptor and ASC, all known as markers for cell death. As described in the bibliography, P2X7 could be found in the supernatant of PBMCs after inflammasome activation (García-Villalba et al., 2022). HMGB1 and ASC, for their part, have been reported to be released in different type of cell death, but not exclusively pyroptosis

(Baroja-Mazo et al., 2014; Franklin et al., 2014; Meynier & Rieux-Laucat, 2019; Teodorovic et al., 2014). Indeed, Basiorka *et al.* demonstrated the presence of ASC oligomers in plasma of MDS patients (Basiorka et al., 2018), supporting that our results in CMML patients.

In addition, we showed that the treatment of a CMML patient carrying the mutation *KRAS*-G12D with anakinra, an IL-1 blocker, blocked the NLRP3 inflammasome activation in *ex vivo* experiments, reducing the number of ASC-specking monocytes, the level of free ASC in plasma and the release of the proinflammatory cytokines IL-1β and IL-18. As it has been recently published, IL-1β contributed to the myeloproliferation (Villatoro et al., 2023). Therefore, our results may lead us to hypothesize that the malignant clones of monocytes found in CMML might depend on IL-1 signalling, and its blockade reduces NLRP3 activation.

Taken together, our study demonstrated that CMML *KRAS*-mut patients present a basal activation of the NLRP3 inflammasome. Also, that IL-1 blockers may be a therapeutic option to improved clinical status of CMML patients. Moreover, our study supports the notion that CMML *KRAS*-mut patients who have a poor response to conventional therapies and poor prognosis could benefit, in the future, from novel therapies blocking the inflammasome such as the recently developed nanobodies against extracellular ASC oligomers.

CONCLUSIONS

1. Survival of patients with intra-abdominal origin sepsis is associated with increase canonical activation of the NLRP3 inflammasome in blood monocytes treated with LPS and ATP.

2. Pyrin inflammasome activation in blood monocytes treated with LPS and TcdB at day one is not associated with the survival of patients suffering intra-abdominal origin sepsis.

3. In the plasma of patients with intra-abdominal origin sepsis the cytokines IL-6, IL-8 and IL-1RA, as well as the acute phase proteins CRP and PCT, were increased when compared to COVID-19 and healthy individuals.

4. In the plasma of COVID-19 patients the cytokine IL-15 and ferritin were increased when compared to healthy individuals and patients with intra-abdominal origin sepsis.

5. The uncertain significance NLRP3 variants V198M and Q703K expressed in HEK293T cells have a similar BRET signal and induce a similar percentage of cells with ASC oligomers than NLRP3 wild-type.

6. The NLRP3 variants R260W, L305P and L353P expressed in HEK293T cells present a diminish in BRET signal in comparation with NLRP3 wild-type at 37ºC and 32ºC.

7. The NLRP3 pathogenic variants R250W and L353P expressed in HEK293T cells induce an increase of the percentage of cells with ASC oligomers at 32ºC when compared to 37ºC.

8. With the exception of the G326E NLRP3 variant, MCC950 inhibitor increases the BRET signal of all the pathogenic NLRP3 variants expressed in HEK293T cells.

9. CY-09 inhibitor decreases the BRET signal of all the pathogenic NLRP3 variants when expressed in HEK293T cells, with the exception of R260W, D303A, D303G, E304K and L353P variants.

10. A patient carrying the postzygotic S171F NLRC4 variant presented an increase in the proportion of monocytes with ASC oligomers and IL-18 release when compared to healthy controls.

11. The NLRC4 pathogenic variants S171F, T117A, T337S, S445P and W665C presented an increase of ASC-specking cells when expressed in HEK293T cells.

12. CAPS patients had an enhancement of the percentage of ASC-specking blood monocytes compared to FMF patients and healthy controls.

13. Patients with relapsing-remitting multiple sclerosis refractory to fingolimod treatment had an increase in monocytes with ASC oligomers after the canonical activation of the NLRP3 inflammasome with LPS and ATP compared with responders and healthy individuals.

14. CMML patients with mutation in *KRAS* had a significantly increase in the percentage of blood monocytes with ASC oligomers when compared to either healthy controls or CMML $KRAS^{WT}$ patients.

15. Anakinra treatment in a CMML patient with a $KRAS^{G12D}$ mutation impairs the canonical NLRP3 inflammasome activation and serves as a bridge therapy to allo-HSCT.

BIBLIOGRAPHY

Abbafati, C., Abbas, K. M., Abbasi-Kangevari, M., Abd-Allah, F., Abdelalim, A., Abdollahi, M., Abdollahpour, I., Abegaz, K. H., et al. (2020). Global burden of 369 diseases and injuries in 204 countries and territories, 1990–2019: a systematic analysis for the Global Burden of Disease Study 2019. *The Lancet*, *396*(10258), 1204–1222.

Abdel Galil, S. M., Ezzeldin, N., & El-Boshy, M. E. (2015). The role of serum IL-17 and IL-6 as biomarkers of disease activity and predictors of remission in patients with lupus nephritis. *Cytokine*, *76*(2), 280–287.

Abers, M. S., Delmonte, O. M., Ricotta, E. E., Fintzi, J., Fink, D. L., Almeida de Jesus, A. A., Zarember, K. A., Alehashemi, S., et al. (2021). An immune-based biomarker signature is associated with mortality in COVID-19 patients. *JCI Insight*, *6*(1).

Aganna, E., Martinon, F., Hawkins, P. N., Ross, J. B., Swan, D. C., Booth, D. R., Lachmann, H. J., Gaudet, R., et al. (2002). Association of mutations in the NALP3/CIAS1/PYPAF1 gene with a broad phenotype including recurrent fever, cold sensitivity, sensorineural deafness, and AA amyloidosis. *Arthritis and Rheumatism*, *46*(9), 2445–2452.

Ahn, M., Chen, V. C. W., Rozario, P., Ng, W. L., Kong, P. S., Sia, W. R., Kang, A. E. Z., Su, Q., Nguyen, L. H., et al. (2023). Bat ASC2 suppresses inflammasomes and ameliorates inflammatory diseases. *Cell*, *186*(10), 2144-2159.e22.

Akira, S., Uematsu, S., & Takeuchi, O. (2006). Pathogen recognition and innate immunity. *Cell*, *124*(4), 783–801.

Akkaya, M., Kwak, K., & Pierce, S. K. (2020). B cell memory: building two walls of protection against pathogens. *Nature Reviews Immunology*, *20*(4), 229–238.

Alarcón-Vila, C., Baroja-Mazo, A., de Torre-Minguela, C., Martínez, C. M., Martínez-García, J. J., Martínez-Banaclocha, H., García-Palenciano, C., & Pelegrin, P. (2020). Cd14 release induced by p2x7 receptor restricts inflammation and increases survival during sepsis. *ELife*, *9*, 1–21.

Albertsmeier, M., Prix, N. J., Winter, H., Bazhin, A., Werner, J., & Angele, M. K. (2017). Monocyte-dependent suppression of T-cell function in postoperative patients and abdominal sepsis. *Shock*, *48*(6), 651–656.

Aldea, A., Campistol, J. M., Arostegui, J. I., Rius, J., Maso, M., Vives, J., & Yagüe, J. (2004). A Severe Autosomal-Dominant Periodic Inflammatory Disorder with Renal AA Amyloidosis and Colchicine Resistance Associated to the MEFV H478Y Variant in a Spanish Kindred: An Unusual Familial Mediterranean Fever Phenotype or Another MEFV-Associated Periodic. *American Journal of Medical Genetics*, *124 A*(1), 67–73.

Alsabani, M., Abrams, S. T., Cheng, Z., Morton, B., Lane, S., Alosaimi, S., Yu, W., Wang, G., et al. (2022). Reduction of NETosis by targeting CXCR1/2 reduces thrombosis, lung injury, and mortality in experimental human and murine sepsis. *British Journal of Anaesthesia*, *128*(2), 283–293.

Alves-Filho, J. C., Spiller, F., & Cunha, F. Q. (2010). Neutrophil paralysis in sepsis. *Shock*, *34*, 15–21.

Anaya, J. M., Gómez, L., & Castiblanco, J. (2006). Is there a common genetic basis for autoimmune diseases? *Clinical and Developmental Immunology*, *13*(2–4), 185–195.

Andreeva, L., David, L., Rawson, S., Shen, C., Pasricha, T., Pelegrin, P., & Wu, H. (2021). NLRP3 cages revealed by full-length mouse NLRP3 structure control pathway activation. *Cell*, *184*(26), 6299-6312.e22.

Angosto-Bazarra, D., Alarcón-Vila, C., Hurtado-Navarro, L., Baños, M. C., Rivers-Auty, J., & Pelegrín, P. (2022). Evolutionary analyses of the gasdermin family suggest conserved roles in infection response despite loss of pore-forming functionality. *BMC Biology*, *20*(1), 1–18.

Angosto-Bazarra, D., Molina-López, C., Peñín-Franch, A., Hurtado-Navarro, L., & Pelegrín, P. (2021). Techniques to study inflammasome activation and inhibition by small molecules. *Molecules*, *26*(6).

Arber, D. A., Orazi, A., Hasserjian, R. P., Borowitz, M. J., Calvo, K. R., Kvasnicka, H. M., Wang, S.

A., Bagg, A., et al. (2022). International Consensus Classification of Myeloid Neoplasms and Acute Leukemias: integrating morphologic, clinical, and genomic data. *Blood*, *140*(11), 1200–1228.

Arend, W. P. (1998). Interleukin-1 receptor antagonist. *Immunologist*, *5*(6), 197–201.

Arend, W. P., Thompson, R. C., & Eisenberg, S. P. (1990). Interleukin 1 Receptor Antagonist Measurement. *Journal of Clinical Investigation*, *85*(5), 1694–1697.

Aróstegui, J. I., Aldea, A., Modesto, C., Rua, M. J., Argüelles, F., González-Enseñat, M. A., Ramos, E., Rius, J., et al. (2004). Clinical and genetic heterogeneity among Spanish patients with recurrent autoinflammatory syndromes associated with the CIAS1/PYPAF1/NALP3 gene. *Arthritis and Rheumatism*, *50*(12), 4045–4050.

Artis, D., & Spits, H. (2015). The biology of innate lymphoid cells. *Nature*, *517*(7534), 293–301.

Arts, R. J. W., Gresnigt, M. S., Joosten, L. A. B., & Netea, M. G. (2017). Cellular metabolism of myeloid cells in sepsis. *Journal of Leukocyte Biology*, *101*(1), 151–164.

Atal, S., & Fatima, Z. (2020). IL-6 Inhibitors in the Treatment of Serious COVID-19: A Promising Therapy? *Pharmaceutical Medicine*, *34*(4), 223–231.

Baker, K. F., & Isaacs, J. D. (2018). Novel therapies for immune-mediated inflammatory diseases: What can we learn from their use in rheumatoid arthritis, spondyloarthritis, systemic lupus erythematosus, psoriasis, Crohn's disease and ulcerative colitis? *Annals of the Rheumatic Diseases*, *77*(2), 175–187.

Baker, P. J., Boucher, D., Bierschenk, D., Tebartz, C., Whitney, P. G., D'Silva, D. B., Tanzer, M. C., Monteleone, M., et al. (2015). NLRP3 inflammasome activation downstream of cytoplasmic LPS recognition by both caspase-4 and caspase-5. *European Journal of Immunology*, *45*(10), 2918–2926.

Ball, D. P., Taabazuing, C. Y., Griswold, A. R., Orth, E. L., Rao, S. D., Kotliar, I. B., Vostal, L. E., Johnson, D. C., et al. (2020). Caspase-1 interdomain linker cleavage is required for pyroptosis. *Life Science Alliance*, *3*(3), 1–11.

Bar-Or, D., Carrick, M., Tanner, A., Lieser, M. J., Rael, L. T., & Brody, E. (2018). Overcoming the Warburg Effect: Is it the key to survival in sepsis? *Journal of Critical Care*, *43*, 197–201.

Baroja-Mazo, A., Martín-Sánchez, F., Gomez, A. I., Martínez, C. M., Amores-Iniesta, J., Compan, V., Barberà-Cremades, M., Yagüe, J., et al. (2014). The NLRP3 inflammasome is released as a particulate danger signal that amplifies the inflammatory response. *Nature Immunology*, *15*(8), 738–748.

Barsalou, J., Blincoe, A., Fernandez, I., Dal-Soglio, D., Marchitto, L., Selleri, S., Haddad, E., Benyoucef, A., et al. (2018). Rapamycin as an adjunctive therapy for NLRC4 associated macrophage activation syndrome. *Frontiers in Immunology*, *9*, 1–6.

Basiorka, A. A., McGraw, K. L., Abbas-Aghababazadeh, F., McLemore, A. F., Vincelette, N. D., Ward, G. A., Eksioglu, E. A., Sallman, D. A., et al. (2018). Assessment of ASC specks as a putative biomarker of pyroptosis in myelodysplastic syndromes: an observational cohort study. *The Lancet Haematology*, *5*(9), e393–e402.

Basiorka, A. A., McGraw, K. L., Eksioglu, E. A., Chen, X., Johnson, J., Zhang, L., Zhang, Q., Irvine, B. A., et al. (2016). The NLRP3 inflammasome functions as a driver of the myelodysplastic syndrome phenotype. *Blood*, *128*(25), 2960–2975.

Bauernfeind, F. G., Horvath, G., Stutz, A., Alnemri, E. S., MacDonald, K., Speert, D., Fernandes-Alnemri, T., et al. (2009). Cutting Edge: NF-κB Activating Pattern Recognition and Cytokine Receptors License NLRP3 Inflammasome Activation by Regulating NLRP3 Expression. *The Journal of Immunology*, *183*(2), 787–791.

Bedaiwi, M. K., Almaghlouth, I., & Omair, M. A. (2021). Effectiveness and adverse effects of anakinra in treatment of rheumatoid arthritis: A systematic review. *European Review for Medical and Pharmacological Sciences*, *25*(24), 7833–7839.

Ben-Chetrit, E., & Touitou, I. (2009). Familial mediterranean fever in the world. *Arthritis Care and*

Research, *61*(10), 1447–1453.

Bertin, J., & DiStefano, P. S. (2000). The PYRIN domain: A novel motif found in apoptosis and inflammation proteins. *Cell Death and Differentiation*, *7*(12), 1273–1274.

Bertoni, A., Penco, F., Mollica, H., Bocca, P., Prigione, I., Corcione, A., Cangelosi, D., Schena, F., et al. (2022). Spontaneous NLRP3 inflammasome-driven IL-1-b secretion is induced in severe COVID-19 patients and responds to anakinra treatment. *Journal of Allergy and Clinical Immunology*, *150*(4), 796–805.

Bessa, J., Meyer, C. A., de Vera Mudry, M. C., Schlicht, S., Smith, S. H., Iglesias, A., & Cote-Sierra, J. (2014). Altered subcellular localization of IL-33 leads to non-resolving lethal inflammation. *Journal of Autoimmunity*, *55*(1), 33–41.

Bhan, C., Dipankar, P., Chakraborty, P., & Sarangi, P. P. (2016). Role of cellular events in the pathophysiology of sepsis. *Inflammation Research*, *65*(11), 853–868.

Bianchi, M. E., Crippa, M. P., Manfredi, A. A., Mezzapelle, R., Rovere Querini, P., & Venereau, E. (2017). High-mobility group box 1 protein orchestrates responses to tissue damage via inflammation, innate and adaptive immunity, and tissue repair. *Immunological Reviews*, *280*(1), 74–82.

Biswas, S. K., & Lopez-Collazo, E. (2009). Endotoxin tolerance: new mechanisms, molecules and clinical significance. *Trends in Immunology*, *30*(10), 475–487.

Biswas, S. K., & Mantovani, A. (2010). Macrophage plasticity and interaction with lymphocyte subsets: Cancer as a paradigm. *Nature Immunology*, *11*(10), 889–896.

Booshehri, L. M., & Hoffman, H. M. (2019). CAPS and NLRP3. *Journal of Clinical Immunology*, *39*(3), 277–286.

Borges, J. P., Sætra, R. S. R., Volchuk, A., Bugge, M., Devant, P., Sporsheim, B., Kilburn, B. R., Evavold, C. L., et al. (2022). Glycine inhibits NINJ1 membrane clustering to suppress plasma membrane rupture in cell death. *ELife*, *11*, 1–24.

Bosmann, M., & Ward, P. A. (2013). The inflammatory response in sepsis. *Trends in Immunology*, *34*(3), 129–136.

Boucher, D., Monteleone, M., Coll, R. C., Chen, K. W., Ross, C. M., Teo, J. L., Gomez, G. A., Holley, C. L., et al. (2018). Caspase-1 self-cleavage is an intrinsic mechanism to terminate inflammasome activity. *The Journal of Experimental Medicine*, 215(3):827-840.

Boxer, M. B., Quinn, A. M., Shen, M., Jadhav, A., Leister, W., Simeonov, A., Auld, D. S., & Thomas, C. J. (2010). A highly potent and selective caspase 1 inhibitor that utilizes a key 3-cyanopropanoic acid moiety. *ChemMedChem*, *5*(5), 730–738.

Bozza, F. A., Salluh, J. I., Japiassu, A. M., Soares, M., Assis, E. F., Gomes, R. N., Bozza, M. T., Castro-Faria-Neto, et al. (2007). Cytokine profiles as markers of disease severity in sepsis: A multiplex analysis. *Critical Care*, *11*(2), 1–8.

Brealey, D., Brand, M., Singer, M., Hargreaves, I., Heales, S., Land, J., Davies, N. A., & Cooper, C. E. (2002). Association between mitochondrial dysfunction and severity and outcome of septic shock. *Lancet*, *360*(9328), 219–223.

Brewer, D. B. (1994). Max schultze and the living, moving, phagocytosing leucocytes: 1865. *Medical History*, *38*(1), 91–101.

Brinkmann, V. (2009). FTY720 (fingolimod) in Multiple Sclerosis: Therapeutic effects in the immune and the central nervous system. *British Journal of Pharmacology*, *158*(5), 1173–1182.

Brinkschulte, R., Fußhöller, D. M., Hoss, F., Rodríguez-Alcázar, J. F., Lauterbach, M. A., Kolbe, C. C., Rauen, M., Ince, S., et al. (2022). ATP-binding and hydrolysis of human NLRP3. *Communications Biology*, *5*(1), 1–12.

Broderick, L., & Hoffman, H. M. (2022). IL-1 and autoinflammatory disease: biology, pathogenesis and therapeutic targeting. *Nature Reviews Rheumatology*, *18*(8), 448–463.

Broz, P. (2023). Unconventional protein secretion by gasdermin pores. *Seminars in Immunology*, *69*, 101811.

Broz, P., & Dixit, V. M. (2016). Inflammasomes: Mechanism of assembly, regulation and signalling. *Nature Reviews Immunology*, *16*(7), 407–420.

Broz, P., Pelegrín, P., & Shao, F. (2020). The gasdermins, a protein family executing cell death and inflammation. *Nature Reviews Immunology*, *20*(3), 143–157.

Broz, P., Ruby, T., Belhocine, K., Bouley, D. M., Kayagaki, N., Dixit, V. M., & Monack, D. M. (2012). Caspase-11 increases susceptibility to Salmonella infection in the absence of caspase-1. *Nature*, *490*(7419), 288–291.

Brubaker, S. W., Bonham, K. S., Zanoni, I., & Kagan, J. C. (2015). Innate immune pattern recognition: A cell biological perspective. In *Annual Review of Immunology* 33, 257-290.

Brydges, S. D., Broderick, L., McGeough, M. D., Pena, C. A., Mueller, J. L., & Hoffman, H. M. (2013). Divergence of IL-1, IL-18, and cell death in NLRP3 inflammasomopathies. *Journal of Clinical Investigation*, *123*(11), 4695–4705.

Buhl, A. L., & Wenzel, J. (2019). Interleukin-36 in infectious and inflammatory skin diseases. *Frontiers in Immunology*, *10*, 1–11.

Buonaguro, F. M., Puzanov, I., & Ascierto, P. A. (2020). Anti-IL6R role in treatment of COVID-19-related ARDS. *Journal of Translational Medicine*, *18*(1), 9–10.

Buras, J. A., Holzmann, B., & Sitkovsky, M. (2005). Model organisms: Animal models of sepsis: Setting the stage. *Nature Reviews Drug Discovery*, *4*(10), 854–865.

Cabeza-Cabrerizo, M., Cardoso, A., Minutti, C. M., Pereira Da Costa, M., & Reis E Sousa, C. (2021). Dendritic Cells Revisited. *Annual Review of Immunology*, *39*, 131–166.

Cai, X., Chen, J., Xu, H., Liu, S., Juang, Q.-X., Halfmann, R., & Chen, Z. (2014). Prion-like Polymerization Underlies Signal Transduction in Antiviral Immune Defense and Inflammasome Activation. *Cell*, *156*(6), 1207–1222.

Callegari, I., Derfuss, T., & Galli, E. (2021). Update on treatment in multiple sclerosis. *Presse Medicale*, *50*(2), 104068.

Canna, S. W., De Jesús, A. A., Sushanth, G., Brooks, S. R., Marrero, B., Liu, Y., Dimattia, M. A., Zaal, K. J. M., Montealegre-Sánchez, G. A., et al. (2014). An activating NLRC4 inflammasome mutation causes autoinflammation with recurrent macrophage activation syndrome. *Nat Genet*, *46*(10), 1140–1146.

Canna, S. W., Girard, C., Malle, L., De Jesus, A. A., Romberg, N., Kelsen, J., Surrey, L. F., Russo, P., et al. (2017). Life-threatening NLRC4-associated hyperinflammation successfully treated with IL-18 inhibition. *Journal of Allergy and Clinical Immunology*, *139*(5), 1698–1701.

Cao, H., Huang, Y., Wang, L., Wang, H., Pang, X., Li, K., Dang, W., Tang, H., et al. (2016). Leptin promotes migration and invasion of breast cancer cells by stimulating IL-8 production in M2 macrophages. *Oncotarget*, *7*(40), 65441–65453..

Carabelli, A. M., Peacock, T. P., Thorne, L. G., Harvey, W. T., Hughes, J., de Silva, T. I., Peacock, S. J., Barclay, W. S., et al. (2023). SARS-CoV-2 variant biology: immune escape, transmission and fitness. *Nature Reviews Microbiology*, *21*(3), 162–177.

Carneiro, L., Magalhaes, J., Philpott, D., & Travassos, L. (2008). Nod-like proteins in inflammation and disease. *Journal of Pathology*, *214*, 136–148.

Case, C. L., Shin, S., & Roy, C. R. (2009). Asc and Ipaf inflammasomes direct distinct pathways for caspase-1 activation in response to Legionella pneumophila. *Infection and Immunity*, *77*(5), 1981–1991.

Cavaillon, J.-M. (2018). Once upon a time. *Invention in the Real: Papers of the Freudian School of Melbourne*, *24*, 11–20.

Cavaillon, J. M., & Adib-Conquy, M. (2006). Bench-to-bedside review: Endotoxin tolerance as a model of leukocyte reprogramming in sepsis. *Critical Care*, *10*(5), 1–8.

Cavalli, G., Colafrancesco, S., Emmi, G., Imazio, M., Lopalco, G., Maggio, M. C., Sota, J., & Dinarello, C. A. (2021). Interleukin 1α: a comprehensive review on the role of IL-1α in the pathogenesis and treatment of autoimmune and inflammatory diseases. *Autoimmunity Reviews*, *20*(3), 102763.

Cayrol, C., & Girard, J. P. (2009). The IL-1-like cytokine IL-33 is inactivated after maturation by caspase-1. *Proceedings of the National Academy of Sciences of the United States of America*, *106*(22), 9021–9026.

Cecconi, M., Evans, L., Levy, M., & Rhodes, A. (2018). Sepsis and septic shock. *The Lancet*, *392*(10141), 75–87.

Chapman, E. A., Lyon, M., Simpson, D., Mason, D., Beynon, R. J., Moots, R. J., & Wright, H. L. (2019). Caught in a trap? Proteomic analysis of neutrophil extracellular traps in rheumatoid arthritis and systemic lupus erythematosus. *Frontiers in Immunology*, *10*, 243.

Charabati, M., Wheeler, M. A., Weiner, H. L., & Quintana, F. J. (2023). Multiple sclerosis: neuroimmune crosstalk and therapeutic targeting. *Cell*, *186*(7), 1309–1327.

Chaudhry, H., Zhou, J., Zhong, Y., Ali, M. M., Mcguire, F., Nagarkatti, P. S., & Nagarkatti, M. (2013). Role of cytokines as a double-edged sword in sepsis. *In Vivo*, *27*(6), 669–684.

Chear, C. T., Nallusamy, R., Canna, S. W., Chan, K. C., Baharin, M. F., Hishamshah, M., Ghani, H., Ripen, A. M., et al. (2020). A novel de novo NLRC4 mutation reinforces the likely pathogenicity of specific LRR domain mutation. *Clinical Immunology*, *211*, 108328.

Chen, J., & Chen, Z. J. (2018). PtdIns4P on dispersed trans-Golgi network mediates NLRP3 inflammasome activation. *Nature*, *564*(7734), 71–76.

Chen, J. Q., Szodoray, P., & Zeher, M. (2016). Toll-Like Receptor Pathways in Autoimmune Diseases. *Clinical Reviews in Allergy and Immunology*, *50*(1), 1–17.

Cheng, S. C., Scicluna, B. P., Arts, R. J. W., Gresnigt, M. S., Lachmandas, E., Giamarellos-Bourboulis, E. J., Kox, M., Manjeri, G. R., et al. (2016). Broad defects in the energy metabolism of leukocytes underlie immunoparalysis in sepsis. *Nature Immunology*, *17*(4), 406–413.

Chiu, S., & Bharat, A. (2016). Role of monocytes and macrophages in regulating immune response following lung transplantation. *Current Opinion in Organ Transplantation*, *21*(3), 239–245.

Chou, W. C., Jha, S., Linhoff, M. W., & Ting, J. P. Y. (2023). The NLR gene family: from discovery to present day. *Nature Reviews Immunology*.

Chu, L. H., Indramohan, M., Ratsimandresey, R. A., Gangopadhyay, A., Morris, E. P., Monack, D. M., Dorfleutner, A., & Stehlik, C. (2018). The oxidized phospholipid oxPAPC protects from septic shock by targeting the non-canonical inflammasome in macrophages. *Nature Communications*, *9*(1).

Clay, G. M., Valadares, D. G., Graff, J. W., Ulland, T. K., Davis, R. E., Scorza, B. M., Zhanbolat, B. S., Chen, Y., et al. (2017). An Anti-Inflammatory Role for NLRP10 in Murine Cutaneous Leishmaniasis. *The Journal of Immunology*, *199*(8), 2823–2833.

Cohen, P. &. (2001). Overview of the Immune System. *Immunology*, *357*, 63–81.

Coll, R. C., Hill, J. R., Day, C. J., Zamoshnikova, A., Boucher, D., Massey, N. L., Chitty, J. L., Fraser, J. A., et al. (2019). MCC950 directly targets the NLRP3 ATP-hydrolysis motif for inflammasome inhibition. *Nature Chemical Biology*, *15*(6), 556–559.

Coll, R. C., Robertson, A. A. B., Chae, J. J., Higgins, S. C., Muñoz-Planillo, R., Inserra, M. C., Vetter, I., Dungan, L. S., et al. (2015). A small-molecule inhibitor of the NLRP3 inflammasome for the treatment of inflammatory diseases. *Nature Medicine*, *21*(3), 248–257.

Coll, R. C., Schroder, K., & Pelegrín, P. (2022). NLRP3 and pyroptosis blockers for treating inflammatory diseases. *Trends in Pharmacological Sciences*, *43*(8), 653–668.

Cosson, C., Riou, R., Patoli, D., Niu, T., Rey, A., Groslambert, M., Chatre, E., Allatif, O., et al. (2023). Functional diversity of NLRP3 gain-of-function mutants associated with CAPS autoinflammation. *BioRxiv*.

Courjon, J., Dufies, O., Robert, A., Bailly, L., Torre, C., Chirio, D., Contenti, J., Vitale, S., et al. (2021). Heterogeneous NLRP3 inflammasome signature in circulating myeloid cells as a biomarker of COVID-19 severity. *Blood Advances*, *5*(5), 1523–1534.

Croce, M., Orengo, A. M., Azzarone, B., & Ferrini, S. (2012). Immunotherapeutic applications of IL - 15 R eview. *Immunotherapy*, *4*(9), 957–969.

Cubillos-Zapata, C., Hernández-Jiménez, E., Toledano, V., Esteban-Burgos, L., Fernández-Ruíz, I., Gómez-Piña, V., del Fresno, C., Siliceo, M., et al. (2014). NFκB2/p100 Is a Key Factor for Endotoxin Tolerance in Human Monocytes: A Demonstration Using Primary Human Monocytes from Patients with Sepsis. *The Journal of Immunology*, *193*(8), 4195–4202.

Cui, Y., Yu, H., Bu, Z., Wen, L., Yan, L., & Feng, J. (2022). Focus on the Role of the NLRP3 Inflammasome in Multiple Sclerosis: Pathogenesis, Diagnosis, and Therapeutics. *Frontiers in Molecular Neuroscience*, *15*, 1–19.

Cuisset, L., Jeru, I., Dumont, B., Fabre, A., Cochet, E., Le Bozec, J., Delpech, M., Amselem, S., et al. (2011). Mutations in the autoinflammatory cryopyrin-associated periodic syndrome gene: Epidemiological study and lessons from eight years of genetic analysis in France. *Annals of the Rheumatic Diseases*, *70*(3), 495–499.

Dagvadorj, J., Mikulska-Ruminska, K., Tumurkhuu, G., Ratsimandresey, R. A., Carriere, J., Andres, A. M., Marek-Iannucci, S., Song, Y., et al. (2021). Recruitment of pro-IL-1α to mitochondrial cardiolipin, via shared LC3 binding domain, inhibits mitophagy and drives maximal NLRP3 activation. *Proceedings of the National Academy of Sciences of the United States of America*, *118*(1), 1–12.

David, J. M., Dominguez, C., Hamilton, D. H., & Palena, C. (2016). The IL-8/IL-8R axis: A double agent in tumor immune resistance. *Vaccines*, *4*(3).

de Almeida, L., Khare, S., Misharin, A. V., Patel, R., Ratsimandresey, R. A., Wallin, M. C., Perlman, H., Greaves, D. R., et al. (2015). The PYRIN Domain-only Protein POP1 Inhibits Inflammasome Assembly and Ameliorates Inflammatory Disease. *Immunity*, *43*(2), 264–276.

de Menthière, C. S., Terrière, S., Pugnère, D., Ruiz, M., Demaille, J., & Touitou, I. (2003). INFEVERS: The registry for FMF and hereditary inflammatory disorders mutations. *Nucleic Acids Research*, *31*(1), 282–285.

De Torre-Minguela, C., Barberà-Cremades, M., Gómez, A. I., Martín-Sánchez, F., & Pelegrín, P. (2016). Macrophage activation and polarization modify P2X7 receptor secretome influencing the inflammatory process. *Scientific Reports*, *6*, 1–11.

De Torre-Minguela, C., del Castillo, P. M., & Pelegrín, P. (2017). The NLRP3 and pyrin inflammasomes: Implications in the pathophysiology of autoinflammatory diseases. *Frontiers in Immunology*, *8*(JAN).

De Torre-Minguela, C., Gómez, A. I., Couillin, I., & Pelegrín, P. (2021). Gasdermins mediate cellular release of mitochondrial DNA during pyroptosis and apoptosis. *FASEB Journal*, *35*(8), 1–16.

Del Valle, D. M., Kim-Schulze, S., Huang, H. H., Beckmann, N. D., Nirenberg, S., Wang, B., Lavin, Y., Swartz, T. H., et al. (2020). An inflammatory cytokine signature predicts COVID-19 severity and survival. *Nature Medicine*, *26*(10), 1636–1643.

Delano, M. J., & Ward, P. A. (2016). The immune system's role in sepsis progression, resolution, and long-term outcome. *Immunological Reviews*, *274*(1), 330–353.

Deng, Y., Deng, F., Pan, Y., Mei, S., Zheng, Z., Min, R., Wu, Z., Li, W., et al. (2022). Streptococcal pyrogenic exotoxin B cleaves GSDMA and triggers pyroptosis. *Nature*, *602*(7897), 496–502.

Deng, Wenmin, Yang, Z., Yue, H., Ou, Y., Hu, W., & Sun, P. (2020). Disulfiram suppresses NLRP3 inflammasome activation to treat peritoneal and gouty inflammation. *Free Radical Biology and Medicine*, *152*, 8–17.

Devant, P., Dong, Y., Mintseris, J., Ma, W., Gygi, S. P., Wu, H., & Kagan, J. C. (2023). Structural insights into cytokine cleavage by inflammatory caspase-4. *Nature*.

Di, A., Xiong, S., Ye, Z., Malireddi, R. K. S., Kometani, S., Zhong, M., Mittal, M., Hong, Z., et al. (2018). The TWIK2 Potassium Efflux Channel in Macrophages Mediates NLRP3 Inflammasome-Induced Inflammation. *Immunity*, *49*(1), 56-65.e4.

Diebolder, C. A., Halff, E. F., Koster, A. J., Huizinga, E. G., & Koning, R. I. (2015). Cryoelectron Tomography of the NAIP5/NLRC4 Inflammasome: Implications for NLR Activation. *Structure*, *23*(12), 2349–2357.

Dinarello, C. A., Simon, A., & van der Meer, J. (2012). Treating inflammation by blocking interleukin-1 in a broad spectrum of diseases. *Nat Rev Drug Discov.*, *11*(8), 633–652.

Dinarello, C. A. (2009). Immunological and inflammatory functions of the interleukin-1 family. *Annual Review of Immunology*, *27*, 519–550.

Dinarello, C. A. (2018). Overview of the IL-1 family in innate inflammation and acquired immunity. *Immunological Reviews*, *281*(1), 8–27.

Dinarello, C. A., Novick, D., Kim, S., & Kaplanski, G. (2013). Interleukin-18 and IL-18 binding protein. *Frontiers in Immunology*, *4*, 1–10.

Dinarello, C. A. (2019). The IL-1 family of cytokines and receptors in rheumatic diseases. *Nature Reviews Rheumatology*, *15*(10), 612–632.

Ding, J., Wang, K., Liu, W., She, Y., Sun, Q., Shi, J., Sun, H., Wang, D. C., et al. (2016). Pore-forming activity and structural autoinhibition of the gasdermin family. *Nature*, *535*(7610), 111–116.

Döcke, W.D., Randow, F., Syrbe, U., Krausch, D., Asadullah, K., Reinke, P., Volk, H.D., & Kox, W. (1997). Monocytes deactivation in septic patients: restoration by INF-y treatment. *Nature Medicine*, *3*, pages 678–681.

Dorfleutner, A., Bryan, N. B., Talbott, S. J., Funya, K. N., Rellick, S. L., Reed, J. C., Shi, X., Rojanasakul, Y., et al. (2007). Cellular pyrin domain-only protein 2 is a candidate regulator of inflammasome activation. *Infection and Immunity*, *75*(3), 1484–1492.

Drouin, M., Saenz, J., & Chiffoleau, E. (2020). C-Type Lectin-Like Receptors: Head or Tail in Cell Death Immunity. *Frontiers in Immunology*, *11,* 251.

Dugar, S., Choudhary, C., & Duggal, A. (2020). Sepsis and septic shock: Guideline-based management. *Cleveland Clinic Journal of Medicine*, *87*(1), 53–64.

Duncan, J. A., & Canna, S. W. (2018). The NLRC4 Inflammasome. *Immunological Reviews*, *281*(1), 115–123.

López-Collazo, E., & del Fresno, C. (2013). Pathophysiology of endotoxin tolerance: Mechanisms and clinical consequences. *Critical Care*, *17*(6), 1–11.

Eberl, G., Colonna, M., Santo, J. P. D., & McKenzie, A. N. J. (2015). Innate lymphoid cells: A new paradigm in immunology. *Science*, *348*(6237).

Economides, A. N., Carpenter, L. R., Rudge, J. S., Wong, V., Koehler-Stec, E. M., Hartnett, C., Pyles, E. A., Xu, X., et al. (2003). Cytokine traps: Multi-component, high-affinity blockers of cytokine action. *Nature Medicine*, *9*(1), 47–52.

Eidt, M. V., Nunes, F. B., Pedrazza, L., Caeran, G., Pellegrin, G., Melo, D. A. S., Possuelo, L., Jost, R. T., et al. (2016). Biochemical and inflammatory aspects in patients with severe sepsis and septic shock: The predictive role of IL-18 in mortality. *Clinica Chimica Acta*, *453*, 100–106.

El-Gabalawy, H., Guenther, L. C., & Bernstein, C. N. (2010). Epidemiology of immune-mediated inflammatory diseases: Incidence, prevalence, natural history, and comorbidities. *Journal of Rheumatology*, *37*(SUPPL. 85), 2–10.

Ellwanger, K., Becker, E., Kienes, I., Sowa, A., Postma, Y., Gloria, Y. C., Weber, A. N. R., & Kufer, T. A. (2018). The NLR family pyrin domain-containing 11 protein contributes to the regulation of

inflammatory signaling. *Journal of Biological Chemistry*, *293*(8), 2701–2710.

Emery, P., Rondon, J., Parrino, J., Lin, Y., Pena-Rossi, C., Van Hoogstraten, H., Graham, N. M. H., Liu, N., et al. (2019). Safety and tolerability of subcutaneous sarilumab and intravenous tocilizumab in patients with rheumatoid arthritis. *Rheumatology (United Kingdom)*, *58*(5), 849–858.

Esquerdo, K. F., Sharma, N. K., Brunialti, M. K. C., Baggio-Zappia, G. L., Assunção, M., Azevedo, L. C. P., Bafi, A. T., & Salomao, R. (2017). Inflammasome gene profile is modulated in septic patients, with a greater magnitude in non-survivors. *Clinical and Experimental Immunology*, *189*(2), 232–240.

Evavold, C. L., Hafner-Bratkovič, I., Devant, P., D'Andrea, J. M., Ngwa, E. M., Boršić, E., Doench, J. G., LaFleur, M. W., et al. (2021). Control of gasdermin D oligomerization and pyroptosis by the Ragulator-Rag-mTORC1 pathway. *Cell*, *184*(17), 4495-4511.e19.

Evavold, C. L., Ruan, J., Tan, Y., Xia, S., Wu, H., & Kagan, J. C. (2018). The Pore-Forming Protein Gasdermin D Regulates Interleukin-1 Secretion from Living Macrophages. *Immunity*, *48*(1), 35-44.e6.

Fahy, R. J., Exline, M. C., Gavrilin, M. A., Bhatt, N. Y., Besecker, B. Y., Sarkar, A., Hollyfield, J. L., Duncan, M. D., et al. (2008). Inflammasome mRNA expression in human monocytes during early septic shock. *American Journal of Respiratory and Critical Care Medicine*, *177*(9), 983–988.

Farahi, N., Singh, N. R., Heard, S., Loutsios, C., Summers, C., Solanki, C. K., Solanki, K., Balan, K. K., et al. (2012). Use of 111-Indium-labeled autologous eosinophils to establish the in vivo kinetics of human eosinophils in healthy subjects. *Blood*, *120*(19), 4068–4071.

Farber, D. L., Netea, M. G., Radbruch, A., Rajewsky, K., & Zinkernagel, R. M. (2016). Immunological memory: Lessons from the past and a look to the future. *Nature Reviews Immunology*, *16*(2), 124–128.

Fink, M. P. (2014). Animal models of sepsis. *Virulence*, *5*(1), 143–153.

Fiore, P. F., Di Matteo, S., Tumino, N., Mariotti, F. R., Pietra, G., Ottonello, S., Negrini, S., Bottazzi, B., et al. (2020). Interleukin-15 and cancer: Some solved and many unsolved questions. *Journal for ImmunoTherapy of Cancer*, *8*(2).

Fischer, S., Stegmann, F., Gnanapragassam, V. S., & Lepenies, B. (2022). From structure to function – Ligand recognition by myeloid C-type lectin receptors. *Computational and Structural Biotechnology Journal*, *20*, 5790–5812.

Fisher, B. A., Veenith, T., Slade, D., Gaskell, C., Rowland, M., Whitehouse, T., Scriven, J., & Parekh, D. (2022). Namilumab or infliximab compared with standard of care in hospitalised patients with COVID-19 (CATALYST): a randomised, multicentre, multi-arm, multistage, open-label, adaptive, phase 2, proof-of-concept trial. *Lancet Respir Med*, *10*, 255–266.

Fisher, C. J., Dhainaut, J. F. A., Opal, S. M., Pribble, J. P., Labrecque, J. F., Catalano, M. A., Balk, R. A., Slotman, G. J., Iet al. (1994). Recombinant Human Interleukin 1 Receptor Antagonist in the Treatment of Patients With Sepsis Syndrome: Results From a Randomized, Double-blind, Placebo-Controlled Trial. *JAMA: The Journal of the American Medical Association*, *271*(23), 1836–1843.

Fitzgerald, K. A., & Kagan, J. C. (2020). Toll-like Receptors and the Control of Immunity. *Cell*, *180*(6), 1044–1066.

Fousek, K., & Claudia Palena, L. A. H. (2021). Interleukin-8: a Chemokine at the Intersection of Cancer Plasticity, Angiogenesis, and Immune Suppression Kristen. *Pharmacol Ther.*, *219*, 107692.

Franchi, L., Eigenbrod, T., & Núñez, G. (2009). Cutting Edge: TNF-α Mediates Sensitization to ATP and Silica via the NLRP3 Inflammasome in the Absence of Microbial Stimulation. *The Journal of Immunology*, *183*(2), 792–796.

Franklin, B. S., Bossaller, L., De Nardo, D., Ratter, J. M., Stutz, A., Engels, G., Brenker, C., Nordhoff, M., et al. (2014). ASC has extracellular and prionoid activities that propagate inflammation. *Nat Immunol*, *15*(8), 727–737.

Franzini, A., Pomicter, A. D., Yan, D., Khorashad, J. S., Tantravahi, S. K., Than, H., Ahmann, J. M., O'Hare, T., et al. (2019). The transcriptome of CMML monocytes is highly inflammatory and reflects

leukemia-specific and age-related alterations. *Blood Advances*, *3*(20), 2949–2961.

Freud, A. G., Yu, J., & Caligiuri, M. A. (2014). Human natural killer cell development in secondary lymphoid tissues. *Seminars in Immunology*, *26*(2), 132–137.

Furman, D., Campisi, J., Verdin, E., Carrera-Bastos, P., Targ, S., Franceschi, C., Ferrucci, L., Gilroy, D. W., et al. (2019). Chronic inflammation in the etiology of disease across the life span. *Nature Medicine*, *25*(12), 1822–1832.

Gabay, C., Lamacchia, C., & Palmer, G. (2010). IL-1 pathways in inflammation and human diseases. *Nature Reviews Rheumatology*, *6*(4), 232–241.

García-Villalba, J., Hurtado-Navarro, L., Peñín-Franch, A., Molina-López, C., Martínez-Alarcón, L., Angosto-Bazarra, D., Baroja-Mazo, A., & Pelegrin, P. (2022). Soluble P2X7 Receptor Is Elevated in the Plasma of COVID-19 Patients and Correlates With Disease Severity. *Frontiers in Immunology*, *13*, 894470.

Garlanda, C., Dinarello, C. A., & Mantovani, A. (2013). The Interleukin-1 Family: Back to the Future. *Immunity*, *39*(6), 1003–1018.

Garlanda, C., Riva, F., Bonavita, E., & Mantovani, A. (2013). Negative regulatory receptors of the IL-1 family. *Seminars in Immunology*, *25*(6), 408–415.

Geering, B., Stoeckle, C., Conus, S., & Simon, H. U. (2013). Living and dying for inflammation: Neutrophils, eosinophils, basophils. *Trends in Immunology*, *34*(8), 398–409.

Geijtenbeek, T. B. H., & Gringhuis, S. I. (2009). Signalling through C-type lectin receptors: Shaping immune responses. *Nature Reviews Immunology*, *9*(7), 465–479.

Geissler, K., Jäger, E., Barna, A., Alendar, T., Ljubuncic, E., Sliwa, T., & Valent, P. (2016). Chronic myelomonocytic leukemia patients with RAS pathway mutations show high in vitro myeloid colony formation in the absence of exogenous growth factors. *Leukemia*, *30*(11), 2280–2281.

Geissmann, F., Manz, M. G., Jung, S., Sieweke, M. H., Merad, M., & Ley, K. (2010). Development of monocytes, macrophages, and dendritic cells. *Science*, *327*(5966), 656–661.

Giamarellos-bourboulis, E. J., Veerdonk, F. L. Van De, Mouktaroudi, M., Raftogiannis, M., Antonopoulou, A., Joosten, L. A. B., Pickkers, P., Savva, A., et al. (2011). Inhibition of caspase-1 activation in gram-negative sepsis and experimental endotoxemia. *Critical Care*, *15*(1), R27.

Gibellini, L., De Biasi, S., Paolini, A., Borella, R., Boraldi, F., Mattioli, M., Lo Tartaro, D., Fidanza, L., et al. (2020). Altered bioenergetics and mitochondrial dysfunction of monocytes in patients with COVID-19 pneumonia. *EMBO Molecular Medicine*, *12*(12), 1–13.

Gil-Lianes, J., Gariup, G., Iranzo-Fernández, P., Mensa-Vilaró, A., Peñín-Franch, A., Hurtado-Navarro, L., Pelegrin, P., & Aróstegui, J. I. (2023). Early-onset recurrent panniculitis as a phenotype of NLRC4-associated autoinflammatory syndrome: Characterization of pathogenicity of the p.Ser445Pro NLRC4 variant. *Australasian Journal of Dermatology*, *64*(2), 260–267.

Ginhoux, F., & Jung, S. (2014). Monocytes and macrophages: Developmental pathways and tissue homeostasis. *Nature Reviews Immunology*, *14*(6), 392–404.

Gram, H. (2020). The long and winding road in pharmaceutical development of canakinumab from rare genetic autoinflammatory syndromes to myocardial infarction and cancer. *Pharmacological Research*, *154*(December 2018), 104139.

Granowitz, E. V., Porat, R., Mier, J. W., Pribble, J. P., Stiles, D. M., Bloedow, D. C., Catalano, M. A., Wolff, S. M., et al. (1992). Pharmacokinetics, safety and immunomodulatory effects of human recombinant interleukin-1 receptor antagonist in healthy humans. *Cytokine*, *4*(5), 353–360.

Gray, E. E., Winship, D., Snyder, J. M., Child, S. J., Geballe, A. P., & Stetson, D. B. (2016). The AIM2-like Receptors Are Dispensable for the Interferon Response to Intracellular DNA. *Immunity*, *45*(2), 255–266.

Gritsenko, A., Green, J. P., Brough, D., & Lopez-Castejon, G. (2020). Mechanisms of NLRP3 priming in inflammaging and age related diseases. *Cytokine and Growth Factor Reviews*, *55*(August), 15–

25.

Groß, C. J., Mishra, R., Schneider, K. S., Médard, G., Wettmarshausen, J., Dittlein, D. C., Shi, H., Gorka, O., et al. (2016). K+ Efflux-Independent NLRP3 Inflammasome Activation by Small Molecules Targeting Mitochondria. *Immunity*, *45*(4), 761–773.

Gu, Z., Gu, L., Eils, R., Schlesner, M., & Brors, B. (2014). Circlize implements and enhances circular visualization in R. *Bioinformatics*, *30*(19), 2811–2812.

Guan, W., Ni, Z., Hu, Y., Liang, W., Ou, C., He, J., Liu, L., Shan, H., et al. (2020). Clinical Characteristics of Coronavirus Disease 2019 in China. *New England Journal of Medicine*, *382*(18), 1708–1720.

Guilliams, M., Mildner, A., & Yona, S. (2018). Developmental and Functional Heterogeneity of Monocytes. *Immunity*, *49*(4), 595–613.

Guo, Y., Hu, K., Li, Y., Lu, C., Ling, K., Cai, C., Wang, W., & Ye, D. (2022). Targeting TNF-α for COVID-19: Recent Advanced and Controversies. *Frontiers in Public Health*, *10*(February), 1–9.

Guo, Yin, Patil, N. K., Luan, L., Bohannon, J. K., & Sherwood, E. R. (2017). The biology of natural killer cells during sepsis. *Immunology*, *153*(2), 190–202.

Guo, Y., Gan, X., Zhou, H., Zhou, H., Pu, S., Long, X., Ren, C., Feng, T., et al. (2020). Fingolimod suppressed the chronic unpredictable mild stress-induced depressive-like behaviors via affecting microglial and NLRP3 inflammasome activation. *Life Sciences*, *263*, 118582.

Hafner-Bratkovič, I. (2017). The NLRC4 inflammasome: The pieces of the puzzle are falling into place. *Inflammasome*, *3*(1), 10–23.

Hagar, J. A., Powell, D. A., Aachoui, Y., Ernst, R. K., & Miao, E. A. (2013). Cytoplasmic LPS activates caspase-11: Implications in TLR4-independent endotoxic shock. *Science*, *341*(6151), 1250–1253.

Halle, A., Hornung, V., Petzold, G. C., Stewart, C. R., Monks, B. G., Reinheckel, T., Fitzgerald, K. A., Latz, E., et al. (2008). The NALP3 inflammasome is involved in the innate immune response to amyloid-β. *Nature Immunology*, *9*(8), 857–865.

Hamarsheh, S., Osswald, L., Saller, B. S., Unger, S., De Feo, D., Vinnakota, J. M., Konantz, M., Uhl, F. M., et al. (2020). Oncogenic KrasG12D causes myeloproliferation via NLRP3 inflammasome activation. *Nature Communications*, *11*(1), 1659.

Harbarth, S., Holeckova, K., Pittet, D., Ricou, B., Grau, G. E., & Vadas, L. (2001). Diagnostic value of procalcitonin, interleukin-6 and Interleukin-8 in Critically Ill Patients Admitted. *American Journal of Respiratory and Critical Care Medicine*, *164*, 396–402.

Hassan, J., Khan, S., Zahra, R., Razaq, A., Zain, A., Razaq, L., & Razaq, M. (2022). Role of Procalcitonin and C-reactive Protein as Predictors of Sepsis and in Managing Sepsis in Postoperative Patients: A Systematic Review. *Cureus*, *14*(11), 1–13.

He, H., Jiang, H., Chen, Y., Ye, J., Wang, A., Wang, C., Liu, Q., Liang, G., Deng, X., et al. (2018). Oridonin is a covalent NLRP3 inhibitor with strong anti-inflammasome activity. *Nature Communications*, *9*(1), 1–12.

He, L., Guo, C., Su, Y., & Ding, N. (2023). The relationship between serum ferritin level and clinical outcomes in sepsis based on a large public database. *Scientific Reports*, *13*(1), 1–12.

He, Y., Zeng, M. Y., Yang, D., Motro, B., & Núñez, G. (2016). NEK7 is an essential mediator of NLRP3 activation downstream of potassium efflux. *Nature*, *530*(7590), 354–357.

Hennig, P., Garstkiewicz, M., Grossi, S., Filippo, M. Di, French, L. E., & Beer, H. D. (2018). The crosstalk between Nrf2 and inflammasomes. *International Journal of Molecular Sciences*, *19*(2), 562.

Henry, B. M., De Oliveira, M. H. S., Benoit, S., Plebani, M., & Lippi, G. (2020). Hematologic, biochemical and immune biomarker abnormalities associated with severe illness and mortality in coronavirus disease 2019 (COVID-19): A meta-analysis. *Clinical Chemistry and Laboratory Medicine*, *58*(7), 1021–1028.

Hettinger, J., Richards, D. M., Hansson, J., Barra, M. M., Joschko, A. C., Krijgsveld, J., & Feuerer, M. (2013). Origin of monocytes and macrophages in a committed progenitor. *Nature Immunology*, *14*(8), 821–830.

Hochheiser, I. V., Pilsl, M., Hagelueken, G., Moecking, J., Marleaux, M., Brinkschulte, R., Latz, E., Engel, C., et al. (2022). Structure of the NLRP3 decamer bound to the cytokine release inhibitor CRID3. *Nature*, *604*(7904), 184–189.

Hoffman, H. M., & Broderick, L. (2016). The role of the inflammasome in patients with autoinflammatory diseases. *Journal of Allergy and Clinical Immunology*, *138*(1), 3–14.

Hoffman, H. M., Gregory, S. G., Mueller, J. L., Tresierras, M., Broide, D. H., Wanderer, A. A., & Kolodner, R. D. (2003). Fine structure mapping of CIAS1: Identification of an ancestral haplotype and a common FCAS mutation, L353P. *Human Genetics*, *112*(2), 209–216.

Hoffman, H. M., Mueller, J. L., Broide, D. H., Wanderer, A. A., & Kolodner, R. D. (2001). Mutation of a new gene encoding a putative pyrin-like protein causes familial cold autoinflammatory syndrome and Muckle-Wells syndrome. *Nature Genetics*, *29*(3), 301–305.

Holley, C. L., & Schroder, K. (2020). The rOX-stars of inflammation: links between the inflammasome and mitochondrial meltdown. *Clinical and Translational Immunology*, *9*(2), 1–13.

Hooftman, A., Angiari, S., Hester, S., Corcoran, S. E., Runtsch, M. C., Ling, C., Ruzek, M. C., Slivka, P. F., et al. (2020). The Immunomodulatory Metabolite Itaconate Modifies NLRP3 and Inhibits Inflammasome Activation. *Cell Metabolism*, *32*(3), 468-478.e7.

Hoogendijk, A. J., Van Vught, L. A., Wiewel, M. A., Fuhler, G. M., Belkasim-Bohoudi, H., Horn, J., Schultz, M. J., Scicluna, B. P., et al. (2019). Kinase activity is impaired in neutrophils of sepsis patients. *Haematologica*, *104*(6), e233–e235.

Hornung, V., Bauernfeind, F., Halle, A., Samstad, E. O., Kono, H., Rock, K. L., Fitzgerald, K. A., & Latz, E. (2008). Silica crystals and aluminum salts activate the NALP3 inflammasome through phagosomal destabilization. *Nature Immunology*, *9*(8), 847–856.

Hoss, F., Rodriguez-Alcazar, J. F., & Latz, E. (2017). Assembly and regulation of ASC specks. *Cellular and Molecular Life Sciences*, *74*(7), 1211–1229.

Hotchkiss, R. S. (2013). Sepsis-induced immunosuppression: From cellular dysfunctions to immunotherapy. *Nat Rev Immunol.*, *13*(12), 862–874.

Hotchkiss, R. S., & Karl, I. E. (2003). The Pathophysiology and Treatment of Sepsis. *New England Journal of Medicine*, *348*(2), 138–150.

Hu, Z., Yan, C., Liu, P., Huang, Z., Ma, R., Zhang, C., Wang, R., Zhang, Y., et al. (2013). Crystal structure of NLRC4 reveals its autoinhibition mechanism. *Science*, *341*(6142), 172–175.

Hu, Z., Zhou, Q., Zhang, C., Fan, S., Cheng, W., Zhao, Y., Shao, F., Wang, H. W., et al. (2015). Structural and biochemical basis for induced self-propagation of NLRC4. *Science*, *350*(6259), 399–404.

Huang, Z., Xie, L., Li, H., Liu, X., Bellanti, J. A., Zheng, S. G., & Su, W. (2019). Insight into interleukin-37: The potential therapeutic target in allergic diseases. *Cytokine and Growth Factor Reviews*, *49*, 32–41.

Humphries, F., Shmuel-Galia, L., Ketelut-Carneiro, N., Li, S., Wang, B., Nemmara, V. V., Wilson, R., Jiang, Z., et al. (2020). Succination inactivates gasdermin D and blocks pyroptosis. *Science*, *369*(6511), 1633–1637.

Hurtado-Navarro, L., Angosto-Bazarra, D., Pelegrín, P., Baroja-Mazo, A., & Cuevas, S. (2022). NLRP3 Inflammasome and Pyroptosis in Liver Pathophysiology: The Emerging Relevance of Nrf2 Inducers. *Antioxidants*, *11*(5), 1–15.

Hurtado-Navarro, L., Baroja-Mazo, A., Martínez-Banaclocha, H., & Pelegrín, P. (2022). Assessment of ASC Oligomerization by Flow Cytometry. *Methods in Molecular Biology*, *2459*, 1–9.

Hurtado-Navarro, L., García-Palenciano, C., & Pelegrín, P. (2023). Inflammasomes in sepsis.

Inflammasome Biology, 369–382.

Ibrahim, J. N., Jounblat, R., Delwail, A., Abou-Ghoch, J., Salem, N., Chouery, E., Megarbane, A., Medlej-Hashim, M., et al. (2014). Ex vivo PBMC cytokine profile in familial Mediterranean fever patients: Involvement of IL-1β, IL-1α and Th17-associated cytokines and decrease of Th1 and Th2 cytokines. *Cytokine*, *69*(2), 248–254.

Ichinohe, T., Yamazaki, T., Koshiba, T., & Yanagi, Y. (2013). Mitochondrial protein mitofusin 2 is required for NLRP3 inflammasome activation after RNA virus infection. *Proceedings of the National Academy of Sciences of the United States of America*, *110*(44), 17963–17968.

Ihim, S. A., Abubakar, S. D., Zian, Z., Sasaki, T., Saffarioun, M., Maleknia, S., & Azizi, G. (2022). Interleukin-18 cytokine in immunity, inflammation, and autoimmunity: Biological role in induction, regulation, and treatment. *Frontiers in Immunology*, *13*, 1–18.

Inohara, N., Chamaillard, M., McDonald, C., & Nuñez, G. (2005). NOD-LRR proteins: Role in host-microbial interactions and inflammatory disease. *Annual Review of Biochemistry*, *74*, 355–383.

Ionescu, D., Peñín-Franch, A., Mensa-Vilaró, A., Castillo, P., Hurtado-Navarro, L., Molina-López, C., Romero-Chala, S., Plaza, S., et al. (2022). First Description of Late-Onset Autoinflammatory Disease Due to Somatic NLRC4 Mosaicism. *Arthritis and Rheumatology*, *74*(4), 692–699.

Itzykson, R., Fenaux, P., Bowen, D., Cross, N. C. P., Cortes, J., De Witte, T., Germing, U., Onida, F., et al. (2018). Diagnosis and Treatment of Chronic Myelomonocytic Leukemias in Adults: Recommendations from the European Hematology Association and the European LeukemiaNet. *HemaSphere*, *2*(6).

Itzykson, R., O., Renneville, A., Gelsi-Boyer, V., Meggendorfer, M., Morabito, M., Berthon, C., Adès, L., Fenaux, P., et al. (2013). Prognostic score including gene mutations in chronic Myelomonocytic Leukemia. *Journal of Clinical Oncology*, *31*(19), 2428–2436.

Iwasaki, A., & Medzhitov, R. (2015). Control of adaptive immunity by the innate immune system. *Nature Immunology*, *16*(4), 343–353.

Iyer, S. S., He, Q., Janczy, J. R., Elliott, E. I., Zhong, Z., Olivier, A. K., Sadler, J. J., Knepper-Adrian, V., et al. (2013). Mitochondrial Cardiolipin Is Required for Nlrp3 Inflammasome Activation. *Immunity*, *39*(2), 311–323.

Jain, S., Gautam, V., & Naseem, S. (2011). Acute-phase proteins: As diagnostic tool. *Journal of Pharmacy and Bioallied Sciences*, *3*(1), 118–127.

Jakubzick, C. V., Randolph, G. J., & Henson, P. M. (2017). Monocyte differentiation and antigen-presenting functions. *Nature Reviews Immunology*, *17*(6), 349–362.

Jamilloux, Y., Magnotti, F., Belot, A., & Henry, T. (2018). The pyrin inflammasome: From sensing RhoA GTPases-inhibiting toxins to triggering autoinflammatory syndromes. *Pathogens and Disease*, *76*(3), 1–9.

Janeway, C. A., & Medzhitov, R. (2002). Innate immune recognition. *Annual Review of Immunology*, *20*(2), 197–216.

Jekarl, D. W., Lee, S. Y., Lee, J., Park, Y. J., Kim, Y., Park, J. H., Wee, J. H., & Choi, S. P. (2013). Procalcitonin as a diagnostic marker and IL-6 as a prognostic marker for sepsis. *Diagnostic Microbiology and Infectious Disease*, *75*(4), 342–347.

Jiang, H., He, H., Chen, Y., Huang, W., Cheng, J., Ye, J., Wang, A., Tao, J., et al. (2017). Identification of a selective and direct NLRP3 inhibitor to treat inflammatory disorders. *Journal of Experimental Medicine*, *214*(11), 3219–3238.

Jiang, H., Swacha, P., & Gekara, N. O. (2021). Nuclear AIM2-Like Receptors Drive Genotoxic Tissue Injury by Inhibiting DNA Repair. *Advanced Science*, *8*(22), 2–11.

Johnson, C. W., Reid, D., Parker, J. A., Salter, S., Knihtila, R., Kuzmic, P., & Mattos, C. (2017). The small GTPases K-Ras, N-Ras, and H-Ras have distinct biochemical properties determined by allosteric effects. *Journal of Biological Chemistry*, *292*(31), 12981–12993.

Jones, A. E., Trzeciak, S., & Kline, J. A. (2009). The Sequential Organ Failure Assessment score for predicting outcome in patients with severe sepsis and evidence of hypoperfusion at the time of emergency department presentation. *Critical Care Medicine*, *37*(5), 1649–1654.

Joosten, L. A. B., Abdollahi-Roodsaz, S., Dinarello, C. A., O'Neill, L., & Netea, M. G. (2016). Toll-like receptors and chronic inflammation in rheumatic diseases: New developments. *Nature Reviews Rheumatology*, *12*(6), 344–357.

Junqueira, C., Crespo, Â., Ranjbar, S., de Lacerda, L. B., Lewandrowski, M., Ingber, J., Parry, B., Ravid, S., et al. (2022). FcγR-mediated SARS-CoV-2 infection of monocytes activates inflammation. *Nature*, *606*(7914), 576–584.

Kalliolias, G. D., Ivashkiv, L. B., & Program, T. D. (2016). TNF biology, pathogenic mechanisms and emerging therapeutic strategies. *Nat Rev Rheumatol.*, *12*(1), 49–62.

Karasawa, T., Komada, T., Yamada, N., Aizawa, E., Mizushina, Y., Watanabe, S., Baatarjav, C., Matsumura, T., et al. (2022). Cryo-sensitive aggregation triggers NLRP3 inflammasome assembly in cryopyrin-associated periodic syndrome. *ELife*, *11*, 1–26.

Kawasaki, Y., Oda, H., Ito, J., Niwa, A., Tanaka, T., Hijikata, A., Seki, R., Nagahashi, A., et al. (2017). Identification of a High-Frequency Somatic NLRC4 Mutation as a Cause of Autoinflammation by Pluripotent Cell-Based Phenotype Dissection. *Arthitis & Rheumatology*, *69*(2), 447–449.

Kayagaki, N., Kornfeld, O. S., Lee, B. L., Stowe, I. B., O'Rourke, K., Li, Q., Sandoval, W., Yan, D., Kang, J., et al. (2021). NINJ1 mediates plasma membrane rupture during lytic cell death. *Nature*, *591*(7848), 131–136.

Kayagaki, N., Stowe, I. B., Alegre, K., Deshpande, I., Wu, S., Lin, Z., Kornfeld, O. S., Lee, B. L., et al. (2023). Inhibiting membrane rupture with NINJ1 antibodies limits tissue injury. *Nature*, *618*.

Kayagaki, N., Stowe, I. B., Lee, B. L., O'Rourke, K., Anderson, K., Warming, S., Cuellar, T., Haley, B., Ret al. (2015). Caspase-11 cleaves gasdermin D for non-canonical inflammasome signalling. *Nature*, *526*(7575), 666–671.

Kayagaki, N., Warming, S., Lamkanfi, M., Walle, L. Vande, Louie, S., Dong, J., Newton, K., et al. (2011). Non-canonical inflammasome activation targets caspase-11. *Nature*, *479*(7371), 117–121. https://doi.org/10.1038/nature10558

Kayagaki, N., Wong, M. T., Stowe, I. B., Ramani, S. R., Gonzalez, L. C., Akashi-takamura, S., Miyake, K., Zhang, J., et al. (2013). *Noncanonical Inflammasome Activation by Intracellular LPS Independent of TLR4*. *130*(September), 1246–1249.

Khoury, J. D., Solary, E., Abla, O., Akkari, Y., Alaggio, R., Apperley, J. F., Bejar, R., Berti, E., et al. (2022). The 5th edition of the World Health Organization Classification of Haematolymphoid Tumours: Myeloid and Histiocytic/Dendritic Neoplasms. *Leukemia*, *36*(7), 1703–1719.

Kim, N. E., Kim, D. K., & Song, Y. J. (2021). Sars-cov-2 nonstructural proteins 1 and 13 suppress caspase-1 and the NLRP3 inflammasome activation. *Microorganisms*, *9*(3), 1–12.

Kitamura, A., Sasaki, Y., Abe, T., Kano, H., & Yasutomo, K. (2014). An inherited mutation in NLRC4 causes autoinflammation in human and mice. *Journal of Experimental Medicine*, *211*(12), 2385–2396.

Kofoed, E. M., Vance, R. E., & Biology, C. (2012). Innate immune recognition of bacterial ligands by NAIPs dictates inflammasome specificity. *Nature*, *477*(7366), 592–595.

Kosiewicz, M. M., Zirnheld, A. L., & Alard, P. (2011). Gut microbiota, immunity, and disease: A complex relationship. *Frontiers in Microbiology*, *2*, 1–11.

Kotas, M.E., & Medzhitov, R. (2015). Homeostasis, Inflammation, and Disease Susceptibility. *Cell*, *160*(5), 816–827.

Koyama, S., Ishii, K. J., Coban, C., & Akira, S. (2008). Innate immune response to viral infection. *Cytokine*, *43*(3), 336–341.

Kratky, W., Reis E Sousa, C., Oxenius, A., & Spörri, R. (2011). Direct activation of antigen-presenting

cells is required for CD8 + T-cell priming and tumor vaccination. *Proceedings of the National Academy of Sciences of the United States of America*, *108*(42), 17414–17419.

Kuek, A., Hazleman, B. L., & Östör, A. J. K. (2007). Immune-mediated inflammatory diseases (IMIDs) and biologic therapy: A medical revolution. *Postgraduate Medical Journal*, *83*(978), 251–260.

Kuemmerle-Deschner, J., Verma, D., Endres, T., Broderick, L., de Jesus, A., Hofer, F., Blank, N., Krause, K., et al. (2017). Clinical and Molecular Phenotypes of Low-Penetrance Variants of NLRP3: Diagnostic and Therapeutic Challenges. *Arthritis & Rheumatology*, *67*(11), 2233–2240.

Kuhlmann, T., Moccia, M., Coetzee, T., Cohen, J. A., Correale, J., Graves, J., Marrie, R. A., Montalban, X., et al. (2023). Multiple sclerosis progression: time for a new mechanism-driven framework. *The Lancet Neurology*, *22*(1), 78–88.

Kuhn, M. (2008). Building predictive models in R using the caret package. *Journal of Statistical Software*, *28*(5), 1–26.

Kumar, H., Kawai, T., & Akira, S. (2011). Pathogen recognition by the innate immune system. *International Reviews of Immunology*, *30*(1), 16–34.

Kumar, B. V, Connors, T., & Farber, D. L. (2019). *Human T cell development, localization, and function throughout life*. *48*(2), 202–213.

Kurowska-Stolarska, M., Stolarski, B., Kewin, P., Murphy, G., Corrigan, C. J., Ying, S., Pitman, N., Mirchandani, A., et al. (2009). IL-33 Amplifies the Polarization of Alternatively Activated Macrophages That Contribute to Airway Inflammation. *The Journal of Immunology*, *183*(10), 6469–6477.

Lamkanfi, M., & Dixit, V. M. (2014). Mechanisms and functions of inflammasomes. *Cell*, *157*(5), 1013–1022.

Lamkanfi, M., Mueller, J. L., Vitari, A. C., Misaghi, S., Fedorova, A., Deshayes, K., Lee, W. P., Hoffman, H. M., et al. (2009). Glyburide inhibits the Cryopyrin/Nalp3 inflammasome. *Journal of Cell Biology*, *187*(1), 61–70.

Lasho, T., & Patnaik, M. M. (2021). Novel therapeutic targets for chronic myelomonocytic leukemia. *Best Practice and Research: Clinical Haematology*, *34*(1), 101244.

Lasigliè, D., Mensa-Vilaro, A., Ferrera, D., Caorsi, R., Penco, F., Santamaria, G., Di Duca, M., Amico, G., et al. (2017). Cryopyrin-associated periodic syndromes in Italian Patients: Evaluation of the rate of somatic NLRP3 mosaicism and phenotypic characterization. *Journal of Rheumatology*, *44*(11), 1667–1673.

Lee, B., Hoyle, C., Wellens, R., Green, J. P., Martin-Sanchez, F., Williams, D. M., Matchett, B. J., Seoane, P. I., et al. (2023). Disruptions in endocytic traffic contribute to the activation of the NLRP3 inflammasome. *Science Signaling*, *16*(773).

Lee, B. L., Stowe, I. B., Gupta, A., Kornfeld, O. S., Roose-Girma, M., Anderson, K., Warming, S., Zhang, J., et al. (2018). Caspase-11 auto-proteolysis is crucial for noncanonical inflammasome activation. *Journal of Experimental Medicine*, *215*(9), 2279–2288.

Lefrançais, E., Duval, A., Mirey, E., Roga, S., Espinosa, E., Cayrol, C., & Girard, J. P. (2014). Central domain of IL-33 is cleaved by mast cell proteases for potent activation of group-2 innate lymphoid cells. *Proceedings of the National Academy of Sciences of the United States of America*, *111*(43), 15502–15507.

Leurs, C. E., Podlesniy, P., Trullas, R., Balk, L., Steenwijk, M. D., Malekzadeh, A., Piehl, F., Uitdehaag, B. M., et al. (2018). Cerebrospinal fluid mtDNA concentration is elevated in multiple sclerosis disease and responds to treatment. *Multiple Sclerosis Journal*, *24*(4), 472–480.

Levy, A. R. R. A., Rojas-villarraga, A., & Levy, R. A. (2000). Cancer and Autoimmunity. In *Cancer and Autoimmunity*.

Levy, R., Gérard, L., Kuemmerle-Deschner, J., Lachmann, H. J., Koné-Paut, I., Cantarini, L., Woo, P., Naselli, A., et al. (2015). Phenotypic and genotypic characteristics of cryopyrin-associated periodic syndrome: A series of 136 patients from the Eurofever Registry. *Annals of the Rheumatic Diseases*, *74*(11), 2043–2049.

Li, P., Li, M., Lindberg, M. R., Kennett, M. J., Xiong, N., & Wang, Y. (2010). PAD4 is essential for antibacterial innate immunity mediated by neutrophil extracellular traps. *Journal of Experimental Medicine*, *207*(9), 1853–1862.

Li, S., Neff, C. P., Barber, K., Hong, J., Luo, Y., Azam, T., Palmer, B. E., Fujita, M., et al. (2015). Extracellular forms of IL-37 inhibit innate inflammation in vitro and in vivo but require the IL-1 family decoy receptor IL-1R8. *Proceedings of the National Academy of Sciences of the United States of America*, *112*(8), 2497–2502.

Liang, J., Alfano, D. N., Squires, J. E., Riley, M. M., Parks, W. T., Kofler, J., El-Gharbawy, A., Madan-Kheterpal, S., et al. (2017). Novel NLRC4 Mutation Causes a Syndrome of Perinatal Autoinflammation With Hemophagocytic Lymphohistiocytosis, Hepatosplenomegaly, Fetal Thrombotic Vasculopathy, and Congenital Anemia and Ascites. *Pediatric and Developmental Pathology*, *20*(6), 498–505.

Lieben, L. (2018). Free IL-18 causes macrophage activation syndrome. *Nature Reviews Rheumatology*, *2018*, 2018.

Lieberman, J., Wu, H., & Kagan, J. C. (2019). Gasdermin D activity in inflammation and host defense. *Science Immunology*, *4*(39), 1–9.

Linarez-Ochoa, N. E., Rodríguez, G., Reyes, I. D., Rico Rivas, K. M., Ramírez, C., & Durón, R. M. (2022). Differences in inflammatory markers between coronavirus disease 2019 and sepsis in hospitalised patients. *Clinical Epidemiology and Global Health*, *15*, 1–6.

Liu, J., Li, S., Liu, J., Liang, B., Wang, X., Wang, H., Li, W., Tong, Q., et al. (2020). Longitudinal characteristics of lymphocyte responses and cytokine profiles in the peripheral blood of SARS-CoV-2 infected patients. *EBioMedicine*, *55,* 102763.

Liu, Y., Dai, Y., Li, Q., Chen, C., Chen, H., Song, Y., Hua, F., & Zhang, Z. (2020). Beta-amyloid activates NLRP3 inflammasome via TLR4 in mouse microglia. *Neuroscience Letters*, *736*, 135279.

Liu, Z. M., Yang, M. H., Yu, K., Lian, Z. X., & Deng, S. L. (2022). Toll-like receptor (TLRs) agonists and antagonists for COVID-19 treatments. *Frontiers in Pharmacology*, *13*, 1–14.

Ljungström, L., Pernestig, A. K., Jacobsson, G., Andersson, R., Usener, B., & Tilevik, D. (2017). Diagnostic accuracy of procalcitonin, neutrophil-lymphocyte count ratio, C-reactive protein, and lactate in patients with suspected bacterial sepsis. *PLoS ONE*, *12*(7), 1–17.

Lopez-Castejón, G., Baroja-Mazo, A., & Pelegrín, P. (2011). Novel macrophage polarization model: From gene expression to identification of new anti-inflammatory molecules. *Cellular and Molecular Life Sciences*, *68*(18), 3095–3107.

López-Collazo, E., Avendaño-Ortiz, J., Martín-Quirós, A., & Aguirre, L. A. (2020). Immune response and COVID-19: A mirror image of sepsis. *International Journal of Biological Sciences*, *16*(14), 2479–2489.

Lozano-Rodríguez, R., Avendaño-Ortíz, J., Montalbán-Hernández, K., Ruiz-Rodríguez, J. C., Ferrer, R., Martín-Quirós, A., Maroun-Eid, C., González-López, J. J., et al. (2023). The prognostic impact of SIGLEC5-induced impairment of CD8+ T cell activation in sepsis. *EBioMedicine*, *25*(97), 104841.

Lu, A., Magupalli, V., Ruan, J., Yin, Q., Maninjay, K., Vos, M., Schröder, G. F., Fitzgerald, K. A., et al. (2014). Unified Polymerization Mechanism for the Assembly of ASC- dependent Inflammasomes. *Cell*, *156*(6), 1193–1206.

Ma, J., Zhu, F., Zhao, M., Shao, F., Yu, D., Ma, J., Zhang, X., Li, W., et al. (2021). SARS-CoV-2 nucleocapsid suppresses host pyroptosis by blocking Gasdermin D cleavage. *The EMBO Journal*, *40*(18), 1–17.

Magnotti, F., Lefeuvre, L., Benezech, S., Malsot, T., Waeckel, L., Martin, A., Kerever, S., Chirita, D., et al. (2019). Pyrin dephosphorylation is sufficient to trigger inflammasome activation in familial Mediterranean fever patients. *EMBO Molecular Medicine*, *11*(11), 1–16.

Magupalli, V. G., Negro, R., Tian, Y., Hauenstein, A. V., Caprio, G. Di, Skillern, W., Deng, Q., et al. (2020). HDAC6 mediates an aggresome-like mechanism for NLRP3 and pyrin inflammasome

activation. *Science*, *369*(6509).

Malhotra, S., Costa, C., Eixarch, H., Keller, C. W., Amman, L., Martínez-Banaclocha, H., Midaglia, L., Sarró, E., et al. (2020). NLRP3 inflammasome as prognostic factor and therapeutic target in primary progressive multiple sclerosis patients. *Brain*, *143*(5), 1414–1430.

Malhotra, S., Rio, J., Urcelay, E., Nurtdinov, R., Bustamante, M. F., Fernandez, O., Oliver, B., Zettl, U., et al. (2015). NLRP3 inflammasome is associated with the response to IFN-b in patients with multiple sclerosis. *Brain*, *138*(3), 644–652.

Man, S. M., Karki, R., Sasai, M., Place, D. E., Kesavardhana, S., Temirov, J., Frase, S., Zhu, Q., et al. (2016). IRGB10 Liberates Bacterial Ligands for Sensing by the AIM2 and Caspase-11-NLRP3 Inflammasomes. *Cell*, *167*(2), 382-396.e17.

Mangan, M. S. J., Olhava, E. J., Roush, W. R., Seidel, H. M., Glick, G. D., & Latz, E. (2018). Targeting the NLRP3 inflammasome in inflammatory diseases. *Nature Reviews Drug Discovery*, *17*(8), 588–606.

Mantovani, A., Sica, A., Sozzani, S., Allavena, P., Vecchi, A., & Locati, M. (2004). The chemokine system in diverse forms of macrophage activation and polarization. *Trends in Immunology*, *25*(12), 677–686.

Marchetti, C., Swartzwelter, B., Gamboni, F., Neff, C. P., Richter, K., Azam, T., Carta, S., Tengesdal, I., et al. (2018). OLT1177, a β-sulfonyl nitrile compound, safe in humans, inhibits the NLRP3 inflammasome and reverses the metabolic cost of inflammation. *Proceedings of the National Academy of Sciences of the United States of America*, *115*(7), E1530–E1539.

Marek-Yagel, D., Berkun, Y., Padeh, S., Abu, A., Reznik-Wolf, H., Livneh, A., Pras, M., & Pras, E. (2009). Clinical disease among patients heterozygous for familial Mediterranean fever. *Arthritis and Rheumatism*, *60*(6), 1862–1866.

Mariathasan, S., Hewton, K., Monack, D. M., Vucic, D., French, D. M., Lee, W. P., Roose-Girma, M., Erickson, S., et al. (2004). Differential activation of the inflammasome by caspase-1 adaptors ASC and Ipaf. *Nature*, *430*(6996), 213–218.

Mariathasan, S., & Monack, D. M. (2007). Inflammasome adaptors and sensors: Intracellular regulators of infection and inflammation. *Nature Reviews Immunology*, *7*(1), 31–40.

Marín-Sánchez, F., Compan, V., Peñín-Franch, A., Tapia-Abellán, A., Gómez, A. I., Baños-Gregori, M. C., Schmidt, F. I., & Pelegrin, P. (2023). ASC oligomer favors caspase-1 CARD domain recruitment after intracellular potassium efflux. *Journal of Cell Biology*, *222*(8), e202003053.

Markov, P. V., Ghafari, M., Beer, M., Lythgoe, K., Simmonds, P., Stilianakis, N. I., & Katzourakis, A. (2023). The evolution of SARS-CoV-2. *Nature Reviews Microbiology*, *21*(6), 361–379.

Markovic, S. S., Jovanovic, M., Gajovic, N., Jurisevic, M., Arsenijevic, N., Jovanovic, M., Mijailovic, Z., Lukic, S., et al. (2021). IL 33 Correlates With COVID-19 Severity, Radiographic and Clinical Finding. *Frontiers in Medicine*, *8*, 1–11.

Martin-Sanchez, F., Diamond, C., Zeitler, M., Gomez, A. I., Baroja-Mazo, A., Bagnall, J., Spiller, D., White, M., et al. (2016). Inflammasome-dependent IL-1β release depends upon membrane permeabilisation. *Cell Death and Differentiation*, *23*(7), 1219–1231.

Martin, G. S., Mannino, D. M., Eaton, S., & Moss, M. (2003). The Epidemiology of Sepsis in the United States from 1979 through 2000. *New England Journal of Medicine*, *348*(16), 1546–1554.

Martínez-García, J. J., Martínez-Banaclocha, H., Angosto-Bazarra, D., de Torre-Minguela, C., Baroja-Mazo, A., Alarcón-Vila, C., Martínez-Alarcón, L., Amores-Iniesta, J., et al. (2019). P2X7 receptor induces mitochondrial failure in monocytes and compromises NLRP3 inflammasome activation during sepsis. *Nature Communications*, *10*(1).

Martinez, F. O., & Gordon, S. (2014). The M1 and M2 paradigm of macrophage activation: Time for reassessment. *F1000Prime Reports*, *6*(March), 1–13.

Martinez, F. O., Helming, L., & Gordon, S. (2009). Alternative activation of macrophages: An immunologic functional perspective. *Annual Review of Immunology*, *27*, 451–483.

Martinon, F., Burns, K., & Tschopp, J. (2002). The Inflammasome: A molecular platform triggering activation of inflammatory caspases and processing of proIL-β. *Molecular Cell*, *10*(2), 417–426.

Martinon, F., Mayor, A., & Tschopp, J. (2009). The inflammasomes: Guardians of the body. *Annual Review of Immunology*, *27*, 229–265.

Mascarenhas, D. P. A., Cerqueira, D. M., Pereira, M. S. F., Castanheira, F. V. S., Fernandes, T. D., Manin, G. Z., Cunha, L. D., & Zamboni, D. S. (2017). Inhibition of caspase-1 or gasdermin-D enable caspase-8 activation in the Naip5/NLRC4/ASC inflammasome. *PLoS Pathogens*, *13*(8), 1–28.

Masters, S. L., Lagou, V., Jéru, I., Baker, P. J., Van Eyck, L., Parry, D. A., Lawless, D., De Nardo, D., et al. (2016). Familial autoinflammation with neutrophilic dermatosis reveals a regulatory mechanism of pyrin activation. *Science Translational Medicine*, *8*(332), 1–10.

McCubrey, J. A., Steelman, L. S., Chappell, W. H., Abrams, S. L., Wong, E. W. T., Chang, F., Lehmann, B., Terrian, D. M., et al. (2007). Roles of the Raf/MEK/ERK pathway in cell growth, malignant transformation and drug resistance. *Biochimica et Biophysica Acta - Molecular Cell Research*, *1773*(8), 1263–1284.

McKee, C. M., & Coll, R. C. (2020). NLRP3 inflammasome priming: A riddle wrapped in a mystery inside an enigma. *Journal of Leukocyte Biology*, *108*(3), 937–952.

McKee, C. M., Fischer, F. A., Bezbradica, J. S., & Coll, R. C. (2021). PHOrming the inflammasome: phosphorylation is a critical switch in inflammasome signalling. *Biochemical Society Transactions*, *49*(6), 2495–2507.

Medzhitov, R. (2007). Recognition of microorganisms and activation of the immune response. *Nature*, *449*(7164), 819–826.

Medzhitov, R. (2008). Origin and physiological roles of inflammation. *Nature*, *454*(7203), 428–435.

Medzhitov, R. (2010). Inflammation 2010: New Adventures of an Old Flame. *Cell*, *140*(6), 771–776.

Medzhitov, R., & Janeway, C. A. (1997). Innate immunity: The virtues of a nonclonal system of recognition. *Cell*, *91*(3), 295–298.

Mehling, M., Brinkmann, V., Antel, J., Bar-Or, A., Goebels, N., Vedrine, C., Kristofic, C., Kuhle, J., et al. (2008). FTY720 therapy exerts differential effects on T cell subsets in multiple sclerosis. *Neurology*, *71*(16), 1261–1267.

Mensa-Vilaro, A., Teresa Bosque, M., Magri, G., Honda, Y., Martínez-Banaclocha, H., Casorran-Berges, M., Sintes, J., González-Roca, E., et al. (2016). Late onset cryopyrin-associated periodic syndrome due to myeloid-restricted somatic NLRP3 mosaicism. *Arthistis & Rheumatology,* 68(12)12, 3035-3041.

Metwaly, A. M., Ghoneim, M. M., Eissa, I. H., Elsehemy, I. A., Mostafa, A. E., Hegazy, M. M., Afifi, W. M., & Dou, D. (2021). Traditional ancient Egyptian medicine: A review. *Saudi Journal of Biological Sciences*, *28*(10), 5823–5832.

Meunier, E., Dick, M. S., Dreier, R. F., Schürmann, N., Broz, D. K., Warming, S., Roose-Girma, M., Bumann, D., et al. (2014). Caspase-11 activation requires lysis of pathogen-containing vacuoles by IFN-induced GTPases. *Nature*, *509*(7500), 366–370.

Meynier, S., & Rieux-Laucat, F. (2019). FAS and RAS related Apoptosis defects: From autoimmunity to leukemia. *Immunological Reviews*, *287*(1), 50–61.

Migliorini, P., Italiani, P., Pratesi, F., Puxeddu, I., & Boraschi, D. (2020). The IL-1 family cytokines and receptors in autoimmune diseases. *Autoimmunity Reviews*, *19*(9), 102617.

Moghaddas, F., Llamas, R., De Nardo, D., Martinez-Banaclocha, H., Martinez-Garcia, J. J., Mesa-Del-Castillo, P., Baker, P. J., Gargallo, V., et al. (2017). A novel Pyrin-Associated Autoinflammation with Neutrophilic Dermatosis mutation further defines 14-3-3 binding of pyrin and distinction to Familial Mediterranean Fever. *Annals of the Rheumatic Diseases*, *76*(12), 2085–2094.

Moghaddas, F., Zeng, P., Zhang, Y., Schützle, H., Brenner, S., Hofmann, S. R., Berner, R., Zhao, Y., et al. (2018). Autoinflammatory mutation in NLRC4 reveals a leucine-rich repeat (LRR)–LRR

oligomerization interface. *Journal of Allergy and Clinical Immunology*, *142*(6), 1956-1967.e6.

Monaco, C., Nanchahal, J., Taylor, P., & Feldmann, M. (2015). Anti-TNF therapy: Past, present and future. *International Immunology*, *27*(1), 55–62.

Mora, J., Schlemmer, A., Wittig, I., Richter, F., Putyrski, M., Frank, A. C., Han, Y., Jung, M., et al. (2016). Interleukin-38 is released from apoptotic cells to limit inflammatory macrophage responses. *Journal of Molecular Cell Biology*, *8*(5), 426–438.

Morante-Palacios, O., Fondelli, F., Ballestar, E., & Martínez-Cáceres, E. M. (2021). Tolerogenic Dendritic Cells in Autoimmunity and Inflammatory Diseases. *Trends in Immunology*, *42*(1), 59–75.

Moreno, R., Rhodes, A., Piquilloud, L., Hernandez, G., Takala, J., Gershengorn, H. B., Tavares, M., Coopersmith, C. M., et al. (2023). The Sequential Organ Failure Assessment (SOFA) Score: has the time come for an update?. *Critical Care*, *27*(1), 1–5.

Moritz Rapp, Wiedemann, G. M., & Sun, J. C. (2019). Memory responses of innate lymphocytes and parallels with T cells. *Physiology & Behavior*, *176*(3), 139–148.

Mousset, C. M., Hobo, W., Woestenenk, R., Preijers, F., Dolstra, H., & van der Waart, A. B. (2019). Comprehensive Phenotyping of T Cells Using Flow Cytometry. *Cytometry Part A*, *95*(6), 647–654.

Muñoz-Planillo, R., Kuffa, P., Martínez-Colón, G., Smith, B. L., Rajendiran, T. M., & Núñez, G. (2013). K+ Efflux Is the Common Trigger of NLRP3 Inflammasome Activation by Bacterial Toxins and Particulate Matter. *Immunity*, *38*(6), 1142–1153.

Munoz, C., Carlet, J., Fitting, C., Misset, B., Blériot, J. P., & Cavaillon, J. M. (1991). Dysregulation of in vitro cytokine production by monocytes during sepsis. *Journal of Clinical Investigation*, *88*(5), 1747–1754.

Murphy, K., & Weaver, C. (2017). Icons used throughout the book. In *Janeway's Immunobiology*.

Murúa, S. R., Farez, M. F., & Quintana, F. J. (2021). The Immune Response in Multiple Sclerosis. *Annual Review of Pathology: Mechanisms of Disease*, *17*, 121–139.

Nadif, R., Zerimech, F., Bouzigon, E., & Matran, R. (2013). The role of eosinophils and basophils in allergic diseases considering genetic findings. *Current Opinion in Allergy and Clinical Immunology*, *13*(5), 507–513.

Nakagawa, K., Gonzalez-Roca, E., Souto, A., Kawai, T., Umebayashi, H., Campistol, J. M., Cañellas, J., Takei, S., et al. (2015). Somatic NLRP3 mosaicism in Muckle-Wells syndrome. A genetic mechanism shared by different phenotypes of cryopyrin-associated periodic syndromes. *Annals of the Rheumatic Diseases*, *74*(3), 603–610.

Napier, B. A., Brubaker, S. W., Sweeney, T. E., Monette, P., Rothmeier, G. H., Gertsvolf, N. A., Puschnik, A., Carette, J. E., et al. (2016). Complement pathway amplifies caspase-11-dependent cell death and endotoxin-induced sepsis severity. *Journal of Experimental Medicine*, *213*(11), 2365–2382.

Netea, M. G., Balkwill, F., Chonchol, M., Cominelli, F., Marc, Y., Giamarellos-bourboulis, E. J., Golenbock, D., Gresnigt, M. S., et al. (2018). *A guiding map for inflammation*. *18*(8), 826–831.

Netea, M. G., Quintin, J., & Van Der Meer, J. W. M. (2011). Trained immunity: A memory for innate host defense. *Cell Host and Microbe*, *9*(5), 355–361.

Netea, M. G., Schlitzer, A., Placek, K., Joosten, L. A. B., & Schultze, J. L. (2019). Innate and Adaptive Immune Memory: an Evolutionary Continuum in the Host's Response to Pathogens. *Cell Host and Microbe*, *25*(1), 13–26.

Netea, M. G., Simon, A., Van De Veerdonk, F., Kullberg, B. J., Van Der Meer, J. W. M., & Joosten, L. A. B. (2010). IL-1β processing in host defense: Beyond the inflammasomes. *PLoS Pathogens*, *6*(2).

Netea, M. G., Van De Veerdonk, F. L., Van Der Meer, J. W. M., Dinarello, C. A., & Joosten, L. A. B. (2015). Inflammasome-independent regulation of IL-1-family cytokines. *Annual Review of Immunology*, *33*, 49–77.

Newton, K., & Dixit, V. M. (2012). Signaling in innate immunity and inflammation. *Cold Spring Harbor Perspectives in Biology*, *4*(3).

Nieto-Torres, J. L., Verdiá-Báguena, C., Jimenez-Guardeño, J. M., Regla-Nava, J. A., Castaño-Rodriguez, C., Fernandez-Delgado, R., Torres, J., Aguilella, V. M., et al. (2015). Severe acute respiratory syndrome coronavirus E protein transports calcium ions and activates the NLRP3 inflammasome. *Virology*, *485*, 330–339.

Nigrovic, P. A., Lee, P. Y., & Hoffman, H. M. (2020). Monogenic autoinflammatory disorders: Conceptual overview, phenotype, and clinical approach. *Journal of Allergy and Clinical Immunology*, *146*(5), 925–937.

Nold, M. F., Nold-Petry, C. A., Zepp, J. A., Palmer, B. E., Bufler, P., & Dinarello, C. A. (2010). IL-37 is a fundamental inhibitor of innate immunity. *Nature Immunology*, *11*(11), 1014–1022.

Novick, D., Kim, S., Kaplanski, G., & Dinarello, C. A. (2013). Interleukin-18, more than a Th1 cytokine. *Seminars in Immunology*, *25*(6), 439–448.

O'Neill, L. A. J., Golenbock, D., & Bowie, A. G. (2013). The history of Toll-like receptors-redefining innate immunity. *Nature Reviews Immunology*, *13*(6), 453–460.

Ohto, U., Kamitsukasa, Y., Ishida, H., Zhang, Z., Murakami, K., Hirama, C., Maekawa, S., & Shimizu, T. (2022). Structural basis for the oligomerization-mediated regulation of NLRP3 in fl ammasome activation. *PNAS*, *11*(43), e2121353119.

Omenetti, A., Carta, S., Delfino, L., Martini, A., Gattorno, M., & Rubartelli, A. (2014). Increased NLRP3-dependent interleukin 1β secretion in patients with familial Mediterranean fever: Correlation with MEFV genotype. *Annals of the Rheumatic Diseases*, *73*(2), 462–469.

Ordás, M. C., Costa, M. M., Roca, F. J., López-Castejón, G., Mulero, V., Meseguer, J., Figueras, A., & Novoa, B. (2007). Turbot TNFα gene: Molecular characterization and biological activity of the recombinant protein. *Molecular Immunology*, *44*(4), 389–400.

Orlowski, G. M., Colbert, J. D., Sharma, S., Bogyo, M., Robertson, S. A., & Rock, K. L. (2015). Multiple Cathepsins Promote Pro–IL-1β Synthesis and NLRP3-Mediated IL-1β Activation. *The Journal of Immunology*, *195*(4), 1685–1697.

Orning, P., Weng, D., Starheim, K., Ratner, D., Best, Z., Lee, B., Brooks, A., Xia, S., et al. (2018). Pathogen blockade of TAK1 triggers caspase-8 dependent cleavage of Gasdermin D and cell death. *Science*, *362*(6418), 1064–1069.

Paidimuddala, B., Cao, J., Nash, G., Xie, Q., Wu, H., & Zhang, L. (2023). Mechanism of NAIP—NLRC4 inflammasome activation revealed by cryo-EM structure of unliganded NAIP5. *Nature Structural and Molecular Biology*, *30*(2), 159–166.

Pan, P., Shen, M., Yu, Z., Ge, W., Chen, K., Tian, M., Xiao, F., Wang, Z., et al. (2021). SARS-CoV-2 N protein promotes NLRP3 inflammasome activation to induce hyperinflammation. *Nature Communications*, *12*(1), 1–17.

Panico, C., & Nylen, E. (2013). Procalcitonin beyond the acute phase: Novel biomediator properties? *BMC Medicine*, *11*(1), 2–5.

Pantsar, T. (2020). The current understanding of KRAS protein structure and dynamics. *Computational and Structural Biotechnology Journal*, *18*, 189–198.

Park, Y. H., Wood, G., Kastner, D. L., & Chae, J. J. (2016). Pyrin Inflammasome Activation and RhoA Signaling in the Autoinflammatory Diseases FMF and HIDS Yong. *Nature Immunology*, *17*(8), 914–921.

Patel, S. (2018). Danger-Associated Molecular Patterns (DAMPs): the Derivatives and Triggers of Inflammation. *Current Allergy and Asthma Reports*, *18*(11).

Patidar, M., Yadav, N., & Dalai, S. K. (2016). Interleukin 15: A key cytokine for immunotherapy. *Cytokine and Growth Factor Reviews*, *31*, 49–59.

Patnaik, M. M., & Lasho, T. (2020). Myelodysplastic syndrome/myeloproliferative neoplasm overlap

syndromes: A focused review. *Hematology (United States)*, *20*(1), 460–464.

Patnaik, M. M., & Tefferi, A. (2018). Chronic myelomonocytic leukemia: 2018 update on diagnosis, risk stratification and management. *American Journal of Hematology*, *93*(6), 824–840.

Pedra, J. H. F., Cassel, S., & Sutterwala, F. (2009). Sensing Pathogens and Danger Signals by the Inflammasome Joao. *Curr Opin Immunol.*, *21*(1), 10–16.

Pelegrín, P. (2011). Many ways to dilate the P2X7 receptor pore. *British Journal of Pharmacology*, *163*(5), 908–911.

Pelegrin, P., & Surprenant, A. (2009). Dynamics of macrophage polarization reveal new mechanism to inhibit IL-1B release through pyrophosphates. *EMBO Journal*, *28*(14), 2114–2127.

Perera, P. Y., Lichy, J. H., Waldmann, T. A., & Perera, L. P. (2012). The role of interleukin-15 in inflammation and immune responses to infection: Implications for its therapeutic use. *Microbes and Infection*, *14*(3), 247–261.

Perregaux, D., & Gabel, C. A. (1994). Interleukin-1β maturation and release in response to ATP and nigericin. Evidence that potassium depletion mediated by these agents is a necessary and common feature of their activity. *Journal of Biological Chemistry*, *269*(21), 15195–15203.

Perschinka, F., Mayerhöfer, T., Lehner, G. F., Hasslacher, J., Klein, S. J., & Joannidis, M. (2022). Immunologic response in bacterial sepsis is different from that in COVID-19 sepsis. *Infection*, *50*(4), 1035–1037.

Pierrakos, C., & Vincent, J. L. (2010). Sepsis biomarkers: A review. *Critical Care*, *14*(1), 1–18.

Pillay, J., Den Braber, I., Vrisekoop, N., Kwast, L. M., De Boer, R. J., Borghans, J. A. M., Tesselaar, K., & Koenderman, L. (2010). In vivo labeling with 2H2O reveals a human neutrophil lifespan of 5.4 days. *Blood*, *116*(4), 625–627.

Pisetsky, D. S., Erlandsson-Harris, H., & Andersson, U. (2008). High-mobility group box protein 1 (HMGB1): An alarmin mediating the pathogenesis of rheumatic disease. *Arthritis Research and Therapy*, *10*(3).

Pizzuto, M., Pelegrin, P., & Ruysschaert, J. M. (2022). Lipid-protein interactions regulating the canonical and the non-canonical NLRP3 inflammasome. *Progress in Lipid Research*, *87*, 101182.

Queen, D., Ediriweera, C., & Liu, L. (2019). Function and Regulation of IL-36 Signaling in Inflammatory Diseases and Cancer Development. *Frontiers in Cell and Developmental Biology*, *7*, 1–13.

Quirant-Sánchez, B., Hervás-García, J. V., Teniente-Serra, A., Brieva, L., Moral-Torres, E., Cano, A., Munteis, E., Mansilla, M. J., et al. (2018). Predicting therapeutic response to fingolimod treatment in multiple sclerosis patients. *CNS Neuroscience and Therapeutics*, *24*(12), 1175–1184.

R Core Team. (2014). *R: a language and environment for statistical computing* (Issue R Foundation for Statistical Computing).

Raghawan, A. K., Ramaswamy, R., Radha, V., & Swarup, G. (2019). HSC70 regulates cold-induced caspase-1 hyperactivation by an autoinflammation-causing mutant of cytoplasmic immune receptor NLRC4. *Proceedings of the National Academy of Sciences of the United States of America*, *116*(43), 21694–21703.

Raghawan, A. K., Ramaswamy, R., & Swarup, G. (2023). Cold-induced loss of interaction with HSC70 triggers inflammasome activity of familial cold autoinflammatory syndrome-causing mutants of NLRP3. *Biochemical and Biophysical Research Communications*, *641*, 42–49.

Rahman, P., Inman, R. D., El-Gabalawy, H., & Krause, D. O. (2010). Pathophysiology and pathogenesis of immune-mediated inflammatory diseases: Commonalities and differences. *Journal of Rheumatology*, *37*(SUPPL. 85), 11–26.

Rathinam, V. A. K., Vanaja, S. K., Waggoner, L., Sokolovska, A., Becker, C., Stuart, L. M., Leong, J. M., & Fitzgerald, K. A. (2012). TRIF licenses caspase-11-dependent NLRP3 inflammasome activation by gram-negative bacteria. *Cell*, *150*(3), 606–619.

Rehwinkel, J., & Gack, M. U. (2020). RIG-I-like receptors: their regulation and roles in RNA sensing. *Nature Reviews Immunology*, *20*(9), 537–551.

Rello, J., Valenzuela-Sánchez, F., Ruiz-Rodriguez, M., & Moyano, S. (2017). Sepsis: A Review of Advances in Management. In *Advances in Therapy* (Vol. 34, Issue 11, pp. 2393–2411). Springer Healthcare.

Repa, A., Bertsias, G. K., Petraki, E., Choulaki, C., Vassou, D., Kambas, K., Boumpas, D. T., Goulielmos, G., et al. (2015). Dysregulated production of interleukin-1β upon activation of the NLRP3 inflammasome in patients with familial Mediterranean fever. *Human Immunology*, *76*(7), 488–495.

Rhodes, A., Evans, L. E., Alhazzani, W., Levy, M. M., Antonelli, M., Ferrer, R., Kumar, A., Sevransky, J. E., et al. (2017). Surviving Sepsis Campaign: International Guidelines for Management of Sepsis and Septic Shock: 2016. In *Intensive Care Medicine* (Vol. 43, Issue 3). Springer Berlin Heidelberg.

Rieber, N., Gavrilov, A., Hofer, L., Singh, A., Öz, H., Endres, T., Schäfer, I., Handgretinger, R., et al. (2015). A functional inflammasome activation assay differentiates patients with pathogenic NLRP3 mutations and symptomatic patients with low penetrance variants. *Clinical Immunology*, *157*(1), 56–64.

Rincon, M. (2012). Interleukin-6: From an inflammatory marker to a target for inflammatory diseases. *Trends in Immunology*, *33*(11), 571–577.

Río, J., Castilló, J., Rovira, A., Tintoré, M., Sastre-Garriga, J., Horga, A., Nos, C., Comabella, M., et al. (2009). Measures in the first year of therapy predict the response to interferon β in MS. *Multiple Sclerosis*, *15*(7), 848–853.

Rittirsch, D., Flierl, M. A., & Ward, P. A. (2008). Harmful molecular mechanisms in sepsis. *Nature Reviews Immunology*, *8*(10), 776–787.

Rittirsch, D., Hoesel, L. M., & Ward, P. A. (2007). The disconnect between animal models of sepsis and human sepsis. *Journal of Leukocyte Biology*, *81*(1), 137–143.

Robin, M., de Wreede, L. C., Padron, E., Bakunina, K., Fenaux, P., Koster, L., Nazha, A., Beelen, D. W., et al. (2022). Role of allogeneic transplantation in chronic myelomonocytic leukemia: an international collaborative analysis. *Blood*, *140*(12), 1408–1418.

Robin, X., Turck, N., Hainard, A., Tiberti, N., Sanchez, J.-C., & Mueller, M. (2011). pROC: an open-source package for R and S+ to analyze and compare ROC curves. *BMC Bioinformatics*, *12*(BMC Bioinformatics), 77.

Rodrigues, T. S., de Sá, K. S. G., Ishimoto, A. Y., Becerra, A., Oliveira, S., Almeida, L., Gonçalves, A. V., et al. (2020). Inflammasomes are activated in response to SARS-cov-2 infection and are associated with COVID-19 severity in patients. *Journal of Experimental Medicine*, *218*(3).

Rogers, C., Fernandes-Alnemri, T., Mayes, L., Alnemri, D., Cingolani, G., & Alnemri, E. S. (2017). Cleavage of DFNA5 by caspase-3 during apoptosis mediates progression to secondary necrotic/pyroptotic cell death. *Nature Communications*, *8*, 1–14.

Rohart, F., Gautier, B., Singh, A., & Lê Cao, K. (2017). mixOmics: An R package for 'omics feature selection and multiple data integration. *PLoS Computational Biology*, *13*(11), 1–14.

Romberg, N., Al Moussawi, K., Nelson-Williams, C., Stiegler, A. L., Loring, E., Choi, M., Overton, J., Meffre, E., et al. (2014). Mutation of NLRC4 causes a syndrome of enterocolitis and autoinflammation. *Nature Genetics*, *46*(10), 1135–1139.

Romberg, N., Vogel, T. P., & Canna, S. W. (2017). NLRC4 inflammasomopathies. *Current Opinion in Allergy and Clinical Immunology*, *17*(6), 398–404.

Rosenberg, H. F., Dyer, K. D., & Foster, P. S. (2013). Eosinophils: Changing perspectives in health and disease. *Nature Reviews Immunology*, *13*(1), 9–22

Rosengren, S., Mueller, J. L., Anderson, J. P., Niehaus, B. L., Misaghi, A., Anderson, S., Boyle, D. L., & Hoffman, H. M. (2007). Monocytes from familial cold autoinflammatory syndrome patients are activated by mild hypothermia. *Journal of Allergy and Clinical Immunology*, *119*(4), 991–996.

Rosser, E. C., & Mauri, C. (2015). Regulatory B Cells: Origin, Phenotype, and Function. *Immunity*, *42*(4), 607–612.

Rowczenio, D. M., Gomes, S. M., Aróstegui, J. I., Mensa-Vilaro, A., Omoyinmi, E., Trojer, H., Baginska, A., Baroja-Mazo, A., et al. (2017). Late-onset cryopyrin-associated periodic syndromes caused by somatic NLRP3 mosaicism-UK single center experience. *Frontiers in Immunology*, *8*, 1410.

Rühl, S., Shkarina, K., Demarco, B., Heilig, R., Santos, J. C., & Broz, P. (2018). ESCRT-dependent membrane repair negatively regulates pyroptosis downstream of GSDMD activation. *Science*, *362*(6417), 956–960.

Saïd-Sadier, N., & Ojcius, D. M. (2014). Alarmins, Inflammasomes and Immunity Pattern recognition receptors in innate immunity. *Biomed Journal*, *35*(6), 437–449.

Saito, S., Nakashima, A., Shima, T., & Ito, M. (2010). Th1/Th2/Th17 and Regulatory T-Cell Paradigm in Pregnancy. *American Journal of Reproductive Immunology*, *63*(6), 601–610.

Salama, C., Han, J., Yau, L., Reiss, W. G., Kramer, B., Neidhart, J. D., Criner, G. J., Kaplan-Lewis, E., et al. (2021). Tocilizumab in Patients Hospitalized with Covid-19 Pneumonia. *New England Journal of Medicine*, *384*(1), 20–30.

Sallman, D. A., & List, A. (2019). The central role of inflammatory signaling in the pathogenesis of myelodysplastic syndromes. *Blood*, *133*(10), 1039–1048.

Santos, J. C., Dick, M. S., Lagrange, B., Degrandi, D., Pfeffer, K., Yamamoto, M., Meunier, E., Pelczar, P., et al. (2018). LPS targets host guanylate-binding proteins to the bacterial outer membrane for non-canonical inflammasome activation . *The EMBO Journal*, *37*(6), 1–19. https://doi.org/10.15252/embj.201798089

Santos, S. S., Carmo, A. M., Brunialti, M. K. C., Machado, F. R., Azevedo, L. C., Assunção, M., Trevelin, S. C., Cunha, F. Q., et al. (2016). Modulation of monocytes in septic patients: preserved phagocytic activity, increased ROS and NO generation, and decreased production of inflammatory cytokines. *Intensive Care Medicine Experimental* , *4*(1), 1–16.

Sarhan, J., Liu, B. C., Muendlein, H. I., Li, P., Nilson, R., Tang, A. Y., Rongvaux, A., Bunnell, S. C., et al. (2018). Caspase-8 induces cleavage of gasdermin D to elicit pyroptosis during Yersinia infection. *Proceedings of the National Academy of Sciences of the United States of America*, *115*(46), E10888–E10897.

Sborgi, L., Rühl, S., Mulvihill, E., Pipercevic, J., Heilig, R., Stahlberg, H., Farady, C. J., Müller, D. J., et al. (2016). GSDMD membrane pore formation constitutes the mechanism of pyroptotic cell death. *The EMBO Journal*, *35*(16), 1766–1778.

Schmitz, J., Owyang, A., Oldham, E., Song, Y., Murphy, E., McClanahan, T. K., Zurawski, G., Moshrefi, M., et al. (2005). IL-33, an interleukin-1-like cytokine that signals via the IL-1 receptor-related protein ST2 and induces T helper type 2-associated cytokines. *Immunity*, *23*(5), 479–490.

Schnappauf, O., Chae, J. J., Kastner, D. L., & Aksentijevich, I. (2019). The Pyrin Inflammasome in Health and Disease. In *Frontiers in immunology* (Vol. 10, p. 1745). NLM (Medline).

Schulte, W., Bernhagen, J., & Bucala, R. (2013). Cytokines in sepsis: Potent immunoregulators and potential therapeutic targets - An updated view. *Mediators of Inflammation*, *2013*.

Schulz, C., Perdiguero, E. G., Chorro, L., Szabo-Rogers, H., Cagnard, N., Kierdorf, K., Prinz, M., Wu, B., et al. (2012). A lineage of myeloid cells independent of myb and hematopoietic stem cells. *Science*, *335*(6077), 86–90.

Sefik, E., Qu, R., Junqueira, C., Kaffe, E., Mirza, H., Zhao, J., Brewer, J. R., Han, A., et al. (2022). Inflammasome activation in infected macrophages drives COVID-19 pathology. *Nature*, *606*(7914), 585–593.

Sester, D. P., Zamoshnikova, A., Thygesen, S. J., Vajjhala, P. R., Cridland, S. O., Schroder, K., & Stacey, K. J. (2016). Assessment of inflammasome formation by flow cytometry. *Current Protocols in Immunology*, *2016*(August), 14.40.1-14.40.29.

Sevin, M., Debeurme, F., Laplane, L., Badel, S., Morabito, M., Newman, H. L., Torres-Martin, M., Yang, Q., et al. (2021). Cytokine-like protein 1–induced survival of monocytes suggests a combined strategy targeting MCL1 and MAPK in CMML. *Blood*, *137*(24), 3390–3402.

Shalova, I. N., Lim, J. Y., Chittezhath, M., Zinkernagel, A. S., Beasley, F., Hernández-Jiménez, E., Toledano, V., Cubillos-Zapata, C., et al. (2015). Human monocytes undergo functional re-programming during sepsis mediated by hypoxia-inducible factor-1α. *Immunity*, *42*(3), 484–498.

Shao, S., Chen, C., Shi, G., Zhou, Y., Wei, Y., Fan, N., Yang, Y., Wu, L., et al. (2021). Therapeutic potential of the target on NLRP3 inflammasome in multiple sclerosis. *Pharmacology and Therapeutics*, *227*, 107880.

Sharif, H., Wang, L., Wang, W. L., Magupalli, V. G., Andreeva, L., Qiao, Q., Hauenstein, A. V., Wu, Z., et al. (2019). Structural mechanism for NEK7-licensed activation of NLRP3 inflammasome. *Nature*, *570*(7761), 338–343.

Sharma, D., & Kanneganti, T. D. (2016). The cell biology of inflammasomes: Mechanisms of inflammasome activation and regulation. *Journal of Cell Biology*, *213*(6), 617–629.

Shi, H., Wang, Y., Li, X., Zhan, X., Tang, M., Fina, M., Su, L., Pratt, D., et al. (2016). NLRP3 activation and mitosis are mutually exclusive events coordinated by NEK7, a new inflammasome component. *Nature Immunology*, *17*(3), 250–258.

Shi, J., Zhao, Y., Wang, K., Shi, X., Wang, Y., Huang, H., Zhuang, Y., Cai, T., et al. (2015). Cleavage of GSDMD by inflammatory caspases determines pyroptotic cell death. *Nature*, *526*(7575), 660–665.

Shi, J., Zhao, Y., Wang, Y., Gao, W., Ding, J., Li, P., Hu, L., & Shao, F. (2014). Inflammatory caspases are innate immune receptors for intracellular LPS. *Nature*, *514*(7521), 187–192.

Shi, X., Sun, Q., Hou, Y., Zeng, H., Cao, Y., Dong, M., Ding, J., & Shao, F. (2023). Recognition and maturation of IL-18 by caspase-4 noncanonical inflammasome. *Nature*, *May*.

Shi, Z. A., Yu, C. X., Wu, Z. C., Chen, C. L., Tu, F. P., & Wan, Y. (2021). The effect of FTY720 at different doses and time-points on LPS-induced acute lung injury in rats. *International Immunopharmacology*, *99*, 107972.

Shimada, K., Crother, T. R., Karlin, J., Dagvadorj, J., Chiba, N., Chen, S., Ramanujan, V. K., Wolf, et al. (2012). Oxidized Mitochondrial DNA Activates the NLRP3 Inflammasome during Apoptosis. *Immunity*, *36*(3), 401–414.

Simon, H. U. (2009). Cell death in allergic diseases. *Apoptosis*, *14*(4), 439–446.

Singer, M., Deutschman, C. S., Seymour, C., Shankar-Hari, M., Annane, D., Bauer, M., Bellomo, R., Bernard, G. R., et al. (2016). The third international consensus definitions for sepsis and septic shock (sepsis-3). *JAMA - Journal of the American Medical Association*, *315*(8), 801–810.

Smith, D. E., Hanna, R., Friend, D., Moore, H., Chen, H., Farese, A. M., MacVittie, T. J., Virca, G. D., et al. (2003). The Soluble Form of IL-1 Receptor Accessory Protein Enhances the Ability of Soluble Type II IL-1 Receptor to Inhibit IL-1 Action. *Immunity*, *18*(1), 87–96.

Smithgall, M. D., Comeau, M. R., Park-Yoon, B. R., Kaufman, D., Armitage, R., & Smith, D. E. (2008). IL-33 amplifies both Th1- and Th2-type responses through its activity on human basophils, allergen-reactive Th 2 cells, iNKT and NK Cells. *International Immunology*, *20*(8), 1019–1030.

Soares, J. L., Oliveira, E. M., & Pontillo, A. (2019). Variants in NLRP3 and NLRC4 inflammasome associate with susceptibility and severity of multiple sclerosis. *Multiple Sclerosis and Related Disorders*, *29*, 26–34.

Solís-Moruno, M., Mensa-Vilaró, A., Batlle-Masó, L., Lobón, I., Bonet, N., Marquès-Bonet, T., Aróstegui, J. I., & Casals, F. (2021). Assessment of the gene mosaicism burden in blood and its implications for immune disorders. *Scientific Reports*, *11*(1), 1–11.

Soriano-Teruel, P. M., García-Laínez, G., Marco-Salvador, M., Pardo, J., Arias, M., DeFord, C., Merfort, I., Vicent, M. J., et al. (2021). Identification of an ASC oligomerization inhibitor for the treatment of inflammatory diseases. *Cell Death and Disease*, *12*(12), 1155.

Straub, R. H., & Schradin, C. (2016). Chronic inflammatory systemic diseases – an evolutionary trade-off between acutely beneficial but chronically harmful programs. *Evolution, Medicine, and Public Health*, eow001.

Subramanian, N., Natarajan, K., Clatworthy, M. R., Wang, Z., & Germain, R. N. (2013). The adaptor MAVS promotes NLRP3 mitochondrial localization and inflammasome activation. *Cell*, *153*(2), 348–361.

Such, E., Germing, U., Malcovati, L., & Hrodek, O. (2013). Development and validation of a prognostic scoring system for patients with chronic myelomonocytic leukemia. *Transfuze a Hematologie Dnes*, *19*(3), 191.

Sun, S., Duan, Z., Wang, X., Chu, C., Yang, C., Chen, F., Wang, D., Wang, C., et al. (2021). Neutrophil extracellular traps impair intestinal barrier functions in sepsis by regulating TLR9-mediated endoplasmic reticulum stress pathway. *Cell Death and Disease*, *12*(6).

Swanson, J., Biology, C., Avenue, L., & Watts, C. (1995). Macropinocytosis. *Trends in Cell Biology*, *5*, 424–428.

Swanson, K. V, Deng, M., & Ting, J. P.-Y. (2019). The NLRP3 inflammasome: molecular activation and regulation to therapeutics. *Nature Reviews Immunology*, *19*(8), 477–489.

Tan, C., Huang, Y., Shi, F., Tan, K., Ma, Q., Chen, Y., Jiang, X., & Li, X. (2020). C-reactive protein correlates with computed tomographic findings and predicts severe COVID-19 early. *Journal of Medical Virology*, *92*(7), 856–862.

Tanaka, N., Izawa, K., Saito, M. K., Sakuma, M., Oshima, K., Ohara, O., Nishikomori, R., Morimoto, T., et al. (2011). High incidence of NLRP3 somatic mosaicism in patients with chronic infantile neurologic, cutaneous, articular syndrome: Results of an international multicenter collaborative study. *Arthritis and Rheumatism*, *63*(11), 3625–3632.

Tanaka, T., Narazaki, M., & Kishimoto, T. (2016). Immunotherapeutic implications of IL-6 blockade for cytokine storm. In *Immunotherapy* (Vol. 8, Issue 8, pp. 959–970). Future Medicine Ltd.

Tang, B. M., Eslick, G. D., Craig, J. C., & McLean, A. S. (2007). Accuracy of procalcitonin for sepsis diagnosis in critically ill patients: systematic review and meta-analysis. *Lancet Infectious Diseases*, *7*(3), 210–217.

Tapia-Abellán, A., Angosto-Bazarra, D., Alarcón-Vila, C., Baños, M. C., Hafner-Bratkovič, I., Oliva, B., & Pelegrín, P. (2021). Sensing low intracellular potassium by NLRP3 results in a stable open structure that promotes inflammasome activation. *Science Advances*, *7*(38), 1–16.

Tapia-Abellán, A., Angosto-Bazarra, D., Martínez-Banaclocha, H., de Torre-Minguela, C., Cerón-Carrasco, J. P., Pérez-Sánchez, H., Arostegui, J. I., & Pelegrin, P. (2019). MCC950 closes the active conformation of NLRP3 to an inactive state. *Nature Chemical Biology*, *15*(6), 560–564.

Tartey, S., & Kanneganti, T. D. (2020). Inflammasomes in the pathophysiology of autoinflammatory syndromes. *Journal of Leukocyte Biology*, *107*(3), 379–391.

Tenthorey, J. L., Kofoed, E. M., Daugherty, M. D., Malik, H. S., & Vance, R. E. (2014). Molecular basis for specific recognition of bacterial ligands by NAIP/NLRC4 inflammasomes. *Molecular Cell*, *54*(1), 17–29.

Teodorovic, L. S., Babolin, C., Rowland, S. L., Greaves, S. A., Baldwin, D. P., Torres, R. M., & Pelanda, R. (2014). Activation of Ras overcomes B-cell tolerance to promote differentiation of autoreactive B cells and production of autoantibodies. *Proceedings of the National Academy of Sciences of the United States of America*, *111*(27).

Teufel, L. U., Arts, R. J. W., Netea, M. G., Dinarello, C. A., & Joosten, L. A. B. (2022). IL-1 family cytokines as drivers and inhibitors of trained immunity. *Cytokine*, *150*, 155773.

Towne, J. E., Renshaw, B. R., Douangpanya, J., Lipsky, B. P., Shen, M., Gabel, C. A., & Sims, J. E. (2011). Interleukin-36 (IL-36) ligands require processing for full agonist (IL-36α, IL-36β, and IL-36γ) or antagonist (IL-36Ra) activity. *Journal of Biological Chemistry*, *286*(49), 42594–42602.

Travers, B. S., & Tsang, B. K. (2022). Multiple sclerosis: diagnosis, disease-modifying therapy and

prognosis. *Australian Journal of General Practice*, *51*(4), 199–206.

Tschopp, J., Martinon, F., & Burns, K. (2003). NALPs: A novel protein family involved in inflammation. *Nature Reviews Molecular Cell Biology*, *4*(2), 95–104.

Vajjhala, P. R., Kaiser, S., Smith, S. J., Ong, Q. R., Soh, S. L., Stacey, K. J., & Hill, J. M. (2014). Identification of multifaceted binding modes for pyrin and ASC pyrin domains gives insights into pyrin inflammasome assembly. *Journal of Biological Chemistry*, *289*(34), 23504–23519.

van Buuren, S., & Groothuis-Oudshoorn, K. (2011). mice: Multivariate imputation by chained equations in R. *Journal of Statistical Software*, *45*(3), 1–67.

Van de Veerdonk, F. &, & Netea, M. G. (2013). New insights in the immunobiology of IL-1 family members. *Frontiers in Immunology*, *4*(JUL), 1–11.

Van De Veerdonk, F. L., & Netea, M. G. (2020). Blocking IL-1 to prevent respiratory failure in COVID-19. *Critical Care*, *24*(1), 1–6.

Van De Veerdonk, F. L., Stoeckman, A. K., Wu, G., Boeckermann, A. N., Azam, T., Netea, M. G., Joosten, L. A. B., Van Der Meer, J. W. M., et al. (2012). IL-38 binds to the IL-36 receptor and has biological effects on immune cells similar to IL-36 receptor antagonist. *Proceedings of the National Academy of Sciences of the United States of America*, *109*(8), 3001–3005.

Van den Bossche, J., Baardman, J., Otto, N. A., van der Velden, S., Neele, A. E., van den Berg, S. M., Luque-Martin, R., Chen, H. J., et al. (2016). Mitochondrial Dysfunction Prevents Repolarization of Inflammatory Macrophages. *Cell Reports*, *17*(3), 684–696.

Van Der Poll, T., Van De Veerdonk, F. L., Scicluna, B. P., & Netea, M. G. (2017). The immunopathology of sepsis and potential therapeutic targets. *Nature Reviews Immunology*, *17*(7), 407–420.

Van Gorp, H., Saavedra, P. H. V., De Vasconcelos, N. M., Van Opdenbosch, N., Walle, L. Vande, Matusiak, M., Prencipe, G., et al. (2016). Familial Mediterranean fever mutations lift the obligatory requirement for microtubules in Pyrin inflammasome activation. *Proceedings of the National Academy of Sciences of the United States of America*, *113*(50), 14384–14389.

Vargas, M., & Rojo, C. (2020). Ferritin levels and COVID-19 Suggested. *Therapeutic Advances in Vaccines*, *9*(5), 2019–2020.

Venables, W. N., & & Ripley, B. D. (2002). *Modern applied statistics with S*. Springer.

Veras, F. P., Pontelli, M. C., Silva, C. M., Toller-Kawahisa, J. E., de Lima, M., Nascimento, D. C., Schneider, A. H., Caetité, D., et al. (2020). SARS-CoV-2-triggered neutrophil extracellular traps mediate COVID-19 pathology. *Journal of Experimental Medicine*, *217*(12).

Villatoro, A., Cuminetti, V., Bernal, A., Torroja, C., Cossío, I., Benguría, A., Ferré, M., Konieczny, J., et al. (2023). Endogenous IL-1 receptor antagonist restricts healthy and malignant myeloproliferation. *Nature Communications*, *14*(1).

Volker-Touw, C. M. L., de Koning, H. D., Giltay, J. C., de Kovel, C. G. F., van Kempen, T. S., Oberndorff, K. M. E. J., Boes, M. L., van Steensel, M. A. M., et al. (2017). Erythematous nodes, urticarial rash and arthralgias in a large pedigree with NLRC4-related autoinflammatory disease, expansion of the phenotype. *British Journal of Dermatology*, *176*(1), 244–248.

Vora, S. M., Lieberman, J., & Wu, H. (2021). Inflammasome activation at the crux of severe COVID-19. *Nature Reviews Immunology*, *21*(11), 694–703. h

Wang, J., Ye, Q., Zheng, W., Yu, X., Luo, F., Fang, R., Shangguan, Y., Du, Z., et al. (2022). Low-ratio somatic NLRC4 mutation causes late-onset autoinflammatory disease. *Annals of the Rheumatic Diseases*, *81*(8), 1173–1178.

Wang, Y., Gao, W., Shi, X., Ding, J., Liu, W., He, H., Wang, K., & Shao, F. (2017). Chemotherapy drugs induce pyroptosis through caspase-3 cleavage of a gasdermin. *Nature*, *547*(7661), 99–103.

Wannamaker, W., Davies, R., Namchuk, M., Pollard, J., Ford, P., Ku, G., Decker, C., Charifson, P., et al. (2007). (S)-1-((S)-2-{[1-(4-amino-3-chloro-phenyl)-methanoyl]-amino}-3, 3-dimethyl-butanoyl)-

pyrrolidine-2-carboxylic acid ((2R,3S)-2-ethoxy-5-oxo- tetrahydro-furan-3-yl)-amide (VX-765), an orally available selective interleukin (IL)-converting enzyme/caspase-1 i. *Journal of Pharmacology and Experimental Therapeutics*, *321*(2), 509–516.

Weinert, C., Grütter, C., Roschitzki-Voser, H., Mittl, P. R. E., & Grütter, M. G. (2009). The Crystal Structure of Human Pyrin B30.2 Domain: Implications for Mutations Associated with Familial Mediterranean Fever. *Journal of Molecular Biology*, *394*(2), 226–236.

Williams, K. L., Lich, J. D., Duncan, J. A., Reed, W., Moore, C., Kurtz, S., Coffield, V. M., Accavitti-, M. A., et al. (2005). *The CATERPILLER Protein Monarch-1 Is an Antagonist of Toll-like Receptor-, Tumor Necrosis Factor α-, and Mycobacterium tuberculosis-induced Pro-inflammatory Signals*. *280*(48), 39914–39924.

Wilson, J. G., Simpson, L. J., Ferreira, A. M., Rustagi, A., Roque, J., Asuni, A., Ranganath, T., Grant, P. M., et al. (2020). Cytokine profile in plasma of severe COVID-19 does not differ from ARDS and sepsis. *JCI Insight*, *5*(17), 1–6.

Wright, S. W., Lovelace-Macon, L., Hantrakun, V., Rudd, K. E., Teparrukkul, P., Kosamo, S., Liles, W. C., Limmathurotsakul, D., et al. (2020). sTREM-1 predicts mortality in hospitalized patients with infection in a tropical, middle-income country. *BMC Medicine*, *18*(1), 1–9.

Wu, J., & Chen, Z. J. (2014). Innate immune sensing and signaling of cytosolic nucleic acids. *Annual Review of Immunology*, *32*, 461–488.

Xia, S., Zhang, Z., Magupalli, V. G., Pablo, J. L., Dong, Y., Vora, S. M., Wang, L., Fu, T. M., et al. (2021). Gasdermin D pore structure reveals preferential release of mature interleukin-1. *Nature*, *593*(7860), 607–611.

Xiao, L., Magupalli, V. G., & Wu, H. (2023). Cryo-EM structures of the active NLRP3 inflammasome disc. *Nature*, *613*(7944), 595–600.

Xiao, W., Mindrinos, M. N., Seok, J., Cuschieri, J., Cuenca, A. G., Gao, H., Hayden, D. L., Hennessy, L., et al. (2011). A genomic storm in critically injured humans. *Journal of Experimental Medicine*, *208*(13), 2581–2590.

Xu, Hao, Yang, J., Gao, W., Li, L., Li, P., Zhang, L., Gong, Y. N., Peng, X., et al. (2014). Innate immune sensing of bacterial modifications of Rho GTPases by the Pyrin inflammasome. *Nature*, *513*(7517), 237–241.

Xu, H., Akinyemi, I. A., Chitre, S. A., Loeb, J. C., Lednicky, J. A., McIntosh, M. T., & Bhaduri-McIntosh, S. (2022). SARS-CoV-2 viroporin encoded by ORF3a triggers the NLRP3 inflammatory pathway. *Virology*, *568*, 13–22.

Xu, J., & Núñez, G. (2023). The NLRP3 inflammasome: activation and regulation. *Trends in Biochemical Sciences*, *48*(4), 331–344.

Yalcinkaya, M., Liu, W., Islam, M. N., Kotini, A. G., Gusarova, G. A., Fidler, T. P., Papapetrou, E. P., Bhattacharya, J., et al. (2021). Modulation of the NLRP3 inflammasome by Sars-CoV-2 Envelope protein. *Scientific Reports*, *11*(1), 1–12.

Yang, D., He, Y., Muñoz-Planillo, R., Liu, Q., & Núñez, G. (2015). Caspase-11 Requires the Pannexin-1 Channel and the Purinergic P2X7 Pore to Mediate Pyroptosis and Endotoxic Shock. *Immunity*, *43*(5), 923–932.

Yang, J., Zhao, Y., Shi, J., & Shao, F. (2013). Human NAIP and mouse NAIP1 recognize bacterial type III secretion needle protein for inflammasome activation. *Proceedings of the National Academy of Sciences of the United States of America*, *110*(35), 14408–14413.

Yang, Z., Shi, J., He, Z., Lu, Y., Xu, Q., Ye, C., Chen, S., Tang, B., et al. (2020). Predictors for imaging progression on chest ct from coronavirus disease 2019 (covid-19) patients. *Aging*, *12*(7), 6037–6048.

Yao, S., Li, L., Sun, X., Hua, J., Zhang, K., Hao, L., Liu, L., Shi, D., et al. (2019). FTY720 Inhibits MPP+-Induced Microglial Activation by Affecting NLRP3 Inflammasome Activation. *Journal of Neuroimmune Pharmacology*, *14*(3), 478–492.

Yeretssian, G., Correa, R. G., Doiron, K., Fitzgerald, P., Dillon, C. P., Green, D. R., Reed, J. C., & Saleh, M. (2011). Non-apoptotic role of BID in inflammation and innate immunity. *Nature*, *474*(7349), 96–99.

Yona, S., Kim, K. W., Wolf, Y., Mildner, A., Varol, D., Breker, M., Strauss-Ayali, D., Viukov, S., et al. (2014). Fate mapping reveals origins and dynamics of monocytes and tissue macrophages under homeostasis. *Immunity*, *38*(1), 79–91.

Yu, J. W., Fernandes-Alnemri, T., Datta, P., Wu, J., Juliana, C., Solorzano, L., McCormick, M., Zhang, Z. J., et al. (2007). Pyrin Activates the ASC Pyroptosome in Response to Engagement by Autoinflammatory PSTPIP1 Mutants. *Molecular Cell*, *28*(2), 214–227.

Zafer, M. M., El-Mahallawy, H. A., & Ashour, H. M. (2021). Severe COVID-19 and sepsis: Immune pathogenesis and laboratory markers. *Microorganisms*, *9*(1), 1–13.

Zanoni, I., Tan, Y., Gioia, M. Di, Broggi, A., Ruan, J., Shi, J., Donado, C. A., Shao, F., et al. (2016). An endogenous caspase-11 ligand elicits interleukin-1 release from living dendritic cells. *Science*, *352*(6290), 1232–1236.

Zelová, H., & Hošek, J. (2013). TNF-α signalling and inflammation: Interactions between old acquaintances. *Inflammation Research*, *62*(7), 641–651.

Zeng, G., Chen, D., Zhou, R., Zhao, X., Ye, C., Tao, H., Sheng, W., & Wu, Y. (2022). Combination of C-reactive protein, procalcitonin, IL-6, IL-8, and IL-10 for early diagnosis of hyperinflammatory state and organ dysfunction in pediatric sepsis. *Journal of Clinical Laboratory Analysis*, *36*(7), 1–9.

Zhang, L., Chen, S., Ruan, J., Wu, J., Tong, A. B., Yin, Q., Li, Y., David, L., et al. (2015). Cryo-EM structure of the activated NAIP2-NLRC4 inflammasome reveals nucleated polymerization. *Science*, *350*(6259), 404–409.

Zhang, L., Sui, R., & Zhang, L. (2022). Fingolimod protects against cerebral ischemia reperfusion injury in rats by reducing inflammatory cytokines and inhibiting the activation of p38 MAPK and NF-κB signaling pathways. *Neuroscience Letters*, *771*(40), 136413.

Zhang, Z., Venditti, R., Ran, L., Liu, Z., Vivot, K., Schürmann, A., Bonifacino, J. S., De Matteis, et al. (2023). Distinct changes in endosomal composition promote NLRP3 inflammasome activation. *Nature Immunology*, *24*(1), 30–41.

Zhao, Y., Qin, L., Zhang, P., Li, K., Liang, L., Sun, J., Xu, B., Dai, Y., et al. (2020). Longitudinal COVID-19 profiling associates IL-1RA and IL-10 with disease severity and RANTES with mild disease. *JCI Insight*, *5*(13), 4–14.

Zhao, Y., Yang, J., Shi, J., Gong, Y. N., Lu, Q., Xu, H., Liu, L., & Shao, F. (2011). The NLRC4 inflammasome receptors for bacterial flagellin and type III secretion apparatus. *Nature*, *477*(7366), 596–602.

Zheng, Y., Humphry, M., Maguire, J. J., Bennett, M. R., & Clarke, M. C. H. (2013). Intracellular Interleukin-1 Receptor 2 Binding Prevents Cleavage and Activity of Interleukin-1α, Controlling Necrosis-Induced Sterile Inflammation. *Immunity*, *38*(2), 285–295.

Zhou, F., Yu, T., Du, R., Fan, G., Liu, Y., Liu, Z., Xiang, J., Wang, Y., et al. (2020). Clinical course and risk factors for mortality of adult inpatients with COVID-19 in Wuhan, China: a retrospective cohort study. *The Lancet*, *395*(10229), 1054–1062.

Zhou, Q., Aksentijevich, I., Wood, G. M., Walts, A. D., Hoffmann, P., Remmers, E. F., Kastner, D. L., & Ombrello, A. K. (2015). Cryopyrin-associated periodic syndrome caused by a myeloid-restricted somatic NLRP3 mutation. *Arthritis and Rheumatology*, *67*(9), 2482–2486.

Zhou, Z., He, H., Wang, K., Shi, X., Wang, Y., Su, Y., Wang, Y., Li, D., et al. (2020). Granzyme A from cytotoxic lymphocytes cleaves GSDMB to trigger pyroptosis in target cells. *Science*, *368*(6494).

Ziegler-Heitbrock, L., & Hofer, T. P. J. (2013). Toward a refined definition of monocyte subsets. *Frontiers in Immunology*, *4*, 1–5.

Zizzo, G., & Cohen, P. (2020). Imperfect storm: is interleukin-33 the Achilles heel of COVID-19? *Lancet Rheumatol*, *2*, e779–90.

SPANISH SUMMARY

1. Introducción

La inflamación es una respuesta esencial del organismo frente a infecciones o alteraciones en los tejidos. En ella participan el sistema inmunitario innato y el adaptativo. El primero de ellos está compuesto por una gran diversidad celular, donde destacan los monocitos, encargados de reconocer, a través de sus receptores, patrones moleculares presentes en los distintos agentes infecciosos o moléculas asociadas a peligro o daño tisular (PAMPs y DAMPs, del inglés *pathogen-associated molecular patterns* y *danger-associated molecular patterns,* respectivamente). Por su parte, el sistema inmunitario adaptativo se encarga del reconocimiento específico de antígenos para los cuales se ha generado una memoria previa. La coordinación y combinación de ambas respuestas inmunitarias conduce a la eliminación de la causa inicial del daño y el restablecimiento de la homeostasis tisular (Medzhitov, 2010; Netea et al., 2018).

Dentro de los receptores de patrones cabe destacar a NLRP3 (del inglés *nucleotide oligomerization domain and leucine rich domain receptor pyrin domain-containing* 3), NLRC4 (del inglés *NLR family CARD domain-containing 4 protein*), y Pirina. Éstos se encuentran en el citoplasma de las células y, aunque no reconocen de forma directa a los *PAMPs* y *DAMPs*, detectan las alteraciones citoplasmáticas inducidas por ellos (p. ej., salida de potasio en el caso de NLRP3, toxina B de *Clostridium difficile* en el caso de Pirina o proteínas bacterianas tales como la flagelina de *Salmonella* y *Legionella* por parte de NLRC4). Una vez activos, estos receptores oligomerizan y forman complejos multiproteicos denominados inflamasomas. La formación del inflamasoma culmina con la activación de la proteasa efectora caspasa-1, lo que a su vez conduce a la secreción de citoquinas proinflamatorias (principalmente la interleuquina (IL)-1β y la IL-18) y a un tipo de muerte celular denominado piroptosis (Martinon et al., 2002). Fallos en la correcta activación de los inflamasomas o mutaciones en los genes que los codifican resultan en un cambio en la estructura de los mismos y en la formación de complejos autoactivos. Esto desemboca en el desarrollo de enfermedades o síndromes autoinflamatorios (de Torre-Minguela et al., 2017).

2. Objetivos

1. Caracterizar los marcadores inflamatorios y la función de los inflamasomas NLRP3 y Pirina en pacientes sépticos de origen intraabdominal.

2. Comparar el patrón de marcadores inflamatorios entre pacientes sépticos de origen intraabdominal y pacientes con COVID-19.

3. Determinar la función de las mutaciones patogénicas que afectan a *NLRP3, NLRC4* y *MEFV* en la activación de los inflamasomas.

4. Analizar la activación de los inflamasomas NLRP3 y Pirina en pacientes con leucemia monocítica crónica y esclerosis múltiple antes y después del tratamiento farmacológico.

3. Materiales y métodos

En esta Tesis se ha caracterizado la función de los inflamasomas NLRP3, NLRC4 y Pirina en muestras de sangre humana. Concretamente, en el estudio de pacientes sépticos de origen abdominal, se recogieron muestras de pacientes con sepsis durante las primeras 24 horas de desarrollo de la sepsis (*n* = 34) y pacientes controles sometidos a una cirugía abdominal sin desarrollo de sepsis (*n* = 36). Asimismo, se han estudiado pacientes portadores de mutaciones asociadas a enfermedades autoinflamatorias. Específicamente, (*n* = 13) pacientes con síndrome periódico asociado a criopirina (*CAPS*, siglas en inglés), (*n* = 4) pacientes con fiebre mediterránea familiar (*FMF*, siglas en inglés) y (*n* = *1*) un paciente con una enfermedad inflamatoria asociada a NLRC4. Además, se ha evaluado el uso de terapias inhibitorias de los componentes del inflamasoma NLRP3 en pacientes con esclerosis múltiple recurrente-remitente (*n* = 12) y pacientes con leucemias mielomonocíticas crónicas (*n* = 5). Cada estudio se ha acompañado con el análisis de donantes sanos (*n* total > 60).

De las muestras de sangre completa se obtuvieron las células mononucleares de sangre periférica (*PBMCs,* acrónimo en inglés), que se cultivaron *in vitro,* y el plasma. En el estudio de pacientes con SARS-CoV-2 se analizaron muestras de plasma de 208 individuos diagnosticados con COVID-19 y de 69 controles sanos obtenidos pre-pandemia.

Para realizar los estudios *in vitro* se ha utilizado la línea celular humana HEK-293T y muestras de médula ósea de ratón, de donde se diferenciaron macrófagos derivados de médula ósea (*BMDMs* o *bone-marrow derived macrophages* en inglés).

Los ensayos *in vitro* han consistido en tratamientos farmacológicos específicos a cada estudio. Generalmente, las células se sembraron a una densidad celular de 10^6 células/ml en placas de 24 pocillos y se incubaron a 37ºC y 5% de CO_2. Las muestras se estimularon con LPS (1.6 µg/ml) durante 3 horas en presencia o ausencia de ATP (3 mM, añadido durante los últimos 30 minutos de incubación), nigericina (10 µM, añadido durante los últimos 30 minutos de incubación), CdtB (1 µg/ml, añadido durante la última hora de

incubación) o con el reactivo FlaTox durante 5 horas. En algunos casos, inhibidores específicos de NLRP3, como MCC950 y CY-09 (10 µM en ambos casos) se añadieron 15 minutos antes del segundo estímulo y se mantuvo durante toda la estimulación. Además, las células de pacientes con síndromes autoinflamatorios, una vez estimuladas, se mantuvieron en un incubador con un 5% de CO_2 tanto a 37ºC como a 32ºC. En todos los ensayos, tras finalizar la estimulación celular, se recogieron y centrifugaron los sobrenadantes para, posteriormente, medir la liberación de citoquinas.

Para obtener los resultados de cada uno de los estudios *in vitro* se emplearon diferentes técnicas. La técnica ELISA (acrónimo del inglés *enzyme-linked immunoSorbent assay:* 'ensayo por inmunoadsorción ligado a enzimas') se utilizó para la determinación de citoquinas liberadas por las células estimuladas (p. ej., IL-1β, IL-6, IL-18, etc.). Como marcador de viabilidad celular se cuantificó la presencia de lactato deshidrogenasa en los sobrenadantes celulares. Para evaluar una batería de marcadores asociados a inflamación en las muestras de plasma se hizo uso de la técnica *multiplexing.* Los ensayos para determinar el porcentaje de monocitos con oligómeros de ASC (del inglés *apoptosis-associated speck-like protein*) fueron realizados por citometría de flujo. Para establecer las poblaciones de monocitos se utilizaron anticuerpos contra los marcadores de membrana CD14 y CD16, y CD15 en el caso de neutrófilos.

Además, se generó una batería de vectores portadores de mutaciones patogénicas de NLRP3 y NLRC4. Para el estudio de su funcionalidad, se transfectaron en HEK293T y se evaluó su expresión, el grado de autoactivación (oligomerización) y la conformación de los inflamasomas mediante electrotransferencia, citometría de flujo y la técnica BRET (*bioluminescent resonance energy transfer,* acrónimo del inglés), respectivamente.

4. Resultados

4.1 La activación del inflamasoma NLRP3, a diferencia del inflamasoma Pirina, se encuentra comprometida en sepsis

La sepsis es considerada una de las principales causas de muerte en las unidades de cuidados intensivos. Está caracterizada por una respuesta inflamatoria sistémica y una fase inmunosupresora que ocurren de forma simultánea.

La cohorte de pacientes sépticos de origen intraabdominal presentó elevados, a día 1, los parámetros de inflamación sistémica y de fallo orgánico, así como una alteración en las poblaciones celulares. Tras analizar la concentración sérica de las citoquinas de la familia de la IL-1, así como otras proteínas relacionadas, se encontró que IL-18, IL-18BP, IL-

1RA, sIL-1RI, sIL-1RII, IL-6, IL-8, TNF-α, M-CSF e IL-15 estaban aumentados en sépticos en comparación con los controles sanos, lo que indicó una respuesta inflamatoria dual en estos pacientes. Las citoquinas IL-6, IL-8, IL-1RA y TNF-α, así como sTREM-1, todos ellos marcadores de predicción de mal pronóstico de la enfermedad, correlacionaron positivamente con la mortalidad.

Nuestro estudio confirmó los resultados previos de nuestro grupo de investigación en los que se identificó un grupo de pacientes sépticos con una respuesta comprometida del inflamasoma NLRP3, pero no del inflamasoma Pirina. Sin embargo, ningún parámetro analizado, como los marcadores bioquímicos o los parámetros de severidad, permitió identificar este grupo de pacientes inmunocomprometidos. Los pacientes con una actividad comprometida del inflamasoma NLRP3 que sobrevivieron y se recuperaron de la sepsis, mejoraron la respuesta del inflamasoma al alta hospitalaria, lo que indicó que la inmunosupresión de NLRP3 es un estado transitorio.

Al comparar el estado inflamatorio de los dos grupos de pacientes sépticos, las citoquinas IL-1β e IL-37 se encontraron elevadas en los pacientes inmunocomprometidos para NLRP3. La IL-37, a diferencia de IL-1β, es una proteína antiinflamatoria conocida por disminuir la producción de citoquinas proinflamatorias mediadas por LPS. Estos resultados podrían indicar que ambas interleuquinas favorecen la desregulación de la respuesta inmunitaria presente en los pacientes sépticos.

El estudio de esta Tesis permite avanzar en la identificación de pacientes sépticos con una respuesta inmunitaria comprometida, siendo esto de vital importancia tanto en el diagnóstico como en el tratamiento de la sepsis.

4. 2 La sepsis y la COVID-19 inducen una secreción diferencial de citoquinas inflamatorias

La enfermedad por COVID-19, al igual que la sepsis, es una enfermedad infecciosa con alta mortalidad. En ambas patologías, un aumento en la edad y en las comorbilidades favorecen el riesgo de padecer una patología severa. Sendos procesos infecciosos están caracterizados por una liberación exacerbada de citoquinas inflamatorias que, en casos severos, inducen un fallo multiorgánico y, en última instancia, el fallecimiento de los pacientes.

El análisis de la cohorte de pacientes con COVID-19 mostró que las proteínas de fase aguda, procalcitonina y proteína C-reactiva, así como el indicador de desregulación inmune, ferritina, aumentaban acorde al incremento de la gravedad clínica. Al comparar

estos resultados con la cohorte de pacientes sépticos de origen abdominal, se observó que la procalcitonina y la proteína C-reactiva se encontraban elevadas en el plasma de los pacientes con sepsis bacteriana, mientras que la ferritina presentaba unos valores superiores en la cohorte de individuos con COVID-19. Probablemente, la hiperferritinemia favorezca el proceso inflamatorio descontrolado que padecen los pacientes con COVID-19.

Además, cuando se evaluó la concentración en plasma de las citoquinas IL-6, IL-1Ra, IL-15 e IL-18 también se encontró un incremento dependiente de la severidad de la infección por COVID-19. Tanto la citoquina IL-6, como las citoquinas IL-1Ra e IL-18, presentaron unos valores muy superiores en los pacientes con sepsis bacteriana. La IL-18, al igual que la interleuquina-1β, participa en la respuesta inmunitaria contra las infecciones, mientras que la IL-1Ra bloquea la señalización de IL-1. En patologías como la sepsis, la concentración sérica de IL-1β es demasiado baja para ser medida, de forma que se considera a la IL-1Ra como un indicador de liberación sistémico de IL-1β. Por tanto, nuestros resultados indican que la señalización mediada por IL-1 y de las citoquinas mediadas por ésta favorecen la respuesta inmunitaria frente a las infecciones bacterianas como la sepsis.

4. 3 Análisis funcional de mutaciones del inflamasoma NLRP3 asociadas a enfermedades inflamatorias

Las variantes de significancia incierta resultan en una patología autoinflamatoria variada en la que la relación genotipo-fenotipo no siempre es fácil de obtener. Nuestro estudio mostró que las variantes de baja penetrancia V198M y Q703K no presentan una activación constitutiva del inflamasoma NLRP3, aunque son capaces de formar oligómeros de ASC tras el estímulo de nigericina. Por el contrario, la variante R488K sí que presentó una activación basal del inflamasoma. Estos resultados indican que las variantes de significancia incierta presentan un fenotipo intermedio entre NLRP3 silvestre y las variantes patogénicas asociadas a NLRP3.

Además, también se estudiaron variantes de NLRP3 asociadas al síndrome autoinflamatorio familiar inducido por frío (siglas en inglés, *FCAS*). Nuestros resultados evidencian que las variantes asociadas a FCAS presentan una estructura abierta en comparación con NLRP3 silvestre, lo que favorece su interacción con la chaperona HSC70. Tras la exposición al frío (32ºC), HSC70 sufre un cambio conformacional que favorece la activación de las variantes asociadas a FCAS, mediado esto por un aumento en la formación de oligómeros de ASC.

Asimismo, se caracterizó una batería de mutaciones en NLRP3 con un patrón de herencia en la línea germinal o por mosaicismo. Las mutaciones en mosaicismo del inflamasoma NLRP3 ocurren por debajo del 15% del total de casos al ser incompatibles con la vida. Aquellas mutaciones que se encontraban en el motivo *Walker B* de NLRP3 presentaron una conformación abierta con un alto porcentaje de formación de oligómeros de ASC. Por otra parte, también se observó que las mutaciones en mosaico K355N, M406V y T433I mostraron un aumento en la formación de oligómeros de ASC. Esto concuerda con el hecho de que se encuentran cerca de la región de NLRP3 que sufre el cambio conformacional asociado a la activación del inflamasoma.

4.4 Activación del inflamasoma NLRP3 en monocitos de pacientes con CAPS y FMF

El síndrome periódico asociado a criopirina y la fiebre mediterránea familiar constituyen dos enfermedades autoinflamatorias causadas por mutaciones de ganancia de función en los genes que codifican a los inflamasomas NLRP3 y Pirina, respectivamente. Los individuos que las padecen sufren brotes inflamatorios recurrentes caracterizados por un aumento en la producción de citoquinas proinflamatorias como la IL-1β. Debido a esto, la mayoría de estudios realizados hasta el momento se han concentrado en pacientes con brotes activos de la enfermedad. Sin embargo, en esta Tesis se han estudiado individuos diagnosticados de CAPS y FMF que se encontraban asintomáticos y bajo tratamiento en el momento del estudio.

Nuestros resultados indican que sólo las mutaciones en *NLRP3*, y no en el gen codificante de Pirina, inducen el estado autoactivo del inflamasoma, tanto en condiciones basales como tras el *priming* con LPS. Además, se ha observado un aumento progresivo en la formación de oligómeros de ASC en los monocitos de los pacientes con CAPS tras diferentes horas del estímulo LPS, siendo esto bloqueado por el inhibidor específico de NLRP3, MCC950. También se ha encontrado que sólo las *PBMCs* de los pacientes con CAPS secretan de forma constitutiva la citoquina IL-18, permaneciendo invariables los niveles de IL-1β y TNF-α entre los donantes sanos y los pacientes con síndromes autoinflamatorios. Las discrepancias entre nuestros resultados con algunos estudios ya publicados podrían explicarse por diversas causas: (i) el protocolo de estimulación de las células en cultivo que podría implicar una activación diferencial en el inflamasoma NLRP3, (ii) la presencia o ausencia de brotes inflamatorios en los pacientes en el momento del estudio y, (iii) el hecho de que aunque las mutaciones asociadas a síndromes autoinflamatorios puedan significar un estado autoactivo del inflamasoma, la señalización y la regulación aguas debajo de este proceso puede ser diferente entre ellas.

Se concluye, por lo tanto, que los niveles de IL-1β no deben considerarse como el único biomarcador de autoinflamación en los pacientes con CAPS y FMF, y que sólo las mutaciones de NLRP3 asociadas a CAPS pueden formar inflamasomas constitutivamente activos.

4.5 Análisis funcional de mutaciones del inflamasoma NLRC4 asociadas a enfermedades inflamatorias

Durante el desarrollo de esta Tesis, se analizó una muestra de sangre procedente de una paciente adulta portadora de la mutación S171F en el gen codificante de NLRC4. Los resultados de los estudios *in vitro* y *ex vivo* de la mutación mostraron un aumento en la formación de oligómeros de ASC, tanto en los monocitos de la paciente como en células HEK293T que expresaban la variante, así como un incremento en la liberación de IL-18. Sin embargo, a diferencia de otros estudios previamente descritos, las células mononucleares de sangre periférica de la paciente no indujeron un aumento en la liberación de IL-1β ni IL-6, tanto en condiciones basales como tras el tratamiento con LPS. Esta deficiencia no pudo atribuirse a un defecto en el *priming* de LPS o en la activación de NFκB. Nuestros resultados apoyan un comportamiento de ganancia de función de la variante S171F, de forma similar a otras mutaciones asociadas a NLRC4 reportadas como causantes de enfermedades autoinflamatorias.

Además, la co-expresión de una batería de mutaciones asociadas a NLRC4 con ASC en el sistema recombinante HEK293T nos permitió analizar, mediante citometría de flujo, la formación de oligómeros de ASC inducidos por estas variantes. Nuestros resultados indican que la sustitución de aminoácidos críticos para la correcta conformación basal inactiva de NLRC4, tales como T177A, pueden inducir un cambio conformacional que favorezca la autoactivación del inflamasoma. Por otra parte, otras mutaciones previamente descritas como patogénicas, como H443P o V341A, no indujeron un aumento en la formación de oligómeros de ASC. Esto podría deberse a que NLRC4, a diferencia de otros inflamasomas como NLRP3, es capaz de interaccionar directamente con pro-caspasa-1 y formar estructuras oligoméricas de forma independiente a la presencia de ASC.

4.6 La inhibición del inflamasoma NLRP3 mediada por Fingolimod como tratamiento de pacientes con esclerosis múltiple

Fingolimod es un fármaco inmunomodulador aprobado para el tratamiento de personas con esclerosis múltiple remitente-recurrente (EMRR). Debido a su mecanismo de

acción, produce una disminución de entre el 60 y el 80% de los linfocitos circulantes en sangre, lo que se traduce en una reducción en el número de linfocitos autoreactivos que llegan al sistema nervioso central. Se ha puesto de manifiesto, en modelos animales de Parkinson y depresión, que dicho tratamiento inhibe el ensamblaje y la activación del inflamasoma NLRP3.

Durante el desarrollo de esta Tesis se tuvo acceso a muestras de sangre de doce pacientes con EMRR en tratamiento con fingolimod. Según el criterio médico fueron clasificados en 'respondedores' y 'no respondedores' al tratamiento tras doce meses del mismo. Tras evaluar la activación del inflamasoma NLRP3 en dichos pacientes, se observó que el tratamiento farmacológico redujo el porcentaje de monocitos con oligómeros de ASC en los pacientes respondedores a los seis meses de tratamiento. Sin embargo, en pacientes no respondedores, no sólo se encontró un aumento en el número de células con oligómeros de ASC, sino también un incremento de muerte celular por piroptosis. Ninguno de estos resultados pudo atribuirse a una variación en las subpoblaciones de monocitos, que permanecieron constantes en ambos grupos de pacientes antes y después del tratamiento.

Además, en los sobrenadantes de las células mononucleares de sangre periférica sin estimular de los pacientes no respondedores se observó un aumento en la producción de TNF-α e IL-6 tras seis meses de tratamiento. En el caso de los pacientes respondedores, el nivel secretado de estas citoquinas fue incluso menor.

Estos resultados sugieren que el tratamiento farmacológico con fingolimod no sólo inhibe la activación del inflamasoma NLRP3, sino que disminuye la ruta de señalización de NF-κB. Por tanto, la falta de inhibición de la activación del inflamasoma NLRP3 en pacientes con EMRR tratados con fingolimod podría identificar individuos refractarios al tratamiento, emergiendo así NLRP3 como un biomarcador.

4.7 Inhibición de la activación del inflamasoma NLRP3 en pacientes con LMMC y *KRAS* mutado mediante el antagonista de IL-1R

Las mutaciones en *RAS* (del inglés *rat* sarcoma) se diagnostican entre el 7% y el 22% de los casos de leucemia mielomonocítica crónica. Entre sus isoformas se encuentra *KRAS* (del inglés, *Kristen RAS*), un oncogén con función de GTPasa implicado en la regulación de la proliferación celular y la muerte por apoptosis. En la bibliografía hay muy pocos estudios que se hayan centrado en analizar la relación del inflamasoma NLRP3 y el desarrollo de los síndromes mielodisplásicos en un contexto humano.

En esta Tesis hemos analizado una cohorte de pacientes con LMMC portadores o no de mutaciones en el oncogén *KRAS*. En los pacientes LMMC *KRAS*-mut se observó un porcentaje elevado (alrededor del 60%) de monocitos con oligómeros de ASC de forma basal. Además, tras la estimulación del inflamasoma NLRP3 con LPS y ATP no se produjo ningún incremento en la liberación de IL-1β. El inhibidor específico de NLRP3, MCC950, redujo significativamente los niveles de IL-1β secretados, pero no la formación de oligómeros de ASC. Esto concuerda con el hecho de que la activación del inflamasoma NLRP3 es un proceso irreversible una vez oligomeriza ASC.

También, se observó que la activación basal de NLRP3 no estaba asociada a un aumento de muerte por piroptosis. Esto sugirió que la liberación de IL-1β podría deberse a un estado hiperactivo en los monocitos cuya muerte celular por piroptosis sería defectuosa.

Asimismo, se ha demostrado que el tratamiento con anakinra en un paciente con LMMC y mutación G12D en *KRAS*, no sólo redujo *ex vivo* el número de monocitos con oligómeros de ASC, sino también la concentración plasmática de ASC y la liberación de las citoquinas proinflamatorias IL-1β e IL-18.

En conjunto, nuestro estudio demostró que los pacientes con LMMC y mutación en *KRAS* presentan una activación basal de inflamasoma NLRP3. Además, el tratamiento con inhibidores de la ruta de señalización de IL-1 podría considerarse como una opción terapéutica en aquellos pacientes refractarios a las terapias convencionales.

5. Conclusiones

1. La supervivencia de los pacientes sépticos de origen intraabdominal a día uno se asocia con un incremento en la activación canónica del inflamasoma NLRP3 en los monocitos estimulados con LPS y ATP.

2. La activación del inflamasoma Pirina en los monocitos de pacientes sépticos de origen intraabdominal a día uno estimulados con LPS y Cdtb no se asocia con la supervivencia de los pacientes.

3. En el plasma de los pacientes sépticos de origen intraabdominal se encontraron elevadas las citoquinas IL-6, IL-8 e IL-1Ra, así como las proteínas de fase aguda PRC y PCT, en comparación con los pacientes control y los pacientes con COVID-19.

4. En el plasma de los pacientes con COVID-19 se encontraron elevados los niveles de la citoquina IL-15 y el marcador inflamatorio ferritina comparados con los pacientes control y los pacientes sépticos de origen intraabdominal.

5. Las variantes de significado incierto de NLRP3 V178M y Q703K expresadas en células HEK293T presentaron una señal BRET y un porcentaje de células con oligómeros de ASC similar a NLRP3 silvestre.

6. Las variantes de NLRP3 R260W, L205P y L353P expresadas en células HEK293T presentaron una disminución de la señal BRET en comparación con NLRP3 silvestre tanto a 37ºC como a 32ºC.

7. Las variantes patogénicas de NLRP3 R260W y L353P expresadas en células HEK293T presentaron un incremento en el porcentaje de células con oligómeros de ASC a 32ºC comparado con el obtenido a 37ºC.

8. Exceptuando la variante de NLRP3 G326E, el inhibidor MCC950 aumentó la señal de BRET en todas las variantes expresadas en células HEK293T y evaluadas en esta Tesis Doctoral.

9. El inhibidor de NLRP3, CY-09, disminuyó la señal BRET de todas las variantes expresadas en células HEK293T y evaluadas en esta Tesis Doctoral, a excepción de las variantes R260W, D303A, D303G, E304L y L353P.

10. El paciente portador de la variante postcigótica de NLRC4 S171 presentó un incremento en la proporción de monocitos con oligómeros de ASC y en la liberación de IL-18 en condiciones basales y tras la estimulación con LPS, comparado con los individuos sanos.

11. Las variantes patogénicas de NLRC4 S171F, T117A, T337S, S445P and W665C mostraron un incremento en el número de células con oligómeros de ASC cuando se expresaron en células HEK293T.

12. Los pacientes con CAPS presentaron un aumento en el porcentaje de monocitos de sangre periférica con oligómeros de ASC en condiciones basales y tras la estimulación con LPS, comparados con los individuos sanos y los pacientes con FMF.

13. Los pacientes con esclerosis múltiple remitente-recurrente refractarios al tratamiento con fingolimod mostraron un incremento en la proporción de monocitos de

sangre periférica con oligómeros de ASC tras la activación canónica del inflamasoma NLRP3 con LPS y ATP después de 6 meses de terapia farmacológica, comparados con los individuos sanos y los pacientes buenos respondedores a la terapia.

14. Los pacientes con leucemia mielomonocítica crónica con mutación en *KRAS* presentaron un aumento significativo en el porcentaje de monocitos de sangre periférica con oligómeros de ASC en condiciones basales y tras la estimulación con LPS, comparados con los individuos control y los pacientes con leucemia mielomonocítica crónica *KRAS* silvestre.

15. El tratamiento con anakinra en un paciente con leucemia mielomonocítica crónica portador de la mutación G12D en el gen *KRAS* alteró la activación del inflamasoma NLRP3 y sirvió como terapia puente previa al trasplante alogénico de células madre.

PUBLICATIONS RESULTING FROM THIS THESIS

1. Published

1. Angosto-Bazarra, D., Molina-López, C.[$], Peñín-Franch, A.[$], **Hurtado-Navarro, L.**[$] & Pelegrín, P. (2021). Techniques to Study Inflammasome Activation and Inhibition by Small Molecules. Molecules (Q2, FI:4.927), 26(6). Doi:10.3390/molecules26061704. Review. *([$]Share second co-autor).*

2. Ionescu, D.*, Peñín-Franch, A.*, Mensa-Vilaro, A., Castillo, P., **Hurtado-Navarro, L.**, Molina-López, C., Romero-Chala, S., Plaza, S., Fabregat, V., Bujan, S., Marques, J., Casals, F., Yague, J., Oliva, B., Fernández-Pereira, L. M., Pelegrín, P. & Aróstegui, J. I. (2022). First Description of Late-Onset Autoinflammatory Disease Due to Somatic NLRC4 Mosaicism. Arthritis Rheumatol (D1, FI: 10.995), 74(4), 692-699. Doi:10.1002/art.41999. *(*Share first autorship).*

3. García-Villalba, J.*, **Hurtado-Navarro, L***., Peñín-Franch, A., Molina-López, C., Martínez-Alarcón, L., Angosto-Bazarra, D., Baroja-Mazo, A. & Pelegrín, P. (2022). Soluble P2X7 receptor is elevated in the plasma of COVID-19 patients and correlates with disease severity. Front Immunol (Q1, FI: 8.787) 18(13), 894470. Doi:10.3389/fimmu.2022.894470. *(*Share first autorship).*

4. Angosto-Bazarra, D., Alarcón-Vila, C., **Hurtado-Navarro, L**., Baños, M. C., Rivers-Auty, J., & Pelegrín, P. (2022). Evolutionary analyses of the gasdermin family suggest conserved roles in infection response despite loss of pore-forming functionality. BMC Biology y (D1, FI: 7.364), 20(1), 1–18. Doi:10.1186/s12915-021-01220-z

5. **Hurtado-Navarro,** L.*, Angosto-Bazarra, D.*, Pelegrín, P., Baroja-Mazo, A., & Cuevas, S. (2022). NLRP3 Inflammasome and Pyroptosis in Liver Pathophysiology: The Emerging Relevance of Nrf2 Inducers. Antioxidants (D1, FI: 7.675), 11(5), 1–15. Doi:10.3390/antiox11050870. Review. *(*Share first autorship).*

6. **Hurtado-Navarro, L**., Baroja-Mazo, A., Martínez-Banaclocha, H., & Pelegrín, P. (2022). Assessment of ASC Oligomerization by Flow Cytometry. Methods in Molecular Biology, 2459, 1–9. Doi:10.1007/978-1-0716-2144-8_1. Book chapter.

7. **Hurtado-Navarro, L**., Baroja-Mazo, A., & Pelegrín, P. (2022). Characterization of P2X7 Receptors in Human Blood Cells. Methods in Molecular Biology, 2510:279-290. Doi: 10.1007/978-1-0716-2384-8_15.

8. **Hurtado-Navarro, L**., García-Palenciano, C., & Pelegrín, P. (2023). Inflammasomes in sepsis. Inflammasome Biology, 369–382. Doi:10.1016/b978-0-323-91802-2.00014-1. Book chapter.

9. Malhotra, S.*, **Hurtado-Navarro, L**.*, Pappolla, A., Villar, L., Río, J., Montalban, X., Pelegrín, P., & Comabella, M. (2023). Increased NLRP3 Inflammasome Activation and Pyroptosis in Patients With Multiple Sclerosis With Fingolimod Treatment Failure. Neurol Neuroimmunol (D1, FI: 11.360), 10 (3) e200100; Doi:10.1212/NXI.0000000000200100. *(*Share first autorship).*

10. Gil-Lianes, J., Gariup, G., Iranzo-Fernández, P., Mensa-Vilaró, A., Peñín-Franch, A., **Hurtado-Navarro, L.,** Pelegrín, P., & Aróstegui, J. I. Early-onset recurrent panniculitis as a phenotype of NLRC4-associated autoinflammatory syndrome: Characterization of pathogenicity of the p.Ser445Pro NLRC4 variant. (2023). Australas J Dermatol (Q3, FI: 2.48), 64(2), 260-267. Doi: 10.1111/ajd.14005.

11. **Hurtado-Navarro, L**.*, Cuenca-Zamora, E.*, Zamora, L., Bellosillo, B., Such, E., Soler-Espejo, E., Martínez-Banaclocha, H., Hernández-Rivas, J., Marco-Ayala, J., Martínez-Alarcón, L., Linares-Latorre, L., García-Ávila, S., Amat-Martínez, P., González,

T., Arnan, M., Pomares-Marín, H., Carreño-Tarragona, G., Chen-Liang, T. H., Herranz, M., García-Palenciano, C., Luz, M. L., Jerez, A., Lozano, M. L., Teruel-Montoya, R., Pelegrín, P., & Ferrer-Marín, F. (2023). NLRP3 inflammasome activation and symptom burden in KRAS-mutated CMML patients is reverted by IL-1 blocking therapy. Accepted in Cell Reports Medicine (D1, FI: 14.3) *(*Share first autorship).*

2. Under review

1. Molina-López, C., **Hurtado-Navarro, L.**, García, C. J., Angosto-Barraza, D., Vallejo, F., Tapia-Abellán, A., Marques-Soares, J. R., Vargas, C., Bujan-Rivas, S., Tomás-Barnerán, F. A., Aróstegui, J. I., & Pelegrín, P. Mutant NLRP3 of Cryopyrin-Associated Periodic Syndromes forms a constitutively active inflammasome and results in alteration in monocyte immunometabolism. *Under review in Nature Communications.*

2. Peñín-Franch, A., **Hurtado-Navarro, L.,** García-Vidal, J. A., Escolar-Reina, P., Medina-Mirapeix, F., & Pelegrín, P. Multiple ASC–dependent inflammasomes drive differential cytokine production in sterile tissue damage. *Under review in Clinical Science.*

3. Schachter, J., Angosto-Bazarra, D., **Hurtado-Navarro, L**., Guijarro, A., Schwarzbaum, P., & Pelegrín, P. Gasdermin D mediates a rapid and transient release of ATP after NLRP3 inflammasome activation. *Under review in Cell Reports.*

3. In preparation

1. **Hurtado-Navarro, L.**, Peñín-Franch, A., Angosto-Bazarra, D., Hernández-Rodríguez, J., Vargas, C., Baroja-Mazo, A., Aróstegui, J.I., & Pelegrín, P. Functional regulation of inflammasomes with NLRP3– and NLRC4–variants associated to autoinflammatory syndromes.

2. **Hurtado-Navarro, L.**, Baroja-Mazo, A., Martínez-Alarcón. L., Ercole, G., Fernández-Pacheco, J., Martínez-Gil, P., Valero-Navarro, G., García-Palenciano, C., & Pelegrín, P. Critical septic patients have an immunesuppression of NLRP3 inflammasome and specific inflammatory profile.

3. **Hurtado-Navarro, L.***, Molina-López, C.*, García-Noguera, D., Mesa del Castillo, P., & Pelegrín, P. Monocytes from Familial Mediterranean fever patients have normal inflammasome activation resulting in exacerbated IL-1β and IL-18 cytokines release. *(*Share first autorship).*

4. Molina-López, C., **Hurtado-Navarro, L.,** O'Neill, L. A., & Pelegrín, P. 4-octylitaconate blocks the constitutive activation of NLPR3 inflammasome of Cryopirin-associated to periodic syndrome.

5. Pizzuto, M., **Hurtado-Navarro, L.[$],** Molina-López, C.[$], Rodríguez-López, S., Ruysschaert, J. M., Schroder, K., & Pelegrín, P. Synthetic Ornithine Lipids Activate Both TLR4 and NLRP3 Inflammasome. *([$]Share second co-autor).*

6. García-Villalba, J., **Hurtado-Navarro, L.,** Angosto-Bazarra, D., Baroja-Mazo, A., Molina-López, C., Peñín-Franch, A., Baños-Gregori, M. C., Gómez, A. I., Baroja-Mazo, A., & Pelegrín, P. The open reading frame ORF7b of the SARS-CoV-2 activates NLRP3.

4. **Awards derived from this Thesis**

1. IX Premio Mejor Proyecto Creación de Empresa "Santander Universidades y Cátedra de Emprendedores, from Banco Santader S.A., 2022.

2. Prize to the best oral communication at the 44º SEBBM Congress (Málaga, 2022). The title of the communication was: “Pyrin inflammasome is active in NLRP3-immunocompromised septic patients”.

3. Prize to the best oral communication at the InflammaZoom Careers Forum (2022) from Abcam. The title of the communication was: “Activation of the Pyrin and NLRP3 inflammasomes during sepsis”.

4. Prize to the best oral communication at the IV *Jornadas Científicas* (Murcia, 2021) from IMIB-Arrixaca. The title of the communication was: “Activation of the Pyrin and NLRP3 inflammasomes during sepsis”.